

# JOINT TRANSPORTATION RESEARCH PROGRAM

INDIANA DEPARTMENT OF TRANSPORTATION  
AND PURDUE UNIVERSITY



## Assessment of Site Variability from Analysis of Cone Penetration Test Data



**Rodrigo Salgado**

**Monica Prezzi**

**Eshan Ganju**

## RECOMMENDED CITATION

Salgado, R., Prezzi, M., & Ganju, E. (2015). *Assessment of site variability from analysis of cone penetration test data* (Joint Transportation Research Program Publication No. FHWA/IN/JTRP-2015/04). West Lafayette, IN: Purdue University. <http://dx.doi.org/10.5703/1288284315523>

## AUTHORS

### Rodrigo Salgado, PhD

Professor of Civil Engineering  
Lyles School of Civil Engineering, Purdue University  
(765) 494-5030  
salgado@purdue.edu  
*Corresponding Author*

### Monica Prezzi, PhD

Professor of Civil Engineering  
Lyles School of Civil Engineering, Purdue University

### Eshan Ganju

Graduate Research Assistant  
Lyles School of Civil Engineering, Purdue University

## ACKNOWLEDGMENTS

This research was funded with support provided by the Indiana Department of Transportation through the Joint Transportation Research Program at Purdue University. The authors would like to thank the agency for the support and are very grateful for the assistance received from the Project Administrators, Samy Nouredin and Timothy Wells, and the Study Advisory Committee (SAC), composed of Athar Khan, Joey Franzino, and Keith Hoernschemeyer, throughout the duration of the project and for their valuable comments and suggestions.

Special thanks are due to Jonathan Paauwe and Joey Franzino and the INDOT drilling crew, Dennis Torrance, Steve Dubac, and Marsell Smith, for their help and support throughout the duration of this project. Thanks are also due to Nayyar Zia Siddiki for his support and valuable comments. In addition, we wish to thank Farhan Rahman for his assistance with some of the research tasks and Anuj Choudhari and Yanfei Ren for their help with the preparation of figures appearing in this report. Last but not least, we also wish to acknowledge Mr. Gerald Verbeek and Geomil Equipment BV for providing a digital cone that was used during the testing.

## JOINT TRANSPORTATION RESEARCH PROGRAM

The Joint Transportation Research Program serves as a vehicle for INDOT collaboration with higher education institutions and industry in Indiana to facilitate innovation that results in continuous improvement in the planning, design, construction, operation, management and economic efficiency of the Indiana transportation infrastructure. [https://engineering.purdue.edu/JTRP/index\\_html](https://engineering.purdue.edu/JTRP/index_html)

Published reports of the Joint Transportation Research Program are available at: <http://docs.lib.purdue.edu/jtrp/>

## NOTICE

The contents of this report reflect the views of the authors, who are responsible for the facts and the accuracy of the data presented herein. The contents do not necessarily reflect the official views and policies of the Indiana Department of Transportation or the Federal Highway Administration. The report does not constitute a standard, specification, or regulation.

## COPYRIGHT

Copyright 2015 by Purdue University. All rights reserved.

Print ISBN: 978-1-62260-344-2

ePUB ISBN: 978-1-62260-345-9

<b>1. Report No.</b> FHWA/IN/JTRP-2015/04	<b>2. Government Accession No.</b>	<b>3. Recipient's Catalog No.</b>	
<b>4. Title and Subtitle</b> Assessment of Site Variability from Analysis of Cone Penetration Test Data		<b>5. Report Date</b> January 2015	<b>6. Performing Organization Code</b>
<b>7. Author(s)</b> Rodrigo Salgado, Monica Prezzi, Eshan Ganju		<b>8. Performing Organization Report No.</b> FHWA/IN/JTRP-2015/04	
<b>9. Performing Organization Name and Address</b> Joint Transportation Research Program Purdue University 550 Stadium Mall Drive West Lafayette, IN 47907-2051		<b>10. Work Unit No.</b>	<b>11. Contract or Grant No.</b> SPR-3408
<b>12. Sponsoring Agency Name and Address</b> Indiana Department of Transportation State Office Building 100 North Senate Avenue Indianapolis, IN 46204		<b>13. Type of Report and Period Covered</b> Final Report	<b>14. Sponsoring Agency Code</b>
<b>15. Supplementary Notes</b> Prepared in cooperation with the Indiana Department of Transportation and Federal Highway Administration.			
<b>16. Abstract</b> <p>Soil property values for use in geotechnical design are often estimated from a limited number of in situ or laboratory tests. The uncertainty involved in estimating soil properties from a limited number of tests can be addressed by quantifying the variability within individual soundings and of the collection of soundings at a site. It has been proposed that factors of safety or resistance factors used in design be linked to site variability. Site variability can be assessed by studying the correlation structure of in situ test data. The cone penetration test (CPT), which is a reliable and widely-accepted in situ test, can be used for this purpose. Soil behavior type (SBT) charts are often used to obtain the subsurface soil profile from CPT parameters such as the cone resistance and the sleeve friction. A soil profile generation algorithm was developed in this research to generate a soil profile from an individual CPT sounding using two modified SBT charts. Soils are variable in both the vertical and horizontal directions. A vertical variability index (VVI) was defined to quantify variability in a CPT sounding. The average of the VVIs for all CPT soundings performed at a site is the site VVI. A site horizontal variability index (site HVI) was also developed, based on cross-correlation between cone resistances, the cone resistance trend differences and the spacing between every pair of CPTs considered, to quantify the soil variability of a site in the horizontal direction. A site variability rating (SVR) system, integrating the vertical and horizontal site variability, was developed to assess the overall site variability. Depending on the SBT chart selected, the soil profile generated using the soil profile generation algorithm may be slightly different; however, the SBT chart effect on the variability indices that compose the SVR index is small. Close agreement was found between the SVRs obtained using the two SBT charts selected for this research. In order to illustrate the use of the algorithms for VVI and HVI calculations and SVR of sites, CPTs from across the state of Indiana were analyzed. CPT data were obtained from Purdue's own database, INDOT's data repository and the U.S. Geological Survey (USGS) website. Site variability is calculated for specific depths of interest. For example, that depth of interest will be shallower for shallow foundations than for deep foundations. Site variability rating maps (SVR maps) for various depths of interest were constructed for the state of Indiana, illustrating the potential use of the site variability assessment methodology. An optimal sounding spacing calculation methodology was also developed to make the site investigation process more efficient, cost-effective and reliable.</p>			
<b>17. Key Words</b> cone penetration test, standard penetration test, site variability, scale of fluctuation, cross-correlation, COV, LRFD, site investigation, CPT sounding spacing		<b>18. Distribution Statement</b> No restrictions. This document is available to the public through the National Technical Information Service, Springfield, VA 22161.	
<b>19. Security Classif. (of this report)</b> Unclassified	<b>20. Security Classif. (of this page)</b> Unclassified	<b>21. No. of Pages</b> 128	<b>22. Price</b>

## EXECUTIVE SUMMARY

### ASSESSMENT OF SITE VARIABILITY FROM ANALYSIS OF CONE PENETRATION TEST DATA

#### Introduction

Site investigation is an important component of every construction project. The main goals of a geotechnical site investigation are (1) to define the soil profile and (2) to estimate the geotechnical properties of the different soils of the soil profile. The soil properties are derived from either *in situ* tests or laboratory tests. However, in both cases the number of *in situ* or laboratory tests is constrained by project budget and time. Since often a limited number of tests are performed, there is uncertainty associated with the soil properties estimated for a site for use in design. This uncertainty is an inevitable part of every geotechnical site investigation, raising the question as to how accurately soil properties derived from laboratory tests or *in situ* tests represent the soil properties of an entire site. Although this uncertainty cannot be eliminated, a site variability assessment may lead to lower or higher resistance factors for use in Load and Resistance Factor Design (LRFD).

In comparison with other *in situ* tests, the Cone Penetration Test (CPT) is considered a reliable tool. The result of the variability study of CPT parameters is helpful during the site investigation and design phases of a project. During the *in situ* investigation phase, the variability of the measured CPT parameters can be assessed in real time. If this variability is deemed high, based on a given number of CPT soundings, additional soundings can be performed to increase the reliability of the estimated soil properties to be used in design, and vice versa. In addition, safety factors or resistance factors to be used in design could be adjusted to reflect the outcome of the variability assessment of the CPT parameters measured for the project site. Therefore, an assessment of site variability can directly benefit a project by optimizing the site investigation cost and increasing the reliability of the foundation design.

#### Findings

In this report, knowledge of spatial statistics was applied to develop a rational methodology to assess site variability using CPT data. The subsurface soil profiles were estimated based on soil behavior type (SBT) charts using a soil profile generation algorithm developed in this research. Then, the vertical variability of each CPT sounding was quantified by a vertical variability index (*VVI*). The average of the *VVIs* for all soundings performed at a site was the site *VVI*. The horizontal variability of the site (site *HVI*) was assessed by considering the

cross-correlation between cone resistances, the cone resistance trend differences, and the spacing between every pair of CPTs.

A site variability rating (SVR) system, integrating the vertical and horizontal site variability, was established to assess the overall site variability. An optimal sounding spacing calculation methodology was also developed to make the site investigation process more efficient, cost-effective, and reliable.

This report includes the following findings:

- The choice of SBT chart influences the soil profile generated using the soil profile generation algorithm; however, its effect on the variability indices that compose the SVR system is small.
- Close agreement was found between the SVRs obtained using the two SBT charts (Robertson, 1990; Tumay, 1985) selected for this research.
- The site variability assessment depends on the soil profile length of the CPT soundings considered in the analyses (the depth of interest will be shallower for shallow foundations than for deep foundations). *VVI* and *HVI* calculations were performed for CPTs available from across the state of Indiana. These calculations, over the long run, can lead to reliable maps of site variability for the state, which would lead to better planning of site investigations and more economical design.

#### Implementation

Site variability rating maps (SVR maps) for various depths of interest were constructed for the state of Indiana, illustrating the potential use of the site variability assessment methodology proposed in this research. SVR maps provide easy visualization of regional site variability.

The following recommendations for implementation are made:

1. continue to develop a comprehensive geotechnical variability database for the state;
2. use CPT instead of SPT whenever possible because of its much greater reliability;
3. measure SPT energy ratio regularly;
4. increase data sampling rate of CPTs;
5. use real-time site variability assessment to establish spacing between CPT soundings;
6. develop a strategy to link LRFD of foundations to site variability assessment;
7. develop site variability iPad® applications to be used in the field by INDOT engineers; and
8. update SVR maps for different soil profile lengths regularly to reflect additional CPT data collected in the context of new INDOT projects.

## CONTENTS

1. INTRODUCTION .....	1
1.1 Introduction .....	1
1.2 Problem statement .....	1
1.3 Research objectives .....	2
1.4 Organization of the report .....	2
2. SOIL PROFILE GENERATION FROM CPT DATA .....	2
2.1 Introduction .....	2
2.2 Review of existing soil behavior type charts .....	2
2.3 Selected SBT charts .....	7
2.4 Soil profile generation .....	9
3. FUNDAMENTAL CONCEPTS OF PROBABILITY AND RANDOM FIELD THEORY .....	20
3.1 Introduction .....	20
3.2 Essentials of probability theory .....	20
3.3 Random field theory .....	21
4. SITE VARIABILITY INDEX .....	25
4.1 Introduction .....	25
4.2 Vertical variability index .....	26
4.3 Horizontal variability index .....	33
4.4 Optimal CPT sounding spacing calculation procedure .....	34
4.5 Site variability rating .....	35
5. SITE VARIABILITY INDEX CALCULATION FOR INDIANA SITES .....	35
5.1 Introduction .....	35
5.2 Sources of CPT data .....	35
5.3 Site variability analysis .....	36
5.4 Soil profile generation .....	39
5.5 Site <i>VVI</i> results .....	39
5.6 SVR results .....	52
6. DEVELOPMENT OF DATA ACQUISITION SYSTEMS .....	68
6.1 Introduction .....	68
6.2 CPT DAQ hardware .....	68
6.3 CPT DAQ and variability analysis software .....	69
6.4 SPT DAQ hardware .....	71
6.5 SPT DAQS .....	71
6.6 SPT energy measurement .....	72
6.7 SPT energy measurement results .....	73
7. CONCLUSIONS AND RECOMMENDATIONS .....	73
REFERENCES .....	74
APPENDICES	
Appendix A. Generated vs. Actual soil profile comparison for indiana sites .....	76
Appendix B. Variability maps for indiana .....	104

## LIST OF TABLES

Table	Page
<b>Table 2.1</b> Soil behavior types in Robertson et al. (1986)	4
<b>Table 2.2</b> Soil behavior types in Robertson (1990)	5
<b>Table 2.3</b> Soil behavior type according to the soil classification index $I_c$ (after Jefferies and Davis, 1991)	6
<b>Table 2.4</b> Sand classification according to density	9
<b>Table 2.5</b> Soil group classification for the modified Tumay (1985) chart	18
<b>Table 2.6</b> Soil group classification for the modified Robertson (1990) chart	18
<b>Table 3.1</b> Auto-correlation function expressions and corresponding scale of fluctuation $SF$	24
<b>Table 4.1</b> Maximum and minimum values of $SF$	30
<b>Table 4.2</b> Maximum and minimum values of COV of cone resistance	30
<b>Table 4.3</b> Minimum and maximum $SF$ , COV and SNC values	30
<b>Table 4.4</b> Minimum and maximum values of DDF and NDLPUL for the modified Tumay (1985) and Robertson (1990) charts	31
<b>Table 4.5</b> Minimum and maximum values of DDF and NDLPUL	32
<b>Table 4.6</b> OV results for soil profile having sand at top followed by clay layers below	32
<b>Table 5.1</b> INDOT CPT data used in the analyses	36
<b>Table 5.2</b> Data collected using Purdue's CPT truck	36
<b>Table 5.3</b> Range of values for the $VVI$ and the various indices making up the $VVI$ for 5 m soil profile length generated using the modified Tumay (1985) chart for INDOT database	46
<b>Table 5.4</b> Results of variability assessment for 5 m soil profile length	55
<b>Table 5.5</b> $SVR$ results for 3 m soil profile length	61
<b>Table 5.6</b> $SVR$ results for 4 m soil profile length	61
<b>Table 5.7</b> $SVR$ results for 5 m soil profile length	62
<b>Table 5.8</b> Maximum and minimum variability values for 5 m soil profile length using the modified Tumay (1985) chart	62
<b>Table 6.1</b> $ER$ (%) obtained from boring 1 at Koleen site	73
<b>Table 6.2</b> $ER$ (%) obtained from SPT 3 at Koleen site	73
<b>Table 6.3</b> $ER$ (%) obtained from SPT 4 at Koleen site	73

## LIST OF FIGURES

Figure	Page
<b>Figure 2.1</b> Begemann (1965) chart	3
<b>Figure 2.2</b> Sanglerat et al. (1974) chart	3
<b>Figure 2.3</b> Schmertmann (1978) chart	3
<b>Figure 2.4</b> Douglas and Olsen (1981) chart	3
<b>Figure 2.5</b> Tumay (1985) chart	4
<b>Figure 2.6</b> Robertson et al. (1986) charts: (a) corrected cone resistance vs. friction ratio chart and (b) corrected cone resistance vs. pore pressure ratio chart	4
<b>Figure 2.7</b> Robertson (1990) charts: (a) normalized cone resistance vs. normalized friction ratio chart and (b) normalized cone resistance vs. pore pressure ratio chart	5
<b>Figure 2.8</b> Senneset et al. (1989) chart	6
<b>Figure 2.9</b> Larson and Mulabdic (1991) chart	6
<b>Figure 2.10</b> Jefferies and Davis (1991) chart	6
<b>Figure 2.11</b> Olsen and Mitchell (1995) chart	7
<b>Figure 2.12</b> Eslami and Fellenius (1997) chart	7
<b>Figure 2.13</b> Ramsey (2002) chart 1	7
<b>Figure 2.14</b> Ramsey (2002) chart 2	8
<b>Figure 2.15</b> Schneider et al. (2008) chart 1	8
<b>Figure 2.16</b> Schneider et al. (2008) chart 2	8
<b>Figure 2.17</b> Schneider et al. (2008) chart 3	8
<b>Figure 2.18</b> Modified Tumay (1985) chart	9
<b>Figure 2.19</b> Modified Robertson (1990) chart	9
<b>Figure 2.20</b> Soil profile generation flowchart – part 1	10
<b>Figure 2.21</b> Soil profile generation flowchart – part 2	10
<b>Figure 2.22</b> Initial soil profile generation for modified Tumay (1985) chart	11
<b>Figure 2.23</b> Thin layer generated by CPT data falling close to boundary line between regions of “clean sand or silty sand” and “clayey sand or silt”	12
<b>Figure 2.24</b> Modified Tumay (1985) chart with examples of CPT data falling near boundary lines	12
<b>Figure 2.25</b> Modified Tumay (1985) chart with $\pm 15\%$ $q_c$ bands	13
<b>Figure 2.26</b> Examples of assignment of secondary soil type(s)	13
<b>Figure 2.27</b> Example of comparison of the average $q_c$ values of thin and thick layers	14
<b>Figure 2.28</b> Assignment of secondary soil type to thin layers	14
<b>Figure 2.29</b> Soil profile checked for SBT chart band approach	15
<b>Figure 2.30</b> Consolidation of a thin layer based on comparison of the average $q_c$ values of the thin and adjacent layers and layer thickness	15
<b>Figure 2.31</b> Thin layers occurring in sequence in a soil profile	16
<b>Figure 2.32</b> Illustration of the proximity ratio	16
<b>Figure 2.33</b> Illustration of a case in which the secondary soil type of a thin layer under consideration matches the primary soil type of an adjacent thin layer and vice-versa	17
<b>Figure 2.34</b> Soil profile checked for consecutive layers of the same soil type	17
<b>Figure 2.35</b> Soil profile checked for the soil group approach	18
<b>Figure 2.36</b> Consolidation of thin layers with adjacent layers of the same soil group	19

<b>Figure 2.37</b>	Soil profile checked for remaining thin layers using the average $q_c$ approach	19
<b>Figure 3.1</b>	Separation distance used in calculation of correlation function	21
<b>Figure 3.2</b>	Calculation of $SF$ from variance function times window length	23
<b>Figure 3.3</b>	Calculation of $SF$ from variance function	23
<b>Figure 3.4</b>	Integration of auto-correlation function for $q_c$	23
<b>Figure 3.5</b>	Example of fitting of generic auto-correlation model: (a) cone resistance profile and (b) correlation coefficient vs. separation distance	24
<b>Figure 3.6</b>	Vanmarcke's simplified method of calculating $SF$	25
<b>Figure 4.1</b>	Soil variability analysis	25
<b>Figure 4.2</b>	Vertical variability index calculation	26
<b>Figure 4.3</b>	Calculation of site vertical variability index	27
<b>Figure 4.4</b>	Calculation of $VVI$	27
<b>Figure 4.5</b>	Calculation of $(VVI)_{IL}$	28
<b>Figure 4.6</b>	Detrending of $q_c$ data	28
<b>Figure 4.7</b>	Idealized plots of $q_c$ vs. depth: (a) low $SF$ with low COV and (b) high $SF$ with high COV	29
<b>Figure 4.8</b>	Flow diagram showing calculation of DDF	31
<b>Figure 4.9</b>	Idealized soil profile for calculation of $[COV(q_c)]_{max}$	32
<b>Figure 4.10</b>	COV of $q_c$ versus length of soil profile	32
<b>Figure 4.11</b>	$HVI$ calculation	33
<b>Figure 4.12</b>	Maximum average $q_c$ difference versus length of soil profile	33
<b>Figure 4.13</b>	$f_2(s)$ function of spacing between soundings	34
<b>Figure 4.14</b>	Optimal spacing between soundings	34
<b>Figure 4.15</b>	Calculation of SVR using $VVI$ and $HVI$	35
<b>Figure 5.1</b>	Vertical variability results for sounding #TB 3 of site 0100521 (LaPorte) for 5 m length of the soil profile using the modified Tumay (1985) chart	37
<b>Figure 5.2</b>	Vertical variability results for sounding #TB 3 of site 0100521 (LaPorte) for 5 m length of the soil profile using the modified Robertson (1990) chart	37
<b>Figure 5.3</b>	Soil profile for Koleen site interpreted from: (a) SPT 01 and (b) CPT 01	38
<b>Figure 5.4</b>	Soil profiles generated using modified Tumay (1985) and modified Robertson (1990) charts for CPT 1 from Koleen site	39
<b>Figure 5.5</b>	Soil profile for Romey site interpreted from: (a) SPT 01 and (b) CPT 01	40
<b>Figure 5.6</b>	Soil profiles generated using modified Tumay (1985) and Robertson (1990) charts for CPT 1 from Romney site	41
<b>Figure 5.7</b>	Soil profile for Flora site interpreted from: (a) SPT 01 and (b) CPT 01	42
<b>Figure 5.8</b>	Soil profiles generated using modified Tumay (1985) and Robertson (1990) charts for CPT 1 from Flora site	43
<b>Figure 5.9</b>	Soil profile for Frankfort site interpreted from: (a) SPT 03 and (b) CPT 02	44
<b>Figure 5.10</b>	Soil profiles generated using modified Tumay (1985) and Robertson (1990) charts for CPT 02 from Frankfort site	45
<b>Figure 5.11</b>	Local averaging for: (a) separation distance=1 and (b) separation distance=2	45
<b>Figure 5.12</b>	Number of crossing equal to 1 for $f_s$ plot for layer 4 of INDOT DES 9700260 (Fort Wayne) CPT sounding #7	46
<b>Figure 5.13</b>	Global and local fluctuation of a soil property with depth	46

<b>Figure 5.14</b> Vertical variability indices for sounding #CPT-9-CG-9 of site 1173689 (LaPorte) for a 5 m soil profile length using the modified Tumay (1985) chart	47
<b>Figure 5.15</b> Cone resistance profile and intra-layer variability indices for sounding #CPT-9-CG-9 of site 1173689 (LaPorte) for a 5 m soil profile length using the modified Tumay (1985) chart	47
<b>Figure 5.16</b> Vertical variability indices for sounding #4 of the Flora site for a 5 m soil profile length using the modified Tumay (1985) chart	48
<b>Figure 5.17</b> Cone resistance profile and intra-layer variability indices for sounding #4 of the Flora site for a 5 m soil profile length using the modified Tumay (1985) chart	48
<b>Figure 5.18</b> Zoomed $q_c$ profile for sounding #4 of the Flora site for a 5 m soil profile length using the modified Tumay (1985)	49
<b>Figure 5.19</b> Soil profile of sounding CPT-2 of site 9700260 (Fort Wayne) for a 5 m soil profile length generated using the modified Tumay (1985) chart and plotted in relevant scale	49
<b>Figure 5.20</b> Normalized error of $q_c$ vs. depth of sounding CPT-2 of site 9700260 (Fort Wayne) for a 5 m soil profile length generated using the modified Tumay (1985) chart	50
<b>Figure 5.21</b> Soil profile for sounding TB – 11 of site 0600337 (Greenfield) for a 5 m soil profile length generated using the modified Tumay (1985) chart	50
<b>Figure 5.22</b> Normalized error of $q_c$ vs. depth for sounding TB – 11 of site 0600337 (Greenfield) for a 5 m soil profile length generated using the modified Tumay (1985) chart	50
<b>Figure 5.23</b> Soil profile for sounding CPT-11-CG-11 of site 1173689 (LaPorte) for a 5 m soil profile length generated using the modified Tumay (1985) chart	51
<b>Figure 5.24</b> Normalized error of $q_c$ vs. depth of sounding CPT-11-CG-11 of site 1173689 (LaPorte) for a 5 m soil profile length	51
<b>Figure 5.25</b> Soil profile of sounding RW-13C of site 0600337 (Greenfield) for a 5 m soil profile length generated using the modified Tumay (1985) chart and plotted in relevant scale	52
<b>Figure 5.26</b> Normalized error of $q_c$ vs. depth of sounding RW-13C of site 0600337 (Greenfield) for a 5 m soil profile length generated using the modified Tumay (1985) chart	52
<b>Figure 5.27</b> COV of cone resistance versus log variability index for a 5 m length soil profile using the modified Tumay (1985) chart	52
<b>Figure 5.28</b> Soil profile of sounding 2 of site 9700260 (Fort Wayne) for a 5 m soil profile length generated using the modified Tumay (1985) chart and plotted in relevant scale	53
<b>Figure 5.29</b> Normalized error of $q_c$ vs. depth of sounding 2 of site 9700260 (Fort Wayne) for 5 m soil profile length generated using the modified Tumay (1985) chart	53
<b>Figure 5.30</b> Soil profile of sounding RW-13C of site 0600337 (Greenfield) for a 5 m soil profile length generated using the modified Tumay (1985) chart	54
<b>Figure 5.31</b> Normalized error of $q_c$ vs. depth of sounding RW-13C of site 0600337 (Greenfield) for a 5 m soil profile length generated using the modified Tumay (1985) chart	55
<b>Figure 5.32</b> Vertical variability for sounding #2 of McCormick site for a 5 m soil profile length using the modified Tumay (1985) chart	56
<b>Figure 5.33</b> Vertical variability of sounding #3 of McCormick site for a 5 m soil profile length using the modified Tumay (1985) chart	56
<b>Figure 5.34</b> Vertical variability of sounding #4 of McCormick site for a 5 m soil profile length using the modified Tumay (1985) chart	57
<b>Figure 5.35</b> Vertical variability of sounding #5 of McCormick site for a 5 m soil profile length using the modified Tumay (1985) chart	57
<b>Figure 5.36</b> Vertical variability of sounding #6 of McCormick site for a 5 m soil profile length using the modified Tumay (1985) chart	58
<b>Figure 5.37</b> Side-by-side comparison of $q_c$ profiles of CPT 1 through CPT 6 for Koleen site	58
<b>Figure 5.38</b> Vertical variability of sounding CPT-2 of site 0100331 (LaPorte) for a 5 m soil profile length using the modified Tumay (1985) chart	59

<b>Figure 5.39</b> Vertical variability of sounding TB-1 of site 0100331 (LaPorte) for a 5 m soil profile length using the modified Tumay (1985) chart	59
<b>Figure 5.40</b> Vertical variability of sounding TB-1a of site 0100331 (LaPorte) for a 5 m soil profile length using the modified Tumay (1985) chart	60
<b>Figure 5.41</b> Side-by-side comparison of $q_c$ profiles for soundings CPT 2, TB-1 and TB-1a of site 0100331 (LaPorte)	60
<b>Figure 5.42</b> Comparison between $VVI$ s obtained using the modified Tumay (1985) and modified Robertson (1990) charts for 3 m soil profile length	62
<b>Figure 5.43</b> Comparison between $VVI$ s obtained using the modified Tumay (1985) and modified Robertson (1990) charts for 4 m soil profile length	62
<b>Figure 5.44</b> Comparison between $VVI$ s obtained using the modified Tumay (1985) and modified Robertson (1990) charts for 5 m soil profile length	62
<b>Figure 5.45</b> Site $VVI$ for 3 m soil profile length using modified Tumay (1985) chart	63
<b>Figure 5.46</b> Site $HVI$ for 3 m soil profile length using modified Tumay (1985) chart	64
<b>Figure 5.47</b> Site $SVR$ for 3 m soil profile length using modified Tumay (1985) chart	65
<b>Figure 5.48</b> Site $VVI$ for 3 m soil profile length using the modified Robertson (1990) chart	66
<b>Figure 5.49</b> Site $SVR$ for 3 m soil profile length using modified Robertson (1990) chart	67
<b>Figure 6.1</b> A simple diagram of CPT DAQ system	68
<b>Figure 6.2</b> Purdue CPT truck	68
<b>Figure 6.3</b> Analog cone	68
<b>Figure 6.4</b> Encoder (mounted)	69
<b>Figure 6.5</b> DAQ box	69
<b>Figure 6.6</b> CPT DAQ software interface	69
<b>Figure 6.7</b> Analyze data form	70
<b>Figure 6.8</b> Input data to analyze	70
<b>Figure 6.9</b> Variability assessment	70
<b>Figure 6.10</b> Analysis properties	70
<b>Figure 6.11</b> SPT instrumented rod	71
<b>Figure 6.12</b> Accelerometer mounted on SPT rod	71
<b>Figure 6.13</b> Using instrumented SPT rod in field	72
<b>Figure 6.14</b> SPT DAQS interface	72
<b>Figure A.1</b> <i>In situ</i> test profiles: (a) SPT profile ( $N_{60}$ values and soil boring description) for SPT 02 and (b) CPT profile (cone resistance, sleeve resistance, friction ratio, variability indices and soil profiles generated using modified Tumay (1985) chart and modified Robertson (1990) chart) for CPT 02 at Koleen site	76
<b>Figure A.2</b> Soil profiles generated using modified Tumay (1985) chart and modified Robertson (1990) chart for CPT 2 from Koleen site	77
<b>Figure A.3</b> <i>In situ</i> test profiles: (a) SPT profile ( $N_{60}$ values and soil boring description) for SPT 05 and (b) CPT profile (cone resistance, sleeve resistance, friction ratio, variability indices and soil profiles generated using modified Tumay (1985) chart and modified Robertson (1990) chart) for CPT 03 at Koleen site	78
<b>Figure A.4</b> Soil profiles generated using modified Tumay (1985) chart and modified Robertson (1990) chart for CPT 3 from Koleen site	79
<b>Figure A.5</b> <i>In situ</i> test profiles: (a) SPT profile ( $N_{60}$ values and soil boring description) for SPT 03 and (b) CPT profile (cone resistance, sleeve resistance, friction ratio, variability indices and soil profiles generated using modified Tumay (1985) chart and modified Robertson (1990) chart) for CPT 04 at Koleen site	80

<b>Figure A.6</b>	Soil profiles generated using modified Tumay (1985) chart and modified Robertson (1990) chart for CPT 4 from Koleen site	81
<b>Figure A.7</b>	<i>In situ</i> test profiles: (a) SPT profile ( $N_{60}$ values and soil boring description) for SPT 02 and (b) CPT profile (cone resistance, sleeve resistance, friction ratio, variability indices and soil profiles generated using modified Tumay (1985) chart and modified Robertson (1990) chart) for CPT 02 at Romney site	82
<b>Figure A.8</b>	Soil profiles generated using modified Tumay (1985) chart and modified Robertson (1990) chart for CPT 2 from Romney site	83
<b>Figure A.9</b>	<i>In situ</i> test profiles: (a) SPT profile ( $N_{60}$ values and soil boring description) for SPT 03 and (b) CPT profile (cone resistance, sleeve resistance, friction ratio, variability indices and soil profiles generated using modified Tumay (1985) chart and modified Robertson (1990) chart) for CPT 03 at Romney site	84
<b>Figure A.10</b>	Soil profiles generated using modified Tumay (1985) chart and modified Robertson (1990) chart for CPT 3 from Romney site	85
<b>Figure A.11</b>	<i>In situ</i> test profiles: (a) SPT profile ( $N_{60}$ values and soil boring description) for SPT 04 and (b) CPT profile (cone resistance, sleeve resistance, friction ratio, variability indices and soil profiles generated using modified Tumay (1985) chart and modified Robertson (1990) chart) for CPT04 at Romney site	86
<b>Figure A.12</b>	Soil profiles generated using modified Tumay (1985) chart and modified Robertson (1990) chart for CPT 4 from Romney site	87
<b>Figure A.13</b>	<i>In situ</i> test profiles: (a) SPT profile ( $N_{60}$ values and soil boring description) for SPT 05 and (b) CPT profile (cone resistance, sleeve resistance, friction ratio, variability indices and soil profiles generated using modified Tumay (1985) chart and modified Robertson (1990) chart) for CPT 05 at Romney site	88
<b>Figure A.14</b>	Soil profiles generated using modified Tumay (1985) chart and modified Robertson (1990) for CPT 5 from Romney site	89
<b>Figure A.15</b>	<i>In situ</i> test profiles: (a) SPT profile ( $N_{60}$ values and soil boring description) for SPT 06 and (b) CPT profile (cone resistance, sleeve resistance, friction ratio, variability indices and soil profiles generated using modified Tumay (1985) chart and modified Robertson (1990) chart) for CPT 06 at Romney site	90
<b>Figure A.16</b>	Soil profiles generated using modified Tumay (1985) chart and modified Robertson (1990) chart for CPT 6 from Romney site	91
<b>Figure A.17</b>	<i>In situ</i> test profiles: (a) SPT profile ( $N_{60}$ values and soil boring description) for SPT 02 and (b) CPT profile (cone resistance, sleeve resistance, friction ratio, variability indices and soil profiles generated using modified Tumay (1985) chart and modified Robertson (1990) chart) for CPT 02 at Flora site	92
<b>Figure A.18</b>	Soil profiles generated using modified Tumay (1985) chart and modified Robertson (1990) chart for CPT 2 from Flora site	93
<b>Figure A.19</b>	<i>In situ</i> test profiles: (a) SPT profile ( $N_{60}$ values and soil boring description) for SPT 03 and (b) CPT profile (cone resistance, sleeve resistance, friction ratio, variability indices and soil profiles generated using modified Tumay (1985) chart and modified Robertson (1990) chart) for CPT 03 at Flora site	94
<b>Figure A.20</b>	Soil profiles generated using modified Tumay (1985) chart and modified Robertson (1990) chart for CPT 3 from Flora site	95
<b>Figure A.21</b>	<i>In situ</i> test profiles: (a) SPT profile ( $N_{60}$ values and soil boring description) for SPT 04 and (b) CPT profile (cone resistance, sleeve resistance, friction ratio, variability indices and soil profiles generated using modified Tumay (1985) chart and modified Robertson (1990) chart) for CPT 04 at Flora site	96
<b>Figure A.22</b>	Soil profiles generated using modified Tumay (1985) chart and modified Robertson (1990) chart for CPT 4 from Flora site	97

<b>Figure A.23</b> <i>In situ</i> test profiles: (a) SPT profile ( $N_{60}$ values and soil boring description) for SPT 06 and (b) CPT profile (cone resistance, sleeve resistance, friction ratio, variability indices and soil profiles generated using modified Tumay (1985) chart and modified Robertson (1990) chart) for CPT 05 at Frank Fort site	98
<b>Figure A.24</b> Soil profiles generated using modified Tumay (1985) chart and modified Robertson (1990) chart for CPT 5 from Frank Fort site	99
<b>Figure A.25</b> <i>In situ</i> test profiles: (a) SPT profile ( $N_{60}$ values and soil boring description) for SPT 07 and (b) CPT profile (cone resistance, sleeve resistance, friction ratio, variability indices and soil profiles generated using modified Tumay (1985) chart and modified Robertson (1990) chart) for CPT06 at Frank Fort site	100
<b>Figure A.26</b> Soil profiles generated using modified Tumay (1985) chart and modified Robertson (1990) chart for CPT 6 from Frank Fort site	101
<b>Figure A.27</b> <i>In situ</i> test profiles: (a) SPT profile ( $N_{60}$ values and soil boring description) for SPT 08 and (b) CPT profile (cone resistance, sleeve resistance, friction ratio, variability indices and soil profiles generated using modified Tumay (1985) chart and modified Robertson (1990) chart) for CPT 07 at Frank Fort site	102
<b>Figure A.28</b> Soil profiles generated using modified Tumay (1985) chart and modified Robertson (1990) chart for CPT 7 from Frank Fort site	103
<b>Figure B.1</b> Site <i>VVI</i> for 3 m soil profile length using modified Tumay (1985) chart	104
<b>Figure B.2</b> Site <i>HVI</i> for 3 m soil profile length	105
<b>Figure B.3</b> <i>SVR</i> for 3 m soil profile length using modified Tumay (1985) chart	106
<b>Figure B.4</b> Site <i>VVI</i> for 3 m soil profile length using modified Robertson (1990) chart	107
<b>Figure B.5</b> <i>SVR</i> for 3 m soil profile length using modified Robertson (1990) chart	108
<b>Figure B.6</b> Site <i>VVI</i> for 4 m soil profile length using modified Tumay (1985) chart	109
<b>Figure B.7</b> Site <i>HVI</i> for 4 m soil profile length	110
<b>Figure B.8</b> <i>SVR</i> for 4 m soil profile length using modified Tumay (1985) chart	111
<b>Figure B.9</b> Site <i>VVI</i> for 4 m soil profile length using modified Robertson (1990) chart	112
<b>Figure B.10</b> <i>SVR</i> for 4 m soil profile length using modified Robertson (1990) chart	113
<b>Figure B.11</b> Site <i>VVI</i> for 5 m soil profile length using modified Tumay (1985) chart	114
<b>Figure B.12</b> Site <i>HVI</i> for 5 m soil profile length	115
<b>Figure B.13</b> <i>SVR</i> for 5 m soil profile length using modified Tumay (1985) chart	116
<b>Figure B.14</b> Site <i>VVI</i> for 5 m soil profile length using modified Robertson (1990) chart	117
<b>Figure B.15</b> <i>SVR</i> for 5 m soil profile length using modified Robertson (1990) chart	118



## 1. INTRODUCTION

### 1.1 Introduction

Site investigation is an important component of every construction project. The main goals of a geotechnical site investigation are (1) to define the soil profile and (2) to estimate the geotechnical properties of the different soils of the soil profile. The soil properties are derived either from *in situ* tests or laboratory tests. However, in either case, the number of *in situ* or laboratory tests is constrained by project budget and time. Since often a limited number of tests is performed, there is uncertainty associated with the soil properties estimated for a site. This uncertainty is an inevitable part of every geotechnical site investigation, raising the question as to how accurately soil properties derived from laboratory or *in situ* tests represent the soil properties of an entire site. Although this uncertainty cannot be eliminated, by studying variability of soil test data, an assessment can be made of the reliability of the property values estimated for use in geotechnical engineering design. This variability assessment for a site may lead to lower or higher resistance factors for use in Load and Resistance Factor Design (LRFD).

In order to address variability of soil properties, researchers have taken advantage of knowledge from statistics and have applied it to quantify spatial variability. Researchers have discovered that soil properties are most often spatially correlated and that correlation becomes increasingly weak with increasing distance between the points considered. A simple mean-value approach, applied to a set of measurements to arrive at a representative soil property value to be used in design, ignores this spatial correlation of soil properties. Therefore, trend or auto-covariance analysis have also been used to study variability of soil properties.

Over the years, the cone penetration test (CPT) has gained acceptance as a fast, reliable and economical tool for *in situ* testing. During a CPT, three main parameters – cone resistance  $q_c$ , sleeve resistance  $f_s$ , and pore pressure  $u$  – are recorded. Typically, soil samples are not collected at the exact location where a CPT sounding is performed. Therefore, soil profiles are inferred from the CPT test data using soil behavior type (SBT) charts. The CPT provides for the entire sounding depth nearly continuous test data, which can be used to estimate soil properties of interest or foundation capacity directly.

Researchers have studied the spatial variability of CPT data (e.g.,  $q_c$  and  $f_s$ ) using different measures of variability (e.g., coefficient of variation and scale of fluctuation). The results of a variability study of CPT parameters are helpful during the site investigation and engineering design phases of a project. During the site investigation phase, if the calculated variability of the CPT parameters is high based on a number of CPTs, additional CPTs can be performed to increase the reliability of the estimated soil properties to be used in design. On the other hand, if the calculated variability of the CPT parameters is low, it may be possible to reduce the number of CPTs from what had been originally decided during the site investigation and planning phases of a project. This approach can save time and costs for a project. However, this option of adjusting the number of CPTs to be performed at a given site is only possible if the

variability of CPT parameters can be calculated in real time in the field.

Whenever an assessment of the variability of the CPT parameters is made, safety factors or resistance factors to be used in design can be adjusted to reflect the outcome of the variability assessment for the project site. For sites with high variability, higher safety factor values or lower soil resistance factors could be used to increase the reliability of the foundation design. Similarly, for sites with low variability, lower safety factor values or higher soil resistance factors could be used to optimize the construction cost. Therefore, an assessment of site variability can directly benefit a project by increasing the reliability of the foundation design and optimizing the associated cost.

According to AASHTO (2007) and Paikowsky (2004), sites can be classified into three categories: low-, average- and high-variability sites. Paikowsky (2004) stated that site variability may be determined based on engineering judgment or approximately assessed from the average values of soil parameters obtained (for example  $q_c$ ) for each bearing layer at a sounding location. Based on the COV (defined as the percentage ratio of the standard deviation to the mean value of the parameter considered) of the soil parameters used for strength analysis, Paikowsky (2004) suggested the categorization of site variability as low ( $COV < 25\%$ ), medium ( $25\% \leq COV \leq 40\%$ ) or high ( $COV \geq 40\%$ ). This classification of sites based on variability of parameters used for strength analysis is attractive because of its multiple potential uses. Knowing the variability of a site, lower or higher resistance factors can be used in LRFD design. Moreover, guidance can be sought from the variability classification of a site regarding the optimum number of test soundings that need to be performed in a project site.

Once CPT data are collected for a large number of different sites, a variability assessment could be performed to provide an indication of the expected variability at different regions of a state and provide guidance regarding the number of CPTs to be performed to obtain reliable site investigation data. Despite the obvious advantages of site variability assessment, currently, there is no robust methodology or framework available that allows quantification of site variability.

### 1.2 Problem Statement

Soil property values for use in geotechnical design are often estimated from a limited number of *in situ* or laboratory tests. The uncertainty involved in estimating soil properties from a limited number of tests can be addressed by quantifying the variability within individual soundings and of the collection of soundings performed at a site. It has been proposed that factors of safety or resistance factors used in design be linked to site variability. In order to develop a comprehensive methodology for site variability assessment, consideration should be given to inter- and intra-layer variability in a soil profile, and both vertical and horizontal variability.

Knowledge of spatial statistics was applied in the development of a rational methodology to assess site variability using CPT data. Subsurface soil profiles are generated from

CPT data using soil behavior type charts. By taking into account the variability of CPT data and occurrence of layers of different soil types in a soil profile, the vertical variability of the soil profile is calculated. A site vertical variability index is calculated as the average of the vertical variability indices of all the CPTs available at a given site. The horizontal variability of the site is assessed by considering for every pair of CPTs in a site, the cross-correlation of cone resistance values, the cone resistance trend differences and the spacing between soundings. A site variability rating system, integrating the vertical and horizontal site variability, was developed to assess the overall site variability. Using the CPT database of the Indiana Department of Transportation (INDOT) and Purdue's CPT database, site variability maps were constructed for different soil profile lengths. An optimal sounding spacing calculation methodology was also developed to make the site investigation process more efficient, cost-effective and reliable.

### 1.3 Research Objectives

This research project has the following main objectives:

1. Development of a data acquisition and analysis system for the CPT;
2. Development of a practical methodology for assessing site variability;
3. Construction of site variability maps for Indiana based on currently available CPT data.

### 1.4 Organization of the Report

This report has seven chapters, organized in the following manner:

- *Chapter 1, Introduction*, provides an introduction to the research work.
- *Chapter 2, Soil Profile Generation from CPT Data*, describes the procedure used to obtain a soil profile using soil behavior type charts.
- *Chapter 3, Fundamental Concepts of Probability and Random Field Theory*, provides a brief review of the statistical tools used to quantify spatial variability.
- *Chapter 4, Results of Site Variability Index Calculations*, explains the methodology developed to calculate vertical variability, horizontal variability and site variability. It also describes the methodology developed to determine optimal CPT spacing in real time during the site investigation phase of a project.
- *Chapter 5, Site Variability Calculations for Indiana Sites*, presents the results of site variability calculations done for the CPT data available for the state of Indiana.
- *Chapter 6, Development of Data Acquisition Systems*, provides details of the developed data acquisition system.
- *Chapter 7, Conclusions and Recommendations*, provides the lessons learned from this research.

## 2. SOIL PROFILE GENERATION FROM CPT DATA

### 2.1 Introduction

The cone penetration test consists of pushing a cone of standard geometry (diameter=35.7mm and apex angle=60°)

into the ground at a standard rate of 20 mm/s while measuring the resistance offered by the soil to penetration (ASTM D5778-12, 2012). Cone resistance  $q_c$ , sleeve resistance  $f_s$  and pore pressure  $u$  are measured in a nearly continuous manner (sampling rate may vary depending on local practice) as the cone penetrates into the ground. The friction ratio  $FR$ , which is defined as the ratio in percent of  $f_s$  to  $q_c$ , together with cone resistance gives an indication of the soil behavior type expected for each layer of the soil profile. A soil profile can be obtained from Standard Penetration Tests (SPT) by collecting samples at the same depth as the SPT tests are performed or from Cone Penetration Tests (CPT) using soil behavior type charts and soil profile interpretation programs commonly available with most CPT rigs (special samplers can also be used with the CPT to collect soil samples at the same time a CPT is performed). A site investigation using the cone penetration test consists of performing the CPT soundings at the project site, developing detailed soil profiles using soil behavior type (SBT) charts, and then selectively sampling and testing soils at different depths to provide additional information regarding ambiguous soil classifications (Robertson & Campanella, 1983).

In this chapter, we review the existing soil behavior type charts available in the literature and a procedure that can be followed to generate a soil profile from CPT data (i.e.,  $q_c, f_s$  and  $FR$ ) and SBT charts. The modifications made to two existing SBT charts, (Robertson, 1990; Tumay, 1985), used in this research to generate soil profiles are also explained.

### 2.2 Review of Existing Soil Behavior Type Charts

Many soil behavior type (SBT) classification charts have been proposed over the years. Some of the early SBT charts are those of Begemann (1965), Sanglerat, Nhim, Sejourne, and Andina (1974), Schmertmann (1978), Douglas and Olsen (1981), Tumay (1985), Robertson, Campanella, Gillespie, and Rice (1986), Senneset, Sandyen, and Janbu (1989), Robertson (1990), Larsson and Mulabdic (1991), and Jefferies and Davis (1991), while some of the more recently proposed SBT charts include Ramsey (2002) and Schneider, Randolph, Mayne, and Ramsey (2008).

Generation of soil profiles from SBT charts is subject to uncertainty. Robertson (2010) gave examples where the soil behavior types obtained from SBT charts were not in agreement with the traditional soil classifications based on grain-size distribution and soil plasticity (e.g., USCS soil classification). According to Robertson (2010), different soil classifications are likely to result, particularly in the mixed soil regions (i.e., sand mixtures and silt mixtures) of the SBT charts. We next discuss the various SBT charts available in the literature.

#### 2.2.1 Begemann (1965) Chart

Figure 2.1 shows one of the earliest SBT charts that was proposed by Begemann (1965) using a mechanical cone. In this SBT chart, a soil type is identified from the cone resistance and sleeve resistance measurements made during testing.

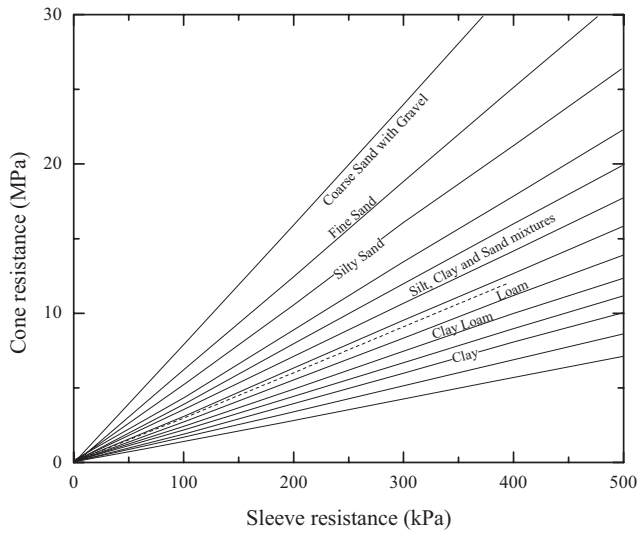


Figure 2.1 Begemann (1965) chart.

### 2.2.2 Sanglerat et al. (1974) Chart

Figure 2.2 shows the SBT chart proposed by Sanglerat et al. (1974). This chart has three primary regions (clay, sand and silt regions) with some overlap between them. This chart is incomplete in the sense that it fails to assign a soil type when the cone resistance and friction ratio of a soil fall outside of these three primary regions.

### 2.2.3 Schmertmann (1978) Chart

Figure 2.3 shows the SBT chart proposed by Schmertmann (1978). Schmertmann (1978) used the Begemann (1965) mechanical cone to perform *in situ* tests in Florida, U.S. According to Schmertmann (1978), it is difficult to apply SBT charts to geologic settings different from those

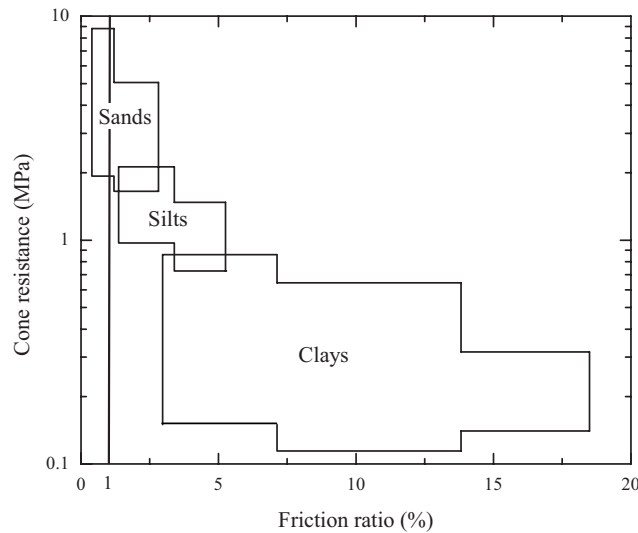


Figure 2.2 Sanglerat et al. (1974) chart.

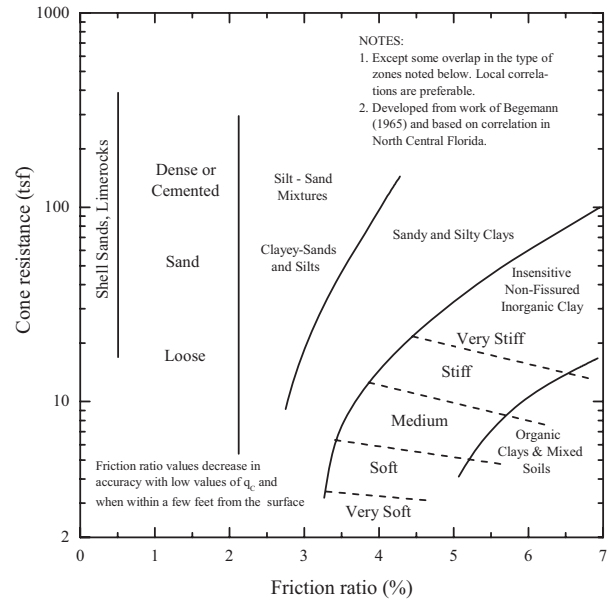


Figure 2.3 Schmertmann (1978) chart.

for which the charts have been developed. In the case of quick clays, Schmertmann (1978) measured friction ratio values as low as 0.1% using a Fugro cone tip. As we can see in Figure 2.3, the regions of this chart have incomplete boundaries.

### 2.2.4 Douglas and Olsen (1981) Chart

Figure 2.4 shows the SBT chart proposed by Douglas and Olsen (1981). In this chart, the soil behavior type is based on the unified soil classification system. These authors pointed out that SBT charts do not provide accurate predictions of soil type as would be obtained from a soil

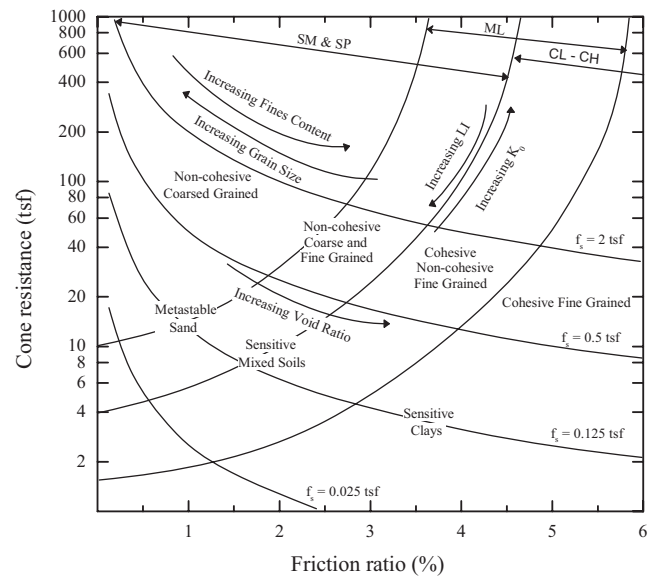


Figure 2.4 Douglas and Olsen (1981) chart.

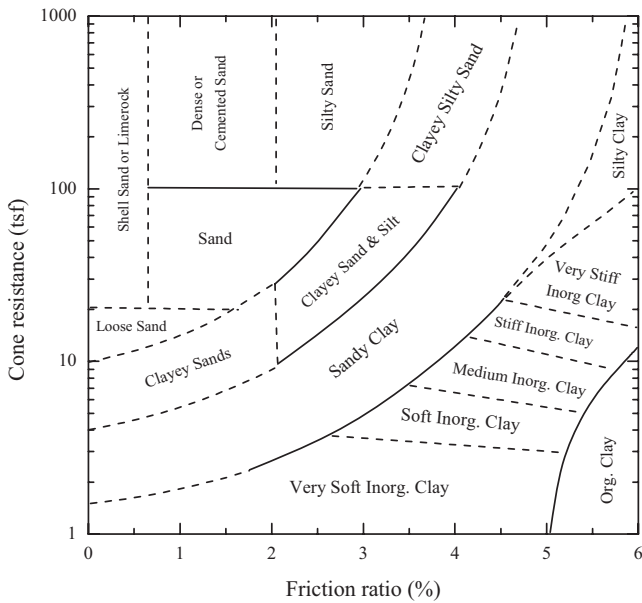


Figure 2.5 Tumay (1985) chart.

classification system but provide instead an indication of soil behavior type.

### 2.2.5 Tumay (1985) Chart

Figure 2.5 shows the SBT chart proposed by Tumay (1985). This SBT chart is a modification of the Schmertmann (1978) chart and is based on data from sites in Louisiana, California, Oklahoma, Utah, Arizona and Nevada, as reported by Douglas and Olsen (1981). This chart depicts the four distinct regions identified by Douglas and Olsen (1981) further subdivided into sub-regions that were sorted out using the Schmertmann (1978) soil classification chart (Tumay, 1985). In this chart, soils with very low friction ratio (near zero) are classified as very soft clay if the cone resistance is less than 0.2 MPa. This most likely represents Schmertmann's measurement of low friction ratios (as low as 0.1%) for quick clays, as mentioned by Schmertmann (1978).

### 2.2.6 Robertson et al. (1986) and Robertson (1990) Charts

Figure 2.6 (a) and (b) show the two SBT charts proposed by Robertson et al. (1986) which have 12 soil behavior types (these are indicated in the charts by zone numbers from 1 to 12). Table 2.1 provides a description of these 12 soil behavior types. The cone resistance  $q_t$  corrected for pore pressure appearing in these charts is defined as:

$$q_t = q_c + (1 - a)u \quad (2.1)$$

where  $u$  is the pore pressure measured at the cone shoulder,  $a$  is the net area ratio ( $a \approx d_{lc}^2/d_c^2$ , where  $d_{lc}$  is the diameter of

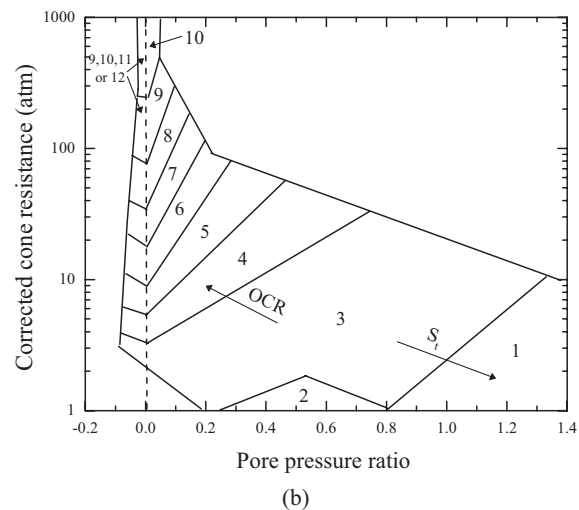
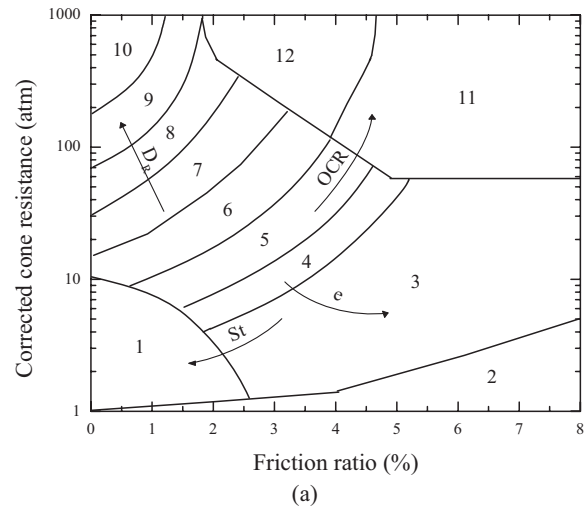


Figure 2.6 Robertson et al. (1986) charts: (a) corrected cone resistance vs. friction ratio chart and (b) corrected cone resistance vs. pore pressure ratio chart.

the load cell support and  $d_c$  is the cone diameter). One of the Robertson et al. (1986) SBT charts [appearing in Figure 2.6

TABLE 2.1  
Soil behavior types in Robertson et al. (1986)

Zone	Soil Behavior Type
1	Sensitive fine grained
2	Organic material
3	Clay
4	Silty clay to clay
5	Clayey silt to silty clay
6	Sandy silt to clayey silt
7	Silty sand to sandy silt
8	Sand to silty sand
9	Sand
10	Gravelly sand to sand
11	Very stiff fine grained
12	Sand to clayey sand

(b)] is based on the corrected cone resistance  $q_t$  and the pore pressure ratio  $Bq$ , obtained from:

$$Bq = \frac{u - u_0}{q_t - \sigma_v} \quad (2.2)$$

where  $u_0$  is the *in situ* pore pressure and  $\sigma_v$  is the total vertical stress.

Although the Robertson et al. (1986) charts are shown in terms of the corrected cone resistance  $q_t$ , it can be used as well with the cone resistance  $q_c$  when the difference between  $q_c$  and  $q_t$  is small; this is not the case in soft, fine-grained soils that generate high pore pressure values during cone penetration (Robertson, 2010).

Figure 2.7 (a) and (b) show the SBT charts proposed by Robertson (1990). Table 2.2 provides a description of the soils in the zones indicated by numbers 1 to 9 in these charts. These charts use normalized cone resistance and normalized friction ratio values. In order to do the normalization,

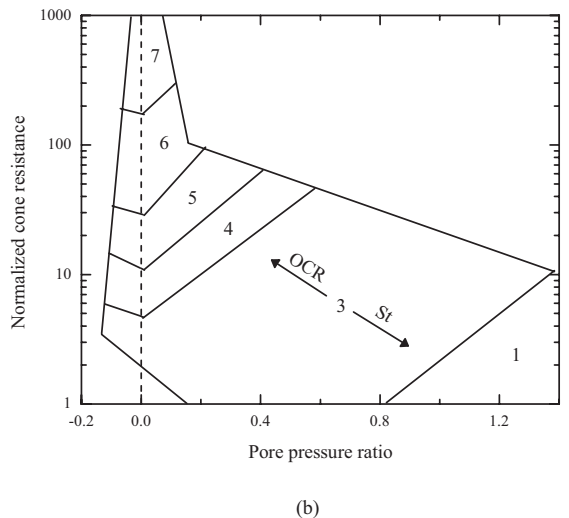
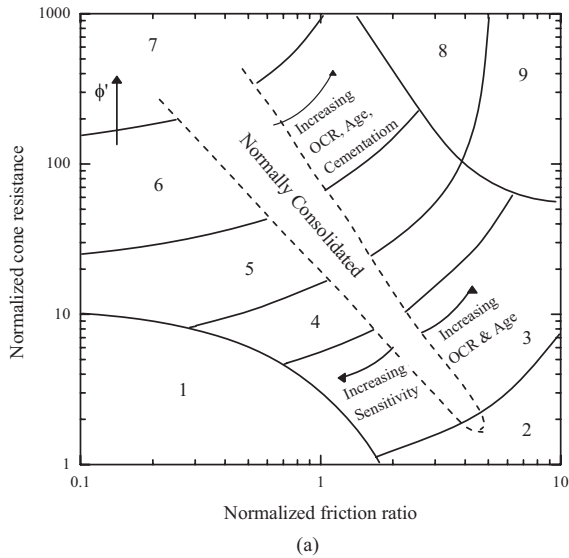


**Figure 2.7** Robertson (1990) charts: (a) normalized cone resistance vs. normalized friction ratio chart and (b) normalized cone resistance vs. pore pressure ratio chart.

**TABLE 2.2**  
**Soil behavior types in Robertson (1990)**

Zone	Soil Behavior Type
1	Sensitive, fine grained
2	Organic soils – peats
3	Clays – clay to silty clay
4	Silt mixtures – clayey silt to silty clay
5	Sand mixtures – silty sand to sandy silt
6	Sands – clean sand to silty sand
7	Gravelly sand to sand
8	Very stiff sand to clayey* sand
9	Very stiff, fine grained*

\* Heavily over-consolidated or cemented.

additional information on the unit weights of the soils found at the site and the ground water elevation are required. The normalized cone resistance  $q_{tn}$  and the normalized friction ratio  $FR_n$  are obtained from:

$$q_{tn} = \frac{q_{c,net}}{\sigma'_v} \quad (2.3)$$

and

$$FR_n = \frac{f_s}{q_{c,net}} \quad (2.4)$$

where the net cone resistance  $q_{c,net}$  is:

$$q_{c,net} = q_t - \sigma_v \quad (2.5)$$

Since the Robertson et al. (1986) SBT charts do not require normalization of CPT parameters, they can be used in real-time as CPT data is being collected in the field, while the Robertson (1990) charts can only be used after post-processing of the CPT data. Robertson et al. (1986) have suggested that, if a CPT extends beyond a depth of about 30 m below the ground surface, then the non-normalized charts should be used with caution. In general, the normalized charts by Robertson (1990) provide more reliable for identification of soil behavior type than the non-normalized charts by Robertson et al. (1986). However, when the *in situ* vertical effective stress is between 50 kPa and 150 kPa, there is often little difference between the resulting normalized and non-normalized soil behavior types (Robertson, 2010).

### 2.2.7 Senneset et al. (1989) Chart

Figure 2.8 shows the SBT chart proposed by Senneset et al. (1989). The maximum corrected cone resistance in this SBT chart is 16 MPa.

### 2.2.8 Larsson and Mulabdic (1991) Chart

Figure 2.9 shows the SBT chart proposed by Larsson and Mulabdic (1991). These authors considered CPT data for clayey soils with a maximum net cone resistance of 4 MPa.

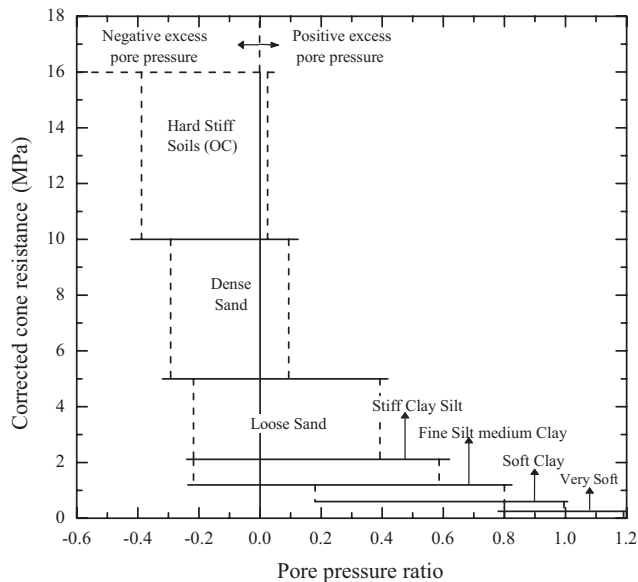


Figure 2.8 Senneset et al. (1989) chart.

2.2.9 Jefferies and Davis (1991) Chart

Figure 2.10 shows the SBT chart proposed by Jefferies and Davis (1991). In this chart, the boundaries between the SBT zones are approximated by concentric circles, with the radius of each circle representing a soil classification index  $I_c$  (Jefferies & Davis, 1991). Table 2.3 shows the soil classification system based on the index  $I_c$ .

2.2.10 Olsen and Mitchell (1995) Chart

Figure 2.11 shows the SBT chart proposed by Olsen and Mitchell (1995) based on the normalization of cone resistance proposed by (Olsen, 1994). The normalized cone resistance  $q_{c,1}$  is calculated as:

$$q_{c,1} = \left( \frac{p_A}{\sigma'_v} \right) q_c \quad (2.6)$$

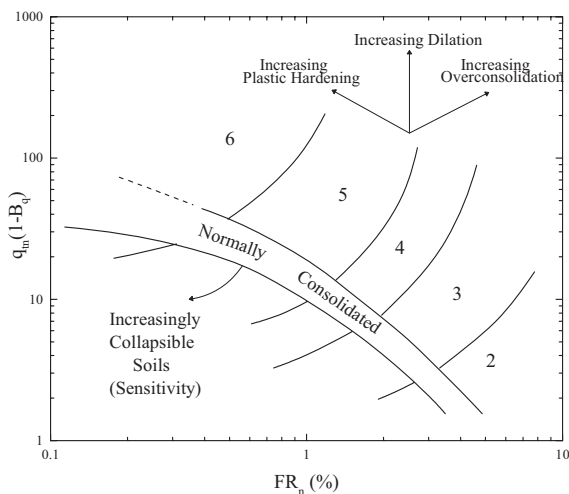


Figure 2.10 Jefferies and Davis (1991) chart.

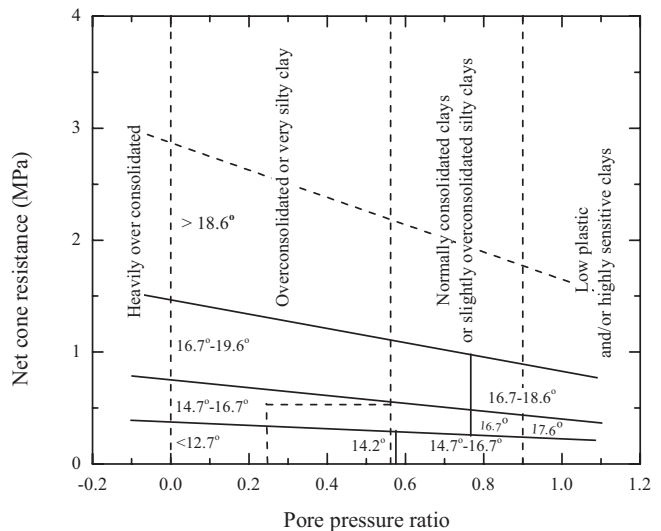


Figure 2.9 Larson and Mulabdic (1991) chart.

where  $p_A$  is a reference stress in the same units as the vertical effective stress  $\sigma'_v$ , and  $C$  is the cone tip normalization exponent.

2.2.11 Eslami and Fellenius (1997) chart

Figure 2.12 shows the SBT chart proposed by Eslami and Fellenius (1997). In this chart, the effective cone resistance is

TABLE 2.3 Soil behavior type according to the soil classification index  $I_c$  (after Jefferies & Davis, 1991)

$I_c$	Zone	Soil Classification
$I_c \leq 1.25$	7	Gravelly sands
$1.25 I_c \leq 1.9$	6	Sands – clean sand to silty sand
$1.90 I_c \leq 2.54$	5	Sand mixtures – silty sand to sandy silt
$2.54 I_c \leq 2.82$	4	Silt mixtures – clayey silt to silty clay
$2.82 I_c \leq 3.22$	3	Clays

NOTES:

1. Sensitive fine grained
2. Organic soils - peats
3. Clays - clay to silty clay
4. Silt mixtures - clayey silt to silty clay
5. Sand mixtures - silty sand to sandy silt
6. Sands - clean sand to silty sand

$$q_m = (q_t - \sigma'_v) \sigma'_v$$

$$FR_n = (f_s / (q_t - \sigma'_v)) 100\%$$

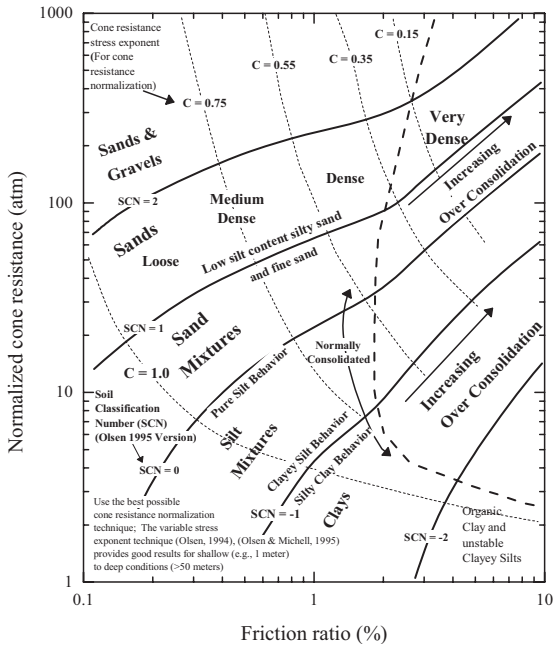


Figure 2.11 Olsen and Mitchell (1995) chart.

obtained by subtracting the pore pressure measured at the cone shoulder from the corrected tip resistance.

### 2.2.12 Ramsey (2002) charts

Figure 2.13 and Figure 2.14 show the SBT charts proposed by Ramsey (2002). The charts were developed using Fugro's database of CPT results with adjacent laboratory test results available. The predicted soil categories obtained by the SBT charts were compared with the soil classifications obtained from laboratory tests (Ramsey, 2002).

### 2.2.13 Schneider et al. (2008) charts

Figure 2.15, Figure 2.16 and Figure 2.17 show the SBT charts proposed by Schneider et al. (2008). These

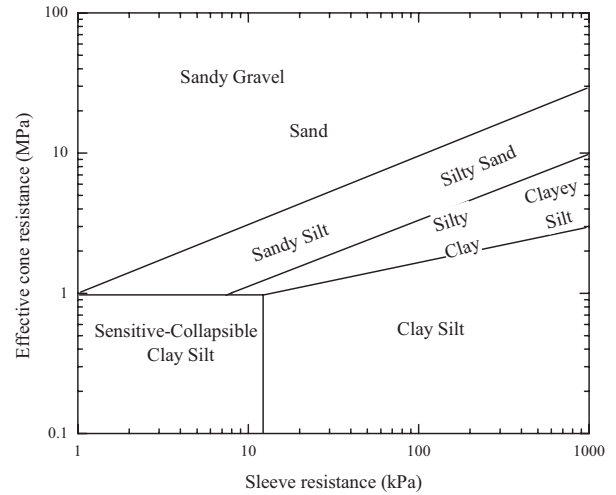


Figure 2.12 Eslami and Fellenius (1997) chart.

authors have incorporated the effects of drainage conditions during cone penetration in the soil behavior type classification.

In these charts, the normalized cone resistance  $q_m = \left( \frac{q_{c,net}}{\sigma'_v} \right)$  is plotted against the ratio of pore pressure change  $\Delta u$  right behind the cone tip normalized with respect to the vertical effective stress or the net cone resistance.

### 2.3 Selected SBT Charts

SBT charts enable us to construct a soil profile from the CPT data. In order to construct a soil profile with only one soil behavior type associated with each layer of the soil profile, we need to work with a chart or charts having each distinct region identifying only a specific type of soil behavior. In this regard, both the Tumay (1985) and Robertson (1990) SBT charts were appealing; however, minor modifications had to be made to these charts to eliminate overlap of SBT regions or some ambiguities.

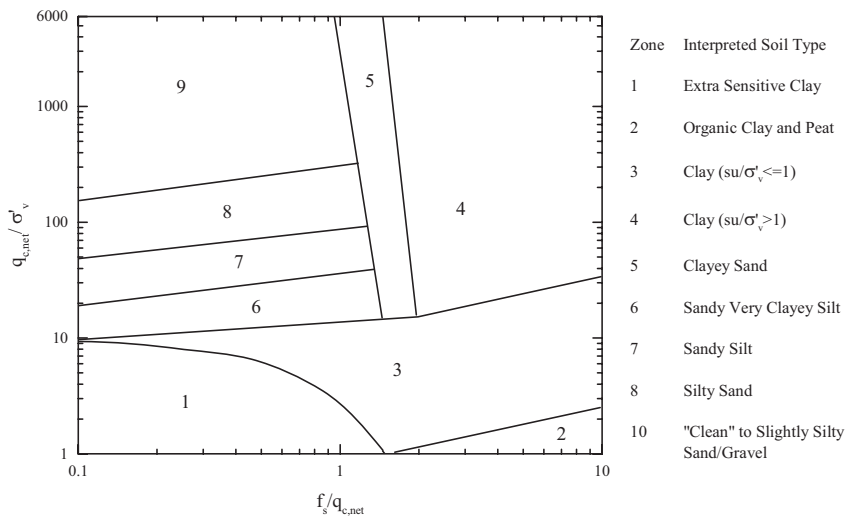


Figure 2.13 Ramsey (2002) chart 1.

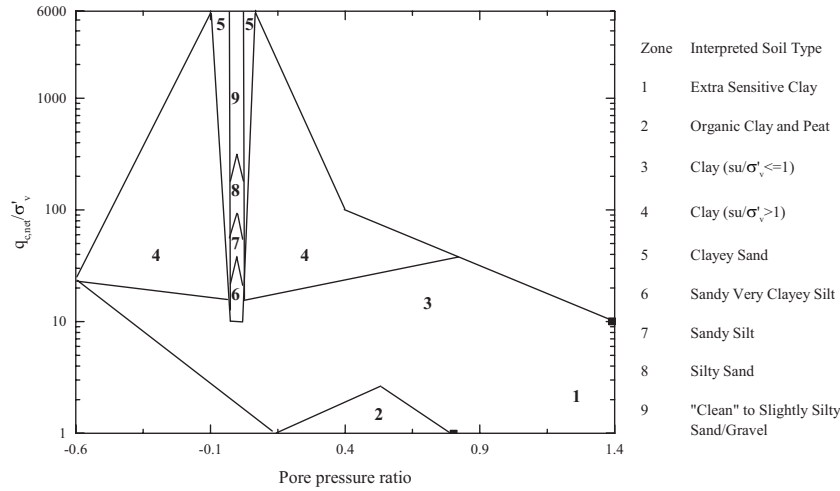


Figure 2.14 Ramsey (2002) chart 2.

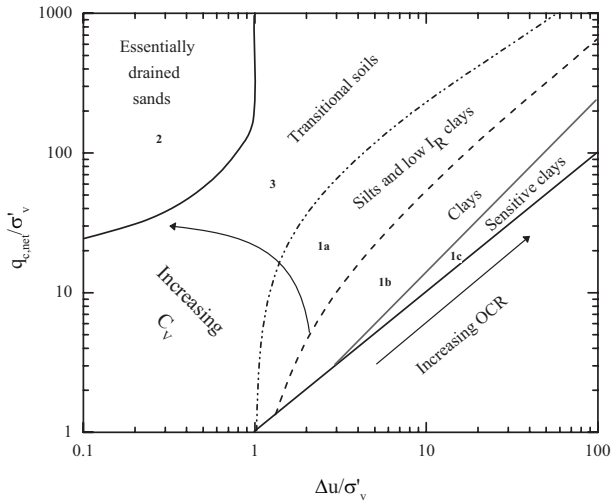


Figure 2.15 Schneider et al. (2008) chart 1.

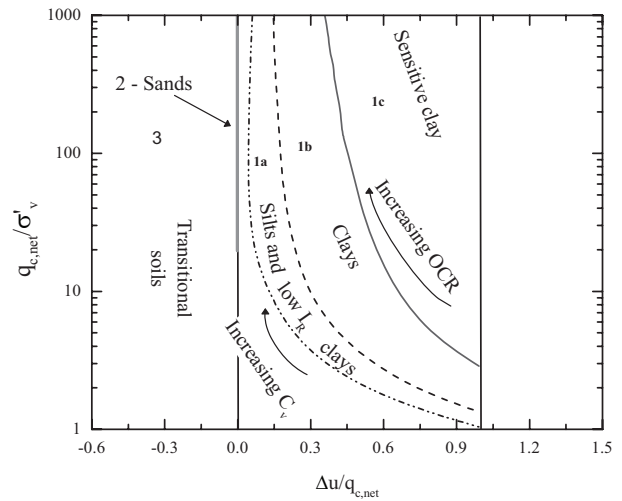


Figure 2.17 Schneider et al. (2008) chart 3.

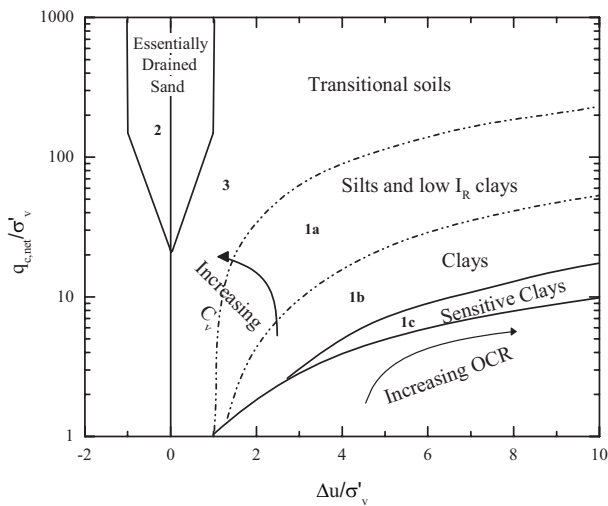


Figure 2.16 Schneider et al. (2008) chart 2.

### 2.3.1 Modified Tumay (1985) Chart

Figure 2.18 shows the modified Tumay (1985) chart used in this research. The following modifications were made to the Tumay (1985) chart:

1. The regions of the original chart ("Loose sand," "Sand," "Shell sand or limerock," "Dense or cemented sand" and "Silty sand") were removed and consolidated into a single SBT region referred to as "Clean sand or silty sand." When a soil falls into this "Clean sand or silty sand" region of the chart, it is further classified into five different subtypes depending on the estimated relative density (from very loose to very dense), as shown in Table 2.4. The relative density of the sandy soil is calculated as (Salgado, 2008):

$$D_R = \frac{\ln\left(\frac{q_c}{p_A}\right) - 0.4947 - 0.841 - 0.1041\phi_c \times \ln\left(\frac{\sigma'_h}{p_A}\right)}{0.0264 - 0.0002\phi_c - 0.0047 \times \ln\left(\frac{\sigma'_h}{p_A}\right)} \leq 100\% \quad (2.7)$$

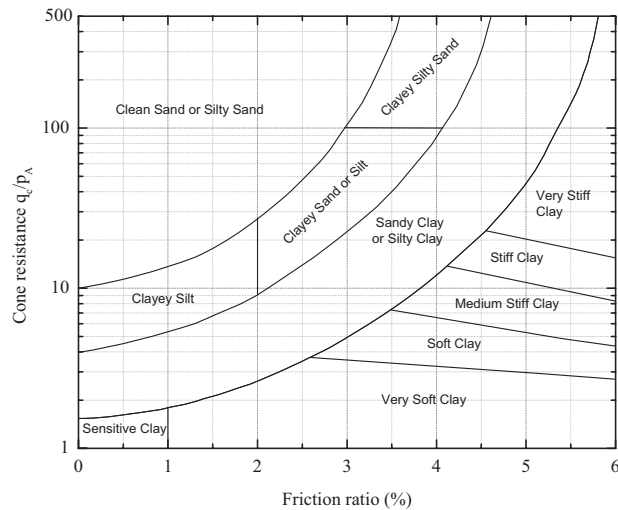


Figure 2.18 Modified Tumay (1985) chart.

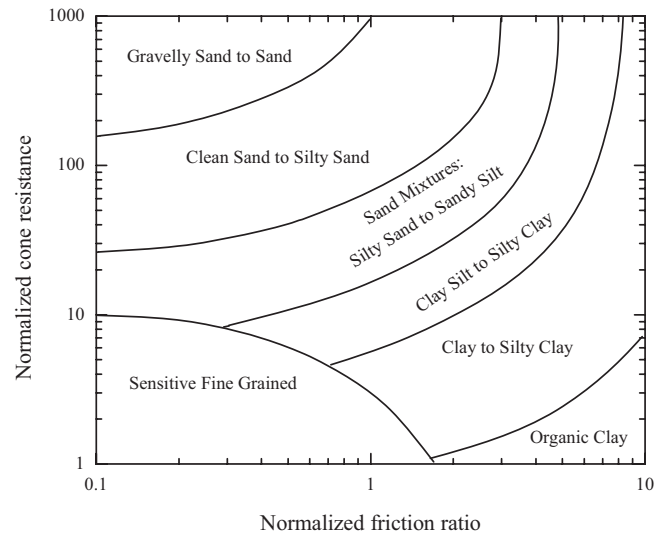


Figure 2.19 Modified Robertson (1990) chart.

TABLE 2.4  
Sand classification according to density

Relative Density (%)	Sand Classification
0–15	Very loose sand
15–35	Loose sand
35–65	Medium dense sand
65–85	Dense sand
85–100	Very dense sand

where  $DR$  is the relative density,  $q_c$  is the cone resistance,  $\phi_c$  is the critical-state friction angle,  $\sigma'_h$  is the horizontal effective stress ( $\sigma'_h = K_0 \sigma'_v$ , where  $K_0$  is the coefficient of lateral earth pressure at-rest) and  $p_A$  is the reference stress.

- The “Silty clay” region in the original chart was removed.
- The “Sandy clay” region in the original chart was renamed “Sandy clay or silty clay.”
- The “Organic clay” region in the original chart was removed. The “Inorganic clay” regions of different stiffnesses in the original chart were changed to “Clay” of different stiffnesses in the modified chart.
- The “Clayey sands” region in the original chart was changed to “Clayey silt” in the modified chart. This was done to be consistent with the expected progressive increase in cone resistance with increasing sand content from “Clayey silt” to “Clayey sand or silt” and then to “Clayey silty sand.”
- A new region, “Sensitive clay,” was added. This region indicates clay with FR less than unity.

### 2.3.2 Modified Robertson (1990) Chart

Figure 2.19 shows the modified Robertson (1990) chart used in this research. The following modifications were made to the original chart:

- The “Organic soils – peats” region (zone 2) was renamed “Organic clay” in the modified chart.

- The “Very stiff sand to clayey sand” region (zone 8) in the original chart was incorporated into two different regions – “Sand mixtures: silty sand to sandy silt” (zone 5 of the original chart) and “Clean sand to silty sand” (zone 6 of the original chart) – in the modified chart. This modification was made by removing the boundary lines between zones 6 and 8 and zones 5 and 8 in the original chart. The boundary line between zones 5 and 6 was extended all the way to the top axis (the normalized friction ratio axis) in the modified chart. The rationale behind this modification is that the “Very stiff sand to clayey sand” region (zone 8) in the original chart indicates similar soil behavior type to those suggested by the “Sand mixtures: silty sand to sandy silt” (zone 5) and “Clean sand to silty sand” (zone 6) regions (this is because zone 8 in the original chart also indicates mixed soil types).
- The “Clean sand to silty sand” region (zone 6) was further classified into five different subtypes depending on the estimated relative density (very loose to very dense). The relative density of the sandy soils was calculated using Equation 2.7.
- The “Very stiff, fine-grained” region (zone 9) in the original chart was incorporated into the “Clay to silty clay” (zone 3 of the original chart) and “Clayey silt to silty clay” (zone 4 of the original chart) regions in the modified chart. This modification was made by removing the boundary lines between zones 4 and 9, and zones 3 and 9. The boundary line between zones 3 and 4 was extended all the way to the top axis (the normalized friction ratio axis) in the modified chart. The rationale behind this modification is that the “Very stiff, fine-grained” (zone 9) region in the original chart indicates similar soil behavior type to those suggested by “Clay to silty clay” (zone 3) and “Clayey silt to silty clay” (zone 4) regions.

### 2.4 Soil Profile Generation

The procedure followed to obtain a soil profile to be used in the site variability analysis consists mainly of two steps:

- Obtain the initial soil profile by plotting CPT data on SBT chart selected;
- Modify the initial soil profile by consolidating thin layers to obtain the final soil profile.

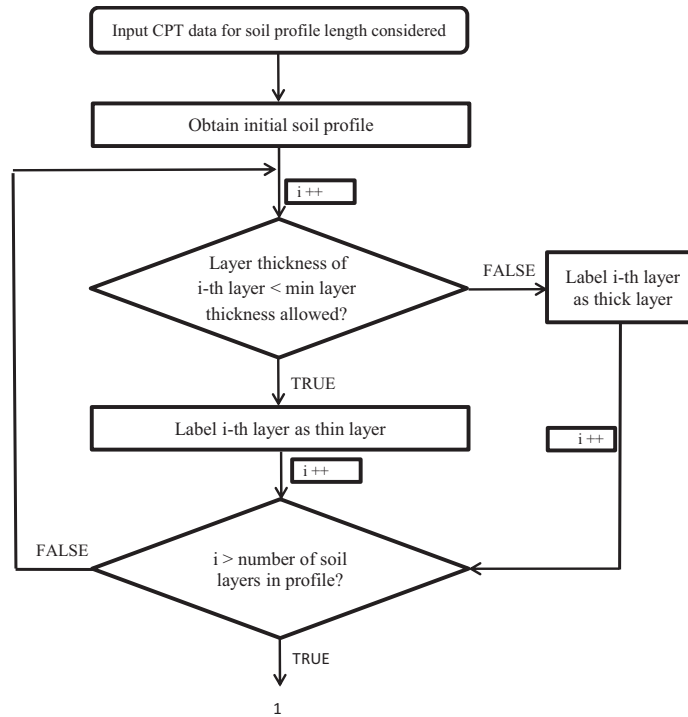


Figure 2.20 Soil profile generation flowchart—part 1.

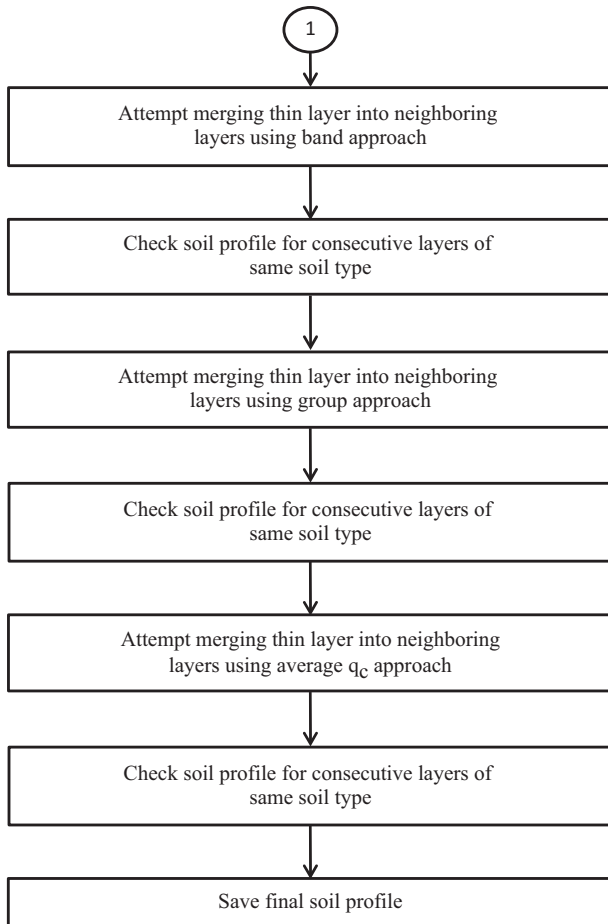


Figure 2.21 Soil profile generation flowchart—part 2.

Figure 2.20 and Figure 2.21 show the steps required to generate a soil profile using CPT data and an SBT chart.

#### 2.4.1 Initial Soil Profile

Either of the two modified SBT charts discussed previously can be used to obtain a soil profile from the CPT data ( $q_c$ ,  $f_s$ ,  $FR$ , pore pressure and possibly other quantities versus depth). The  $FR$  and  $q_c$  values (these parameters may need to be normalized depending on the chart used) obtained at each depth are first plotted on the selected SBT chart. Then a “primary soil behavior type” is assigned to each depth depending on where the point [e.g., point with coordinates  $FR$  and  $q_c/p_A$  for the modified Tumay (1985) chart] falls on the SBT chart selected. This process is repeated for all depths of the CPT sounding for which data was obtained. Subsequently, all adjacent depths with the same SBT classification are grouped into initial soil layers. All the initial soil layers put together define the initial soil profile. Figure 2.22 shows the algorithm used to obtain the initial soil profile.

#### 2.4.2 Occurrence of Thin Layers in Initial Soil Profile

The initial soil profile consists of layers of various thicknesses. Some layers can be quite thin (e.g., only a few centimeters thick). However, since the standard cone has a diameter of 35.7 mm, it has a minimum resolution for layer

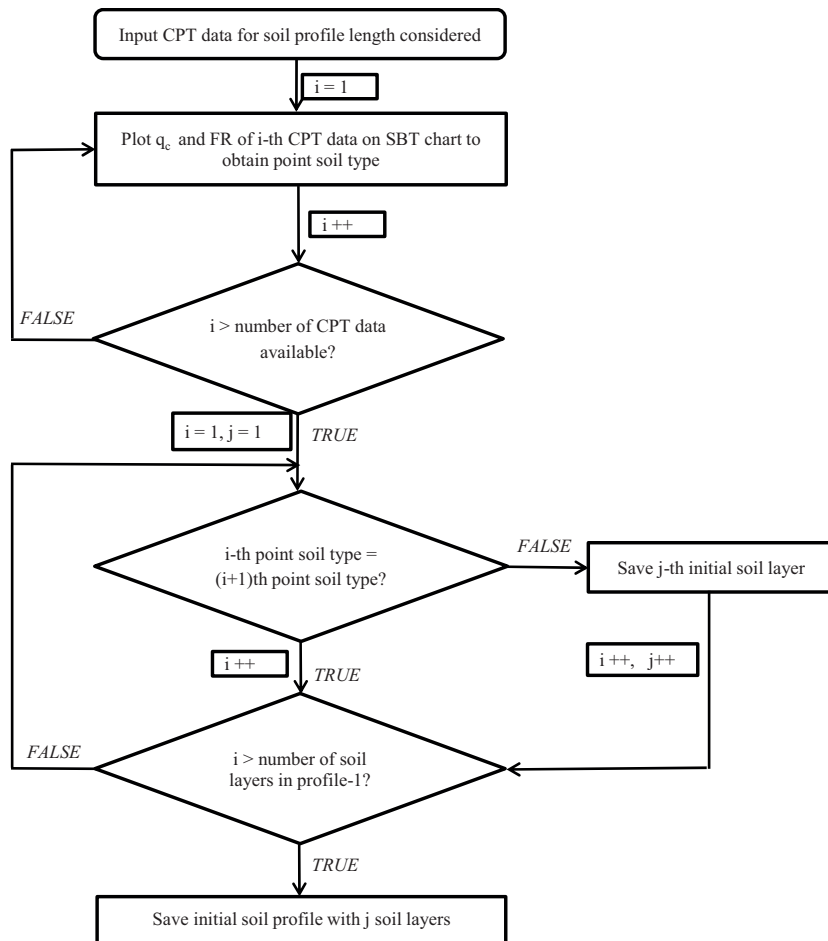


Figure 2.22 Initial soil profile generation for modified Tumay (1985) chart.

identification. The reason for this limitation is that the cone needs to penetrate a certain depth into a given layer to develop the cone resistance that is representative of that layer. This distance is referred to as the development distance. In addition, as the cone approaches a layer of different stiffness, it will start sensing its presence a few cone diameters ahead of the interface between the layers. This distance is referred to as the sensing distance.

These development and sensing distances depend on the relative stiffness of the layers being traversed by the cone. If both the sensing and development distances (which, when added up, are of the order of a few cone diameters in thickness) are considered, then layers thinner than approximately 15–20 cm cannot be properly detected by the cone. Accordingly, this research considers a layer having a thickness of 15 cm or less (corresponding to about 4.2 standard cone diameters) a thin layer.

All thin layers in the initial soil profile are absorbed into thick layers by the soil profile generation algorithm according to three different approaches:

- SBT chart band approach (consolidation of thin layers into adjacent layers considering secondary soil type(s) classification);
- Soil group approach (consolidation of thin layers into

adjacent layers of the same soil group);

- Average  $q_c$  approach (consolidation of thin layers into adjacent layers with similar average  $q_c$ ).

These approaches are explained in detail next.

### 2.4.3 SBT Chart Band Approach

The SBT chart band approach was developed to address the uncertainty associated with the location of the boundary lines between regions defining different soil behavior types in a chart. When generating a soil profile, it is possible that a very thin layer can be produced by CPT data plotting very close to a boundary line between two soil behavior types in the SBT chart. A thin layer produced in this manner can be argued to actually be part of a layer adjacent to it in the soil profile. This situation occurs whenever CPT data from thin layers plot near the SBT chart boundary lines. In such cases, thin layers are consolidated into adjacent thick or thin layers with the same soil type as that in the neighboring region of the SBT chart.

Figure 2.23 shows an idealized segment of a soil profile where we can see two layers: one thin layer of type “Medium dense sand” and one thick layer of type “Clayey sand or silt.” Consider that the thin layer of “Medium dense

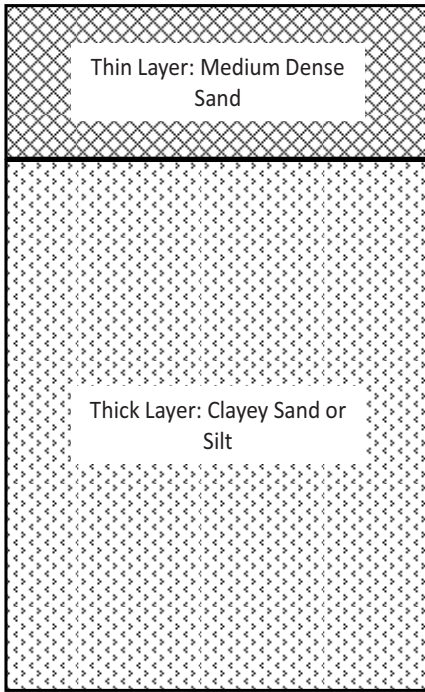


**Figure 2.23** Thin layer generated by CPT data falling close to boundary line between regions of “clean sand or silty sand” and “clayey sand or silt.”

sand” was produced by CPT data falling close to the boundary line between the above mentioned two soil behavior types in the Tumay (1985) chart, as shown in Figure 2.24.

In this example, this thin layer, classified as “Medium dense sand” in the initial soil profile, can be given a secondary soil behavior type classification of “Clayey sand

or silt” (because the point representing the thin layer is very near the boundary with the “Clayey sand or silt” region of the chart). The thin layer can then be consolidated into the adjacent “Clayey sand or silt” thick layer since the secondary soil behavior classification of the thin layer matches the primary soil behavior classification of the thick layer.

**2.4.3.1 Development of SBT chart with bands.** Upper and lower lines, parallel to the existing boundary lines between soil behavior types, were added to the modified SBT charts used in this research. These upper and lower lines define bands in the SBT charts. Figure 2.25 shows the modified version of Tumay (1985) chart with  $\pm 15\%$   $q_c$  dashed lines defining these bands. The soil profile generation algorithm checks whether a thin layer has a  $q_c$  and  $FR$  combination (normalization of these parameters may be needed depending on the chart used) that falls within these bands. If so, the thin layer can be absorbed into a neighboring thick layer if it has the soil type in the region next to this band.

For every thin layer in the initial soil profile, first the average  $q_c$  and the average  $FR$  values are calculated. The average  $q_c$  and  $FR$  values are then plotted on the modified SBT chart. Whenever a point representing a thin layer falls within a band of the SBT chart, the thin layer gets assigned not only the soil behavior type of the region it is in but also, as a secondary soil type assignment, the soil type of the region the band borders with. If the point falls at the intersection of two bands, it gets assigned two secondary soil behavior types. Figure 2.26 shows two examples of secondary soil type assignment. In one case, a thin soil layer of type “clean sand or silty sand” is assigned a secondary soil type of “clayey sand or silt.” In the other case shown in Figure 2.26, a thin soil layer of type “very soft clay” gets two secondary soil type assignments: “sandy clay or silty clay” and “soft clay,” as there are two adjacent boundaries near the point representing the thin layer.

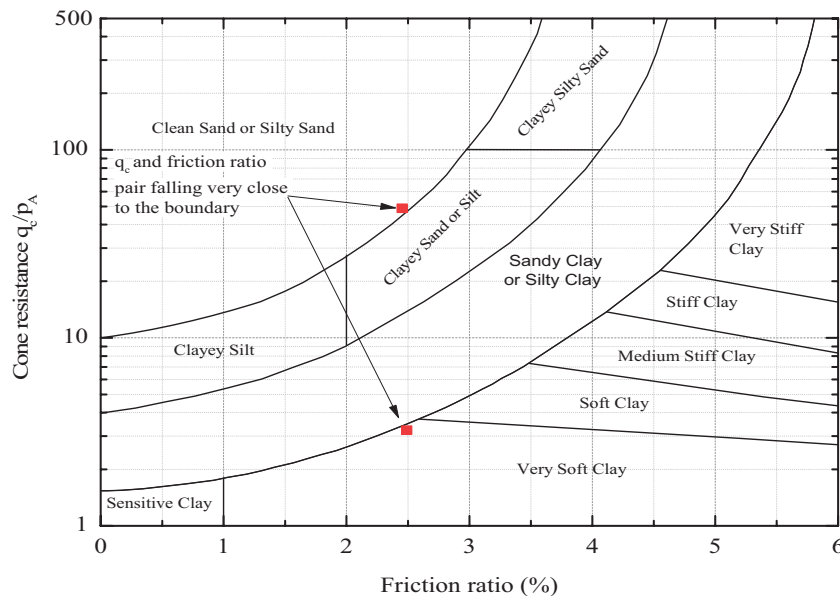


**Figure 2.24** Modified Tumay (1985) chart with examples of CPT data falling near boundary lines.

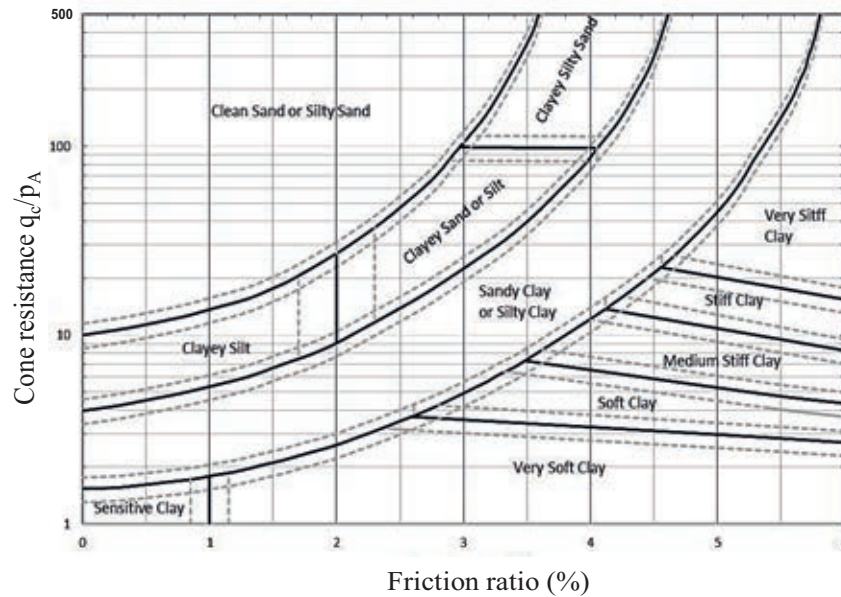


Figure 2.25 Modified Tumay (1985) chart with  $\pm 15\%$   $q_c$  bands.

Although a secondary soil type of a thin layer may match the primary soil type of an adjacent layer, these layers may have quite different values of cone resistance. Such a case is illustrated in Figure 2.27. To address this, the soil profile generation algorithm first compares the average cone resistance of the thin layer under consideration with those of the layers adjacent to it. If the average  $q_c$  of the thin layer is within  $\pm 25\%$  of the average  $q_c$  values of the adjacent layers, then the thin layer is incorporated into an adjacent layer whenever the secondary soil type assigned to the thin layer matches the primary soil type of the adjacent layer. The resulting layer

(composed of the thin layer and the adjacent layer) gets the primary soil type of the layer with the largest thickness.

If the two adjacent layers are thin layers and one of the two layers does not have a secondary soil type assigned to it, then the combination is attempted only based on the secondary soil type assigned to the layer that has it. If the two layers are combined, the resulting layer takes the primary soil type of the layer without a secondary soil type. The consolidation of thin layers using the modified SBT chart with bands described above is hereafter referred to as the “SBT chart band approach.” Figure 2.28 and Figure 2.29

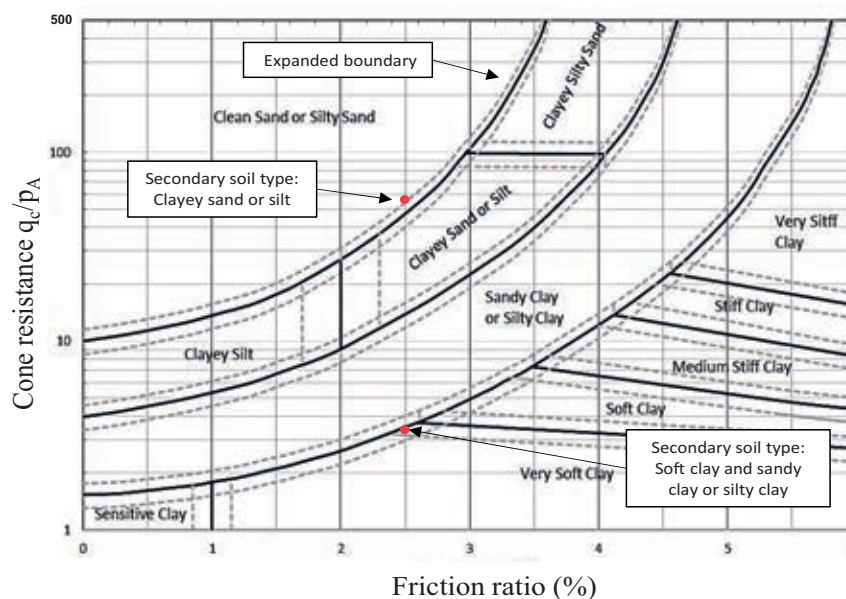


Figure 2.26 Examples of assignment of secondary soil type(s).

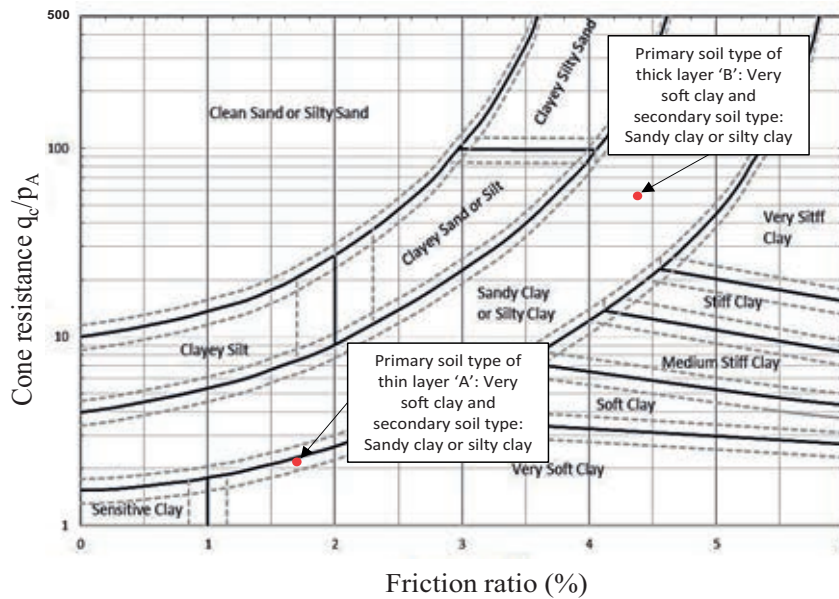


Figure 2.27 Example of comparison of the average  $q_c$  values of thin and thick layers.

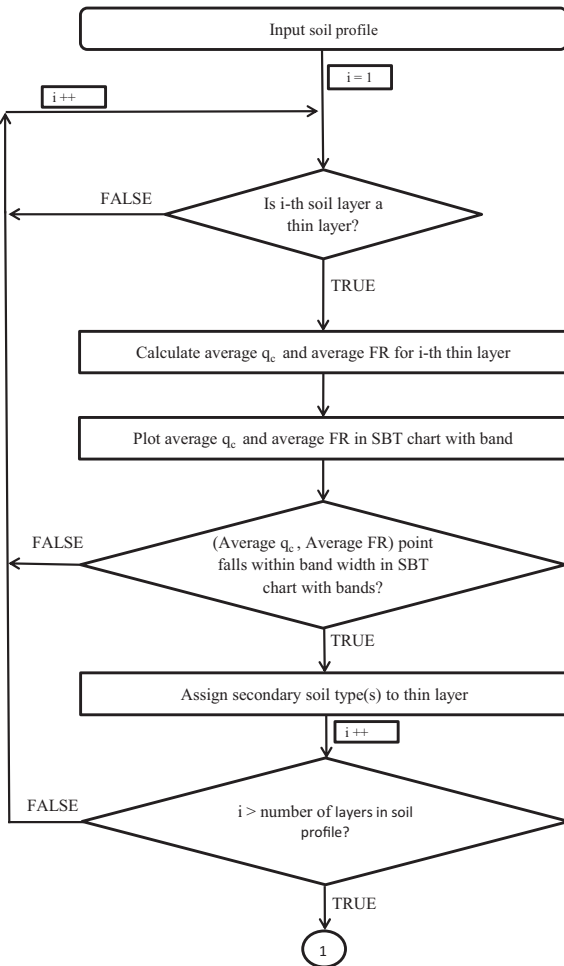


Figure 2.28 Assignment of secondary soil type to thin layers.

show the algorithms developed for consolidation of thin layers using the SBT band approach. As shown in the flow charts, first the thin layers identified in the initial soil profile are assigned secondary soil types whenever the points with average  $FR$  and  $q_c$  values fall within the bands of the modified SBT chart selected. Secondly, the cone resistance values (the average  $q_c$  of the thin layer should be within  $\pm 25\%$  of the average  $q_c$  values of the adjacent layers for consolidation of layers to be allowed) and soil types are compared to decide whether the thin layer can be incorporated into the adjacent layers or not.

**2.4.3.2 Application of the SBT chart band approach.** A thin layer may be located at the very top or at the very bottom of the soil profile. A topmost thin layer only has an adjacent layer (thin or thick) below it, whereas a thin layer at the bottom of the soil profile only has an adjacent (thin or thick) layer above it. Thin layers may also occur at any other location in the soil profile intercalated between other layers, which again may be thin or thick. When a single thin layer is sandwiched between two thick layers and the secondary soil type of the thin layer is the same as the primary soil type of one of the adjacent thick layers, then the thin layer is absorbed into the thick layer that has satisfied the soil type matching requirement. However, if the secondary soil type of the thin layer matches the soil type of both of the adjacent thick layers, then the thin layer is incorporated into the adjacent thick layer whose average  $q_c$  is closer to that of the thin layer. If the secondary soil type(s) of a thin layer under consideration matches the primary soil type of only one of the layers adjacent to it, then these two layers are consolidated.

In case the soil type(s) assigned to the thin layer under consideration matches the soil types of both the layers

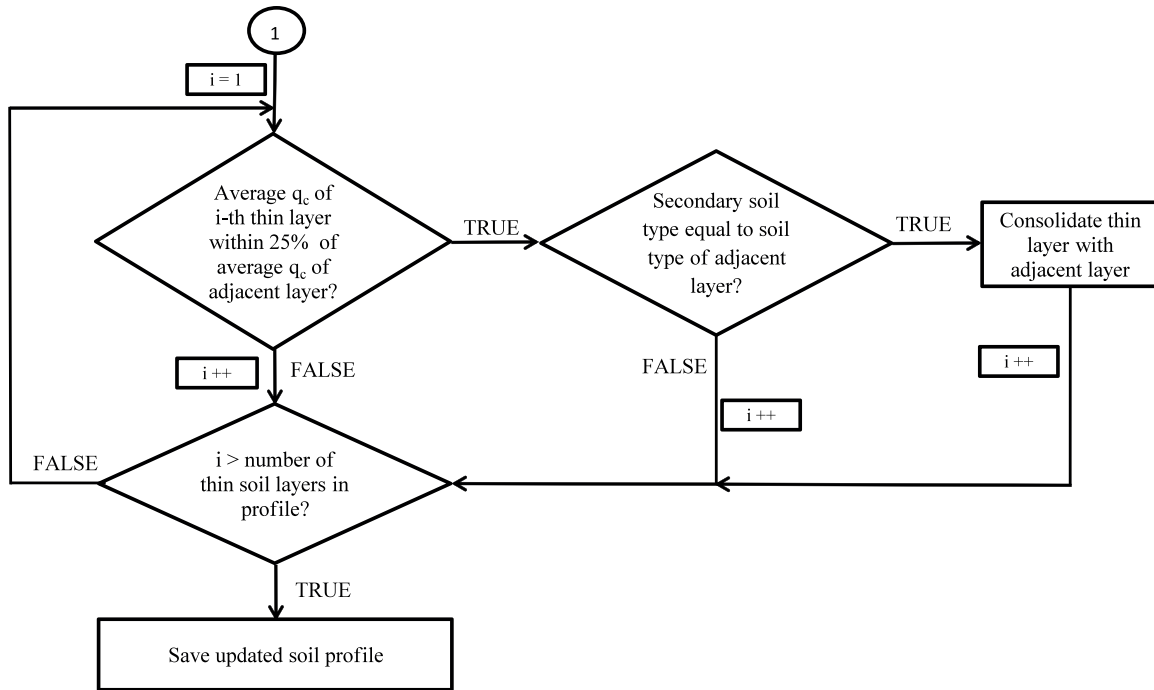


Figure 2.29 Soil profile checked for SBT chart band approach.

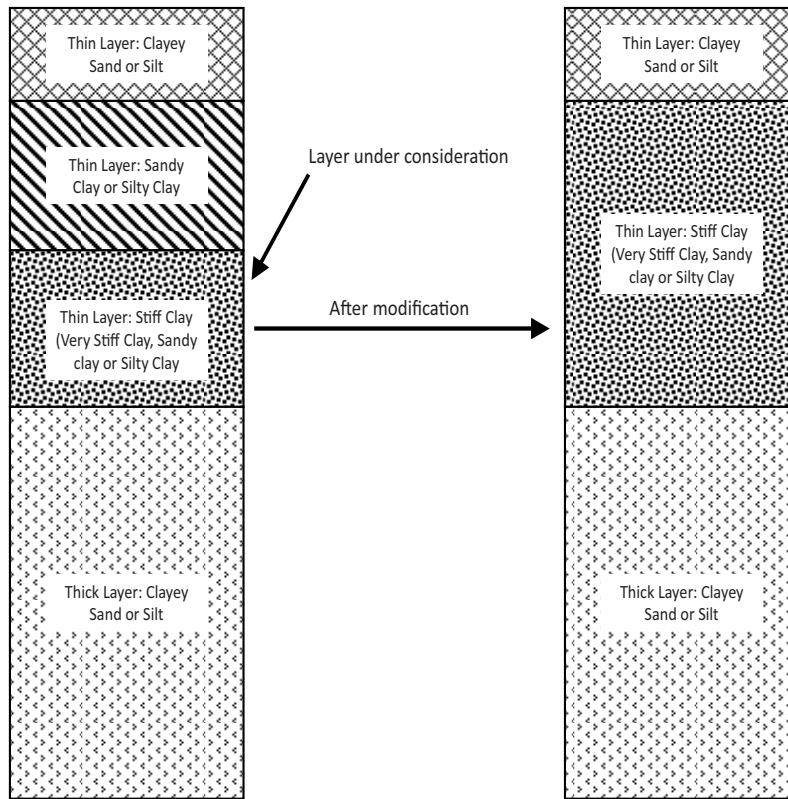


Figure 2.30 Consolidation of a thin layer based on comparison of the average  $q_c$  values of the thin and adjacent layers and layer thickness.

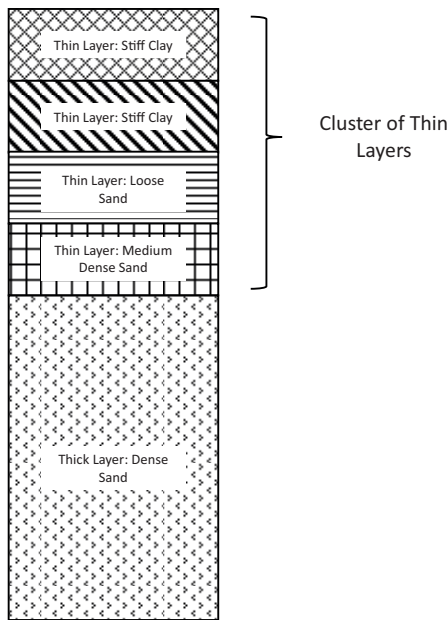


Figure 2.31 Thin layers occurring in sequence in a soil profile.

adjacent to it, as illustrated in Figure 2.30, the average  $q_c$  values of the adjacent layers are compared with the average  $q_c$  value of the thin layer under consideration. The adjacent layer with average  $q_c$  closer to the average  $q_c$  of the thin layer under consideration is consolidated with it, as shown in Figure 2.30, where the consolidated

layer has the soil type of the thin layer under consideration initially since it is thicker than the layer above it with similar average  $q_c$ .

Thin layers may also appear in clusters, as shown in Figure 2.31. Whenever thin layers appear clustered together, the first thin layer to be considered when using the SBT chart band approach is the one whose average  $(FR, q_c)$  point falls nearest to any of the boundary lines of the modified SBT chart [this distance is calculated as the vertical distance from the boundary line to the average  $(FR, q_c)$  point representing the thin layer]. The closer a point is to an SBT chart boundary line, the more likely it is for the primary soil type assignment not to be accurate.

In order to decide which of the thin layers in a cluster of thin layers is considered first when using the SBT chart band approach, the vertical distance from the average  $(FR, q_c)$  point representing a thin layer to a boundary line in the modified SBT chart is calculated for each of the thin layers. This vertical distance is expressed as the ratio of the difference in cone resistance values between the point representing the thin layer and the original boundary line of the modified SBT chart to the difference in cone resistance values between the band line and the original boundary line of the modified SBT chart. This ratio is referred to as the proximity ratio. The thin layer in the cluster with the smallest value of the proximity ratio is considered first. A value of zero for this ratio indicates that the average  $(FR, q_c)$  point representing the thin layer falls exactly on the boundary line, while a value of 100% indicates that the average  $(FR, q_c)$  point representing the thin layer falls exactly on the band line. This is illustrated in Figure 2.32,

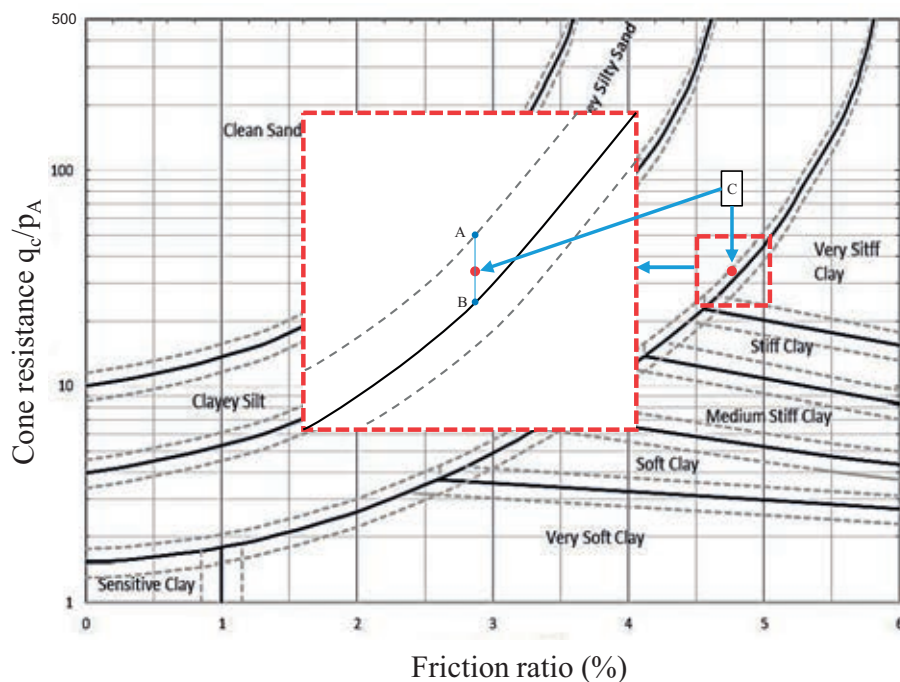
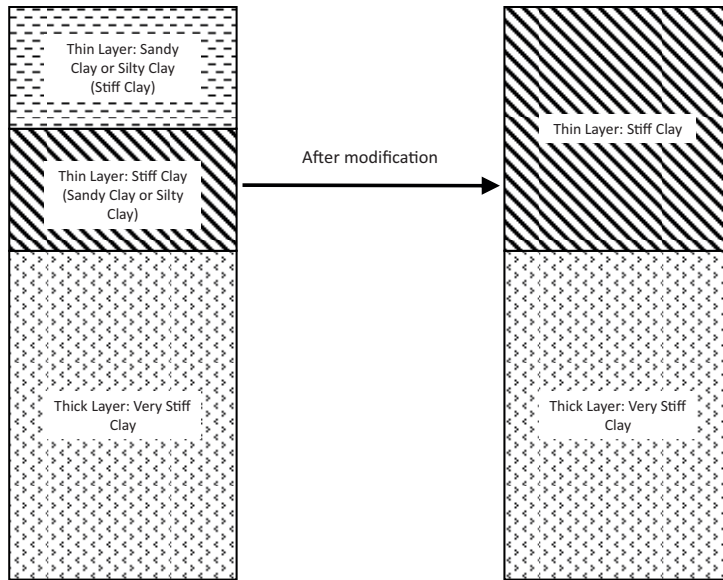
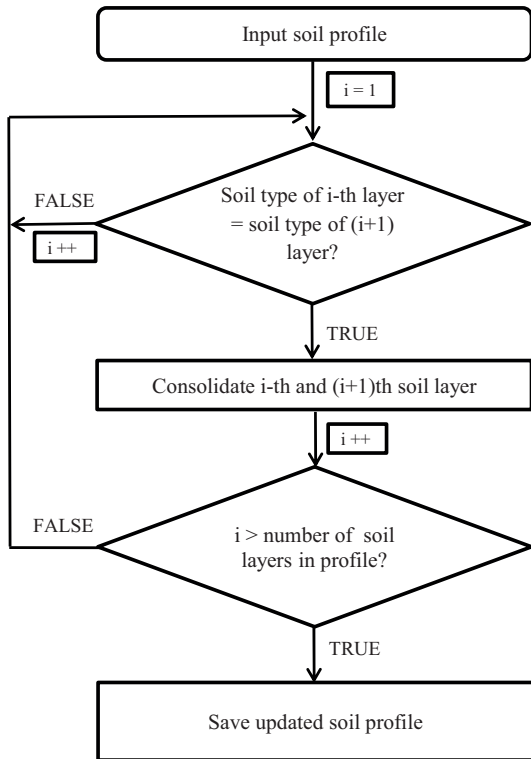


Figure 2.32 Illustration of the proximity ratio.



**Figure 2.33** Illustration of a case in which the secondary soil type of a thin layer under consideration matches the primary soil type of an adjacent thin layer and vice-versa



**Figure 2.34** Soil profile checked for consecutive layers of the same soil type.

where point C represents the average  $(FR, q_c)$  of a thin layer. The proximity ratio is zero when a point falls on the original SBT chart boundary line (e.g., point A in

Figure 2.32) and is 100% when a point falls on a band line (e.g., point B in Figure 2.32). A very low proximity ratio indicates that the average  $(FR, q_c)$  point representing the thin layer is very close to the boundary line, which suggest that there is a high probability that the thin layer is actually part of an adjacent layer in the soil profile. Thin layer consolidation progresses by considering next the thin layer in the cluster of thin layers having the second lowest proximity ratio and so on.

When the secondary soil type of a thin layer under consideration matches the primary soil type of an adjacent thin layer and vice-versa, the soil type of the combined layer will be that of the thicker of the two layers Figure 2.33, which shows two soil profiles, illustrates this case. The soil profile on the right is obtained after modification of the left soil profile according to the SBT band approach. The two top layers of the left soil profile are both thin layers. Their secondary soil types are shown within parentheses in the figure. The topmost thin layer is thinner than the thin layer below it. The secondary soil type of the thinner soil layer (stiff clay) is the same as the primary soil type of the adjacent thin layer. At the same time, the secondary soil type of the thin layer under consideration (sandy clay or silty clay) is the same as the primary soil type of the topmost thin layer. The right soil profile shows the two top thin layers consolidated into a single layer of stiff clay.

#### 2.4.4 Consolidation of Adjacent Layers of the Same Soil Type

After the initial soil profile is modified according to the modified SBT chart band approach, the resultant soil profile

TABLE 2.5  
Soil group classification for the modified Tumay (1985) chart

Soil Group	Soil Types
Sand	Clean sand or silty sand (very loose to very dense)
Clay	Sensitive clay, very soft clay, soft clay, medium stiff clay, stiff clay, very stiff clay
Mixed soil	Clayey silt, clayey sand or silt, clayey silty sand, sandy clay or silty clay

may have adjacent layers of the same soil type. The soil profile is checked for the occurrence of adjacent layers of the same soil type, and, whenever soil layers of the same soil type occur in sequence, these are consolidated. Figure 2.34 shows the algorithm used to consolidate consecutive layers of the same soil type.

#### 2.4.5 Soil Group Approach

After the soil profile is modified using the modified SBT chart band approach and the soil layers appearing in sequence are consolidated when they are of the same soil type, thin layers may still remain in the soil profile. The soil group approach is used to further consolidate these remaining thin layers. Table 2.5 and Table 2.6 show the soil group classification for the modified Tumay (1985) chart and the modified Robertson (1990) chart, respectively. The general algorithm to consolidate thin soil layers with adjacent layers of the same group is shown in Figure 2.35.

In the soil group approach, thin layers are consolidated when they belong to the same soil group. When thin layers appear in a cluster, the process starts with the thinnest layer in the sequence. The consolidated layer always inherits the soil type of the layer adjacent to it that belongs to the same soil group as the thin layer under consideration (since the adjacent layer is always thicker than the thin layer under consideration).

As an illustration, in the leftmost plot of Figure 2.36, the soft clay layer (3rd layer of the profile) is combined with the thin stiff clay layer (2nd layer of the profile) since they belong to the same soil group. Since the stiff clay layer is thicker than the soft clay layer, the consolidated layer is stiff clay, as shown in the middle plot of Figure 2.36. This stiff clay layer, which is still a thin layer, is further consolidated with the overlying very stiff clay layer, as

TABLE 2.6  
Soil group classification for the modified Robertson (1990) chart

Soil Group	Soil Types
Sand	Gravelly sand to sand (very loose to very dense); clean sand to silty sand (very loose to very dense)
Clay	Organic clay; sensitive fine grained
Mixed soil	Sand mixtures: silty sand to sandy silt; clayey silt to silty clay; clay to silty clay

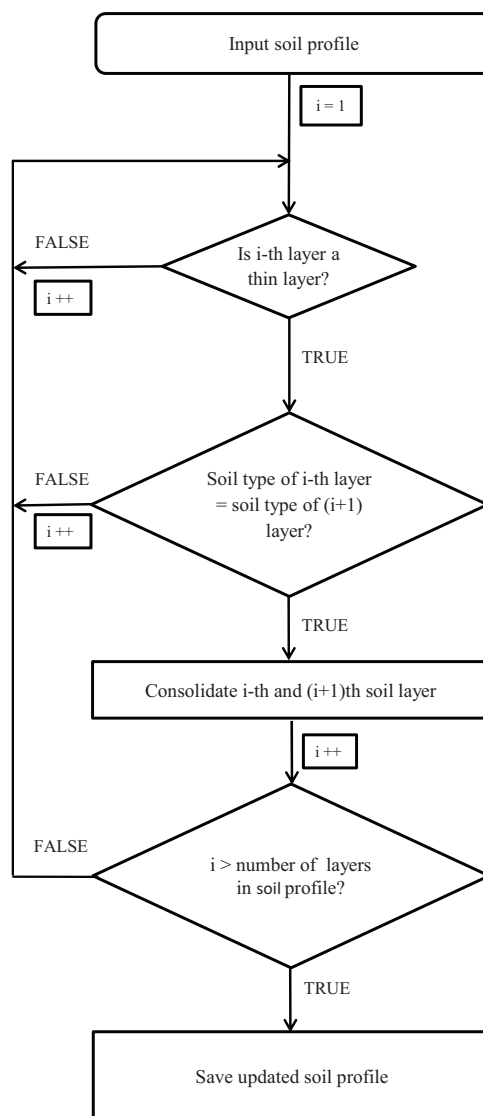


Figure 2.35 Soil profile checked for the soil group approach.

shown in the right most plot of Figure 2.36. Also, in the leftmost plot, the thin loose sand layer is consolidated with the thick dense sand layer since they belong to the same soil group.

If the thin layer under consideration belongs to the same soil group as both the layer above and the one below it, consolidation is based on proximity of the average  $q_c$  values. After consolidating thin layers with adjacent layers of the same soil group, the soil profile is again checked for adjacent layers of the same soil type, and if layers of the same soil type occur in sequence, then these layers are consolidated.

#### 2.4.6 Average $q_c$ Approach

The average  $q_c$  approach is the last approach used to consolidate thin layers still remaining in a soil profile. This approach consists of consolidating thin layers with the adjacent

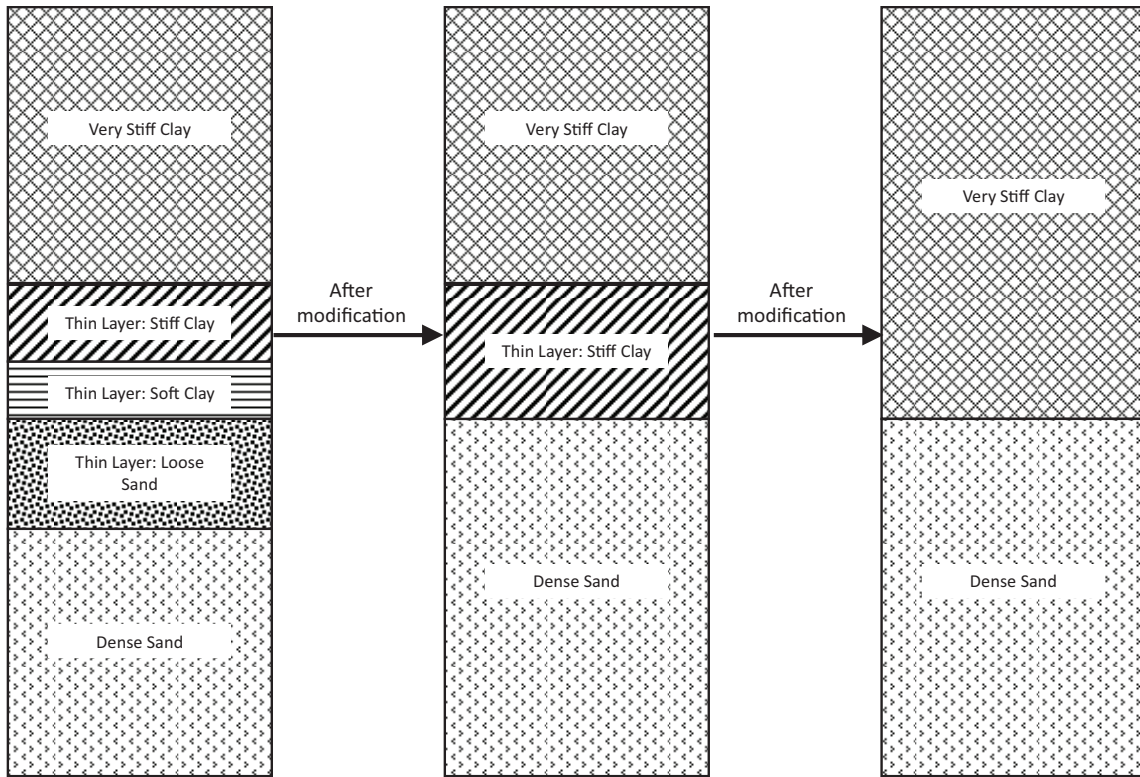


Figure 2.36 Consolidation of thin layers with adjacent layers of the same soil group.

layer having the closest average  $q_c$  value. In the case of a cluster of thin layers, the modification process starts with the thinnest layer in the sequence. If a thin layer is at the very top or at the

very bottom of the soil profile, then it is discarded from the soil profile. Figure 2.37 shows the algorithm used to consolidate thin layers using the average  $q_c$  approach.

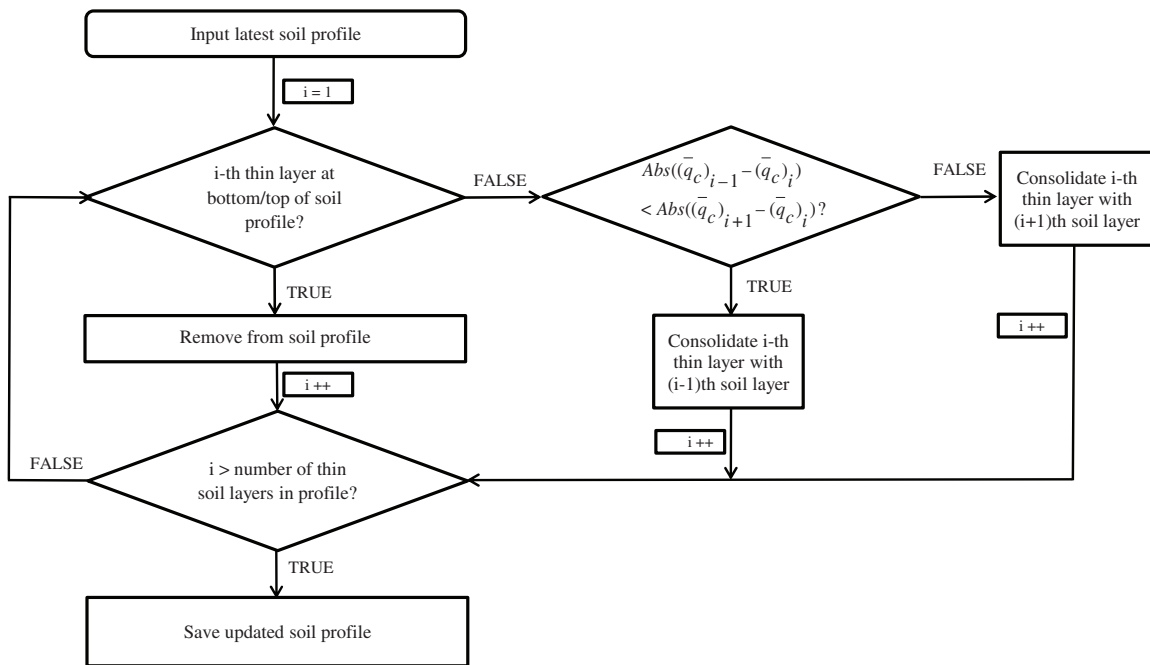


Figure 2.37 Soil profile checked for remaining thin layers using the average  $q_c$  approach.

### 3. FUNDAMENTAL CONCEPTS OF PROBABILITY AND RANDOM FIELD THEORY

#### 3.1 Introduction

Soil properties are variable from one location to another as a result of the soil formation processes. Statistics and probabilistic tools can be used to assess the spatial variability of soil properties. For proper use of statistics and probability theory, a sufficiently large dataset is required to establish reliable relationships and minimize the possibility of biases within the data. The CPT satisfies this requirement, but most other geotechnical investigation tools, the SPT included, do not. The CPT is, as a result, the focus of this research. In this chapter, we briefly review some key concepts from probability theory and random field theory that will be used in other chapters to develop the site variability assessment methodology proposed in this report.

#### 3.2 Essentials of Probability Theory

##### 3.2.1 Random Variables

Variables whose value is not set but instead can change each time an experiment is run under what is believed to be the exact same conditions are called random variables. If we plot the values of the random variable versus the number of times that value is observed divided by the total number of observations, we obtain the variable's probability density function (pdf, for short).

##### 3.2.2 Probability Mass Function

The set of all possible values of a random variable  $X$  (i.e., the set of all possible outcomes of an experiment whose output is the random variable) is the sample space  $S$ . The probability mass function (pmf) of  $X$  shows the probability of  $X$  taking a particular value  $x$  when the sample space is discrete. The probability mass function of  $X$  is  $f_X(x) = P(X = x)$ . The sum of all values of a pmf over the sample space  $S$  is unity. The cumulative mass function (cmf) is a function of the independent random variable given by the probability of the random variable having a value less or equal to a particular value.

##### 3.2.3 Probability Density Function, Central Tendency, and Dispersion

In a continuous sample space, the probability of a random variable  $X$  taking a particular value is always zero, so a probability mass function cannot be defined. However, the probability of the random variable taking a value within a range can be defined and is not necessarily zero. A probability density function (pdf) can be then defined that gives the probability  $f_X(x)dx$  of  $X$  falling between  $x$  and  $x + dx$ . The probability of a random variable  $X$  taking a value between  $a$  and  $b$  is  $P[a < X < b] = \int_a^b f_X(x)dx$ . Similarly to the cumulative mass function defined for a discrete sample

space, a cumulative density function (cdf) gives the probability of a continuous random variable taking a value less than or equal to a particular realization of the random variable.

The most common measures of central tendency of data are the mean, median and mode. The mean is the average of a data set. The median is the value such that half of the data is greater than the median, and half, is less. The mode is the value that occurs most frequently within a dataset. The most common measures of dispersion in data are the variance and the standard deviation. The variance  $\sigma_X^2$  of a random variable  $X$  is defined as:

$$\sigma_X^2 = Var[X] = E[(X - \mu_X)^2] = \begin{cases} \sum_x (x - \mu_X)^2 f_X(x) & \text{for discrete } X \\ \int_{-\infty}^{\infty} (x - \mu_X)^2 f_X(x) dx & \text{for continuous } X \end{cases} \quad (3.1)$$

where  $\mu_X$  is the expected value of  $X$  and the probabilities  $P(X)$  work as the weights in the calculation of the expected value of the squared differences.

The standard deviation  $SD(X)$  is the square root of the variance:

$$SD(X) = \sqrt{\frac{\sum_{i=1}^n (x_i - \mu_X)^2}{n}} \quad (3.2)$$

where  $n$  is the population size, and  $\mu_X$  is again the expected value of  $X$ .

In order to calculate the standard deviation based on a sample, the denominator in Equation 3.2 is replaced by  $(n - 1)$  to account for bias due to sample size. The coefficient of variation  $COV$  of the data is calculated by dividing the standard deviation by the data mean:

$$COV = \frac{SD_X}{\mu_X} \quad (3.3)$$

##### 3.2.4 Conditional Probability and Joint Probability Distribution

Let's assume that  $A$  and  $B$  are two experiments or events. If  $A$  and  $B$  are not independent, then the question of to what extent the probability of event  $A$  is affected by the occurrence of event  $B$  may be of interest. The conditional probability of event  $A$ , given that the probability of event  $B$ , is denoted as  $P[A|B]$  and can be calculated from:

$$P[A|B] = \frac{P[A \text{ and } B]}{P[B]} \quad (3.4)$$

The definition of probability distribution can be extended to the case of multiple random variables. Taking two discrete variables  $X$  and  $Y$  to illustrate the concept, the joint probability mass function of discrete random variables  $X$  and  $Y$  is:

$$f_{X,Y}(x,y) = P[(X = x) \text{ and } (Y = y)] \quad (3.5)$$

Similarly, the joint cumulative mass function of  $X$  and  $Y$  is:

$$F_{X,Y}(x,y) = P[(X \leq x) \text{ and } (Y \leq y)] \quad (3.6)$$

In the case of multiple random variables another useful concept is the marginal distribution. The marginal distribution of  $X$  is obtained by summing (if  $X$  and  $Y$  are discrete random variables) or integrating (if  $X$  and  $Y$  are continuous random variables) the joint probability distribution of  $X$  and  $Y$  over all possible values of  $Y$  (i.e., the sample space of  $Y$ ).

### 3.2.5 Covariance

The covariance is the extension of the concept of variance to two random variables. Let  $X$  and  $Y$  be random variables with joint probability distribution  $f_{XY}(x,y)$ . The covariance of  $X$  and  $Y$  is defined as:

$$\begin{aligned} COV(X, Y) &= E[(X - \mu_X)(Y - \mu_Y)] \\ &= \sum_x \sum_y (x - \mu_X)(y - \mu_Y)f_{XY}(x,y) \end{aligned} \quad (3.7)$$

for discrete  $X$  and  $Y$ , and

$$\begin{aligned} COV(X, Y) &= E[(X - \mu_X)(Y - \mu_Y)] \\ &= \int_{-\infty}^{\infty} \int_{-\infty}^{\infty} (x - \mu_X)(y - \mu_Y)f_{XY}(x,y)dx dy \end{aligned} \quad (3.8)$$

for continuous  $X$  and  $Y$ .

When the covariance of the two random variables  $X$  and  $Y$  is normalized by the product of their standard deviations, we obtain the correlation coefficient of the two random variables:

$$\rho_{XY} = \frac{COV(X, Y)}{\sigma_X \sigma_Y} \quad (3.9)$$

The value of the correlation coefficient ranges from  $-1$  to  $+1$ . The correlation coefficient of two random variables is a measure of the degree of linear dependence between the two variables. When the absolute value of the correlation coefficient value is unity, it indicates that the two random variables are perfectly linearly related. A positive correlation coefficient indicates that, when one variable increases, the other increases as well; while the opposite is true when the correlation coefficient is negative.

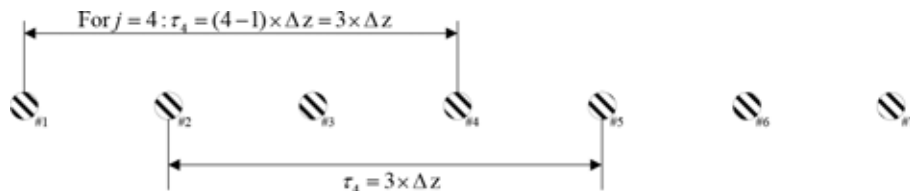


**Figure 3.1** Separation distance used in calculation of correlation function.

## 3.3 Random Field Theory

### 3.3.1 Random Field

A random field  $X(\mathbf{x})$  assigns a random variable  $X$  to the position vector  $\mathbf{x}$  identifying a point in the domain of the random field. A random field could, in a thought experiment, be characterized by outcomes of numerous experiments performed at different locations of the domain, each identified by a set of coordinates. We can say that the random field is discrete or continuous depending on whether  $X$  can take continuous or discrete values over the domain.

Random field theory is a dimensional extension of time series analysis. A time series is a sequence of data recorded at specific times, generally spaced at equal time intervals. The main feature of time series analysis is the recognition that values that are close in time are much more strongly correlated than those separated by larger time intervals. In random field theory, we have a space domain instead of a time domain. Since space can be considered in all of its three dimensions, a random field can be one-, two- or three-dimensional.

### 3.3.2 Auto-Correlation

The auto-correlation of a random field quantifies the strength of the correlation between values taken by a random variable at equally spaced points in a random field. The auto-correlation of  $X = X(z)$  first requires calculation of the covariance of the random field. The covariance is intended to capture the degree of correlation between values of  $X$  at points  $x_i$  and  $x_{i+j-1}$  distant  $\tau_j$  for all values of  $i$  in a range of interest. Let us say that there are  $n$  such points, the covariance  $C(\tau_j)$  is then given by:

$$C(\tau_j) = \frac{1}{n} \sum_{i=1}^{n-j+1} (x_i - \mu_X)(x_{i+j-1} - \mu_X) \quad (3.10)$$

where  $x_i = X(z_i)$ ,  $\mu_X$  is the mean of  $X$ , and  $j \geq 1$  is an integer related to the separation distance  $\tau_j$  through:

$$\tau_j = (j - 1)\Delta z \quad (3.11)$$

where  $\Delta z$  is the minimum distance considered between any two consecutive points. Clearly, to a given value of  $j$  corresponds a value of  $\tau_j$  and to that a value of  $C$ . Figure 3.1 illustrates how data points that enter the summation of Equation 3.10 are determined for  $j = 4$ .

The auto-correlation  $\rho$  of the random field is given by:

$$\rho(\tau_j) = \frac{C(\tau_j)}{C(\tau_1)} \quad (3.12)$$

### 3.3.3 Stationarity

Suppose that a random process is at state  $x_i^*$  at time  $t_i$ , i.e.,  $X_i = X_{(t_i)} = x_i^*$ . The probability that, in the next step, the random process will be at state  $x_{i+1}^*$  is called the transition probability between  $i$  and  $i+1$  and is given:

$$p_{i,i+1} = P[X_{i+1} = x_{i+1}^* | x_i^*, X_{i-1} = x_{i-1}^*, \dots, X_1 = x_1^*, X_0 = x_0^*] \quad (3.13)$$

In a stationary Markov process, the future state of a random process is only dependent on the present state (and not at all dependent on the past), that is:

$$\begin{aligned} p_{i,i+1} &= P[X_{i+1} = x_{i+1}^* | X_i = x_i^*, X_{i-1} = x_{i-1}^*, \dots, X_1 = x_1^*, X_0 = x_0^*] \\ &= P[X_{i+1} = x_{i+1}^* | X_i = x_i^*] \end{aligned} \quad (3.14)$$

Stationarity implies that the one-step transition probability remains constant over time (or space). This means that, as an example, if the probability of going from state  $i$  in step 9 to state  $j$  in step 10 is 0.8, the probability of the random process to go from state  $i$  in step 900 to state  $j$  in step 901 will also be 0.8. The concept of stationarity is extensible to continuous-time (continuous-state) random processes as well.

*Stationarity* or *statistical homogeneity* means that the joint pdf of two random variables in a random process is independent of the absolute temporal or spatial positions of the two random variables: it only depends on the temporal or spatial separation. The strict stationarity assumption also implies that, the mean, covariance and higher order moments are constant over space (or time). A random process is said to be second-order stationary (exhibiting a stationarity that is sometimes referred to as weak stationarity) if the mean is constant over space or time, and the covariance is dependent only upon the separation distance of the random variables.

Various statistical tests have been used to assess stationarity of data [e.g., statistical runs test, Spearman's rank coefficient test, Kendall's tau test, modified Bartlett's statistic (MBS) test and modified Bartlett's statistic revised (MBSR) test]. In these tests, the stationarity assessment is made for a particular confidence level. Kendall's tau test (KTT) is one of the most widely used tests for stationarity assessment found in the literature.

KTT requires the calculation of a test statistic  $\tau$ , which is the measure of association within the sample (Daniel, 1990). The test statistic is given by:

$$\tau = \frac{P - Q}{n(n-1)/2} \quad (3.15)$$

where  $n$  is the number of observations,  $P$  is the number of observation pairs in natural order and  $Q$  is the number of observations in reverse natural order.

The numbers of observations in natural and reverse natural order are calculated in the following manner:

- Arrange the observations ( $X_i, Y_i$ ) in columns such that  $X$  increases from the top to the bottom.
- Compare each  $Y$  value with the  $Y$  value appearing below it. A pair of  $Y$  values is in natural order if the  $Y$  below is greater

than the  $Y$  above. The number of pairs in natural order  $P$  and the number of pairs in reverse natural order  $Q$  are counted.

KTT statistics range from  $+1$  to  $-1$ . It is  $+1$  when all the pairs are in natural order indicating perfect correlation. It is  $-1$  when all the pairs are in reverse natural order, indicating perfect inverse correlation. A KTT statistic close to zero indicates stationarity of the data. A KTT statistic value can be compared with a critical value associated with a confidence level (e.g., 95%) to determine whether there is stationarity (the critical KTT values are tabulated in, for example, Daniel, 1990). For a large number of observations ( $n > 40$ ), Daniel (1990) has recommended calculating a  $z$  value as:

$$z = \frac{3\tau\sqrt{n(n-1)}}{\sqrt{2(2n+5)}} \quad (3.16)$$

This  $z$  value is approximately normally distributed with mean 0 and variance 1. For 95% confidence level, if the absolute value of  $z$  is less than 1.96, the data can be assumed to be stationary.

### 3.3.4 Variance Function

Let  $X_T(t)$  be a random field obtained by local averaging of a random field  $X(t)$  over a window length  $T$ :

$$X_T(t) = \frac{1}{T} \int_{t-T/2}^{t+T/2} X(\eta) d\eta \quad (3.17)$$

The variance function  $\gamma = \gamma(T)$  is defined as the ratio of the (reduced) variance of  $X_T$  to the (original) variance of  $X$ :

$$\gamma(T) = \frac{\text{Var}[X_T(t)]}{\text{Var}[X(t)]} \quad (3.18)$$

The variance function drops from 1 as the window of local averaging  $T$  increases from zero (an infinitesimal length).

### 3.3.5 Scale of Fluctuation

A common measure of variability of a random process is the scale of fluctuation or correlation length, denoted by  $SF$  or  $\theta$ . The correlation length is the distance within which points are significantly correlated. Vanmarcke (1983) has defined  $\theta$  as:

$$\theta = \lim_{T \rightarrow \infty} T\gamma(T) \quad (3.19)$$

where  $\gamma = \gamma(T)$  is the variance function. The correlation length can also be calculated using the auto-correlation function. It can be shown that the correlation length is the area under the auto-correlation function  $\rho$ :

$$\theta = \int_{-\infty}^{\infty} \rho(\tau) d\tau = 2 \int_0^{\infty} \rho(\tau) d\tau \quad (3.20)$$

Correlation length is really only meaningful for strictly non-negative auto-correlation functions; since  $-1 \leq \rho \leq 1$ , one could conceivably have an oscillatory auto-correlation function whose integrated area is zero but which has significant correlations (positive or negative) over significant

distances (Fenton & Griffiths, 2008). For this reason, in order to calculate the correlation length, a non-negative auto-correlation model (e.g., exponential auto-correlation functions) is fit to the calculated correlation coefficient values, and the correlation length is then taken as twice the area under the correlation function curve (when the correlation function values are plotted against separation distances). Another practice is to consider only the positive area under the correlation function curve before it first becomes negative.

In the section in sequence, methods most often mentioned in the literature to estimate the scale of fluctuation are discussed.

### 3.3.6 Determination of the Scale of Fluctuation

**3.3.6.1 Methods based on the variance function.** The scale of fluctuation can be directly calculated using the definition of correlation length given by (Vanmarcke, 1983), that is, using Equation 3.19. In order to calculate the correlation length, first the variance of the data series is calculated. That is the reference variance. Subsequently, new data series are obtained by local averaging of the data series with increasing window lengths, and a new variance is calculated for the modified series obtained for each window length. As the window length increases, the variance of the local-averaged series decreases. The ratio of the new variance to the reference variance is, according to Equation 3.18, the variance function  $\gamma = \gamma(T)$ .

Variance function values are multiplied by the corresponding window lengths, and the results are plotted versus the window length. The first peak of the resultant plot is noted and the associated variance function times the window length value is taken as an estimate of the correlation length or scale of fluctuation. Figure 3.2 provides an example of this method.

A method proposed by Wickremesinghe (1989) relies on plotting the variance function (instead of the variance function times the window length) versus the window length.

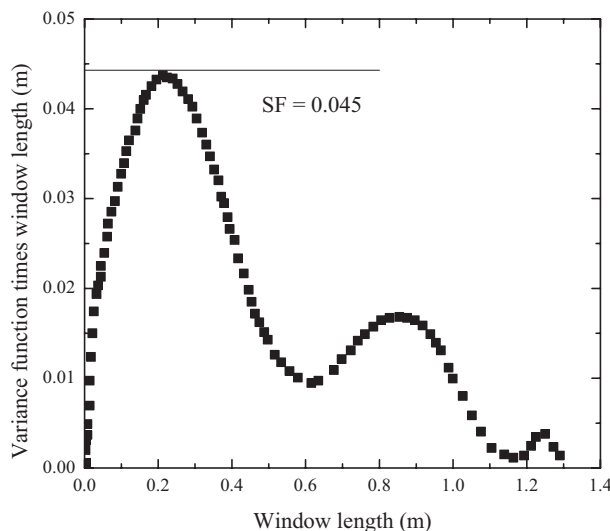


**Figure 3.2** Calculation of  $SF$  from variance function times window length.

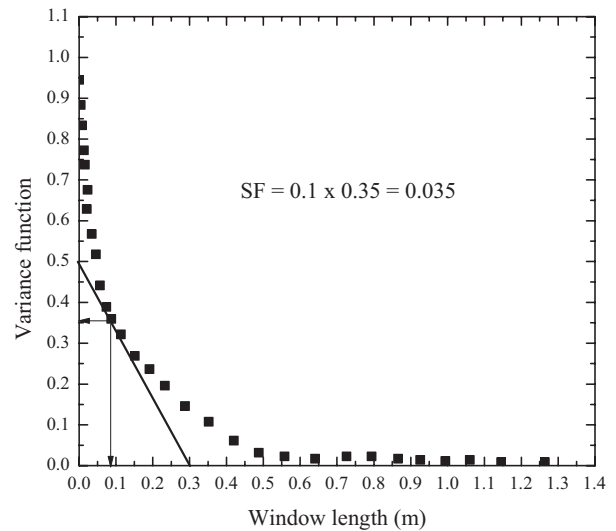


**Figure 3.3** Calculation of  $SF$  from variance function.

The window length corresponding to the point of maximum curvature on the plot is the scale of fluctuation. An example of this method is illustrated in Figure 3.3 for the same data of Figure 3.2.

**3.3.6.2 Direct integration of auto-correlation function over window length.** This method determines the correlation length directly from the experimental auto-correlation versus window length plot. Since the correlation length is only meaningful for strictly non-negative correlation functions (Fenton & Griffiths, 2008), it is generally taken as twice the positive area under the correlation function versus the separation distance plot before the correlation function value first becomes negative. In Figure 3.4, a correlation coefficient of a random variable versus window length is shown. The  $SF$  is equal to twice the positive area under the correlation curve. Also shown in the figure is an exponential fit to the values of

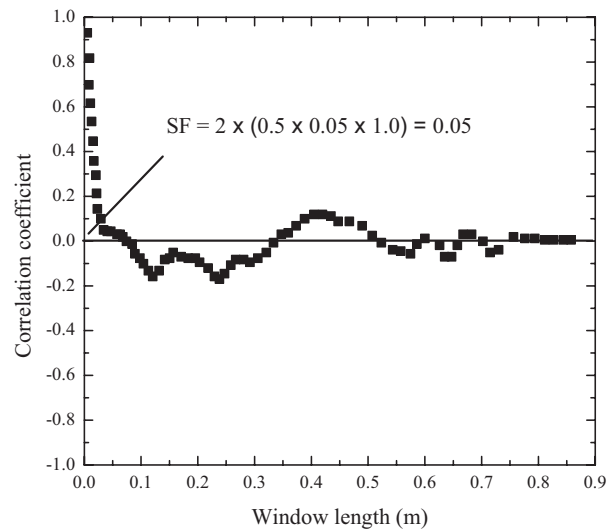


**Figure 3.4** Integration of auto-correlation function for  $q_c$ .

the auto correlation coefficient up to and including the first zero crossing, which could be used to perform the integration.

**3.3.6.3 Method based on integration of fit to auto-correlation data over separation distance.** Another procedure to obtain the correlation length is to fit an auto-correlation relationship to the plot of the auto-correlation coefficient versus separation distance. The correlation length can then be directly calculated by integrating the fitted correlation model following Equation 3.20. Some of the commonly used correlation models and the corresponding *SF* are shown in Table 3.1.

Figure 3.5 shows a  $q_c$  versus depth plot (data from CPT #6 performed at the McCormick site, to be discussed later in the report), along with examples of fitting an exponential and a squared exponential correlation coefficient relationship to the CPT data.

**3.3.6.4 Bartlett’s limit method.** The estimated auto-correlation coefficients become less reliable with increasing separation distances, and are deemed not significantly different from zero inside the Bartlett’s limit (Priestley, 1981; Brockwell & Davis, 1991; as cited in Uzielli, Vannucchi, & Phoon, 2005). The Bartlett’s limit  $l_B$  can be obtained from the number of available data points  $n_d$  using:

$$l_B = \frac{1.96}{\sqrt{n_d}} \quad (3.21)$$

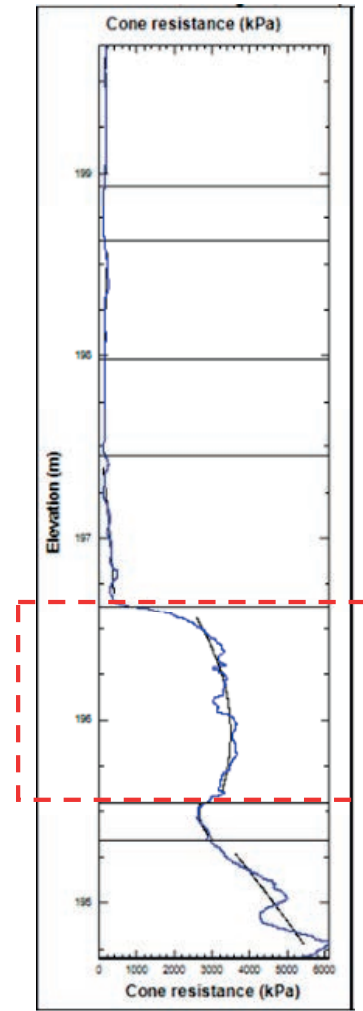
In the auto-correlation function versus window length plot, the window length at which the auto-correlation function first intersects the Bartlett’s limit is known as the Bartlett’s distance. Jaksa, Kaggwa, and Brooker (1999), working with Keswick clay, found that the scale of fluctuation can be approximated well by the Bartlett’s distance.

**3.3.6.5 Vanmarcke’s (1977) simplified method.** As shown in Figure 3.6, if a trendline is fit to the  $q_c$  versus depth (or elevation) plot, the trendline is crossed multiple times. The vertical distance between two crossings of the trendline will be referred to as the crossing distance. All the points between two crossings are on one side of the trend line and can be considered to be well correlated. Since the scale of fluctuation or correlation length also indicates a length within which data are strongly correlated, the crossing distances can be used to estimate the correlation length. Vanmarcke (1977) has shown that the scale of fluctuation may be estimated using:

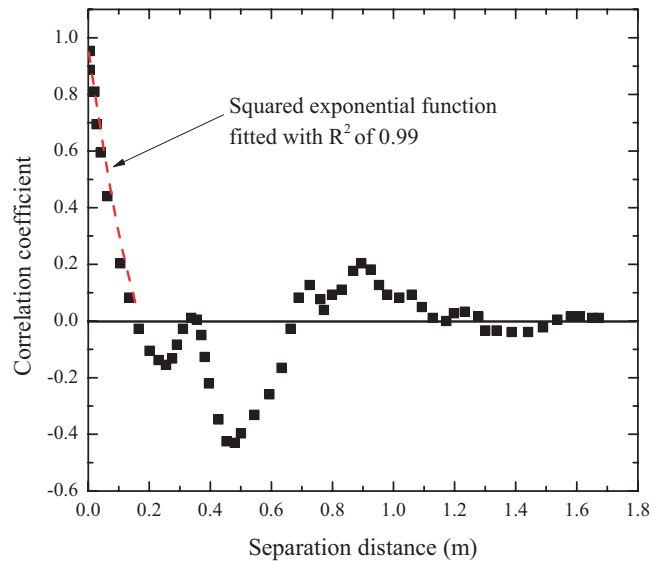
TABLE 3.1  
Auto-correlation function expressions and corresponding scale of fluctuation *SF*

Auto-Correlation Model	Equation	<i>SF</i>
Single exponential	$\rho(\Delta z) = \exp\left(\frac{-\Delta z}{a}\right)$	$2a^\#$
Squared exponential	$\rho(\Delta z) = \exp\left(-\left(\frac{\Delta z}{b}\right)^2\right)$	$b^\# \sqrt{\pi}$
Cosine exponential	$\rho(\Delta z) = \exp\left(\frac{-\Delta z}{c}\right) \cos\left(\frac{\Delta z}{c}\right)$	$c^\#$
Second-order Markov	$\rho(\Delta z) = \left(1 + \frac{\Delta z}{d}\right) \exp\left(\frac{-\Delta z}{d}\right)$	$4d^\#$

<sup>#</sup> Fitting parameters for correlation models



(a)



(b)

**Figure 3.5** Example of fitting of generic auto-correlation model: (a) cone resistance profile and (b) correlation coefficient vs. separation distance.

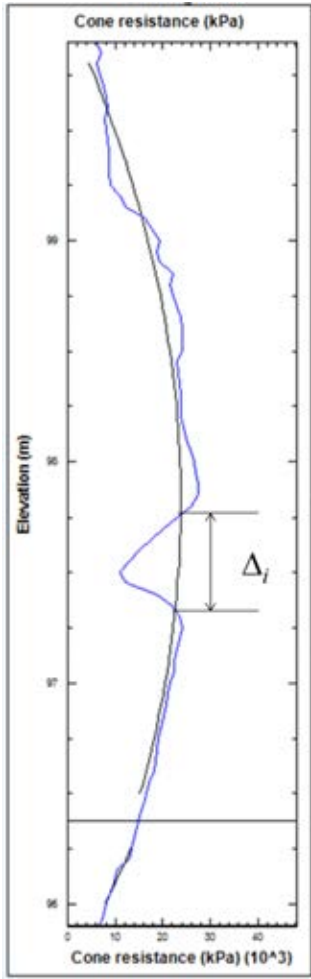


Figure 3.6 Vanmarcke's (1977) simplified method of calculating  $SF$ .

$$SF \approx \bar{\Delta} \sqrt{\frac{2}{\pi}}$$

$$\bar{\Delta} = \frac{1}{n_c - 1} \sum_{i=1}^{n_c} \Delta_i$$

where  $\tau_j = (j-1)\Delta z =$  separation distance,  $\Delta z =$  distance between adjacent data points,  $j$  ( $1 \leq j < n$ ) is an integer related to the separation distance, and  $n =$  number of data points considered in the calculation.

For a stationary random field, the semivariogram and covariance functions are related through:

$$2V(\tau) = \sigma^2 - C(\tau) \quad (3.25)$$

where  $\tau =$  separation distance,  $\sigma^2 =$  variance,  $V(\tau) =$  semivariogram function, and  $C(\tau) =$  covariance function.

Semivariogram models can be fitted to experimental semivariogram data to obtain the correlation length.

## 4. SITE VARIABILITY INDEX

### 4.1 Introduction

In order to quantify site variability, the following steps are required: i) soil profile generation, ii) quantification of vertical variability, iii) quantification of horizontal variability and iv) integration of vertical and horizontal variability into a site variability rating system (see Figure 4.1). The soil profile is obtained using an SBT chart, as discussed in chapter 2. Once the soil profile is established, the vertical variability index  $VVI$ , which reflects variability in  $q_c$ ,  $f_s$ , layering and other factors for each CPT sounding, and the horizontal variability index  $HVI$ , which is based on the cross-correlation between cone resistance logs, cone resistance trend differences and the spacing between every pair of CPTs, are calculated. Taking into account both of these indices, the variability of the site is established according to a site variability rating system that produces a number SVR that takes values between 0 and 1 (or 0 and 100%).

$$SF \approx \bar{\Delta} \sqrt{\frac{2}{\pi}} \quad (3.22)$$

where

$$\bar{\Delta} = \frac{1}{n_c - 1} \sum_{i=1}^{n_c} \Delta_i \quad (3.23)$$

is the average crossing length,  $\Delta_i =$  individual crossing lengths and  $n_c =$  number of crossings.

**3.3.6.6 Method based on fitting semivariogram models.** A concept similar to the auto-correlation coefficient is the semivariogram. In contrast to the auto-correlation coefficient, which measures the degree of correlation between data points separated by some separation distance, the semivariogram function  $V(\tau)$  measures the lack of correlation between data points. The semivariogram is defined as half of the expected value of the squared differences between points separated by a specific distance:

$$V(\tau_j) = \frac{1}{2(n-j)} \sum_{i=1}^{n-j} (x_{i+j} - x_i)^2 \quad (3.24)$$

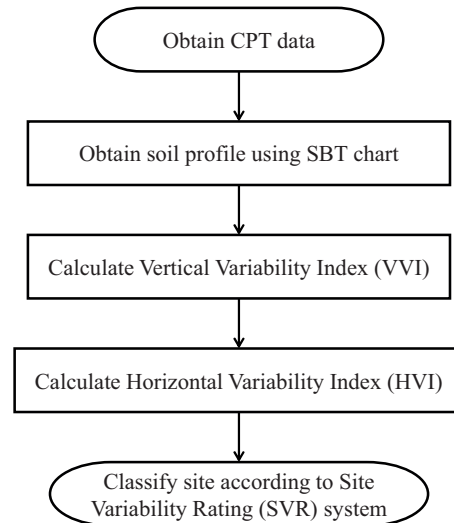
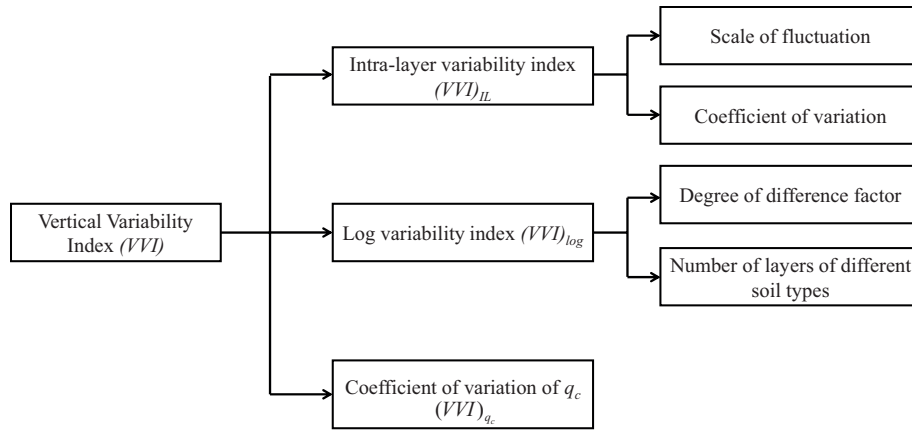


Figure 4.1 Soil variability analysis.



**Figure 4.2** Vertical variability index calculation.

## 4.2 Vertical Variability Index

The vertical variability index  $VVI$  of a CPT sounding is calculated based on an analysis of the soil profile combined with the CPT data. Figure 4.2 shows how the  $VVI$  is calculated. The vertical variability index of a sounding has three components: i) the intra-layer variability index  $(VVI)_{IL}$ , ii) the log variability index  $(VVI)_{log}$  and iii) the  $(VVI)_{qc}$ , which is calculated based on the coefficient of variation of the  $q_c$  of the sounding. The  $(VVI)_{IL}$  is calculated from the scale of fluctuation and coefficient of variation of  $q_c$  and  $f_s$  of each soil layer in the soil profile length being considered. The  $(VVI)_{log}$  attempts to capture the vertical variability of the soil profile introduced by the observed layering. The  $(VVI)_{qc}$  is related to the coefficient of variation calculated for all  $q_c$  values of the sounding or of the soil profile length being considered.

The sounding  $VVI$  is calculated for each of the CPT soundings available at a given site (indicating the vertical variability along the soil profile length considered in the calculations). The site  $VVI$ , which is the average of the  $VVI$ s for all the CPT soundings, reflects the variability in the vertical direction for the entire site. As shown in Figure 4.1, after the site  $VVI$  calculation, a site  $HVI$ , which indicates the site variability in the horizontal direction, is calculated.

In determining the length of the CPT sounding to analyze, the intended geotechnical application should be considered. For roadway applications, a depth of a few meters from the ground surface would be sufficient. For shallow foundations, a multiple of foundation width ranging from one for bearing capacity calculations to as much as four for settlement calculations would need to be considered. For deep foundations, the length of the pile plus five times the pile diameter for single piles or group width for pile groups would be needed. Site variability, therefore, is inextricably linked to the depth of interest for the particular application being contemplated.

Typically, at each site, the depth reached in each CPT sounding is different and depends on specific soil conditions at each given location. In site variability calculations, the soundings must be processed so that the same length of

sounding is being considered in site  $VVI$  calculations. Additionally, comparison across sites, as already stated, are only possible for the same soil profile length. The common soil profile length can be established in different ways. Usually, the same initial and final elevation would define this common elevation range but a different approach, such as using geological information to establish different top and bottom elevations for each sounding (while always maintaining the same soil profile length), would also be possible.

Figure 4.3, Figure 4.4, Figure 4.5 and Figure 4.6 show the various steps that need to be followed to calculate a site vertical variability index. As shown in Figure 4.3, the site  $VVI$  calculation involves calculation of the  $VVI$ s of all of the CPTs available at a site. Figure 4.4 shows the algorithm to calculate  $VVI$  for a particular CPT sounding. Figure 4.5 provides the steps required for the calculation of the intra-layer variability index, which requires detrending of the CPT data first. Figure 4.6 shows the detrending procedure.

### 4.2.1 Consideration of Sensing and Development Distances

As discussed in Chapter 2, the cone can sense not only the soil in its immediate vicinity but also the soil ahead of and behind it. These distances are known as the sensing and development distances (Arshad et al., 2014). As a result, CPT data within the sensing and development distances should be discarded when strict adherence to values that apply only to that layer is desired. In this research, the cone sensing and development depths were considered to be equal to twice the cone diameter ( $\approx 7$  cm), so, for each soil layer of the soil profile, the CPT data within 7 cm from either layer boundary were discarded in the CPT sounding  $VVI$  calculations. If the sum of the sensing and development lengths ( $= 4$  cone diameters  $\approx 14$  cm) were discarded from the top and bottom of a thin layer of thickness of 15 cm, there would be no data left to process. Therefore, the sensing and development lengths are discarded only when the layer thickness is greater than 30 cm (all the data is used in calculations for layers with thickness less than 30 cm).

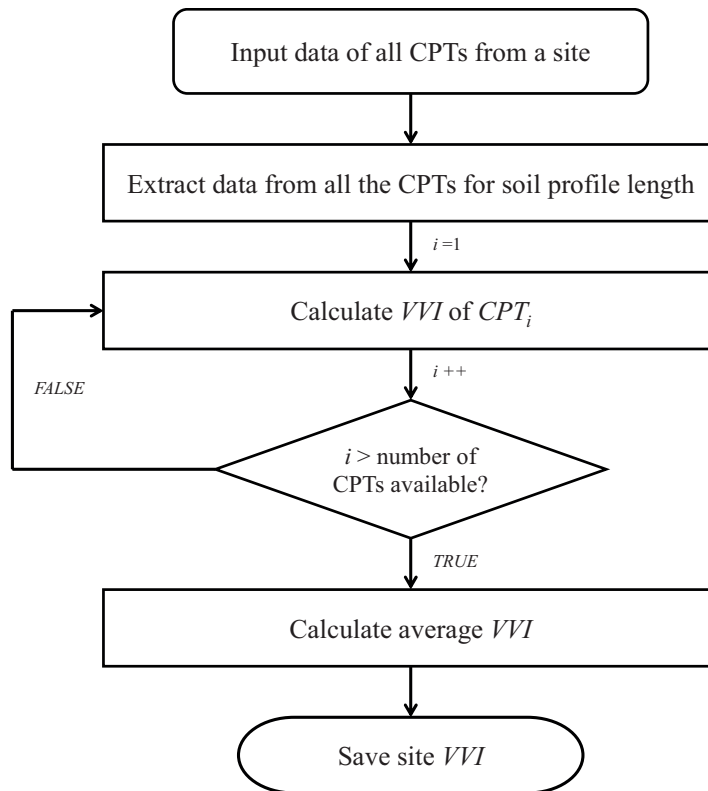


Figure 4.3 Calculation of site vertical variability index.

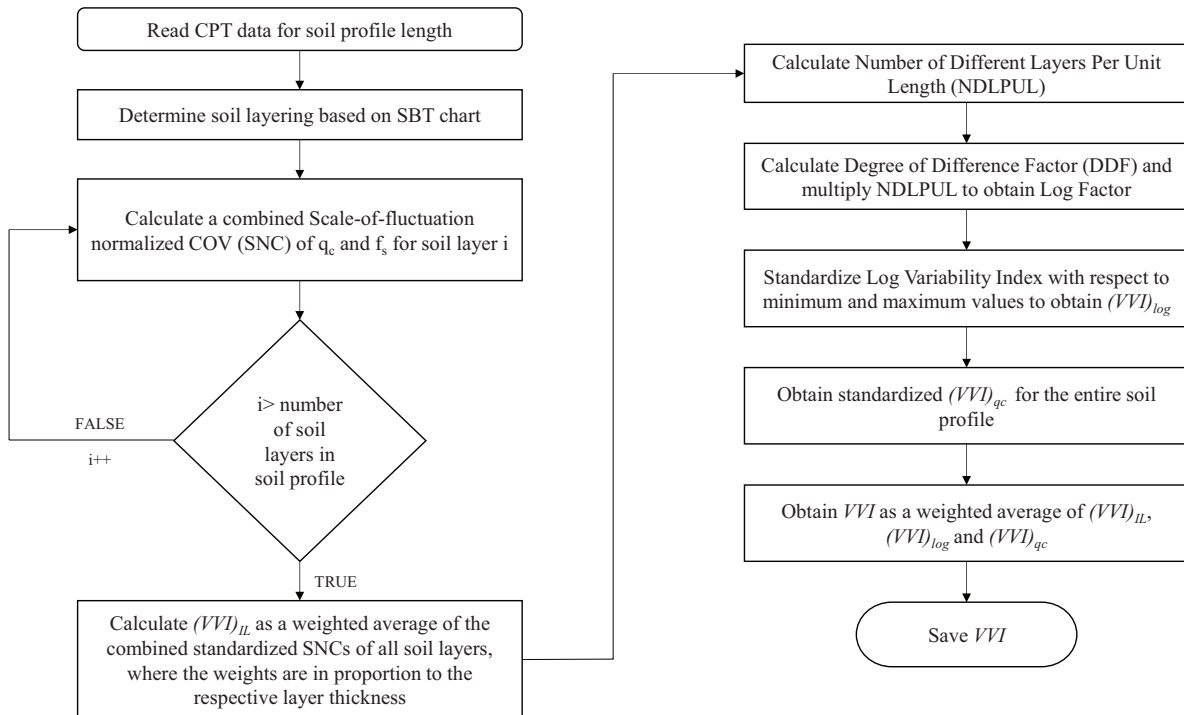


Figure 4.4 Calculation of VVI.

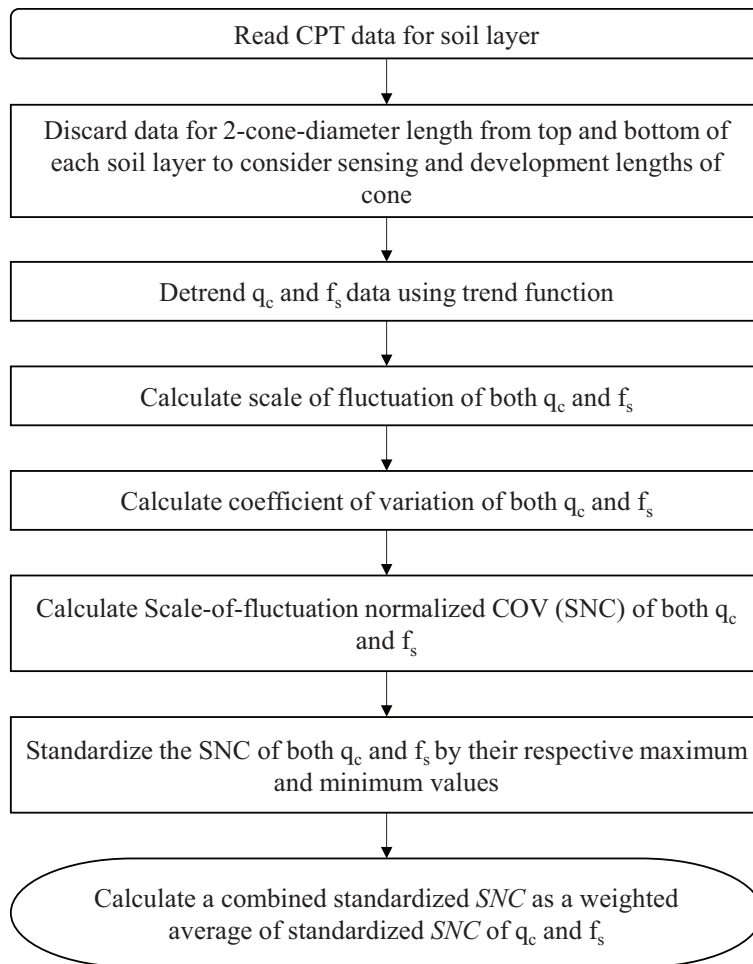


Figure 4.5 Calculation of  $(VVI)_{IL}$ .

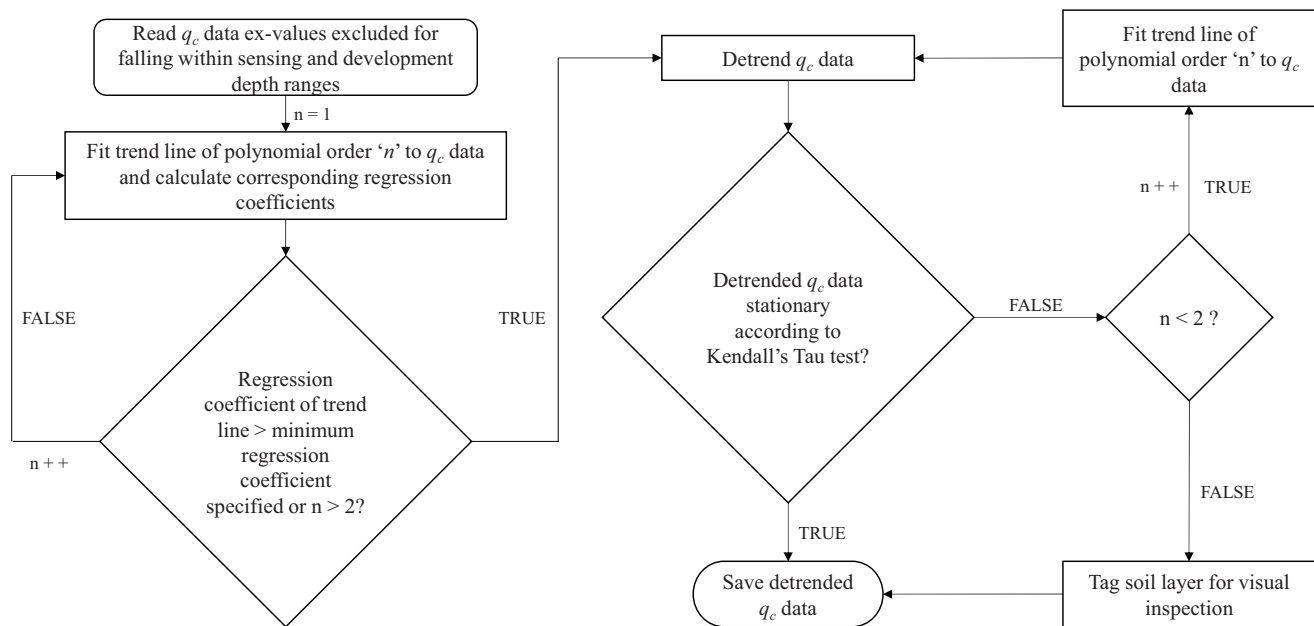


Figure 4.6 Detrending of  $q_c$  data.

The CPT data considered in the variability analysis are from two sources: INDOT CPT data and CPT data collected using Purdue’s CPT truck. INDOT CPT data was recorded every 5 cm of cone penetration, while the CPT data collected using Purdue’s CPT truck were recorded at every 2 mm of cone penetration. Therefore, compared to the INDOT CPT data, for a unit of length, about 25 times more data points were collected in the case of the Purdue database. For a layer thickness of 15 cm (the minimum layer thickness considered in this research), there are 76 CPT data points in the Purdue database, while there are only 4 CPT data points for the INDOT database.

#### 4.2.2 Fit of a Trend Function and Calculation of Scale of Fluctuation and Coefficient of Variation within a Layer

Trend functions are required to detrend the  $q_c$  and  $f_s$  data of each soil layer. Detrending of CPT data is necessary to make it stationary, as explained in section 3.3.3. Figure 4.6 shows the algorithm used to detrend  $q_c$  data. Polynomials of different orders are considered as trend functions. The higher the order of the polynomial used to detrend the data, the less the variability of the data with respect to the trendline. For this reason, a maximum polynomial of order 2 is used to detrend the data in this research.

First, an attempt is made to fit a polynomial of order 1 to the data. The regression coefficient  $R$  is calculated. If the  $R$  value is less than 0.85, a polynomial of order 2 will be required. A polynomial of order 2 is also required if the first fit attempt fails the Kendall Tau test (KTT) discussed in Chapter 3. The KTT with 5% significance

level was used in this research. In most cases, either a straight line or a parabola will fit the data satisfactorily; if not, data are tagged for visual inspection. Once the trend has been fit to the data, the scale of fluctuation is determined using Vanmarcke’s (1977) simplified method (see Chapter 3) and the coefficient of variation is calculated as described next.

Suppose, a function  $x = f(z)$  represents the relationship between two random variables  $X$  and  $Z$  ( $X$  could represent  $q_c$  and  $Z$  could represent depth, for example). The COV of  $X$  can be calculated as:

$$COV_X \approx \sqrt{\frac{\sum_{i=1}^n \left(\frac{x_i - f(z_i)}{f(z_i)}\right)^2}{(n-1)}} = \sqrt{\frac{\sum_{i=1}^n (w_i^*)^2}{n-1}} \quad (4.1)$$

where  $n$  = number of data points and  $w^*$  = normalized error.

Considering that  $f(z) = E(X)$  and the average of the normalized error  $\bar{w}^* = 0$ , we obtain:

$$COV_X = \sqrt{\frac{\sum_{i=1}^n (w_i^* - \bar{w}^*)^2}{n-1}} = \sigma_{w^*} \quad (4.2)$$

#### 4.2.3 Intra-Layer Variability

Intra-layer variability appears as either oscillations of the dependent variable around the trend, which is captured by the coefficient of variation, or by the frequency with which these oscillations occur (which is captured by the scale of fluctuation). Figure 4.7(a) and (b) show idealized plots of  $q_c$  vs. depth. The scale of fluctuation of  $q_c$  in Figure 4.7(a) is smaller than that in Figure 4.7(b) (which would be suggestive of higher variability), but its coefficient of variation is also lower (suggesting lower variability). This example illustrates

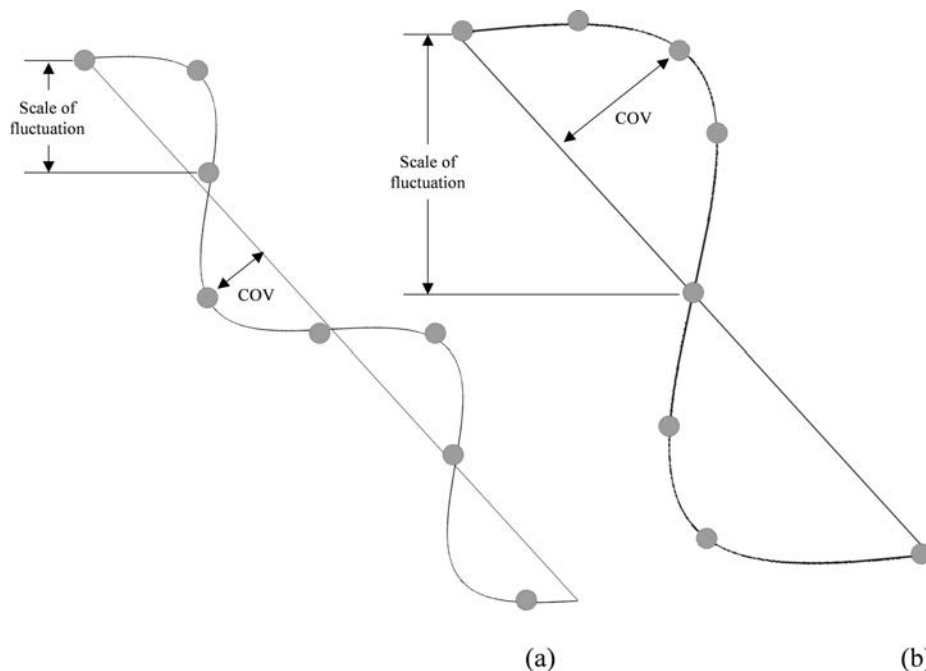


**Figure 4.7** Idealized plots of  $q_c$  vs. depth: (a) low SF with low COV and (b) high SF with high COV.

TABLE 4.1  
Maximum and minimum values of  $SF$  (modified after Uzielli et al., 2007)

Property	Notation	Soil type	Testing Method	$SF$ (m)
Cone tip resistance	$q_c$	Sand, clay	CPT	0.1–3.0
Cone tip resistance	$q_c$	Offshore soils	CPT	0.3–0.4
Corrected cone tip resistance	$q_t$	Clay	CPTU	0.2–0.5
Dimensionless, stress-normalized cone tip resistance	$qc1N$	Fine-grained soils	CPT	0.1–0.6
Dimensionless, stress-normalized cone tip resistance	$qc1N$	Intermediate soils	CPT	0.3–1.0
Dimensionless, stress-normalized cone tip resistance	$qc1N$	Coarse-grained soils	CPT	0.4–1.1
Sleeve resistance	$f_s$	Sand	CPT	1.3
Sleeve resistance	$f_s$	Deltaic soils	CPT	0.3–0.4
Stress-normalized friction ratio	$FR_n$	Fine-grained soils	CPT	0.1–0.5
Stress-normalized friction ratio	$FR_n$	Intermediate soils	CPT	0.1–0.6
Stress-normalized friction ratio	$FR_n$	Coarse-grained soils	CPT	0.2–0.6

that, to quantify variability of a layer, we must consider both the scale of fluctuation and the standard deviation. The way we do that is to define the scale-of-fluctuation normalized COV, denoted as  $SNC$ , which is obtained simply from:

$$SNC = \frac{COV}{SF} L_R \quad (4.3)$$

where  $L_R$  = reference length (1m, 3.281ft or equivalent in other units).

The  $VVI$  (see Figure 4.2) is a weighted average of three separate variability indices: an intra-layer component, a log component and a component related to the COV of  $q_c$ . The three components must be normalized before the average is taken so that each is a number between 0 and 1 (or, equivalently, a percentage between 0 and 100%). In order to standardize the  $SNC$ , maximum and minimum values of  $SNC$  are required.

#### 4.2.4 Minimum and Maximum Values of $SNC$ and $(VVI)_{IL}$

Researchers have calculated  $SF$  for different soil parameters and for different soil types. Table 4.1, modified after (Uzielli, Lacasse, & Nadim, 2007), shows ranges of  $SF$  values calculated in the vertical directions for different soil types. The  $SF$  of  $q_c$  and  $f_s$  ranges from 0.1 to 3 m. Jaksa et al. (1999) worked with Keswick clay layers and found that the  $SF$  of  $q_c$  ranged from 63 to 255 mm, with a mean of 151 mm, while the COV of  $q_c$  was around 30%. Table 4.2, modified after Phoon and Kulhawy (1999), shows COV of  $q_c$  for different soil types; the COV of  $q_c$ , according to these authors, is quite large, ranging from less than 20% to 60%. However, the table suggests that the COV of  $q_c$  is greater in sand than in clay. For a uniform sand layer, Foye (2005)

TABLE 4.2  
Maximum and minimum values of COV of cone resistance (modified after Phoon & Kulhawy, 1999)

Test Type	Property	Soil Type	Mean (MPa)	COV (%)
CPT	$q_t$	Clay	0.5–2.5	<20
	$q_c$	Clay	0.5–2.0	20–40
	$q_c$	Sand	0.5–30.0	20–60

reported COV of  $q_c$  of about 8%, while Foye, Salgado, and Scott (2006) reported COV of  $q_c$  for clay of about 6%.

Table 4.3 shows the maximum and minimum  $SF$ , COV and  $SNC$  values of  $q_c$  and  $f_s$  used in this research for standardization purposes. Regardless of soil type, the maximum value of  $SF$  of both  $q_c$  and  $f_s$  was taken as 2 m; the minimum value of  $SF$  of  $q_c$  was taken as 50 mm, while that of  $f_s$  was taken as 40 mm. The maximum value of COV for  $q_c$  was taken as 15%, while that of  $f_s$  was taken as 20%. The minimum COV of  $q_c$  and of  $f_s$  was taken as the theoretical minimum, i.e., 0%. We assumed slightly higher maximum COV value for  $f_s$  in comparison to that of  $q_c$  and slightly lower minimum  $SF$  value for  $f_s$  in comparison to that of  $q_c$  is because  $f_s$  data is less reliable (more variable) than  $q_c$  data. In order to calculate the maximum  $SNC$  value for  $q_c$ , the maximum COV is divided by the minimum  $SF$  and then multiplied by the reference length of 1 m. When processing a CPT sounding,  $SNC$  values are capped by the maximum  $SNC$  value. The combined  $SNC$  value is the weighted average of the  $SNC$ s of  $q_c$  and  $f_s$ ; an 80% weight is given to the  $SNC$  of  $q_c$  and a 20% weight to the  $SNC$  of  $f_s$ .

The intra-layer  $VVI$ , before normalization, is calculated as a weighted average of the  $SNC$ s of all the layers of the segment of the soil profile being considered. The weights for the  $SNC$  values of each layer are the soil layer thicknesses.

#### 4.2.5 Calculation of the Log Variability Index

The  $(VVI)_{IL}$ , discussed in the previous section, takes into account the intra-layer variability of the soil profile through the  $SNC$ . The overall variability of the soil profile also depends on inter-layer variability; it is addressed by considering:

TABLE 4.3  
Minimum and maximum  $SF$ , COV and  $SNC$  values

	$q_c$			$f_s$		
	$SF$ (m)	COV (%)	$SNC$	$SF$ (m)	COV (%)	$SNC$
<b>Min.</b>	0.05	0	0	0.04	0	0
<b>Max.</b>	2	15	15/0.05 = 300	2	20	20/0.04 = 500

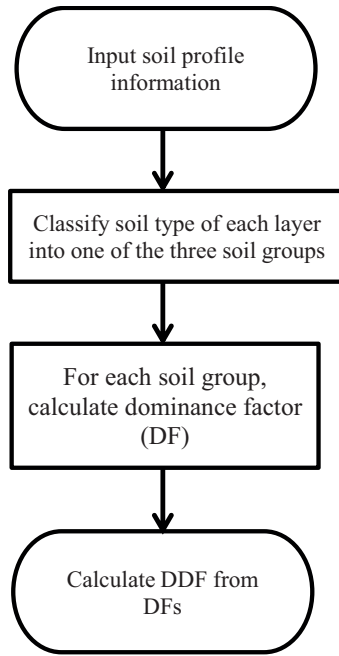


Figure 4.8 Flow diagram showing calculation of DDF.

1. the number of layers along the soil profile per unit length of soil profile;
2. the ratio of the number of different soil layer types to the total number of soil layers; and
3. the dominance of any particular soil group (the broad soil groups are shown in Table 2.5 for the modified Tumay (1985) SBT chart and in Table 2.6 for the modified Robertson (1990) chart, respectively).

The log  $VVI$  is calculated from the number of soil layers of different types in the soil profile and the degree of difference factor  $DDF$ , which accounts for the dominance of any particular soil group. A simple flow diagram in Figure 4.8 shows how to calculate the  $DDF$ . The dominance factor  $DF$  of each soil group is first calculated by dividing the total number of soil layers of that group by the total number of layers in the soil profile:

$$DF_i = \frac{N_i}{N} \quad (4.4)$$

where  $DF_i$  is the dominance factor of the  $i^{th}$  group,  $N$  is the number of layers in a soil profile,  $N_i$  is the total number of layers of the  $i^{th}$  group in the soil profile, and  $i = s, c$  and  $ms$ , where  $s = \text{sand}$ ,  $c = \text{clay}$  and  $ms = \text{mixed soils}$ .

The degree of difference factor  $DDF$  is given by:

$$DDF = \frac{1}{SD(DF_s, DF_c, DF_{ms})} \quad (4.5)$$

where  $SD$  is the standard deviation.

A low  $DDF$  value indicates high dominance of a particular soil group and therefore low vertical variability of the soil profile.

The  $(VVI)_{log}^*$ , before normalization, is calculated as:

$$(VVI)_{log}^* = (DDF)(NDLPUL) \quad (4.6)$$

TABLE 4.4  
Minimum and maximum values of DDF and NDLPUL for the modified Tumay (1985) and Robertson (1990) charts

	Modified Tumay (1985)		Modified Robertson (1990)	
	NDLPUL	DDF	NDLPUL	DDF
Min.	0.1	2.12	0.1	2.12
Max.	6.7	18.4	6.7	4.2

where  $NDLPUL$  = number of different layers per unit length.

#### 4.2.6 Standardization of Log VVI

As for the other indices, the objective of standardization of the log  $VVI$  is to have it range from 0 to 100%. The  $(VVI)_{log}$  has two components:  $DDF$  and  $NDLPUL$ . Therefore, the minimum and maximum value of the  $(VVI)_{log}$  depends on the minimum and maximum values of  $DDF$  and  $NDLPUL$ . The maximum value of  $NDLPUL$  is 6.7 (=  $L_R/\text{minimum layer thickness} = 100/15$ ). The minimum value of  $NDLPUL$  occurs when we have one thick soil layer. In this research, the minimum  $NDLPUL$  is taken as 0.1 (which would be the value of  $NDLPUL$  for a profile consisting of a single soil layer with a thickness of 10m).

The minimum value of  $DDF$  is obtained when all layers of a soil profile belong to only one soil group (say, sand). Hence, the dominance factor of sand is one, while for clay and mixed soil it is zero. The resultant  $DDF$  is 2.12. Therefore, the minimum value of  $DDF$  for both the modified Tumay (1985) and Robertson (1990) is 2.12, as shown in Table 4.4.

To obtain a realistic maximum value of  $DDF$ , the SBT charts are considered. For example, for the modified Tumay (1985) chart, there are a total of 15 different soil types: 5 belong to the sand soil group, 6 to the clay soil group and the remaining 4 to the mixed soil group. We can construct an idealized soil profile that has 15 different soil layers. Each of these soil layers has one of the 15 different soil types in the modified Tumay (1985) chart. This soil profile can be considered to have almost equal dominance of all three soil groups. For this soil profile, the maximum value of  $DDF$  is 18.4. Now, doing the same for the modified Robertson (1990), there are 15 different soil types, with 10 soil types belonging to the sand soil group, 2 belonging to the clay soil group and 3 belonging to the mixed soil group, which leads to a  $DDF$  of 4.2 if each of the 15 layers is assumed to be of a different soil type. This low value of  $DDF$  (compared to what was obtained from the modified Tumay, 1985) is influenced by the greater number of different soil types belonging to the sand soil group. Table 4.4 provides the maximum and minimum values of  $NDLPUL$  and  $DDF$  discussed so far.

Table 4.5 shows the maximum and minimum values of the product of  $NDLPUL$  by  $DDF$ . The minimum values of  $NDLPUL$  and  $DDF$  are the same for both the modified Tumay (1985) and Robertson (1990) charts. These values are also the same values shown in Table 4.4. However, the maximum values of  $NDLPUL$  and  $DDF$  are reduced from

TABLE 4.5  
Minimum and maximum values of DDF and NDLPUL

	Modified Tumay (1985) Chart			Modified Robertson (1990) Chart		
	NDLPUL	DDF	(NDLPUL) (DDF)	NDLPUL	DDF	(NDLPUL) (DDF)
Min.	0.1	2.12	0.212	0.1	2.12	0.212
Max.	3	10	30	2	5	10

the maximum values given in Table 4.5 to obtain more realistic limits. These limits are also set to adjust for the fact that the Robertson (1990) chart has an unbalance between the number of soils considered to be clay or mixed soil versus sand.

Whenever the calculated value of the log  $VVI$  is less than the minimum or greater than the maximum values given in Table 4.5, the calculated value is replaced by the minimum or the maximum values.

#### 4.2.7 Calculation of the COV of $q_c$ of Soil Profile

The  $(VVI)_{log}$  does not fully reflect the variability in a sounding. For example, the  $DDF$  component would treat the transition of a loose sand layer to a soft clay layer the same way it would the transition of a very dense layer to a very soft clay layer. We need, as a result, also to consider the most important source of variability across layers, which is that of  $q_c$ . In order to address this, a direct calculation of COV of  $q_c$  of the entire soil profile is made. To standardize the COV of  $q_c$ , thereby obtaining  $(VVI)_{q_c}$ , a maximum COV of  $q_c$  for the particular length of soil profile under consideration is used.

**4.2.7.1. Calculation of maximum COV of  $q_c$  of sounding.** In order to calculate the maximum value  $[COV(q_c)]_{max}$  of the COV of the cone resistance for a sounding, an idealized, highly variable soil profile is considered, as shown in Figure 4.9. The idealized soil profile must have high standard deviation and low mean value of  $q_c$ . A soil profile containing mostly a reasonably soft clay layer and a thin sand layer would fit this requirement. The thickness of this clay layer is allowed to change, which lets us analyze soil profiles of various thicknesses. The sand layer thickness remains the same (0.5 m) for all soil profile thicknesses considered. All soil profiles are somewhat over-consolidated (a surcharge of 100 kPa is assumed to have been applied and then removed, with consolidation allowed). The plot of maximum  $COV_{q_c}$  vs the length of soil profile is shown in Figure 4.10 and in tabular form in Table 4.6. Depending on the length of soil profile considered in the analysis, the maximum  $COV_{q_c}$  is chosen accordingly.

#### 4.2.8 Calculation of VVI and site VVI

The  $VVI$  of a sounding is calculated as:

$$VVI = w_{log}(VVI)_{log} + w_{IL}(VVI)_{IL} + w_{q_c}(VVI)_{q_c} \quad (4.7)$$

where  $w_{log}$ ,  $w_{IL}$  and  $w_{q_c}$  are the weights assigned to each of the three components of the  $VVI$  (0.2, 0.3 and 0.5 were used,

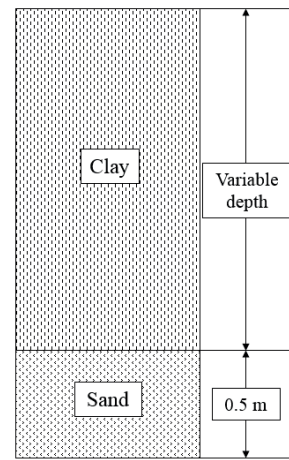


Figure 4.9 Idealized soil profile for calculation of  $[COV(q_c)]_{max}$ .

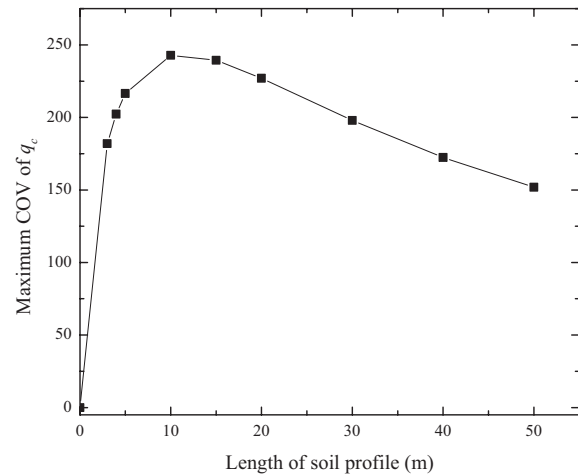


Figure 4.10 COV of  $q_c$  versus length of soil profile.

TABLE 4.6  
COV results for soil profile having sand at top followed by clay layers below

Length of Soil Profile	Soil Layer Type in the Bottom 0.5 m	Soil Layer Type on Top of Sand Layer	Standard Deviation	Mean (kPa)	COV (%)
3	Sand	Clay	2396	1317	181
4	Sand	Clay	2425	1198	202
5	Sand	Clay	2434	1124	216
10	Sand	Clay	2413	993	242
15	Sand	Clay	2380	994	239
20	Sand	Clay	2352	1036	227
30	Sand	Clay	2314	1169	197
40	Sand	Clay	2293	1330	172
50	Sand	Clay	2285	1504	151

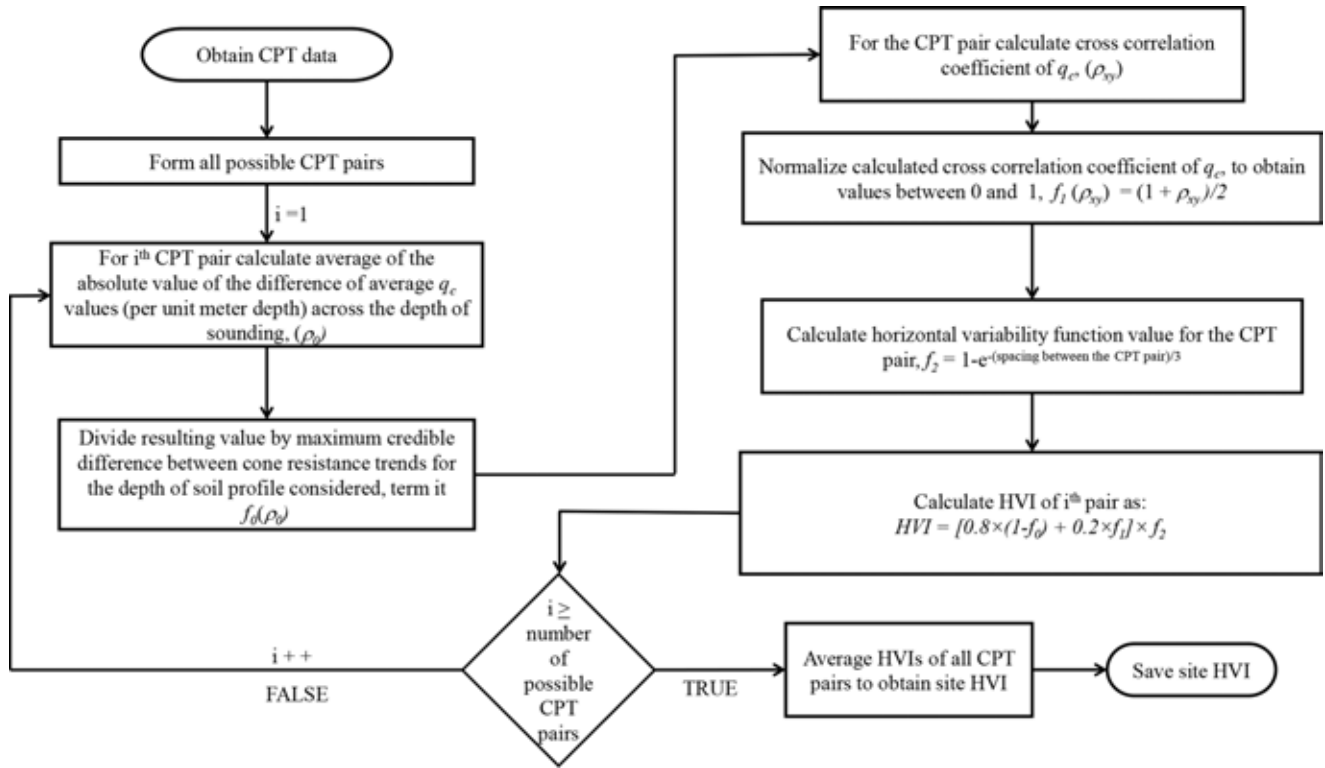


Figure 4.11 HVI calculation.

respectively). The site *VVI* is calculated as the average of all the *VVIs* obtained for all the CPTs available for a site.

### 4.3 Horizontal Variability Index

The horizontal variability index is calculated in terms of how well  $q_c$  correlates across soundings. Figure 4.11 shows how the *HVI* is obtained. First, pairs of CPT soundings are formed from the available CPTs. For every pair of CPTs,

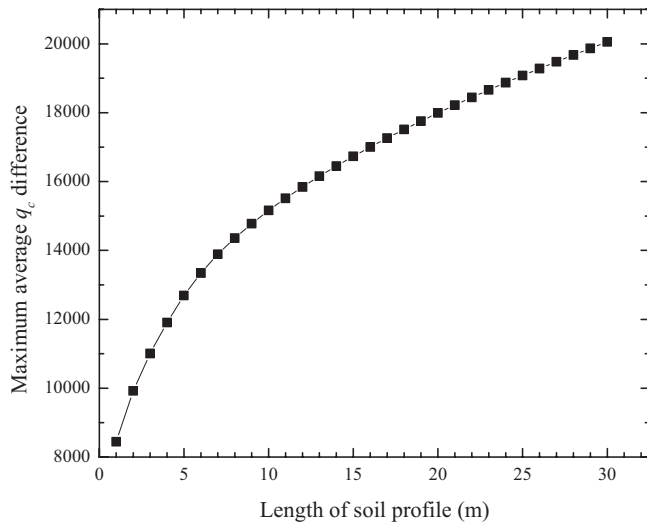


Figure 4.12 Maximum average  $q_c$  difference versus length of soil profile.

two quantities are computed for the cone resistance: a measure of the difference between the trends of cone resistance  $q_c$  with depth (denoted here as  $|\Delta q_{c,avg}|$ ) and the cross-correlation coefficient of  $q_c$ .

In order to quantify the difference between the  $q_c$  trends, the absolute value of the average difference is calculated for depth increments of one meter, and the average of these values are then calculated. The resulting value is then divided by the maximum credible difference between cone-resistance trends for the depth of soil profile considered. This maximum value is obtained by considering two idealized soil profiles, one with an extremely soft clay layer throughout, and one with a sand with 85% relative density throughout. The resulting values in the difference between trends is shown in Figure 4.12.

The variability associated with differences between the cone resistance trends can be expressed by the ratio  $\rho_0 = \rho_0(|\Delta q_{c,avg}|)$ :

$$\rho_0(|\Delta q_{c,avg}|) = \frac{|\Delta q_{c,avg}|}{|\Delta q_{c,avg}|_{\max}} \quad (4.8)$$

Calculation of the cross-correlation coefficient requires first the calculation of the cross-covariance. The cross-covariance  $C_{xy}$  of two signals  $X$  and  $Y$ , each containing  $N$  points, can be calculated as:

$$C_{xy} = \frac{1}{N} \sum_{i=0}^{N-1} (x_i - \bar{x})(y_i - \bar{y}) \quad (4.9)$$

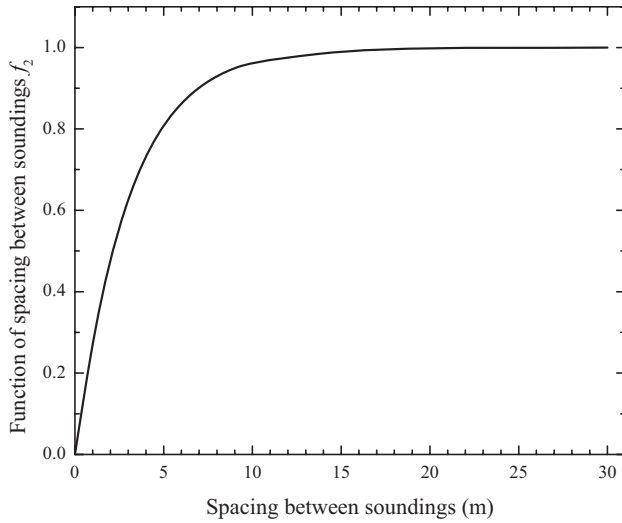


**Figure 4.13**  $f_2(s)$  function of spacing between soundings.

The cross-correlation coefficient  $\rho_{xy}$  is then calculated from:

$$\rho_{xy} = \frac{C_{xy}}{\sigma_x \sigma_y} \quad (4.10)$$

where  $\sigma_x$  and  $\sigma_y$  are the standard deviations of  $X$  and  $Y$ . The cross-correlation coefficient takes values in the  $-1$  to  $+1$  range. We need an index that takes values between 0 and 1 or 0 and 100% that is related to the cross-correlation coefficient. The function  $f_1(\rho)$ , defined below, is just such a function:

$$f_1(\rho) = \frac{\rho + 1}{2} \quad (4.11)$$

Once the cross-correlation coefficient of  $q_c$  has been calculated, a weighted average of it, with weight of 20%, and the trend difference  $|\Delta q_{c,avg}|$ , with weight of 80%, is calculated. The only missing component in an  $HVI$  calculation is the distance between the soundings.

A high cross-correlation value and small trend difference of a CPT pair indicates high correlation and similarity between the two CPTs, and this suggests low variability in the horizontal direction for the site. However, two nearby CPTs will naturally have a high cross correlation value and a small cone resistance trend difference. Therefore, we need to take the spacing  $s$  between CPT soundings into account when calculating the  $HVI$  from trend difference and cross-correlation coefficient values. To calculate the  $HVI$ , a horizontal variability function  $f(|\Delta q_{c,avg}|, \rho, s)$  is formed to take into account both the variability measures (difference in

cone resistance trends and cross correlation) and the spacing between the CPT soundings:

$$f(|\Delta q_{c,avg}|, \rho, s) = [0.8 \times \{1 - f_0 \times (|\Delta q_{c,avg}|)\} + 0.2 \times f_1(\rho)] \times f_2(s) \quad (4.12)$$

The function  $f_2(s)$  is formulated to decay towards zero as the spacing approaches zero:

$$f_2(s) = 1 - e^{-\frac{s}{3}} \quad (4.13)$$

meaning that horizontal variability must not be considered low if the spacing is very small. Figure 4.13 shows the plot of  $f_2(s)$ . It can be seen to be approximately equal to 1 for spacings exceeding 15 m, which is considered sufficient for the cross-correlation coefficient to render a strong indication of whether variability exists in the horizontal direction without any correction.

The  $HVI$  is calculated based on the average of the horizontal variability function  $f(|\Delta q_{c,avg}|, \rho, s)$  for all CPT pairs at the site:

$$HVI = 1 - \frac{\sum_{i=1}^n f(|\Delta q_{c,avg}|_i, \rho_i, s_i)}{n} \quad (4.14)$$

It takes values between 0 and 1.

#### 4.4 Optimal CPT Sounding Spacing Calculation Procedure

The cost of a geotechnical site investigation is directly related to the number of tests performed. The decision on the number of tests that should be performed or the spacing between soundings depends on the geologic conditions and variability of the site. Optimization of the spacing between soundings can reduce the site investigation cost, and, at the same time, increase the reliability of the soil parameters used in design. Optimal spacing can be determined in real time based on the variability of the site as determined based on soundings already performed.

Figure 4.14 shows two soundings (CPT  $i-1$  and CPT  $i$ ) with a center-to-center spacing  $s(i-1, i)$ . The optimal spacing  $s(i, i+1)$  for the subsequent sounding needs to be determined based on the variability of the soil properties observed for the last two soundings. The calculation of the optimal spacing between soundings uses the same methodology developed to calculate horizontal site variability. In the optimal spacing calculation between CPT  $i$  and CPT  $i+1$ , the cross-correlation coefficient of  $q_c$  and the cone resistance trend difference are calculated, averaged with 20% and 80% weights, and then multiplied by a function of distance between the soundings according to Equation 4.12

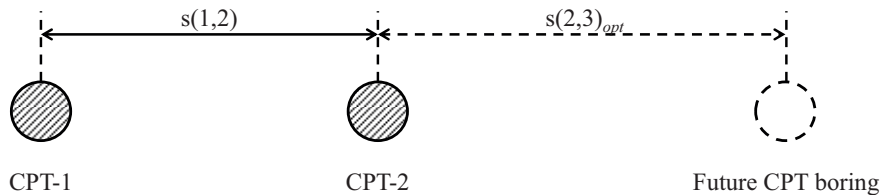


**Figure 4.14** Optimal spacing between soundings.

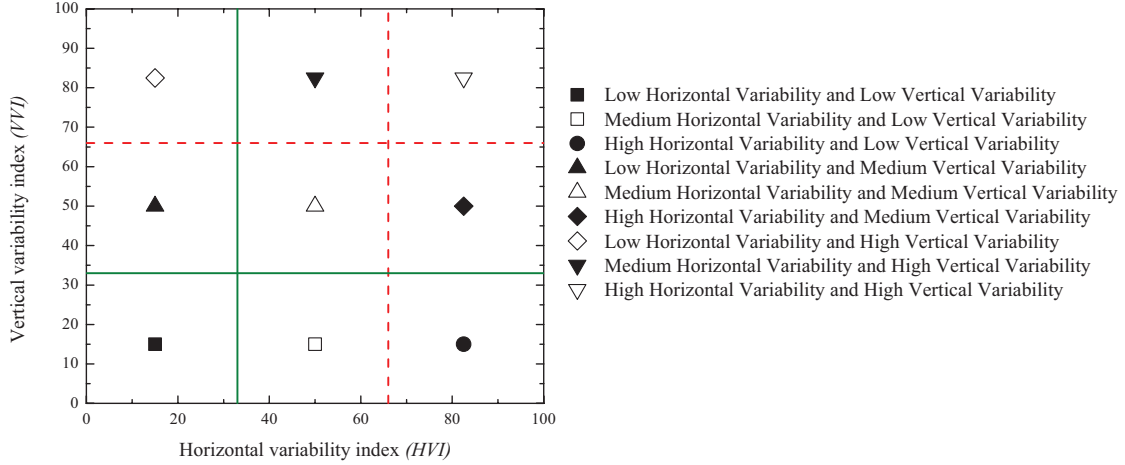


Figure 4.15 Calculation of SVR using VVI and HVI.

and Equation 4.13, consolidated next into one equation with notation specific to soundings CPT  $i$  and CPT  $i + 1$ :

$$f(|\Delta q_{c,avg}|_{ij}, \rho_{i-1,i}, s_{i-1,i}) = \left(0.8 \times \left(1 - \frac{|\Delta q_{c,avg}|}{|\Delta q_{c,avg}|_{max}}\right) + 0.2 \times \frac{\rho_{i-1,i} + 1}{2}\right) \times \left(1 - e^{-\frac{s_{i-1,i}}{3}}\right) \quad (4.15)$$

Next, the horizontal variability factor  $HVF$  is calculated by subtracting the horizontal variability function value from unity:

$$HVF = 1 - f(|\Delta q_{c,avg}|_{ij}, \rho_{i-1,i}, s_{i-1,i}) \quad (4.16)$$

$HVF$  values range from 0 to 1. A high  $HVF$  indicates either little correlation between the two CPTs considered or excessive proximity of the two soundings, with little confidence in horizontal variability estimation as a result. The calculated  $HVF$  is compared with a reference value  $HVF_{ref} = 0.5$ . The suggested optimal spacing  $(s_{i,i+1})_{opt}$  between CPT  $i$  and CPT  $i + 1$  is then calculated as:

$$(s_{i,i+1})_{opt} = (1.5 - HVF) \times s_{i-1,i} \quad (4.17)$$

If the calculated value of  $HVF$  is greater than 0.5, the spacing for the subsequent sounding is decreased. If the calculated value of  $HVF$  is less than 0.5, then the spacing for the subsequent sounding is increased. Since the spacing between CPT  $i - 1$  and CPT  $i$  already reflects the variability observed between previous soundings, horizontal variability observed across the site is indirectly reflected in the new spacing being calculated.

The algorithm discussed so far is directly applicable to soundings performed in line. If soundings are distributed in two dimensions, a possible algorithm is to simply iterate over all pairs of soundings and calculate  $HVF$  for each. An average  $HVF$  can then be computed and substituted into Equation 4.17 to obtain the new spacing. This means

that the new sounding will be at a distance no greater from any sounding than this computed spacing.

#### 4.5 Site Variability Rating

The average VVI and HVI (both of which range from 0 to 100%) of a site define its variability. It is not possible to combine them numerically because they are fundamentally different, but it is possible to classify a site as being of low (L), medium (M) or high (H) variability in the horizontal or vertical direction, depending on whether the HVI or VVI fall in the 0–33%, 33–66% or 66–100% range. We can then establish a rating, defined in terms of a string variable with two characters, each of which may assume the values, L, M or H, as shown in Figure 4.15.

### 5. SITE VARIABILITY INDEX CALCULATION FOR INDIANA SITES

#### 5.1 Introduction

The site variability calculation methodology developed in this research was applied to different sites in Indiana. The site variability rating SVR (discussed in the previous chapter) was determined for these sites, and site variability maps were developed for Indiana. In this chapter, we present these results and discuss how they can evolve into a powerful tool for risk assessment in geotechnical design and construction in the state of Indiana.

#### 5.2 Sources of CPT Data

In order to apply the SVR methodology developed in this research, CPT data from two sources have been considered: Purdue's own database and INDOT's data repository. The sites considered for analysis are those where at least 4 nearby CPTs were performed. Table 5.1 shows the CPT data

TABLE 5.1  
INDOT CPT data used in the analyses

DES	County	District (INDOT Classification)	Approximate Location Information	Latitude	Longitude
14050	LaPorte	LaPorte	Ramp from EB US 20 to EB US 20/35	41.6925	-86.8045
100385	Newton	LaPorte	Bridge over best ditch, 3.28 miles W of US 41	41.1524	-87.5132
0100521	White	LaPorte	Bridge over Big creek, 3.32 miles S of US 24	40.7011	-86.8715
0300310	Allen	Fort Wayne	US 24 Bypass, Near Naumee River	41.1083	-84.9505
0300970	Steuben	Fort Wayne	Sr 427 Over Chad Ditch (Black Creek)	41.5600	-84.9040
0301066	White	LaPorte	Over big creek, 1.69 miles N of I-65	40.7010	-87.0412
0301070	White	LaPorte	Over a drainage Swale, 2.82 miles N of I-65	40.7012	-86.7943
0301071	White	LaPorte	Over a tributary to Hoagland Ditch, 5.22 miles N of I-65	40.7305	-87.0412
0301142	Elkhart	Fort Wayne	Township Ditch, 2.56 mile N of SR 119	41.5448	-86.0016
0301143	Elkhart	Fort Wayne	Bridge over Nunemaker ditch, 4.63 miles N of SR 119	41.5779	-86.0021
0400006	Newton	LaPorte	1.7 miles E of US 41	41.0138	-87.4235
0400007 A	Newton	LaPorte	Over Molson/Bergren Ditch, 3.6 miles E of US 41	41.0138	-87.3808
0401113	Elkhart	Fort Wayne	Over Wagner Ditch, 3.86 miles W of SR 15 in the Fort Wayne District	41.4462	-85.9186
0401159	Lagrange	Fort Wayne	CR 600S	41.5534	-85.5783
0600165	Miami	Fort Wayne	On SR 16 from the town of twelve mile to US 31	40.8665	-86.2253
0600336	Howard	Greenfield	On CR 50N (Carter) over US 31	40.4841	-86.0857
0600337	Howard	Greenfield	On CR 200N (Morgan) over US 31	40.5059	-86.0890
0710146	Jasper	LaPorte	Various locations in Jasper County	40.8855	-87.2001
0800807	Warrick	Vincennes	0.62 mile E of SR 161	38.2034	-87.0802
0801027	Hancock	Greenfield	0.53 mile N of I70 (CR 300N)	39.8320	-85.7706
0810115	Steuben	Fort Wayne	Over Little Turtle Creek, 3.41 miles E of SR 327	41.5394	-85.1153
0810222	Gibson	Vincennes	At junction with SR 65, 4.71 miles E of Illinois state line	38.3558	-87.6871
0900103	Grant	Fort Wayne	Various locations in Grant, Allen, DeKalb and Steuben Counties	40.4804	-85.5521
0900103a	Allen	Fort Wayne	Various locations in Grant, Allen, DeKalb and Steuben Counties	41.1228	-85.1896
0900103b	Steuben	Fort Wayne	Various locations in Grant, Allen, DeKalb and Steuben Counties	41.6360	-85.0481
0900104	Lake	LaPorte	Various locations in Jasper, Newton and Lake Counties	41.4916	-87.3204
0900105	Jackson	Seymour	Various locations in Clark, Scott, Jackson, Bartholomew and Shelby Counties	38.9017	-85.8212
0901897	Daviess	Vincennes	Glendale State Fish and Wildlife area	38.5392	-87.0495
8823155	Warrick	Vincennes	From 6th St to 0.90 mile E of W UAB of Boonville (Phase II)	38.0422	-87.2710
9031790	DeKalb	Fort Wayne	At 3.7 miles N of SR 8 over Mason Ditch	41.4090	-84.8831
9700260	Allen	Fort Wayne	Scott Rd to Hadley Rd	41.0745	-85.2534
9904180	Adams	Fort Wayne	From 0.87 miles E to 1.27 miles E of US 27	40.8321	-84.9580
0100331	LaPorte	LaPorte	Bridge over abandoned Railroad, 5.68 miles E of US 20	41.6878	-86.8133
1006389	Decatur	Seymour	SR 3 16.06 miles north of SR 7 at RP 60 + 26.	39.2450	-85.5761
1173689	Jasper	LaPorte	CSB on I-65 from 3.06 miles N of SR 14 to 4.25 miles N of SR 10	41.1197	-87.2666

obtained from INDOT. The designation number DES used by INDOT for their projects is also shown in the table. Each DES refers to one site where multiple CPTs were performed. The INDOT CPT data used here were obtained from soundings in which  $q_c$  was recorded at every 5 cm.

Table 5.2 shows the locations where CPTs were performed using Purdue's CPT rig. Purdue cone resistance data are recorded at every 2 mm.

TABLE 5.2  
Data collected using Purdue's CPT truck

Data	Designation	County	Latitude	Longitude
Purdue	Koleen	Greene	38.9620	-86.8310
	Purdue Campus	Tippecanoe	40.4257	-86.9316
	Romney	Tippecanoe	40.2308	-86.9067
	Frankfort	Clinton	40.2777	-86.5342
	Fort Wayne	Allen	41.0910	-84.9810
	Flora	Carroll	40.5332	-86.5273
	McCormick	Tippecanoe	40.4261	-86.9317

### 5.3 Site Variability Analysis

As discussed in chapter 4, site variability analysis is done in four steps: (i) soil profile generation, (ii) vertical variability analysis, (iii) horizontal variability analysis, and (iv) site variability assessment based on the results of the vertical and horizontal variability calculations. The generated soil profiles and the different variability indices  $[(VVI)_{IL}, (VVI)_{log}$  and  $(VVI)_{q_c}]$  that make up the vertical variability index  $VVI$  for a given CPT sounding are shown in each figure provided in this chapter. Both the modified Tumay (1985) and Robertson (1990) SBT charts were used to generate the soil profiles from CPT data.

Figure 5.1 shows the soil profile generated using the soil profile generation algorithm (see chapter 4) together with the results for CPT sounding TB-3 of site 0100521 for a 5 m length of the soil profile. The modified Tumay (1985) chart was used to generate the soil profile. Figure 5.2 shows the generated soil profile and variability results for the same sounding (TB - 3 of site 0100521), but this time using the modified Robertson (1990) chart. The headers of

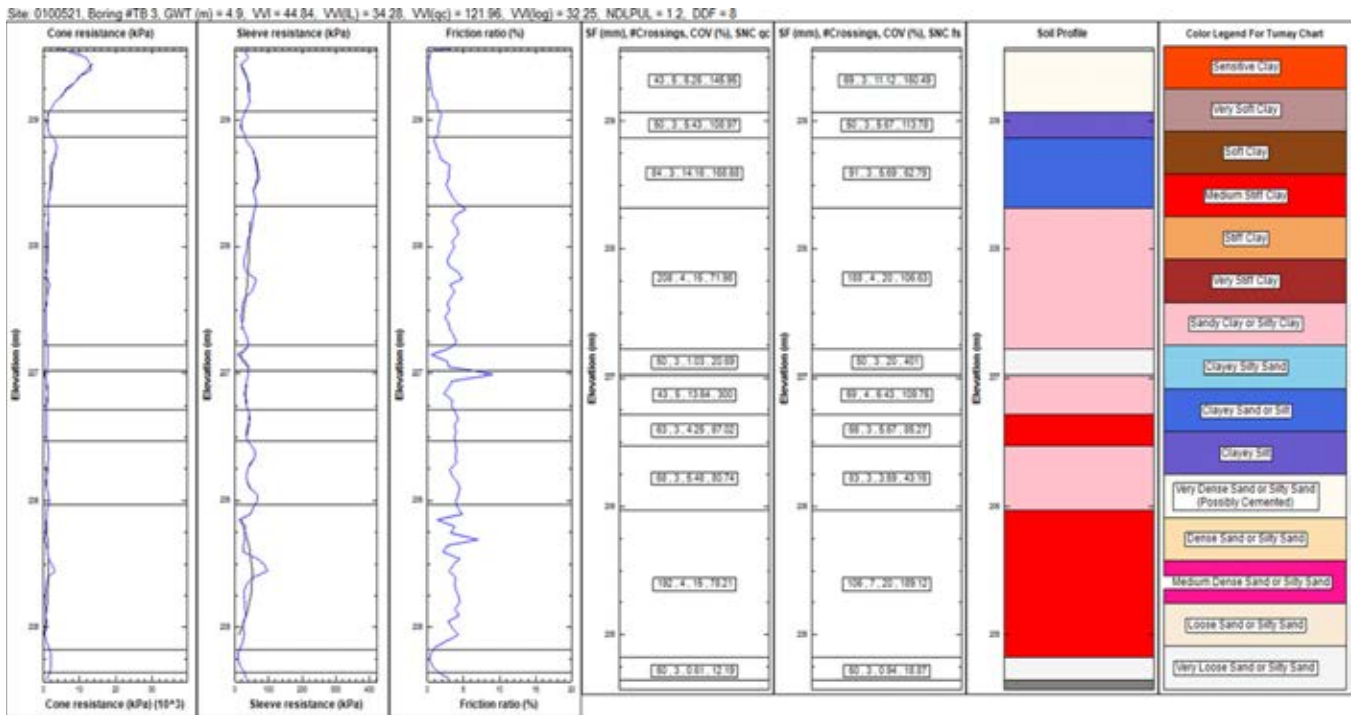


**Figure 5.1** Vertical variability results for sounding #TB 3 of site 0100521 (LaPorte) for 5 m length of the soil profile using the modified Tumay (1985) chart.

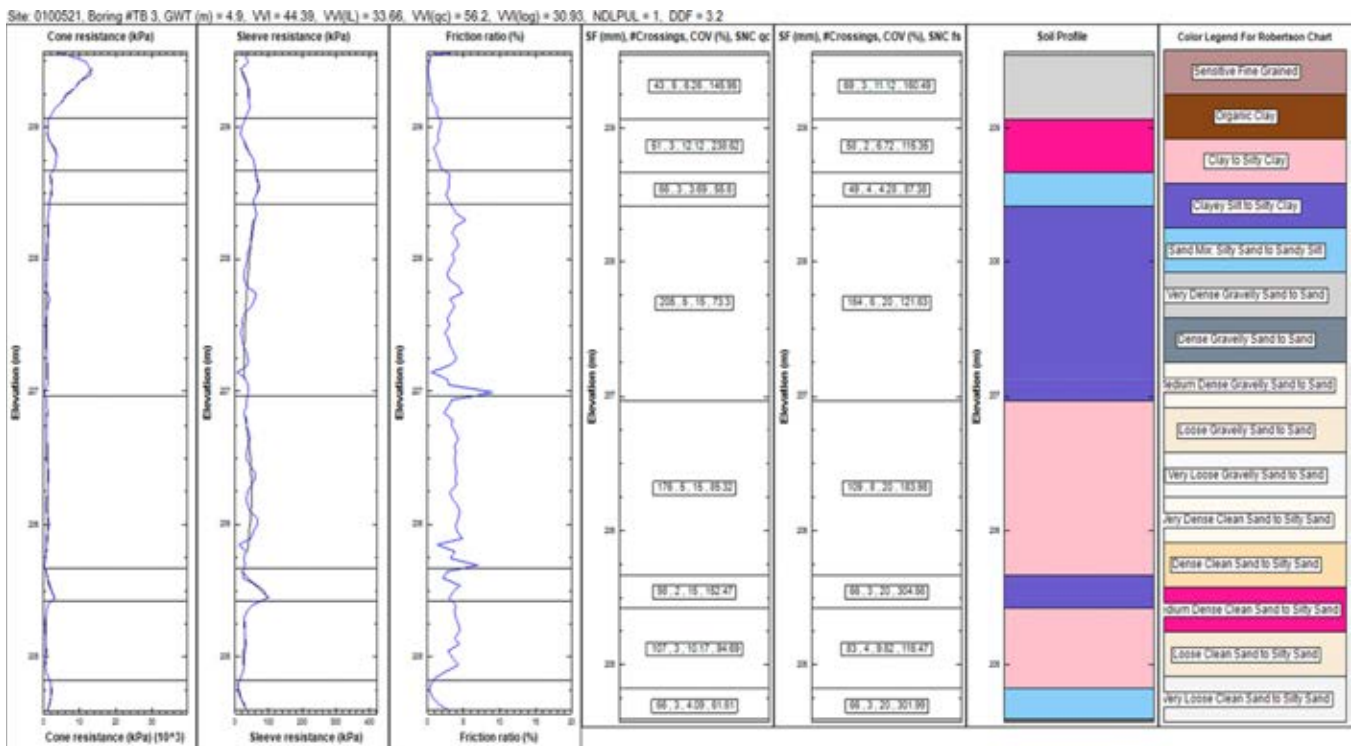
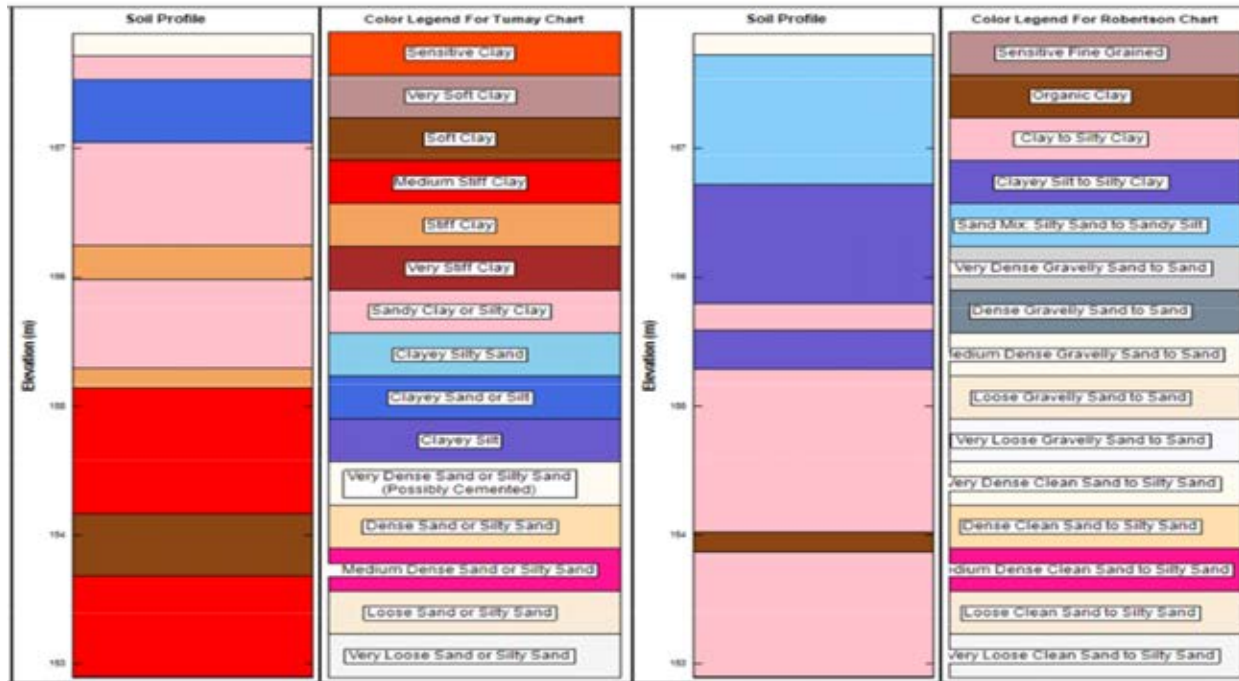


**Figure 5.2** Vertical variability results for sounding #TB 3 of site 0100521 (LaPorte) for 5 m length of the soil profile using the modified Robertson (1990) chart.

Site: Koleen Interstate 69 Expansion Site		Final Depth (m): 9.15		
Date: 16-Jul-12		Groundwater Depth (m): 2.18		
Boring: 1		Drill Rig: ATV		
Surface Elevation (m): 158.84		Drilling Method: <b>K2.SLD</b> /1650.D. H.S.A.		
Depth (m)	USCS	Description	N <sub>60</sub> (Blows)	Remarks
1.07-1.52	CL	Moist, stiff, lean <u>CLAY</u>	11.2	
2.59-3.05		grading wet and firm	6.6	
4.12-4.57			7.2	
5.64-6.10		grading stiff	9.7	
7.16-7.62		grading soft	3.3	
8.69-9.15		grading firm	6.5	The boring was terminated at 9.15 meters.

(a)



(b)

Figure 5.3 Soil profile for Koleen site interpreted from: (a) SPT 01 and (b) CPT 01.

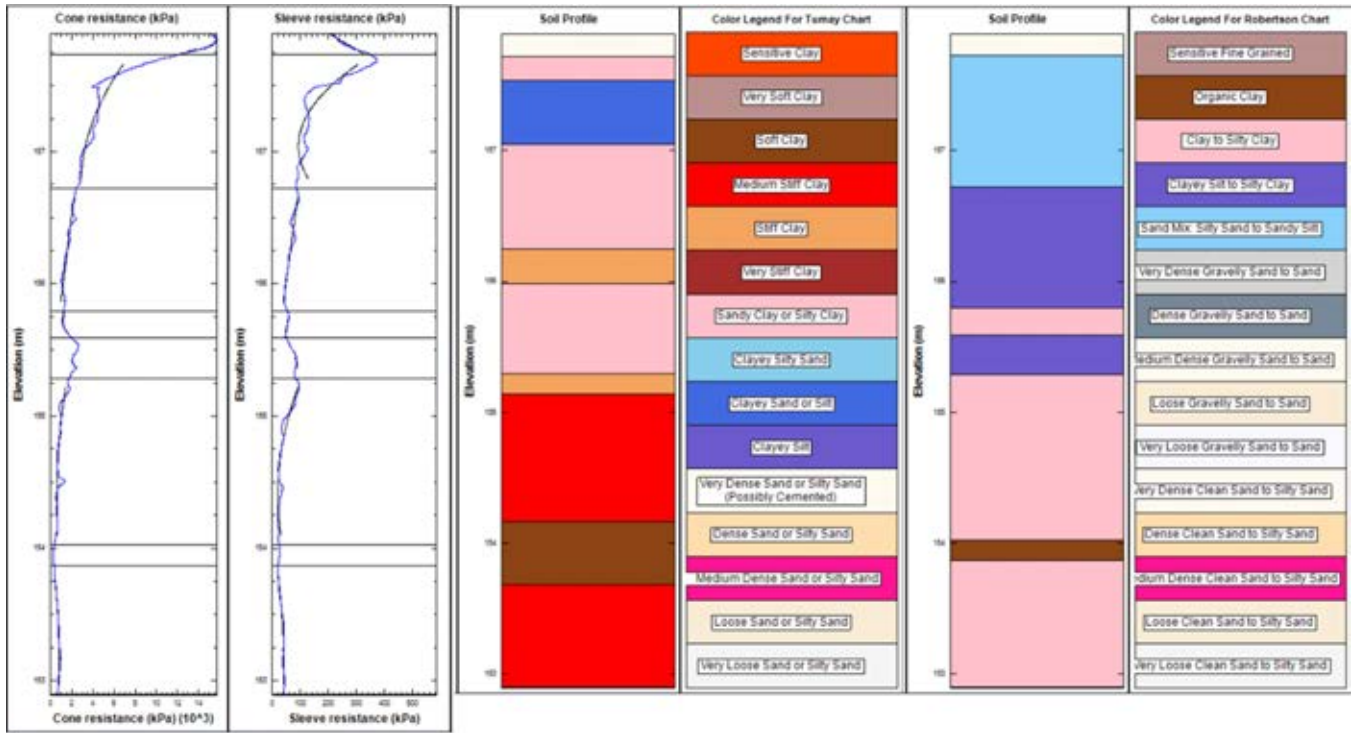


**Figure 5.4** Soil profiles generated using modified Tumay (1985) and modified Robertson (1990) charts for CPT 1 from Koleen site.

Figure 5.1 and Figure 5.2 show the values of the different components that enter the calculation of the *VVI* of a site, as explained earlier. The scale of fluctuation, the number of crossings between the CPT parameter profile and the trend function within a layer, the COV and the scale of fluctuation-normalized COV (SNC) values for each layer are shown in the figures as well. In the subsequent sections, the soil profile generation and the variability results are discussed.

**5.4 Soil Profile Generation**

In order to validate the soil profile generation algorithm used in this report, borings were drilled at a distance of approximately 1 m from the CPTs that were considered for the variability analyses of the Koleen, Romney, Flora and Frankfort sites. Several borings are available for each of these four sites. Soil profiles established from the soil samples collected during the SPTs performed for each boring were compared with the soil profiles generated with the soil profile generation algorithm. One soil profile is discussed in this section; the remaining soil profiles are shown in Appendix A.

Figure 5.3 (a) and (b) show the soil profile obtained from soil samples collected from SPT01 and those obtained from the SBT charts using sounding CPT 01 for the Koleen site. Figure 5.4 shows the two soil profiles obtained from the modified Tumay (1985) and modified Robertson (1990) charts along with  $q_c$  and  $FR$  profiles. The same is done for the other sites in Figure 5.5 through Figure 5.10.

Figure 5.3 and Figure 5.4 show that the Koleen site has a thick clayey layer, which was captured by both of the soil profiles obtained using SBT charts. For the other soil

profiles, both SBT charts produced reasonable results. The modified Robertson (1990) chart does not produce as many distinct clay regions as the modified Tumay (1985) chart. The only distinct clay regions in the soil profile obtained using the modified Robertson (1990) chart are “sensitive fine grained” and “organic clay.” Layers classified as clay of different stiffnesses according to the modified Tumay (1985) chart are sometimes classified as mixed soil (e.g., “clayey silt to silty clay”) according to the modified (Robertson 1990) chart. This appears, for example, in the case of CPT 02 for the Frankfort site shown in Figure 5.10. In general though, reasonable agreement exists between the soil profile from the borings and those based the CPT soil behavior charts.

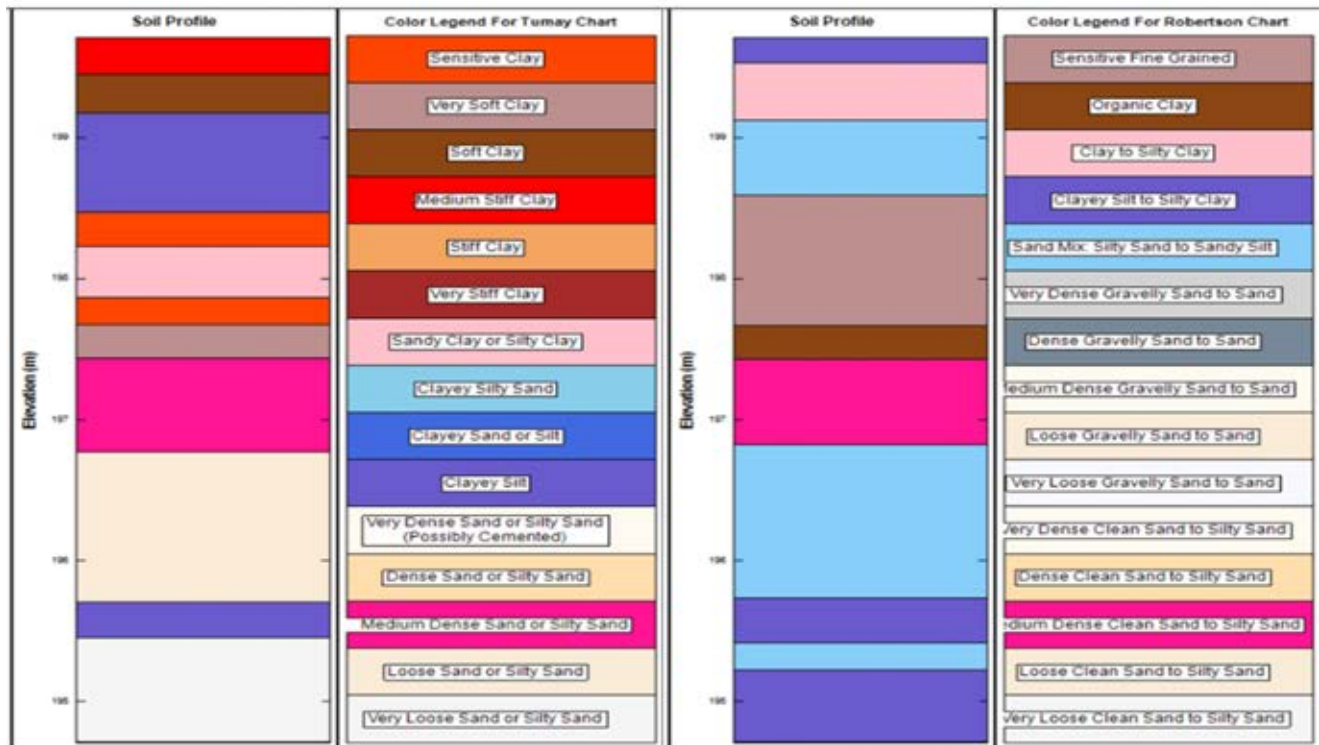
**5.5 Site *VVI* Results**

CPTs available at different locations start and end at different elevations. Additionally, site variability depends on the length of the soil profile considered. In order to compare variability across sites, it is essential to do so always for the same depth below the ground level. In this report, comparisons are made for soil profile lengths of 3, 4 and 5 m. Since many of the CPT soundings in the database are shallow, use of a soil profile length greater than 5 m would significantly reduce the number of soundings available for comparison.

The spacing between CPTs is important for site variability analyses. In the horizontal variability analysis, as discussed in chapter 5, the spacings between CPTs are directly used in the calculations. In transportation applications, CPTs are often performed at large spacings. If the spacing between CPTs is too large, then they should not be considered to belong to one site. In this research, the maximum spacing

Site: Romney Maintenance Unit		Final Depth (m): 6.10		
Date: 9-Jan-12		Groundwater Depth (m): 5.49		
Boring: 1		Drill Rig: ATV		
Surface Elevation (m): 233.23		Drilling Method: SPT/1650.D. H.S.A.		
Depth (m)	USCS	Description	N <sub>60</sub> (Blows)	Remarks
1.07-1.52	SP-SC	Moist, dense, poorly-graded SAND w/ silty clay and gravel	30.4	Water table encountered at 5.49 meters. The boring was terminated at 6.10 meters.
2.59-3.05	SW-SC	Moist, dense, well-graded SAND w/ silty clay and gravel	45.2	
4.12-4.57	ML	Moist, very stiff, sandy SILT	18.6	
5.64-6.10	SM	Wet, medium dense, silty SAND	14.0	

(a)



(b)

Figure 5.5 Soil profile for Romey site interpreted from: (a) SPT 01 and (b) CPT 01.

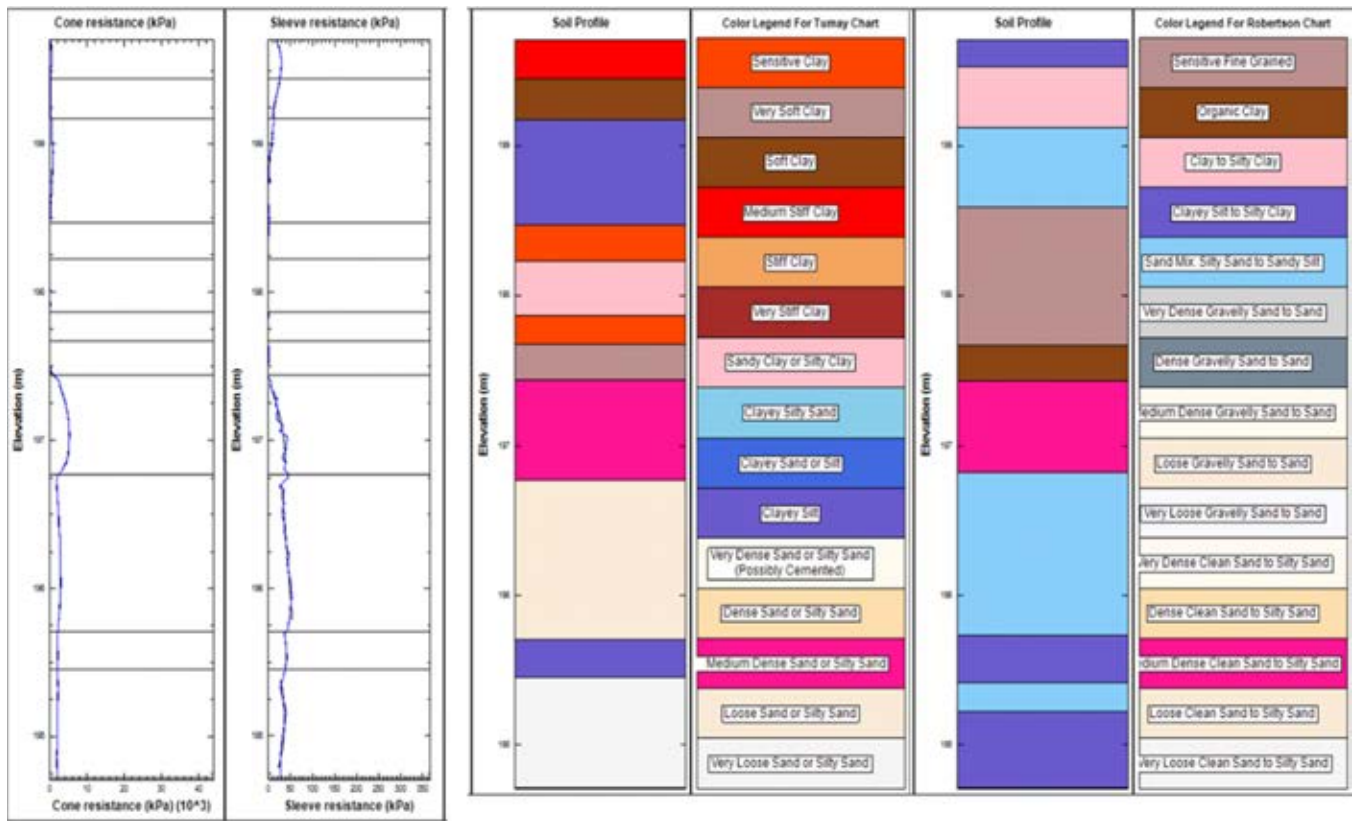


Figure 5.6 Soil profiles generated using modified Tumay (1985) and Robertson (1990) charts for CPT 1 from Romney site.

between any two CPTs considered to belong to the same site is 100 m.

### 5.5.1 SF Results

There are several methods that can be used to calculate SF. In this section, we discuss the applicability of the different methods to this research. As discussed in chapter 2, according to the variance function approach, SF calculation is based on the correlation length definition given by Vanmarcke (1983), i.e., SF is calculated using Equation 3.19, where SF is taken as the window length times the variance function when the window length reaches infinity. In practice, the variance function times the window length value associated with the first peak observed in the variance function times the window length vs. window length plot is taken as an estimate of the correlation length or scale of fluctuation (see Figure 3.2).

INDOT CPT data used in the site variability analysis were recorded at every 5 cm of cone penetration. Exclusion of the sensing and development lengths, assumed equal to 2 cone diameters each, from each layer, as discussed in section 4.2.1, means that thin layers would have only a few data points available. For example, for INDOT data, a 30-cm-thick layer has 7 data points. However, since 14 cm are discarded (corresponding to 4 data points) to account for the sensing and development lengths, only 3 data points remain.

When using the variance function approach to calculate SF, we first need to calculate the variance function value for

different window lengths, as discussed in section 3.3.4. Then, we must plot the variance function times the separation distance versus the separation distance. The number of data points shown in this plot will be equal to the number of different separation distance that can be considered. The calculation of variance function requires calculation of a reference variance: in this particular case, the variance for the three data points. Next, we form new datasets after local averaging of the original dataset with increasing separation distance.

Starting with separation distance equal to zero, the new data set is exactly the same as the original dataset. Therefore, the new variance is the same as the reference variance, and the variance function value will be unity. Next, we will consider a separation distance equal to 1. The new data set after local averaging will have 2 points, as shown in Figure 5.11(a). The new variance will be calculated for this new data set and the corresponding variance function value will be calculated by dividing the new variance by the reference variance. Next, for a separation distance of 2, the new dataset will have only one data point, as shown in Figure 5.11 (b). A dataset consisting of only one point doesn't have any variance, so the variance function cannot be calculated. Hence, when there are only 3 points available, only window lengths of 0 and 1 can be considered. When the variance function times separation distance values are plotted versus the separation distance values, the resultant plot has only 2 points. Therefore, for thin layers, the variance function approach cannot be used to calculate SF.

It is expected that the correlation structure of a soil property is well captured in a correlation coefficient versus

Site: Flora Maintenance Unit		Final Depth (m): 4.57		
Date: 9-Aug-11		Groundwater Depth (m): 2.74		
Boring: 3		Drill Rig: Truck		
Surface Elevation (m): 216.16		Drilling Method: <del>SLP</del> /1650.D. H.S.A.		
Depth (m)	USCS	Description	N <sub>60</sub> (Blows)	Remarks
1.07-1.52	SC-SM	Moist, medium dense, silty clayey SAND	18.5	
2.59-3.05	SP-SC	Wet, medium dense, poorly-graded SAND w/ silty clay	13.7	Water table encountered at 2.74 meters.
4.12-4.57	SP	Wet, medium dense, poorly-graded SAND	14.7	Sand was flowing into the hollow stem augers. The boring was terminated at 4.57 meters.

(a)



(b)

Figure 5.7 Soil profile for Flora site interpreted from: (a) SPT 01 and (b) CPT 01.

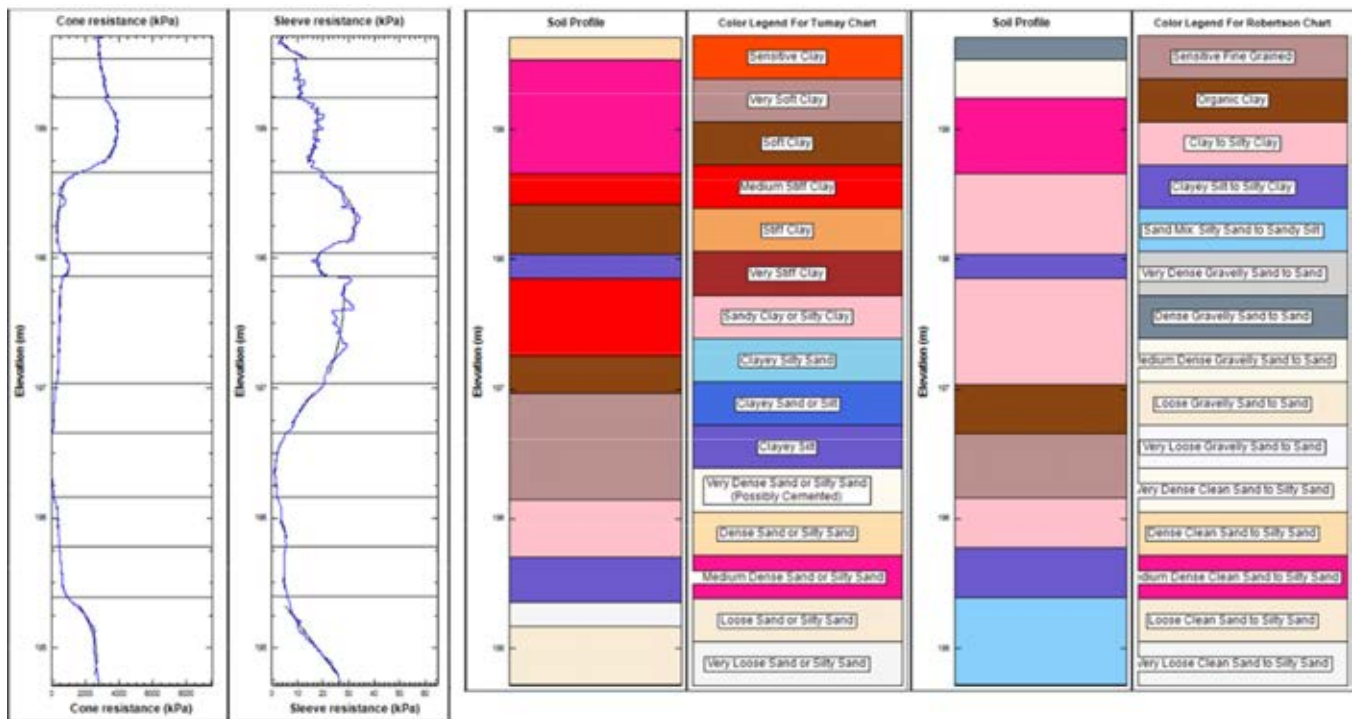


Figure 5.8 Soil profiles generated using modified Tumay (1985) and Robertson (1990) charts for CPT 1 from Flora site.

separation distance plot. However, when the available data points for analysis is small, the extent to which the correlation coefficient versus separation distance plot actually shows the correlation structure of a soil property within a particular soil layer is uncertain. Therefore, the “fitting auto-correlation models” or “integration of auto-correlation function” approaches are also not applicable to calculate *SF* for thin soil layers.

Application of the Bartlett’s limit approach to calculate *SF* involves using Equation 3.21 to calculate Bartlett’s distance. For four data points, a Bartlett’s limit  $LB = 1.96/3^{0.5} = 1.13$  results, and thus there is no intersection between Bartlett’s limit and the correlation coefficient versus separation distance. Therefore, this approach cannot be used to calculate *SF* when the number of data points available for any layer is less than 4.

Vanmarcke’s (1977) simplified method takes into account the crossing lengths and was used to calculate *SF* for thin soil layers. When using Vanmarcke’s (1977) simplified method, it is possible that the CPT parameter (say  $q_c$ ) and the trend line intersect only once. In this case there is no crossing length, and therefore Vanmarcke’s simplified method is not applicable, as shown in Figure 5.12. In such cases, the exponential auto-correlation model fitting approach is used instead to calculate *SF*.

**5.5.1.1 *SF* and COV analysis.** *SF* of  $q_c$  and of  $f_s$  values were obtained for each layer, rather than for the entire soil profiles, since the analysis of the correlation structure of a soil property should be limited to the domain where a particular type of soil exists with approximately the same state. Presumably, if the domain

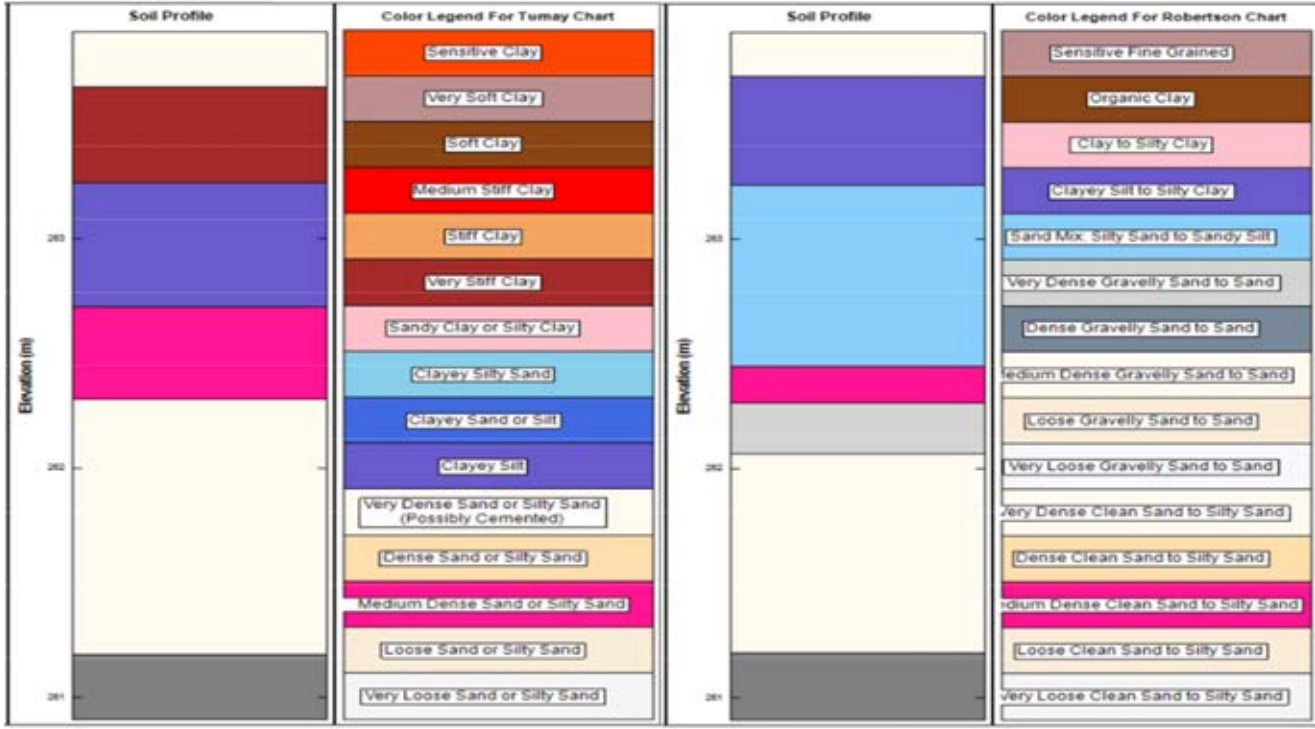
is well defined, the size of the domain should not influence the *SF* value.

Figure 5.13 shows a soil property (cone resistance) fluctuating with depth. A trend line is fitted through the data to help with visualization of the scale of fluctuation of the soil property. It can be seen that the scale of fluctuation from Figure 5.13 is controlled by the global fluctuation of the soil property, with the effect of local fluctuation being secondary. Therefore, the scale of fluctuation is large.

Three methodologies are used to eliminate thin layers when generating a final soil profile from CPT data; these are the SBT chart band approach, the soil group approach and the average  $q_c$  approach. The aim of all of these approaches is to eliminate thin layers, and the order of their application is consistent with the degree of acceptability of these approaches. A minimum layer thickness of 15 cm was set in the soil profile generation methodology. A thin layer is added to the layer above or the one below it, according to a set of criteria (see chapter 4). The addition of a thin layer to a layer increases the COV of that layer. In this research, the COV was calculated using Equation 4.2 (Foye, Abou-Jaoude, Prezzie, & Salgado, 2009; Foye, Prezzi, & Salgado, 2011), which requires the calculation of the normalized error  $w^*$ , as shown in Equation 4.1. The normalized error corresponds to the random component of the variable, so its calculation involves detrending the data by its trend function value and then normalizing the detrended value by the trend function value. The maximum COV of  $q_c$  and  $f_s$  was set to 15% and 20%, respectively. Therefore, if the calculated COV of  $q_c$  or  $f_s$  is greater than 15% or 20%, respectively, then it is replaced with the maximum allowable COV.

Site: Frankfort Maintenance Unit		Final Depth (m): 4.57		
Date: 4-Jan-12		Groundwater Depth (m): 3.81		
Boring: 3		Drill Rig: ATV		
Surface Elevation (m): 264.33		Drilling Method: <del>SLD</del> /1650.D, H.S.A.		
Depth (m)	USCS	Description	N <sub>60</sub> (Blows)	Remarks
1.07-1.52	SM	Moist, medium dense, silty SAND	26.1	Water table encountered at 3.81 meters. The boring was terminated at 4.57 meters.
2.59-3.05	SP-SC	Moist, medium dense, poorly graded SAND w/ silty clay	19.1	
4.12-4.57	SM	Wet, dense, silty SAND	33.1	

(a)



(b)

Figure 5.9 Soil profile for Frankfort site interpreted from: (a) SPT 03 and (b) CPT 02.

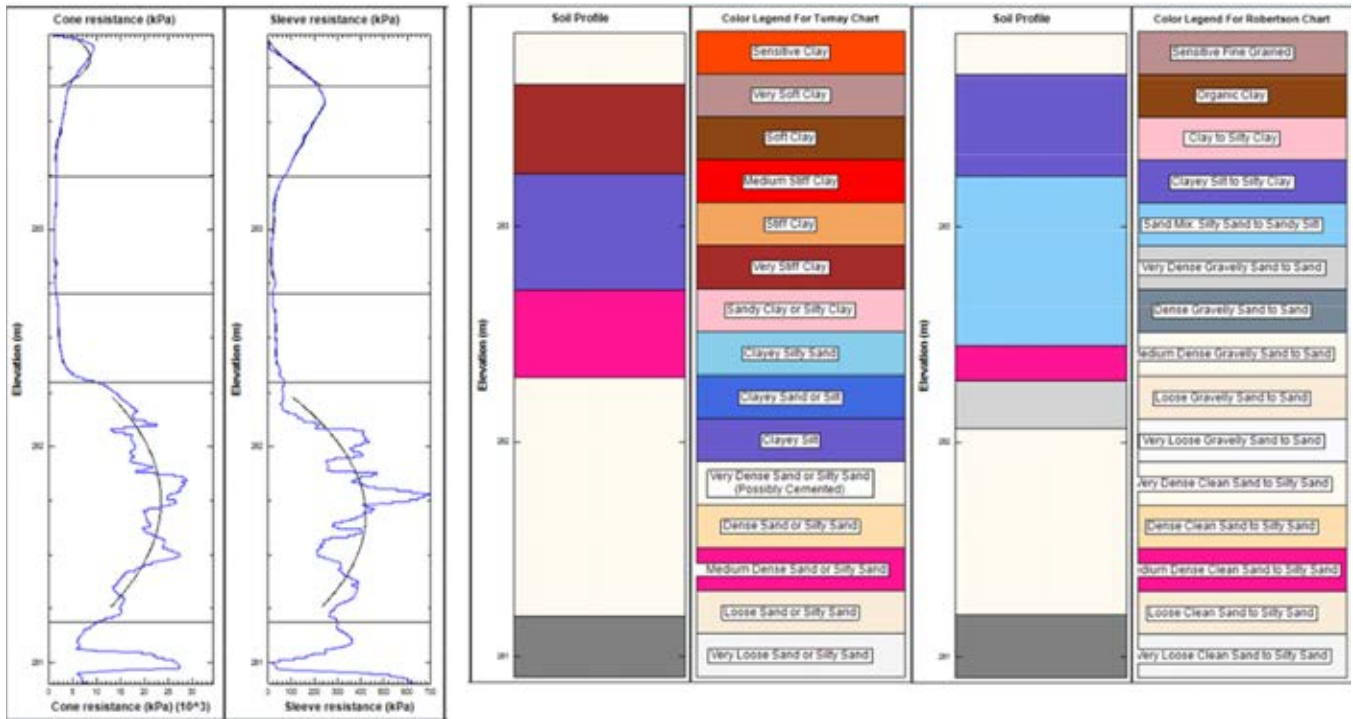


Figure 5.10 Soil profiles generated using modified Tumay (1985) and Robertson (1990) charts for CPT 02 from Frankfort site.

### 5.5.2 Intra-Layer Variability Index

The  $(VVI)_{IL}$  captures the intra-layer variability of a soil layer. Table 5.3 shows the range of values obtained for the  $VVI$  and the various indices making up the  $VVI$  for a 5 m soil profile length generated using the modified Tumay (1985) chart for the INDOT database. The  $(VVI)_{IL}$  component ranges from 9 to 61.5.

Figure 5.14 shows the soil profile for sounding #CPT-9-CG-9 of site 1173689. As discussed in 4.2.3, the  $(VVI)_{IL}$  is calculated from the scale of fluctuation-normalized COV SNC of  $q_c$  and  $f_s$  of all the soil layers in a soil profile. The allowable ranges of SNC for  $q_c$  and  $f_s$  are 0 to 300 and 0 to 500, respectively. As can be seen from Figure 5.14 and Figure 5.15, the maximum SNC value of  $q_c$  is 48 while the maximum SNC of  $f_s$  is equal to 71. The soil profile has a thick, very dense sand layer. The fluctuations in both the  $q_c$  and  $f_s$  profiles have contributed towards producing high values of COV for both  $q_c$  and  $f_s$ . The actual COV of  $q_c$  is 17.9%; however the maximum COV of  $q_c$  was set to 15%. Due to the fact that the comparatively large fluctuations have occurred within large distances, high values of scale

of fluctuations have resulted. Therefore, the  $(VVI)_{IL}$  is quite low.

Figure 5.16 shows the soil profile for sounding #4 of the Flora site. This CPT has a maximum  $(VVI)_{IL}$  of 63.39. As can be seen in Figure 5.16 and Figure 5.17, the SNC values of  $q_c$  and  $f_s$  are quite high. In Figure 5.16, multiple layers have the highest SNC values for  $q_c$  and  $f_s$  of 300 and 500, respectively. For several thin layers, the scale of fluctuation values are quite low, but the corresponding COVs are moderate to high, and therefore, high SNC values are obtained. To aid in the visualization of the fluctuations, a zoomed in version of the  $q_c$  profile is shown in Figure 5.18. The comparatively large number of crossings led to low values of  $SF$ .

### 5.5.3 COV of Cone Resistance

For visual verification of the effectiveness of the COV of cone resistance, normalized error plots may be used. In such plots, the normalized error in  $q_c$  is given by:

$$w_{q_{c,i}} = \frac{q_{c,i} - \bar{q}_{c,i}}{\bar{q}_{c,i}} \quad (5.1)$$

where  $w_{q_{c,i}}$  is the normalized error of  $q_c$  with respect to the trend in  $q_c$  for a depth  $z_i$ ,  $q_{c,i}$  is the cone resistance at  $z_i$  and  $\bar{q}_{c,i}$  is the value of  $q_c$  on the trend line.

Figure 5.19 shows 5 m of the soil profile of sounding CPT-2 of site 9700260 (Fort Wayne) generated using the modified Tumay (1985) chart. The lowest value of the COV of cone resistance (=19.5) was found for this sounding (CPT 2 of site 9700260). Figure 5.19 shows that the soil profile is dominated by loose sand and that the  $q_c$  fluctuates around 2000 kPa.

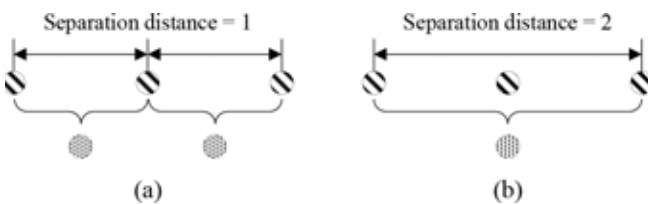
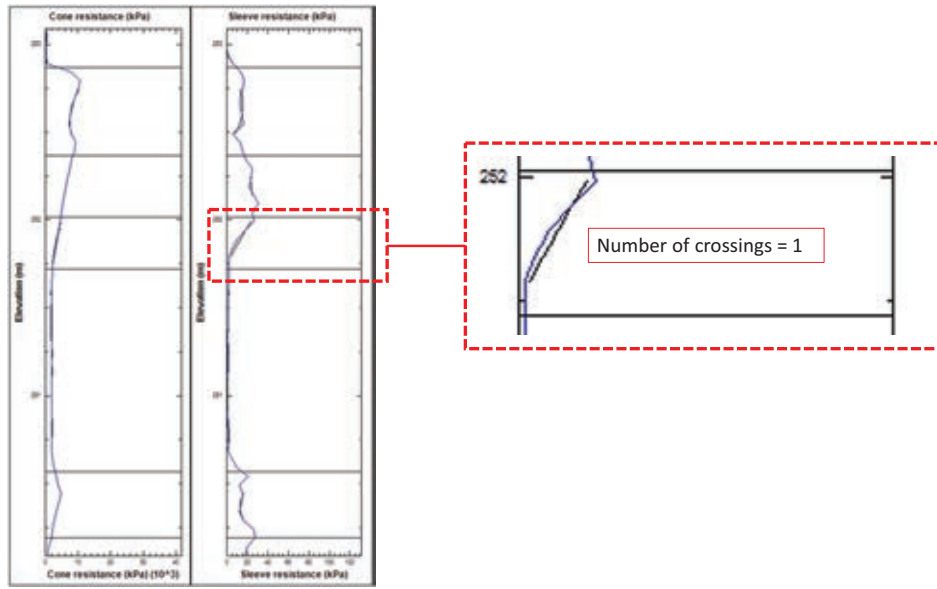


Figure 5.11 Local averaging for: (a) separation distance = 1 and (b) separation distance = 2.



**Figure 5.12** Number of crossing equal to 1 for  $f_s$  plot for layer 4 of INDOT DES 9700260 (Fort Wayne) CPT sounding #7.

Towards the top of the profile there is a comparatively thin layer of “clayey silt” with a  $q_c$  value of about 300 kPa. Figure 5.19 is in a  $q_c$  scale of 0 to 4200 kPa. It is clear that a naïve impression of variability may result from visual inspection of the plot, depending on the scale selected for the plot. In Figure 5.20, it can be seen that the fluctuation of the normalized error of  $q_c$  with respect to the trend in  $q_c$  is indeed minimal, with only some fluctuation towards the top

of the profile caused by the presence of clayey silt and dense sand layers (the rest of the sounding consisting of loose and very loose sand layers). This fluctuation is small, with normalized error staying within the  $-1$  to  $+1$  range.

Figure 5.21 shows the soil profile of sounding TB – 11 of site 0600337 for a 5 m soil profile length generated using the modified Tumay (1985) chart. The soil profile in Figure 5.21 consists of clay near the top, mixed soil layers in the middle and dense sand near the bottom. In Figure 5.22 it can be seen that the fluctuation of the normalized error of  $q_c$  with respect to the trend in  $q_c$  is high towards the bottom of the profile, ranging from  $-1$  to  $+6$ .

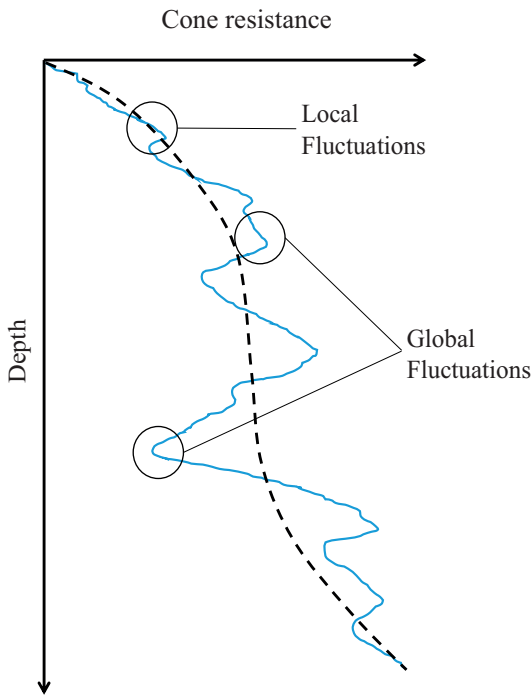


**Figure 5.13** Global and local fluctuation of a soil property with depth.

#### 5.5.4 Log Variability Index

The calculation of the log variability index that enters the  $VVI$  calculation involves calculation of the degree of difference factor  $DDF$  and of the number of different layers per unit length  $NLPL$ , as shown in Figure 4.2. A soil profile having dominance of a particular soil group is expected to have a low value of  $DDF$ , while a soil profile without dominance of any particular soil group is expected to have a high value of  $DDF$ .

**TABLE 5.3**  
Range of values for the  $VVI$  and the various indices making up the  $VVI$  for 5 m soil profile length generated using the modified Tumay (1985) chart for INDOT database

	$VVI$	$DDF$	$NLPL$	$(VVI)_{IL}$	$(VVI)_{log}$	$(VVI)_{q_c}$
Min.	13.8	2.1	0.4	8.26	2.14	17.66
Max.	57.07	21.1	1.7	41.34	100	2.14

Site: 1173689, Boring #CPT-9-CG-9, GWT (m) = 6.5, VI = 15.25, VI(L) = 8.26, VI(qc) = 23.54, VI(log) = 4.99, NDLPUL = 0.8, DDF = 2.1

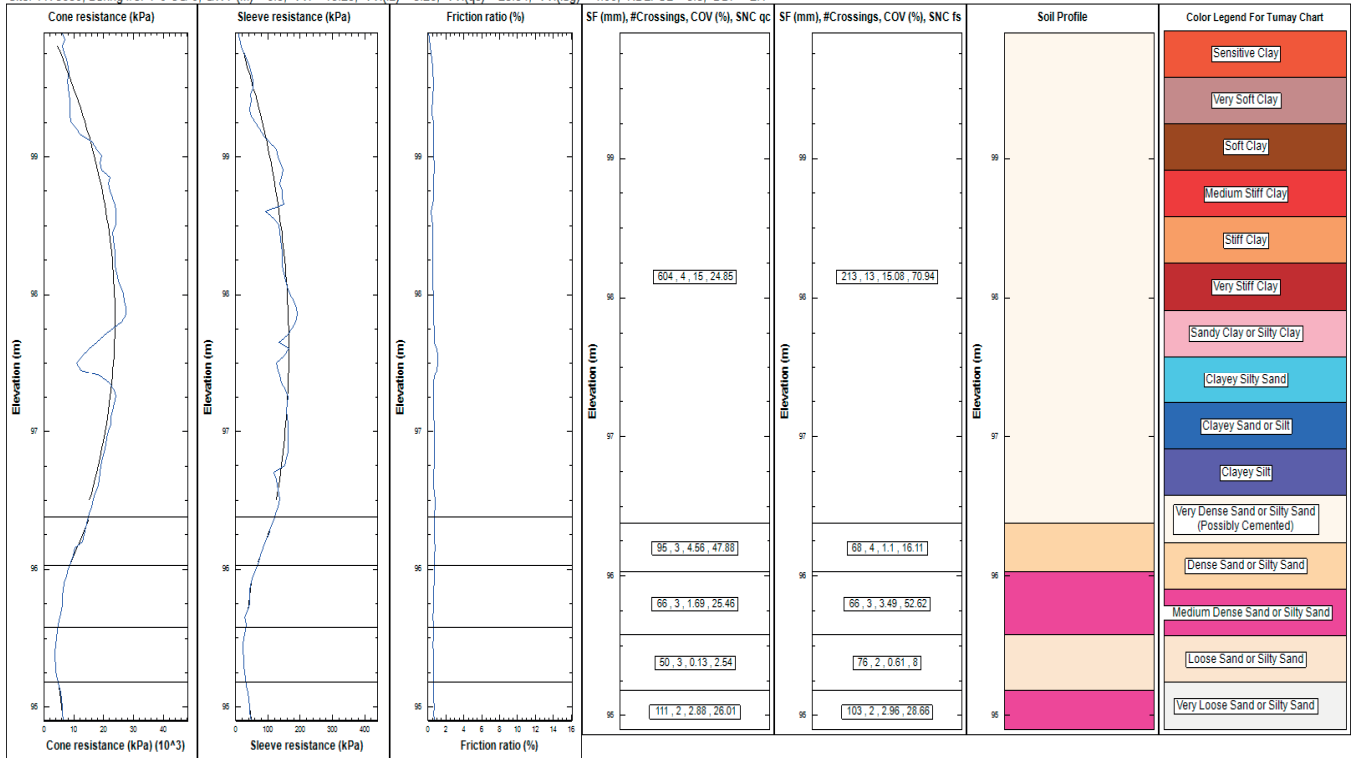


Figure 5.14 Vertical variability indices for sounding #CPT-9-CG-9 of site 1173689 (LaPorte) for a 5 m soil profile length using the modified Tumay (1985) chart.

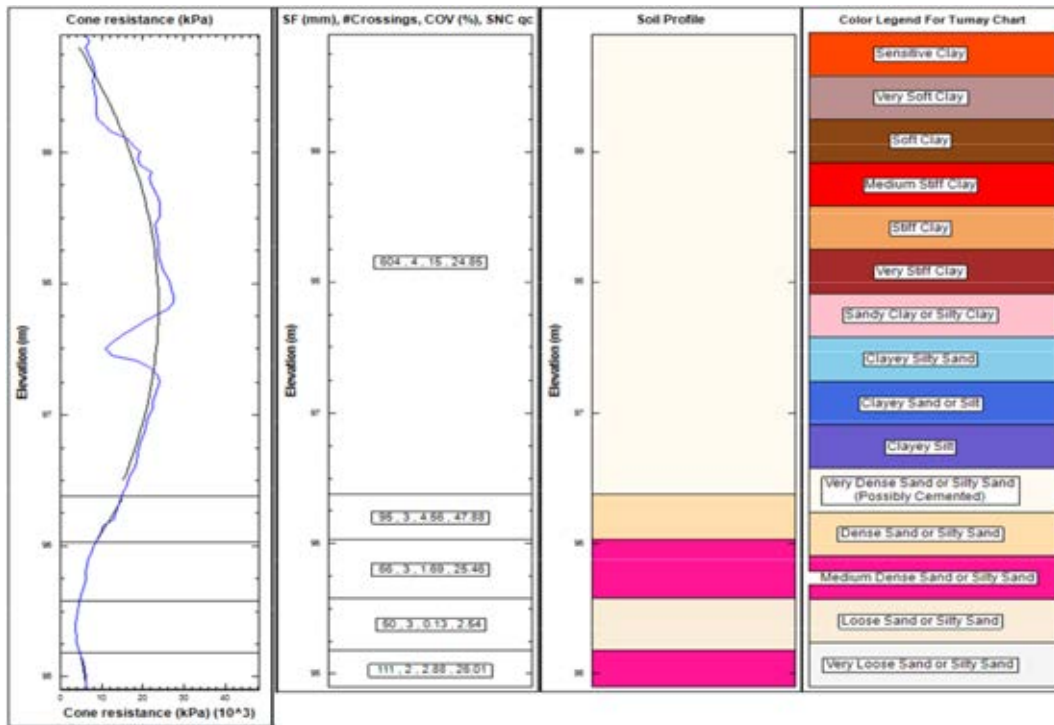


Figure 5.15 Cone resistance profile and intra-layer variability indices for sounding #CPT-9-CG-9 of site 1173689 (LaPorte) for a 5 m soil profile length using the modified Tumay (1985) chart.

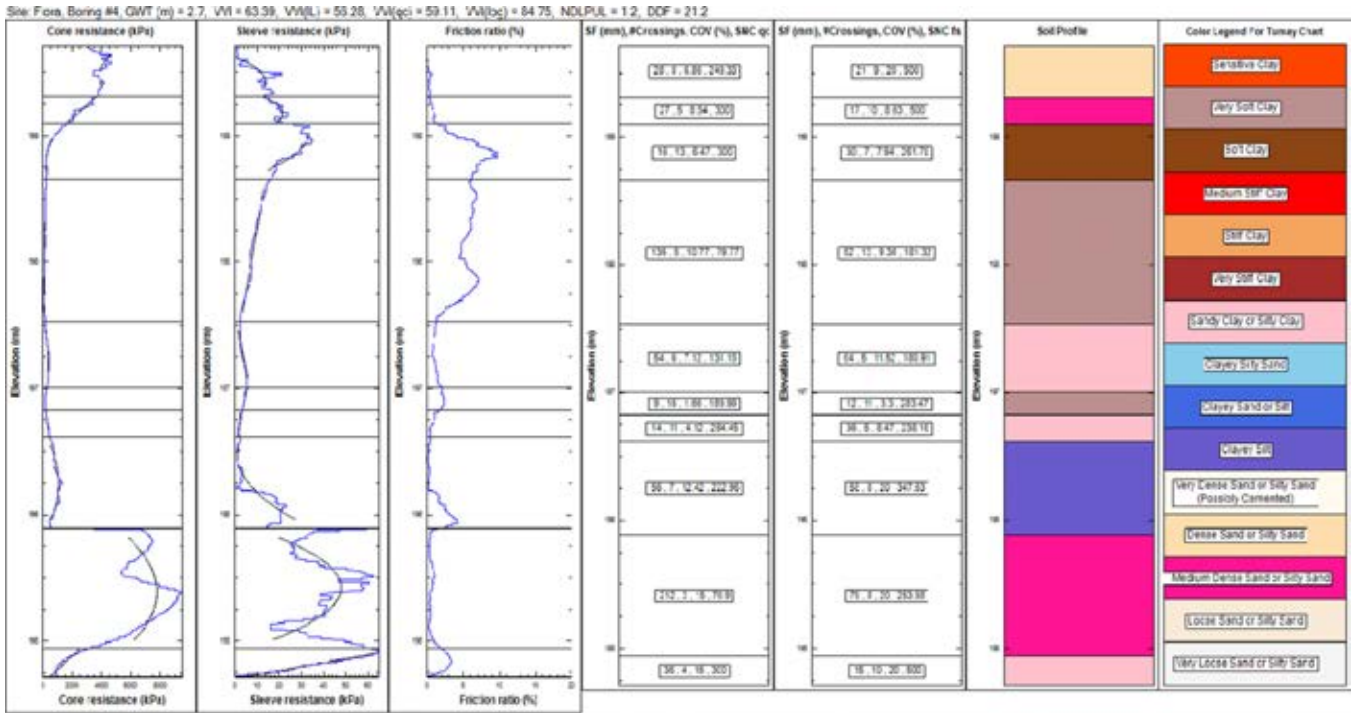


Figure 5.16 Vertical variability indices for sounding #4 of the Flora site for a 5 m soil profile length using the modified Tumay (1985) chart.

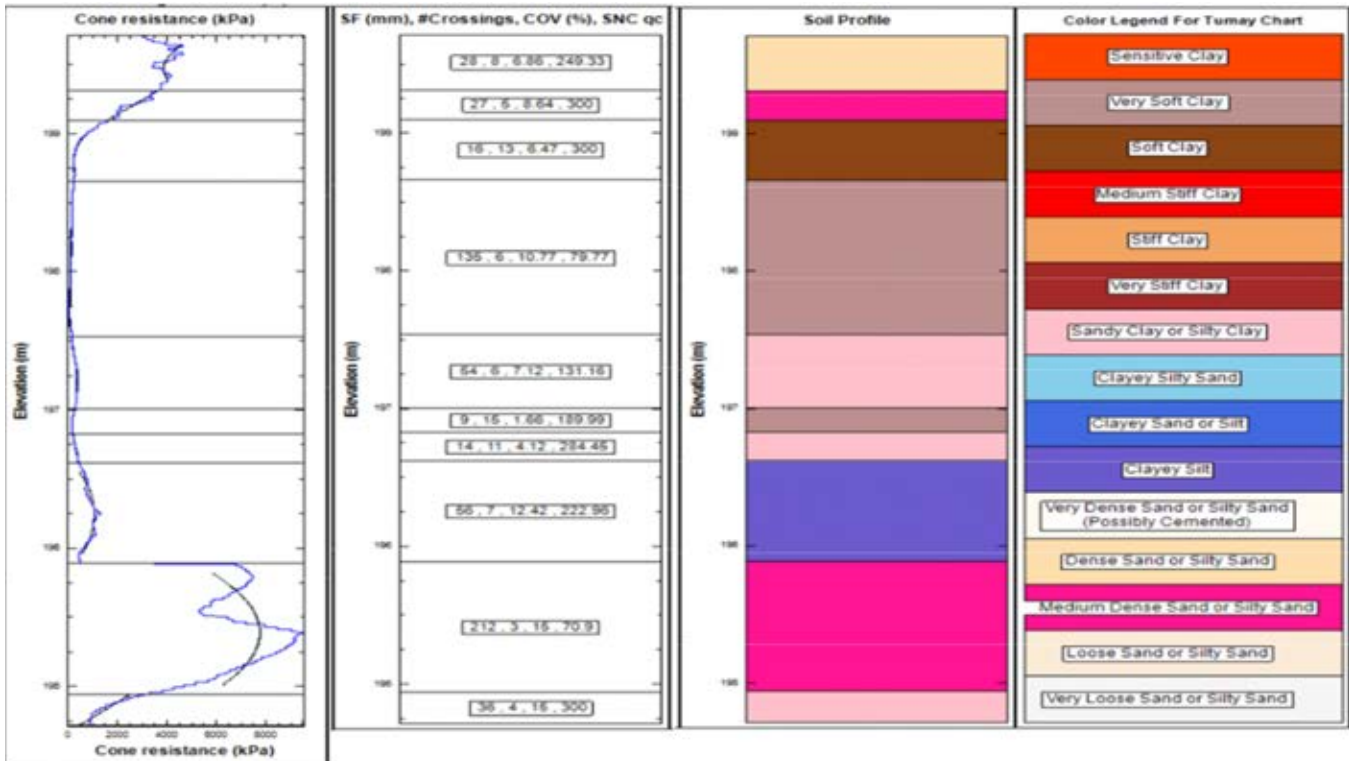


Figure 5.17 Cone resistance profile and intra-layer variability indices for sounding #4 of the Flora site for a 5 m soil profile length using the modified Tumay (1985) chart.

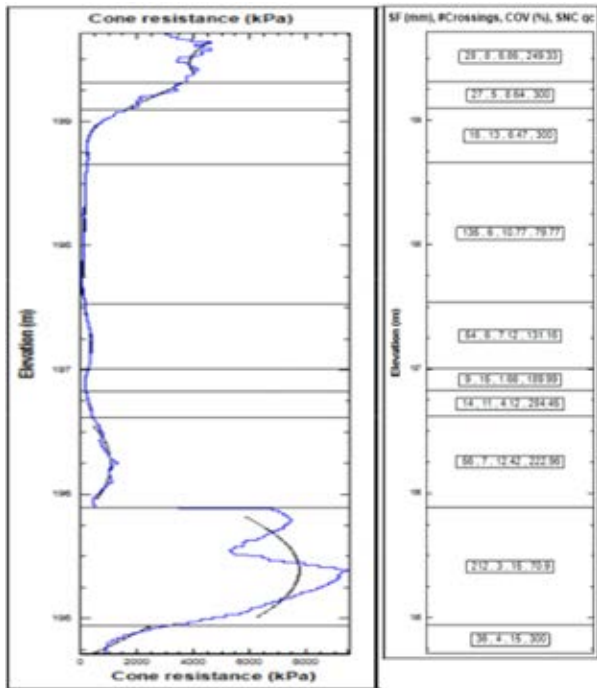


Figure 5.18 Zoomed  $q_c$  profile for sounding #4 of the Flora site for a 5 m soil profile length using the modified Tumay (1985).

A low log variability index is expected for a soil profile with repetition of soil layers and dominance of a particular soil group. Figure 5.23 shows the soil profile of sounding CPT-11-CG-11 of site 1173689 for a 5 m soil profile length generated using the modified Tumay (1985) chart. The soil profile is composed entirely of sand layers. CPT-11-CG-11 of site 1173689 is one of the soundings with the lowest log variability index ( $=2.1$ ). Figure 5.24 shows the normalized error of  $q_c$  vs. depth for sounding CPT-11-CG-11 of site 1173689 (LaPorte).

Figure 5.25 shows the soil profile of sounding RW-13C of site 0600337 for a 5 m soil profile length generated using the modified Tumay (1985) chart. Sounding RW-13C of site 0600337 has the highest log variability index ( $=79.9$ ). The soil profile has a total of 8 soil layers. Except for the two soil layers of sandy clay or silty clay, all the other layers are of different soil type. A high density of different layers, and no dominance of a particular soil group results in a high log variability index ( $=79.9$ ). Figure 5.26 shows the normalized error of  $q_c$  vs. depth for this profile, which ranges from  $-1$  to  $+4$ , resulting in a high COV of the cone resistance of 63.34.

### 5.5.5 Relationship between COV of Cone Resistance and Log Variability Index

In the two examples discussed earlier (sounding CPT-11-CG-11 of site 1173689, with low log variability index, and sounding RW-13C of site 0600337, with high variability index), it is observed that a low log variability index ( $=2.1$ ) is

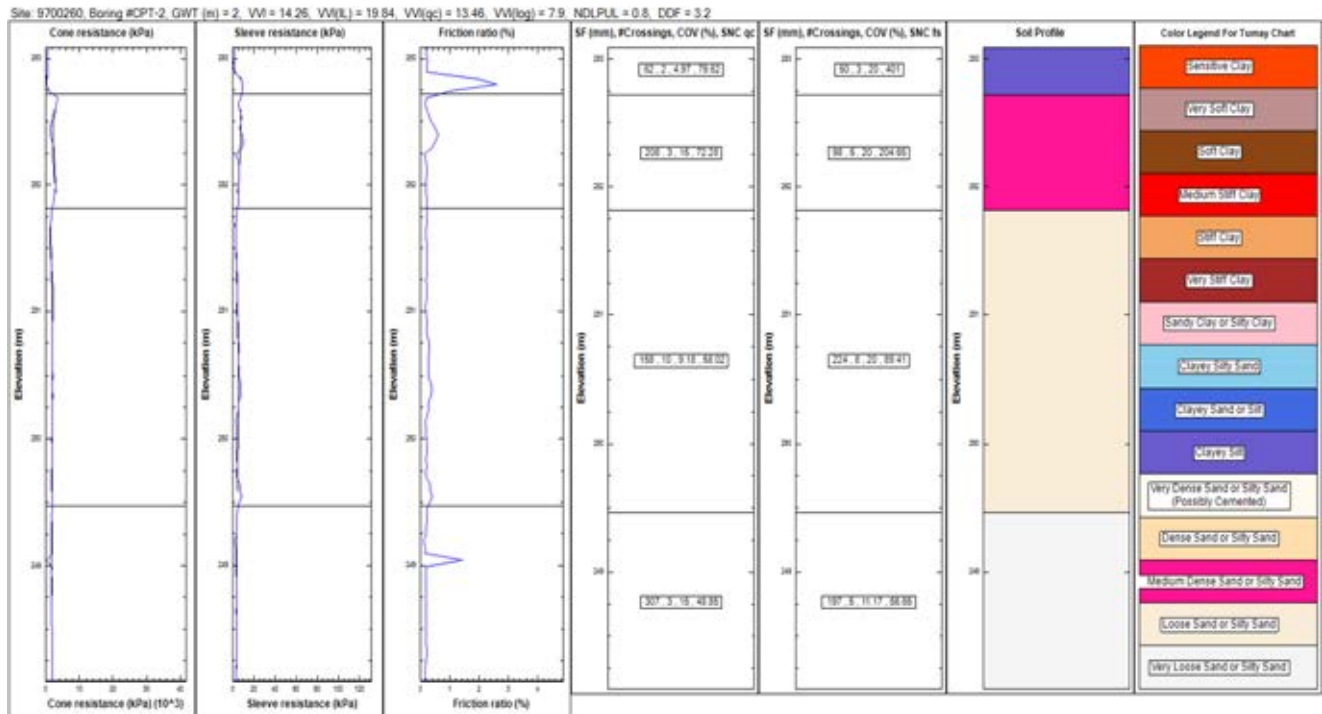
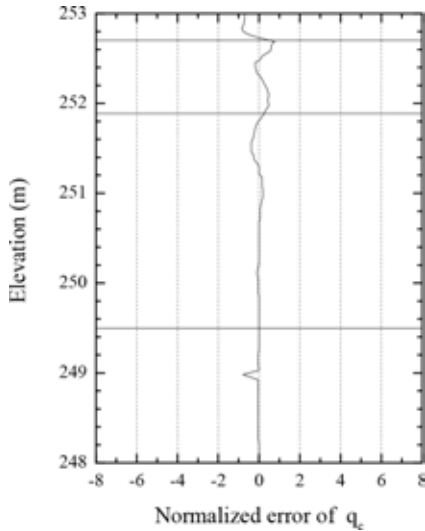
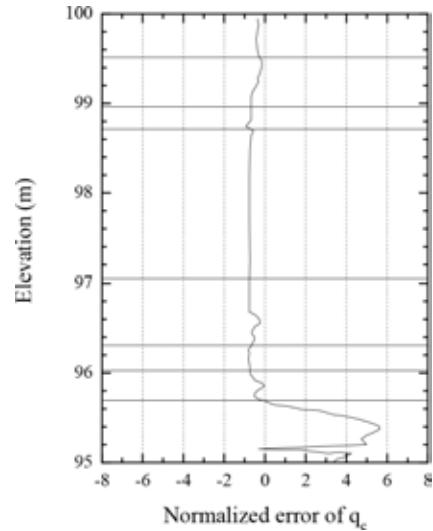


Figure 5.19 Soil profile of sounding CPT-2 of site 9700260 (Fort Wayne) for a 5 m soil profile length generated using the modified Tumay (1985) chart and plotted in relevant scale.



**Figure 5.20** Normalized error of  $q_c$  vs. depth of sounding CPT-2 of site 9700260 (Fort Wayne) for a 5 m soil profile length generated using the modified Tumay (1985) chart.



**Figure 5.22** Normalized error of  $q_c$  vs. depth for sounding TB-11 of site 0600337 (Greenfield) for a 5 m soil profile length generated using the modified Tumay (1985) chart.

accompanied by a low COV of cone resistance ( $=25.6$ ), while a high log variability index ( $=79.9$ ) is accompanied by a high COV of cone resistance ( $=92$ ). To investigate whether there is a relationship of proportionality between the log variability index and the COV of the cone resistance, all available CPTs for 5 m soil profile lengths were compared. Figure 5.27 shows that the correlation between the COV of cone resistance and the log variability index is not strong. The reason for this is that it is possible that a soil profile may have a relatively large number of different soil

layers with comparable  $q_c$  values, for example, which would mean high log variability index but low COV of cone resistance. These two indices therefore do reflect different aspects of variability in the soil profile and are not redundant.

#### 5.5.6 Soil Profiles with Low and High VVI

Of all the soundings analyzed, sounding CPT 2 of site 9700260 (Fort Wayne) produces the lowest (14.26) VVI,

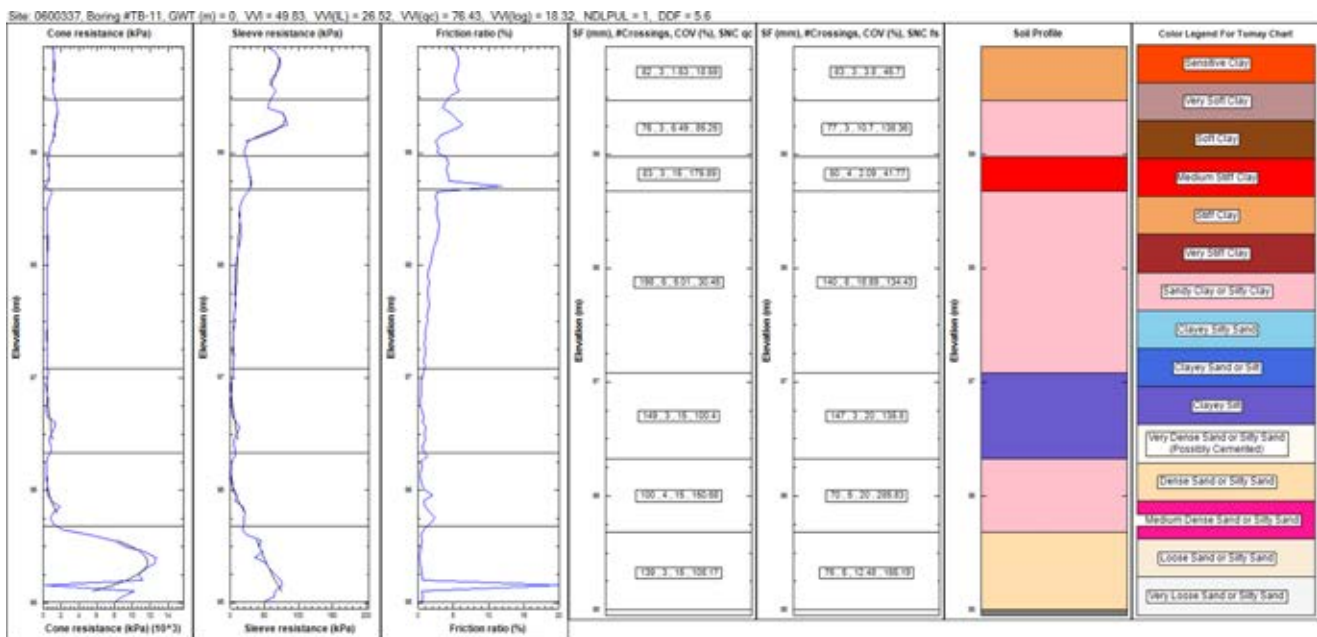


**Figure 5.21** Soil profile for sounding TB-11 of site 0600337 (Greenfield) for a 5 m soil profile length generated using the modified Tumay (1985) chart.

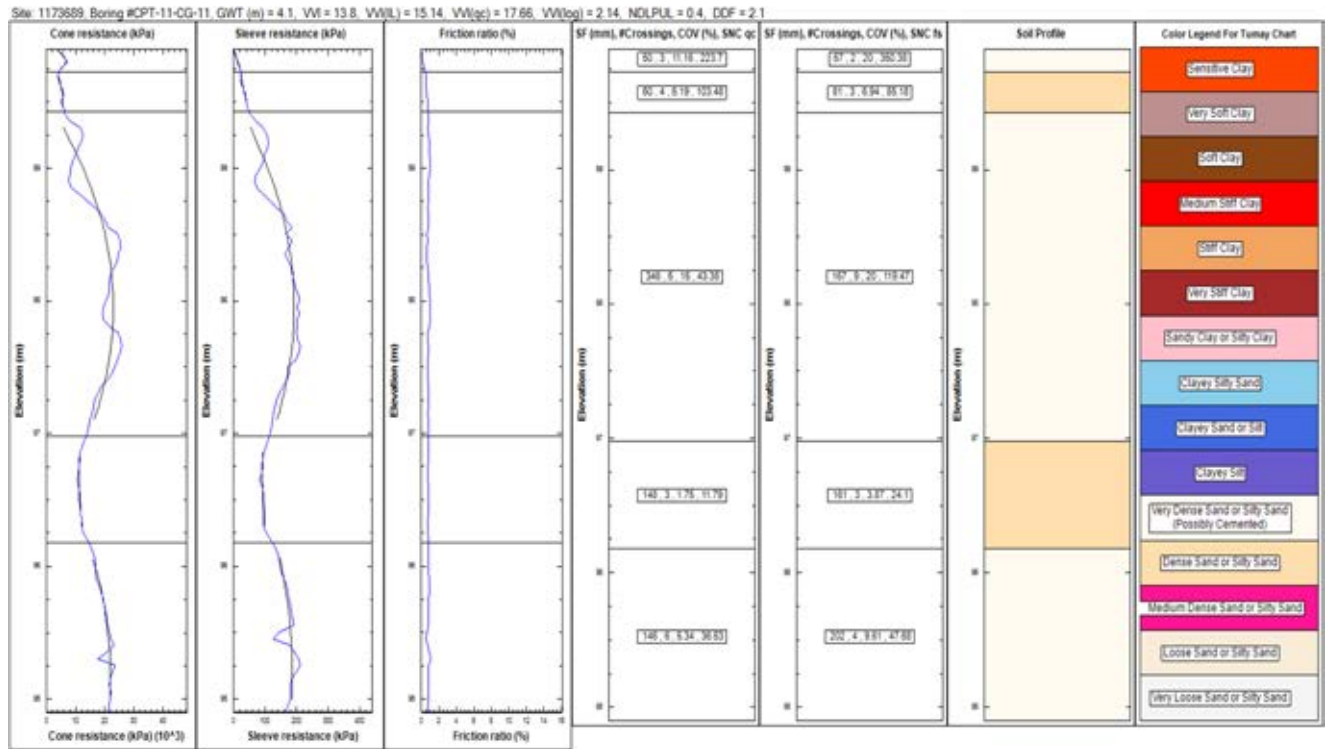


**Figure 5.23** Soil profile for sounding CPT-11-CG-11 of site 1173689 (LaPorte) for a 5 m soil profile length generated using the modified Tumay (1985) chart.

while sounding RW-13C of site 600337 produces the highest (57.07) *VVI* (5 m soil profile length).

Figure 5.28 shows the soil profile of sounding 2 of site 9700260 (Fort Wayne) for a 5 m soil profile length generated using the modified Tumay (1985) chart, and Figure 5.29 shows the normalized error of  $q_c$  vs. depth of sounding 2 of site 9700260 (Fort Wayne) for a 5 m soil profile length

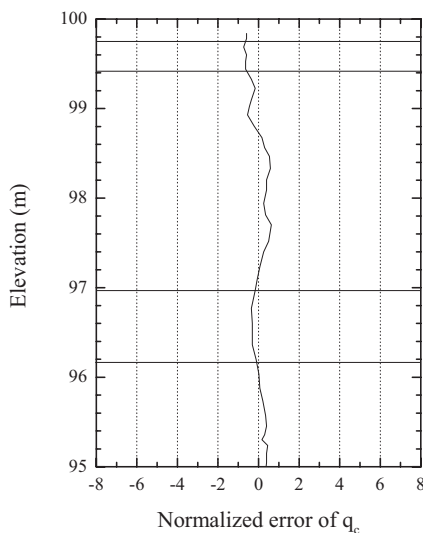


**Figure 5.24** Normalized error of  $q_c$  vs. depth of sounding CPT-11-CG-11 of site 1173689 (LaPorte) for a 5 m soil profile length.

generated using the modified Tumay (1985) chart. The soil profile has a low intra-layer variability index of 19.84 and a low COV of cone resistance of 13.46. The occurrence of low COV of cone resistance is better illustrated in Figure 5.29, where we can see that the normalized error of  $q_c$  is bound within +1 and -1. The soil profile consists mostly of sands and a top layer of mixed soil producing a low log variability index of 7.9.

Figure 5.30 shows the soil profile of sounding RW-13C of site 0600337 (Greenfield) for a 5 m soil profile length generated using the modified Tumay (1985) chart in relevant scale and Figure 5.31 shows the normalized error in  $q_c$  vs. depth of sounding RW-13C of site 0600337 for a 5 m soil profile length generated using the modified Tumay (1985) chart. The soil profile is highly variable, with the presence of very stiff to very soft clay near the top, mixed soil layers in the middle and very dense sand towards the bottom. As a consequence, the soil profile has a very high log variability index of 80.68 and a very high COV of cone resistance of 91.64 (see Figure 5.31).

Table 5.4 summarizes the variability calculation results of all the sites in the Purdue and INDOT databases using both the modified Tumay (1985) and the modified Robertson (1990) SBT charts for a soil profile length of 5 m. The McCormick site has the lowest site *HVI* (= 16), while the site with DES #100331 (LaPorte) has the highest (= 76) site *HVI*. Figure 5.32 through Figure 5.36 show the soil profiles for soundings 1 to 5 of the McCormick site. The similarities among the soundings are noticeable; all of the soundings in general have a

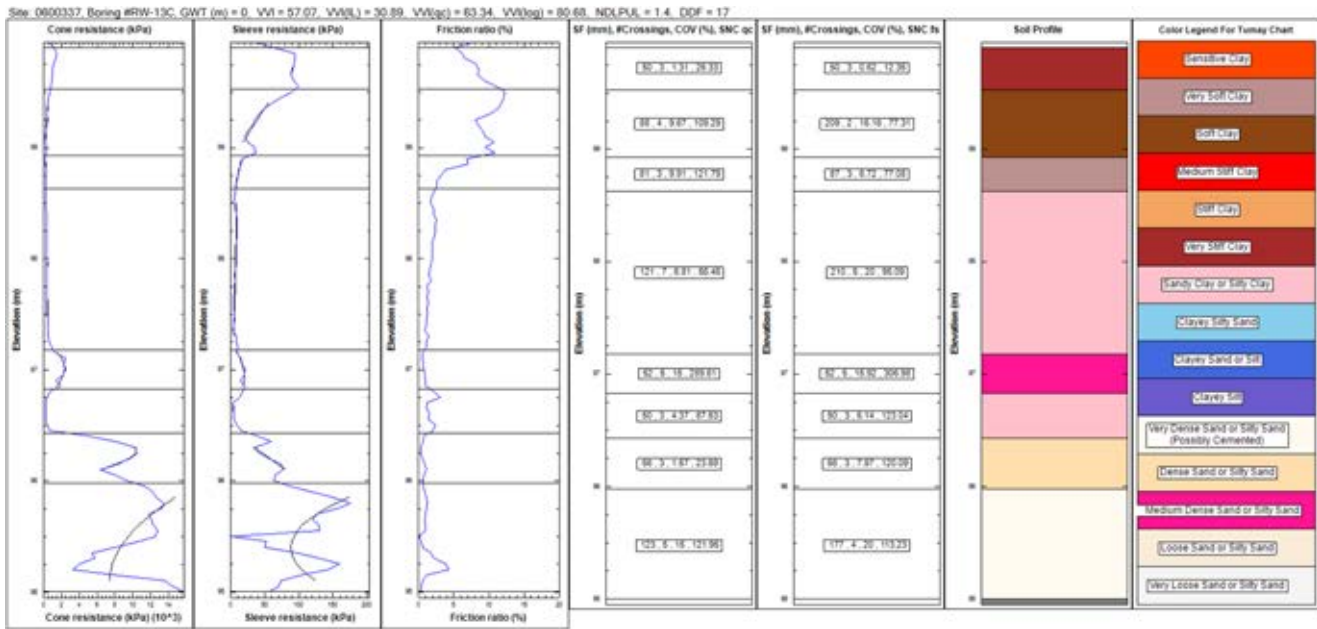


**Figure 5.25** Soil profile of sounding RW-13C of site 0600337 (Greenfield) for a 5 m soil profile length generated using the modified Tumay (1985) chart and plotted in relevant scale.

clayey soil layer towards the top that is underlain by sand layers. In Figure 5.37, the  $q_c$  profiles of the soundings from the McCormick site are arranged side-by-side to better visualize the similarities of the soundings, which produce a very low site *HVI*.

The soil profiles of the soundings from site 100331 are shown in Figure 5.38, Figure 5.39 and Figure 5.40. The soil profiles are, in general, comprised of sand layers of different densities with some clayey and mixed soil layers. The dissimilarity among the  $q_c$  profiles are noticeable from Figure 5.41, which shows the  $q_c$  profiles side by side. This dissimilarity has contributed towards a high site *HVI* of 76.

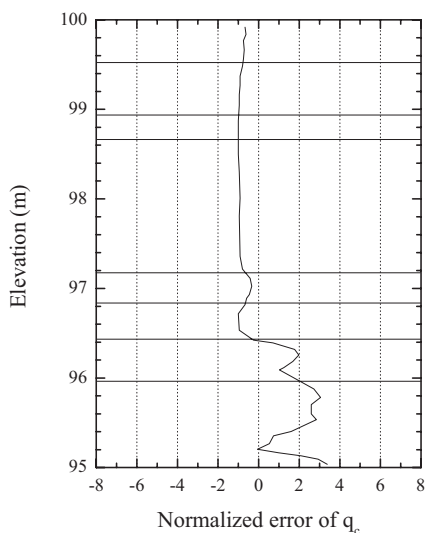


**Figure 5.26** Normalized error of  $q_c$  vs. depth of sounding RW-13C of site 0600337 (Greenfield) for a 5 m soil profile length generated using the modified Tumay (1985) chart.

## 5.6 SVR Results

Table 5.5, Table 5.6, Table 5.7 and Table 5.8 show the variability results for 3 m, 4 m and 5 m soil profile lengths, respectively. As the depth interval increased, the number of available sites for analysis decreased.

### 5.6.1 Comparison of Variability Results Obtained Using the Modified Tumay (1985) and Modified Robertson (1990) Charts

Table 5.5, Table 5.6, Table 5.7 and Table 5.8 show that the variability results obtained using the modified Tumay

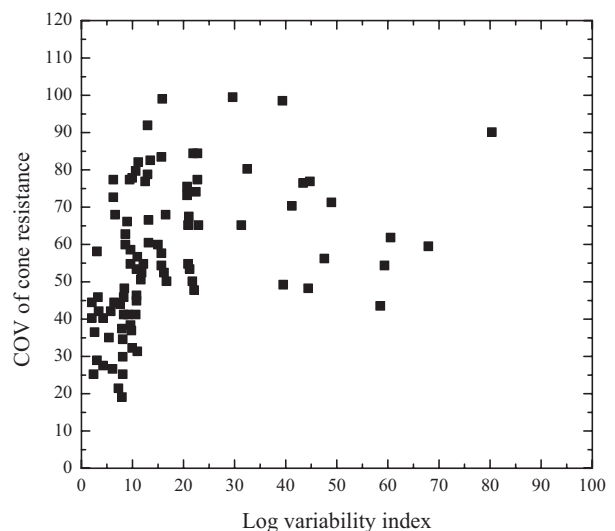


**Figure 5.27** COV of cone resistance versus log variability index for a 5 m length soil profile using the modified Tumay (1985) chart.

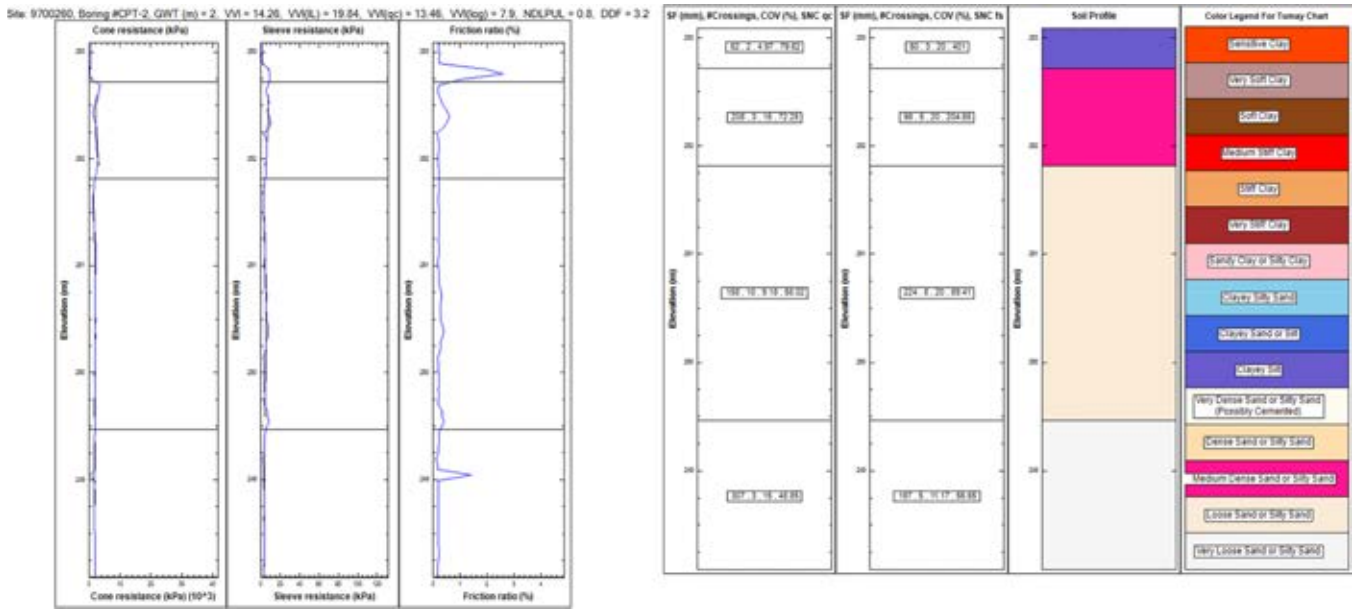


**Figure 5.28** Soil profile of sounding 2 of site 9700260 (Fort Wayne) for a 5 m soil profile length generated using the modified Tumay (1985) chart and plotted in relevant scale.

(1985) and modified Robertson (1990) charts are similar in most cases. In Figure 5.42, Figure 5.43 and Figure 5.44, the site *VVI*s obtained using the modified Tumay (1985) chart are plotted in the horizontal axis and the site *VVI*s for the corresponding sites obtained using the modified Robertson (1990) chart are plotted in the vertical axis. Use of the modified Robertson (1990) chart yields a slightly higher *VVI* than the modified Tumay (1985) chart.

5.6.2 Variability Maps for Indiana

Figure 5.45 shows a map of the state of Indiana with site *VVI* results for a 3 m soil profile length using the modified

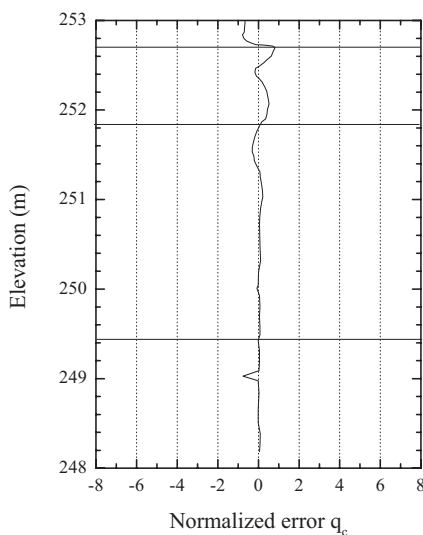


**Figure 5.29** Normalized error of *qc* vs. depth of sounding 2 of site 9700260 (Fort Wayne) for 5 m soil profile length generated using the modified Tumay (1985) chart.

Tumay (1985) chart. The map is divided into counties. The site *VVI* have been divided into low (L,  $VVI < 33\%$ ), medium (M,  $33 \leq VVI < 67\%$ ) and high variability (H,  $67 \leq VVI \leq 100\%$ ). Figure 5.46 shows the calculated site *HVI* for the same sites (also classified using L, M and H, like the *VVI*, to indicate low, medium and high variability in the horizontal direction). Figure 5.47 shows the corresponding SVR map using the modified Tumay (1985) chart. Sites are classified by two symbols, the first (L, M or H) corresponding to the average *VVI* for the site and the second (also L, M or H) to the site *HVI*. So, a site designated as HH would be highly variable in both the horizontal and the vertical directions, whereas a site designated as LL would be a low variability site.

Figure 5.48 and Figure 5.49 show the site *VVI* and SVR maps obtained using the modified Robertson (1990) chart for a 3 m soil profile length. Higher values for the *VVI* result when the modified Robertson (1990) chart is used instead of the modified Tumay (1985) chart, as can be also seen in Figure 5.42. Results in Figure 5.44 show that the site *VVI* is between 45 and 50 in the case of the modified Tumay (1985) chart, while it is near 50 in the case of the modified Robertson (1990) chart. Therefore, depending on the SBT chart used, slightly different site variability classification may result.

In Appendix B, Figure B.6 through Figure B.10 show the site *VVI*, the site *HVI* and SVR maps for 4 m soil profile length and Figure B.11 through Figure B.15 show the site *VVI*, the site *HVI* and SVR maps for 5 m soil profile length.

As can be observed in the SVR maps for the state of Indiana, more CPTs are required to increase the current database of test results. This is needed to enhance our mapping of the spatial variability of *in situ* soils in the state of Indiana. To this end, a properly established procedure

Site: 0600337, Boring #RW-13C, GWT (m) = 0, V<sub>I</sub> = 57.07, V<sub>V</sub>(LL) = 30.89, V<sub>V</sub>(qc) = 63.54, V<sub>V</sub>(log) = 60.66, NDLPLJL = 1.4, DOF = 17

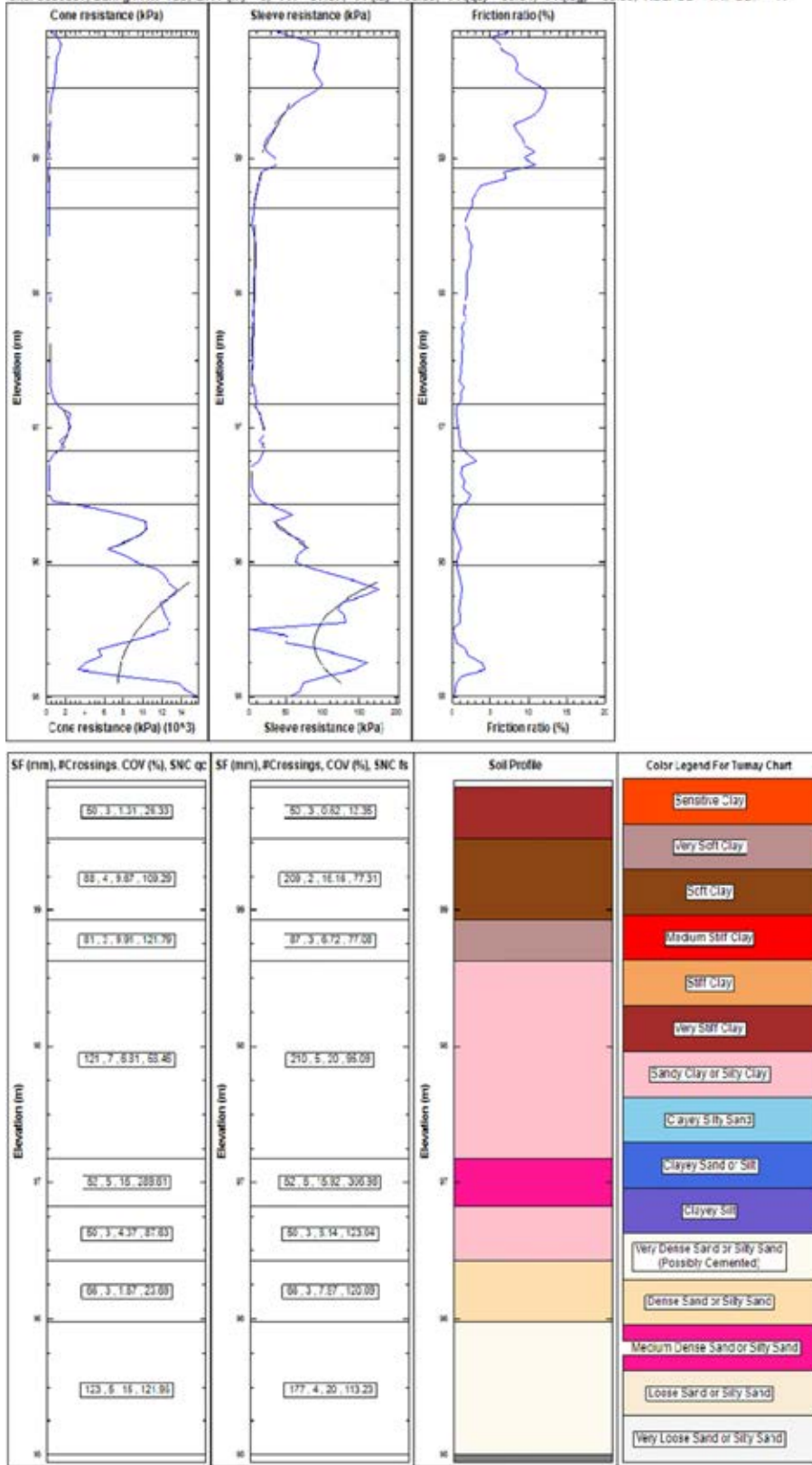
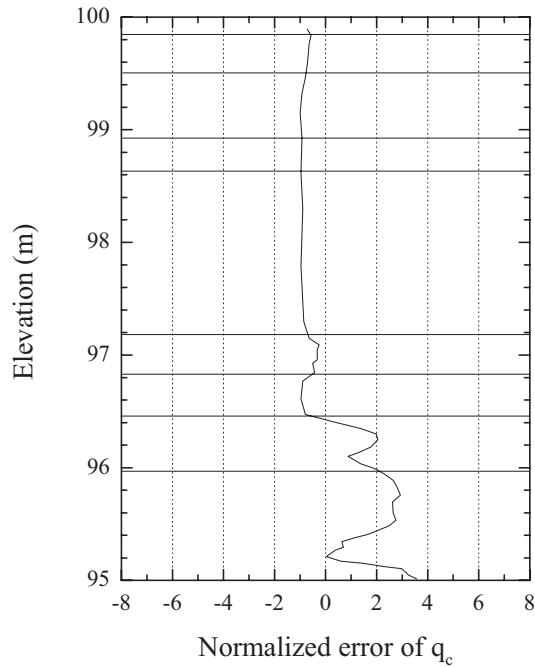


Figure 5.30 Soil profile of sounding RW-13C of site 0600337 (Greenfield) for a 5 m soil profile length generated using the modified Tumay (1985) chart.



**Figure 5.31** Normalized error of  $q_c$  vs. depth of sounding RW-13C of site 0600337 (Greenfield) for a 5 m soil profile length generated using the modified Tumay (1985) chart.

needs to be followed when performing CPTs in the field. The recommended procedure is outlined below:

1. Perform a CPT at an initial location at the test site;
2. Perform a second CPT at a measured distance from the first CPT location;
3. Based on the previous two CPTs, calculate the optimum spacing using the algorithm outlined in section 4.4;

4. Perform the next CPT at calculated optimum spacing from the previous CPT location;
5. Repeat steps 3 and 4 until an adequate number of tests have been performed to characterize the spatial variability of *in situ* soil at the site.

It is recommended that a minimum of five CPTs be performed per 1000 m<sup>2</sup> to properly characterize the *in situ*

**TABLE 5.4**  
Results of variability assessment for 5 m soil profile length

DES#/Site Name	Location		Modified Tumay (1985) Chart			Modified Robertson (1990) Chart		
	County	District	Site VVI	Site HVI	SVR	Site VVI	Site HVI	SVR
100521	White	LaPorte	43	26	ML	45	26	ML
401113	Elkhart	Fort Wayne	48	25	ML	41	25	ML
600337	Howard	Greenfield	37	24	ML	36	24	ML
710722	Steuben	Fort Wayne	27	37	LM	31	37	LM
810115	Daviess	Vincennes	32	53	MM	36	53	MM
901897	LaPorte	LaPorte	31	22	LL	34	22	ML
100331	Jasper	LaPorte	28	76	LH	32	76	LH
1173689	Warrick	Vincennes	18	62	LM	20	62	LM
8823155	DeKalb	Fort Wayne	29	22	LL	31	22	LL
9031790	Allen	Fort Wayne	32	29	LL	35	29	ML
9700260	White	LaPorte	26	24	LL	30	24	LL
Koleen	—	—	46	33	ML	46	33	ML
Romney	—	—	31	79	LH	32	79	LH
McCormick	—	—	35	16	ML	36	16	ML
Flora	—	—	54	23	ML	52	23	ML

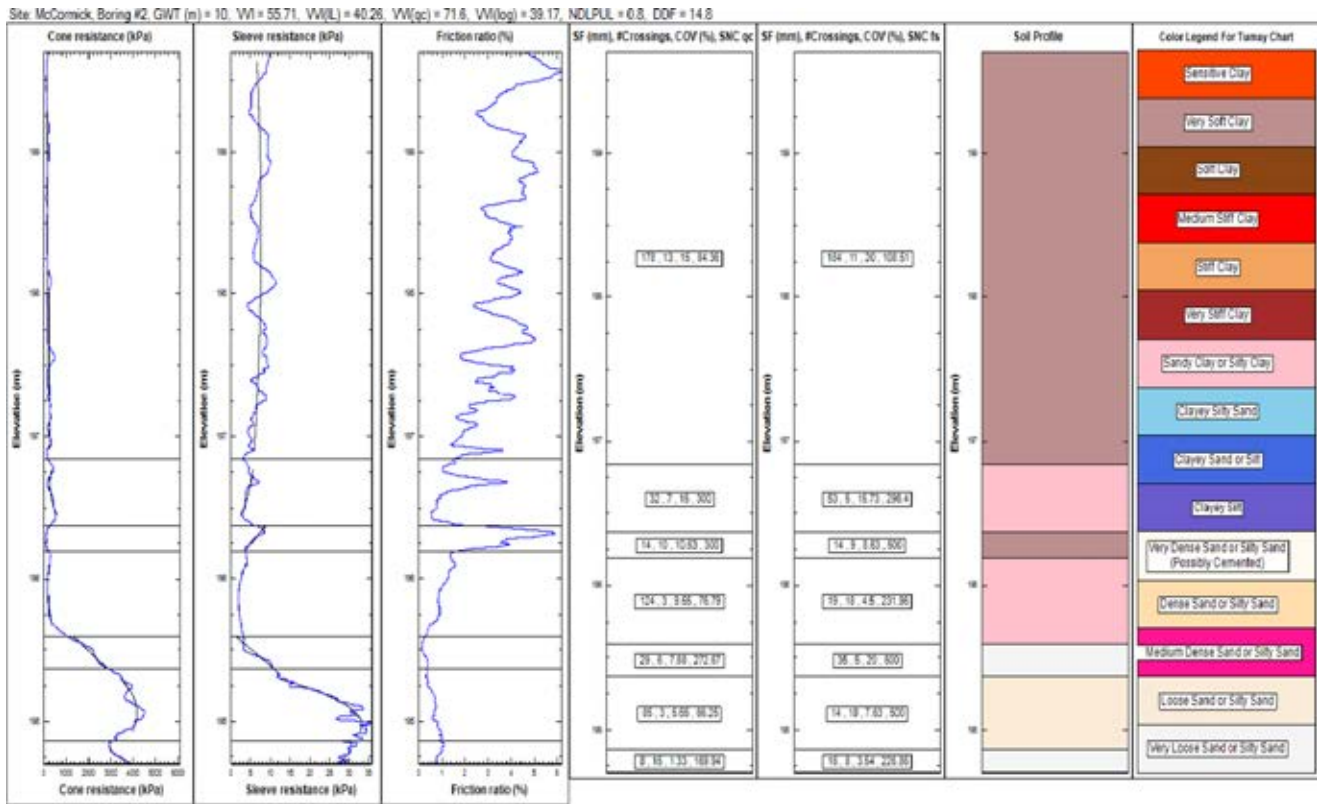


Figure 5.32 Vertical variability for sounding #2 of McCormick site for a 5 m soil profile length using the modified Tumay (1985) chart.

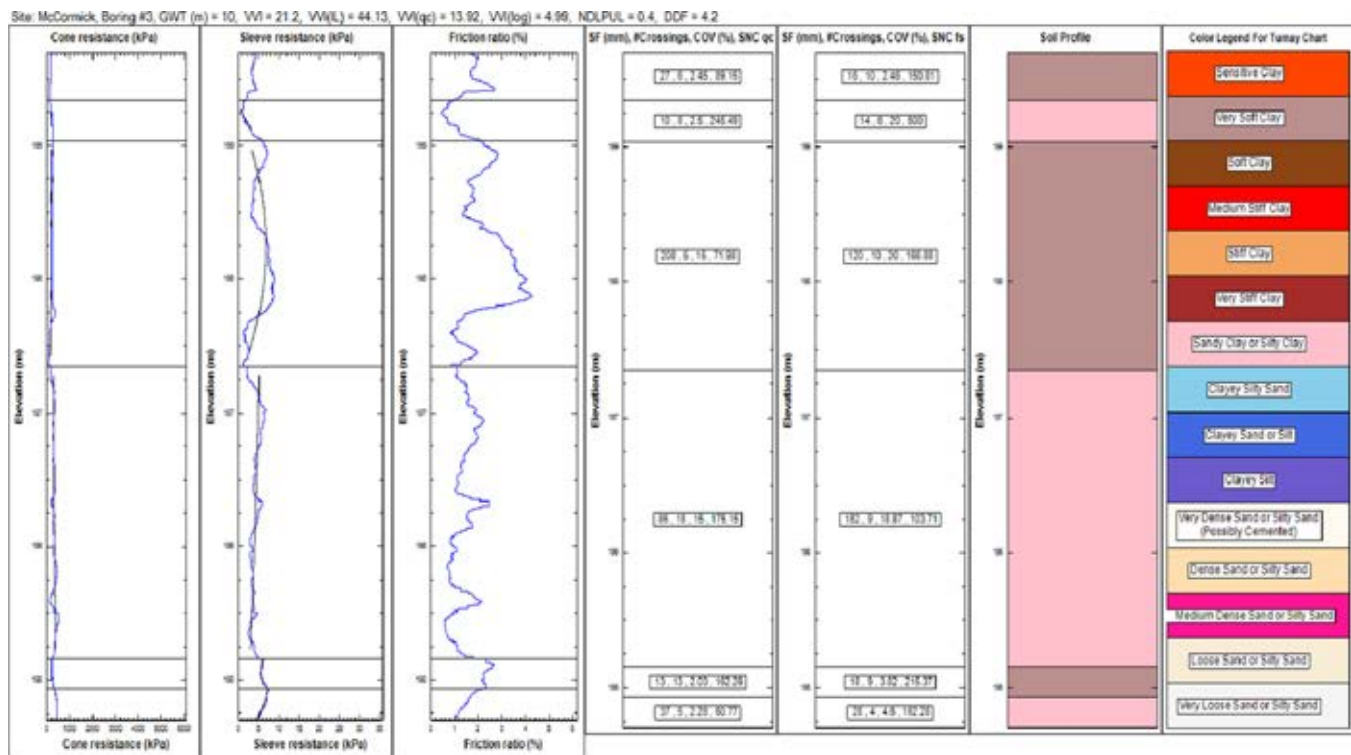


Figure 5.33 Vertical variability of sounding #3 of McCormick site for a 5 m soil profile length using the modified Tumay (1985) chart.

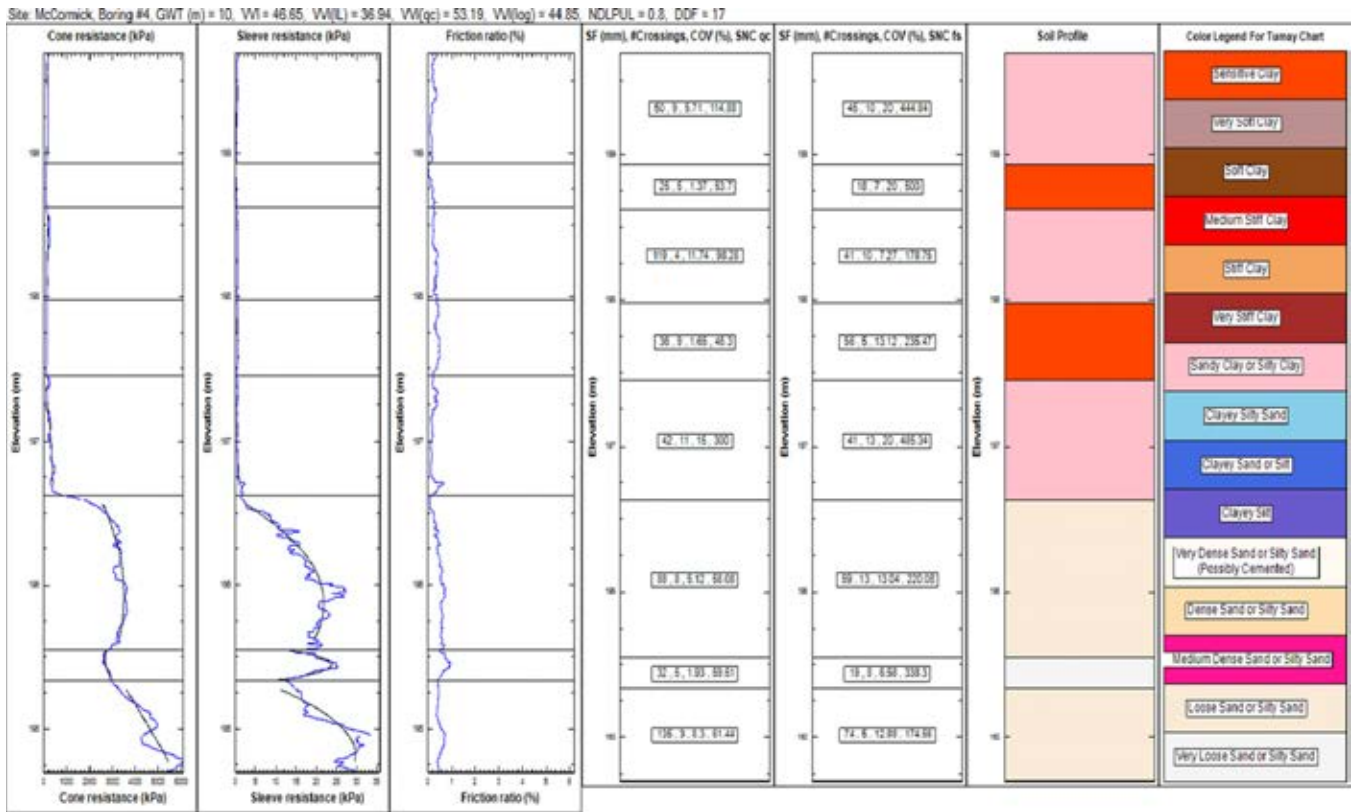


Figure 5.34 Vertical variability of sounding #4 of McCormick site for a 5 m soil profile length using the modified Tumay (1985) chart.

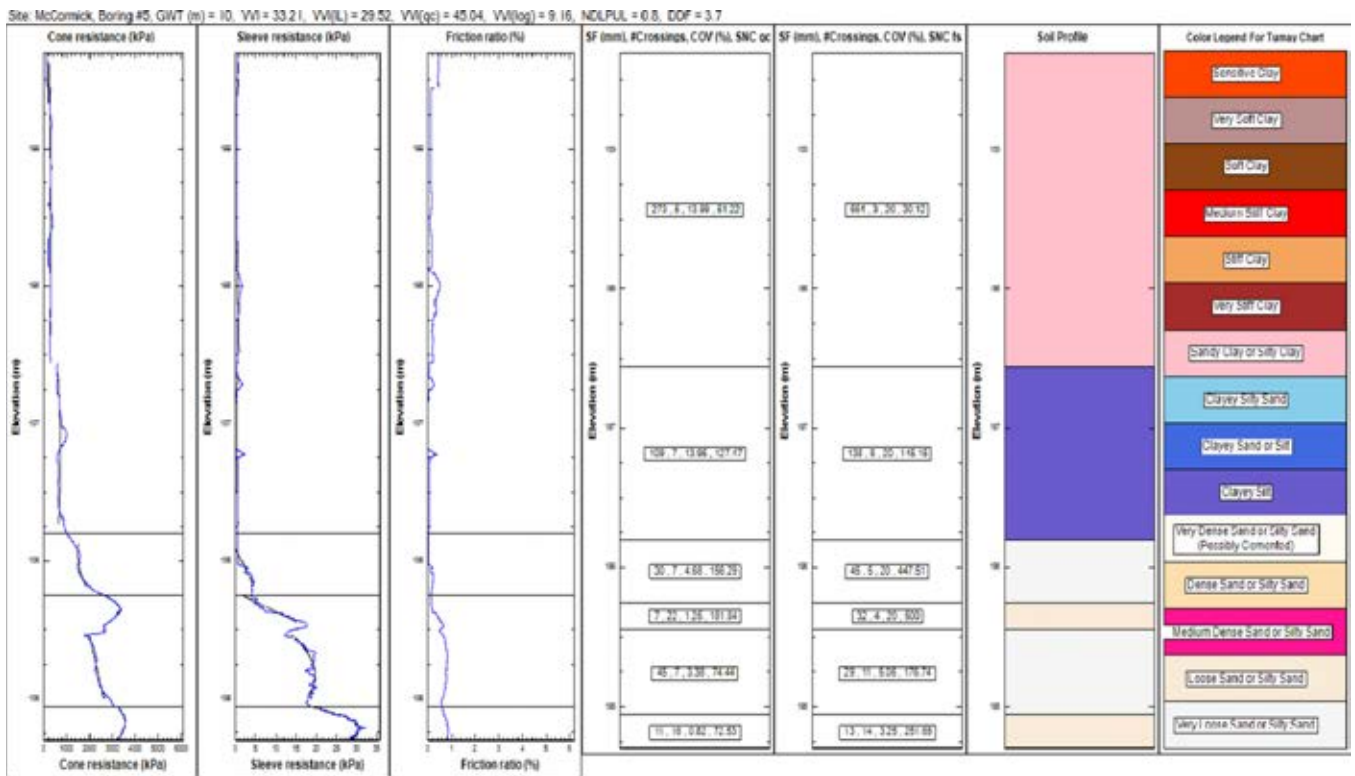


Figure 5.35 Vertical variability of sounding #5 of McCormick site for a 5 m soil profile length using the modified Tumay (1985) chart.

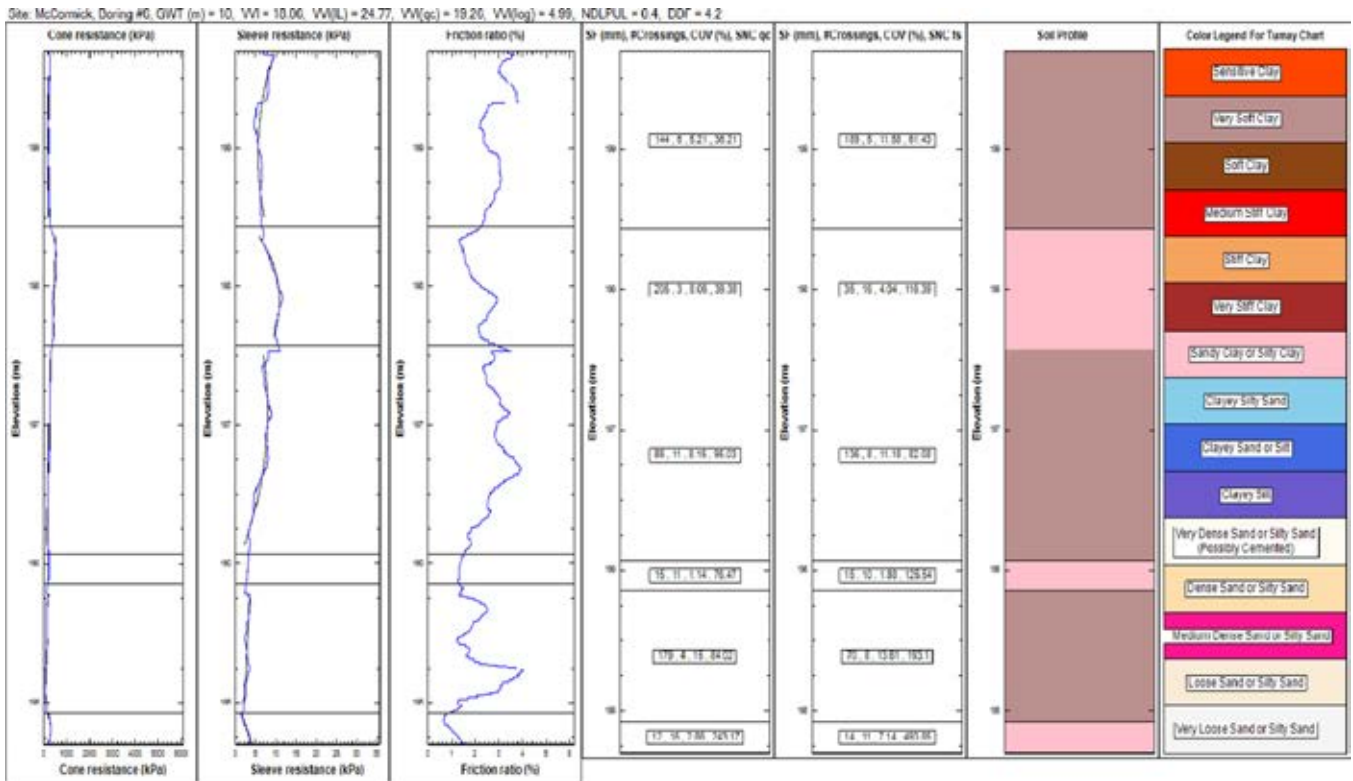


Figure 5.36 Vertical variability of sounding #6 of McCormick site for a 5 m soil profile length using the modified Tumay (1985) chart.

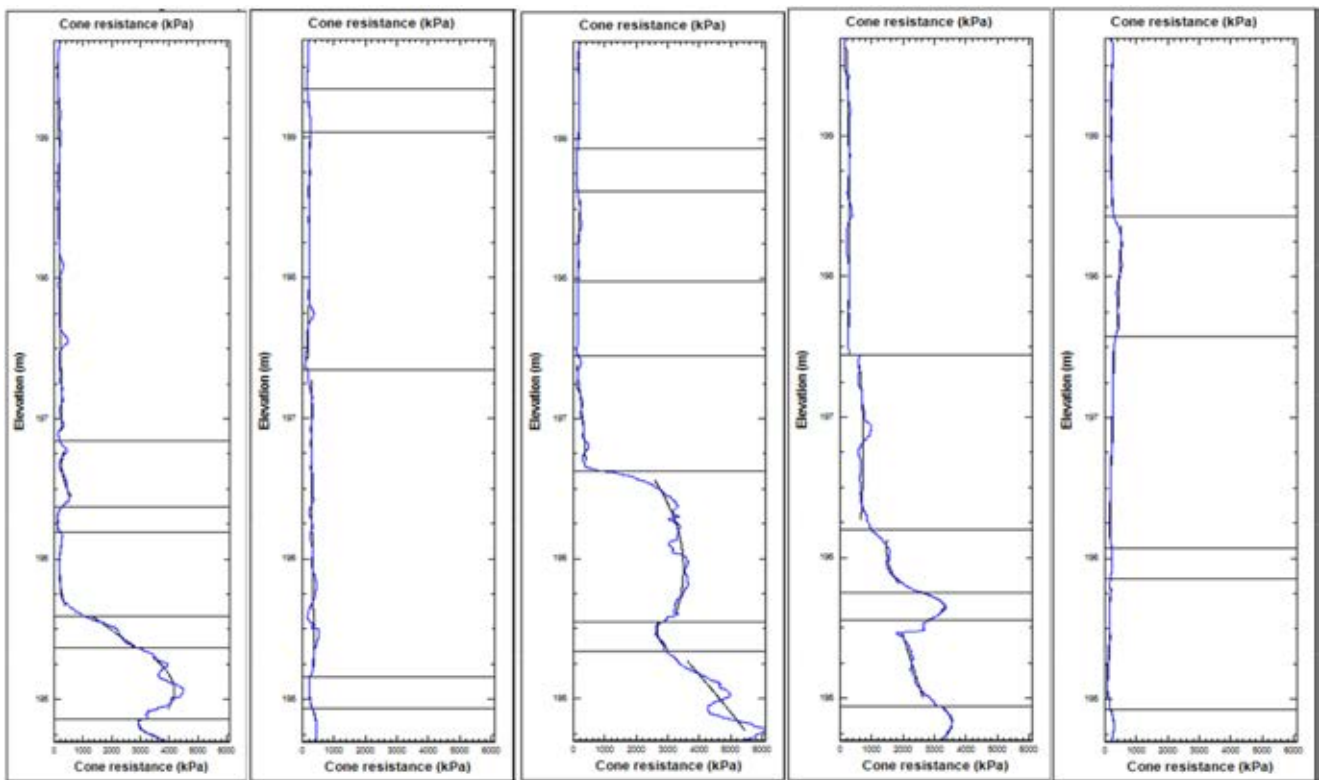


Figure 5.37 Side-by-side comparison of  $q_c$  profiles of CPT 1 through CPT 6 for Kolen site.

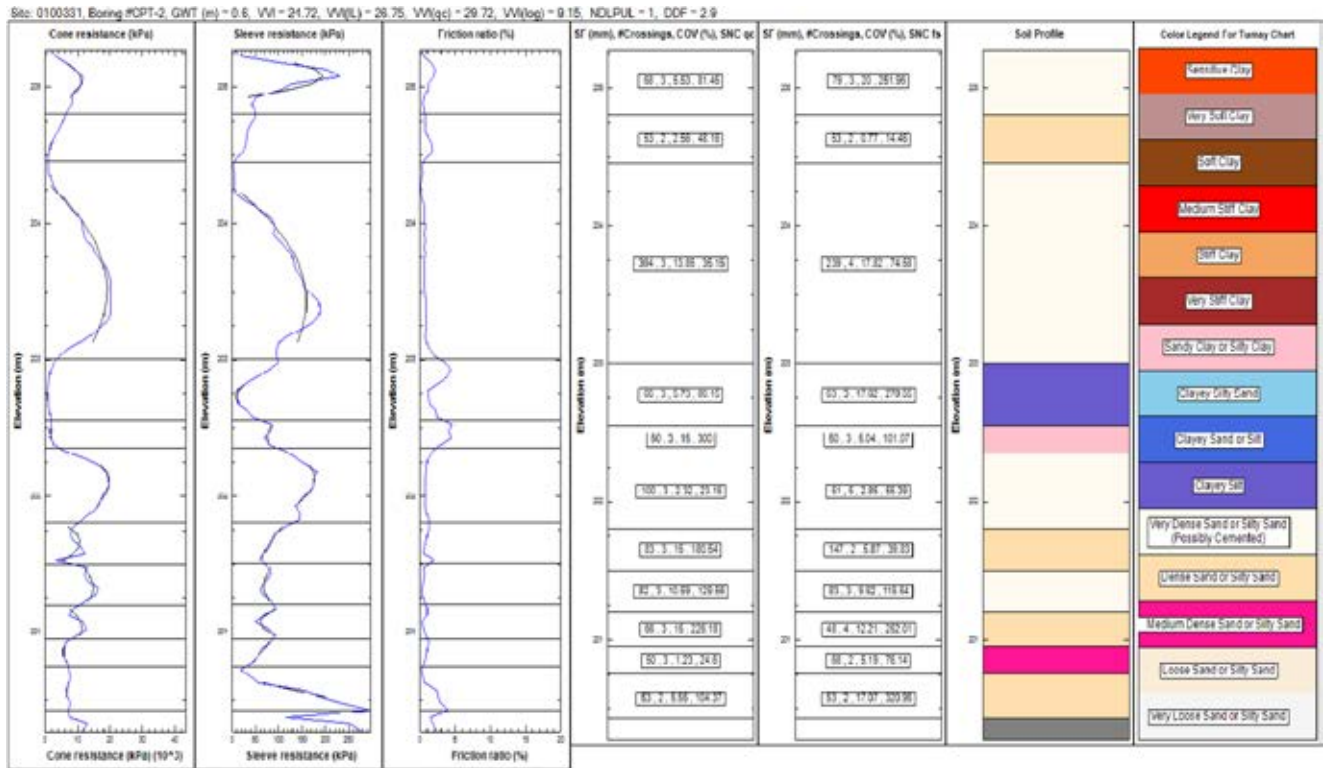


Figure 5.38 Vertical variability of sounding CPT-2 of site 0100331 (LaPorte) for a 5 m soil profile length using the modified Tumay (1985) chart.

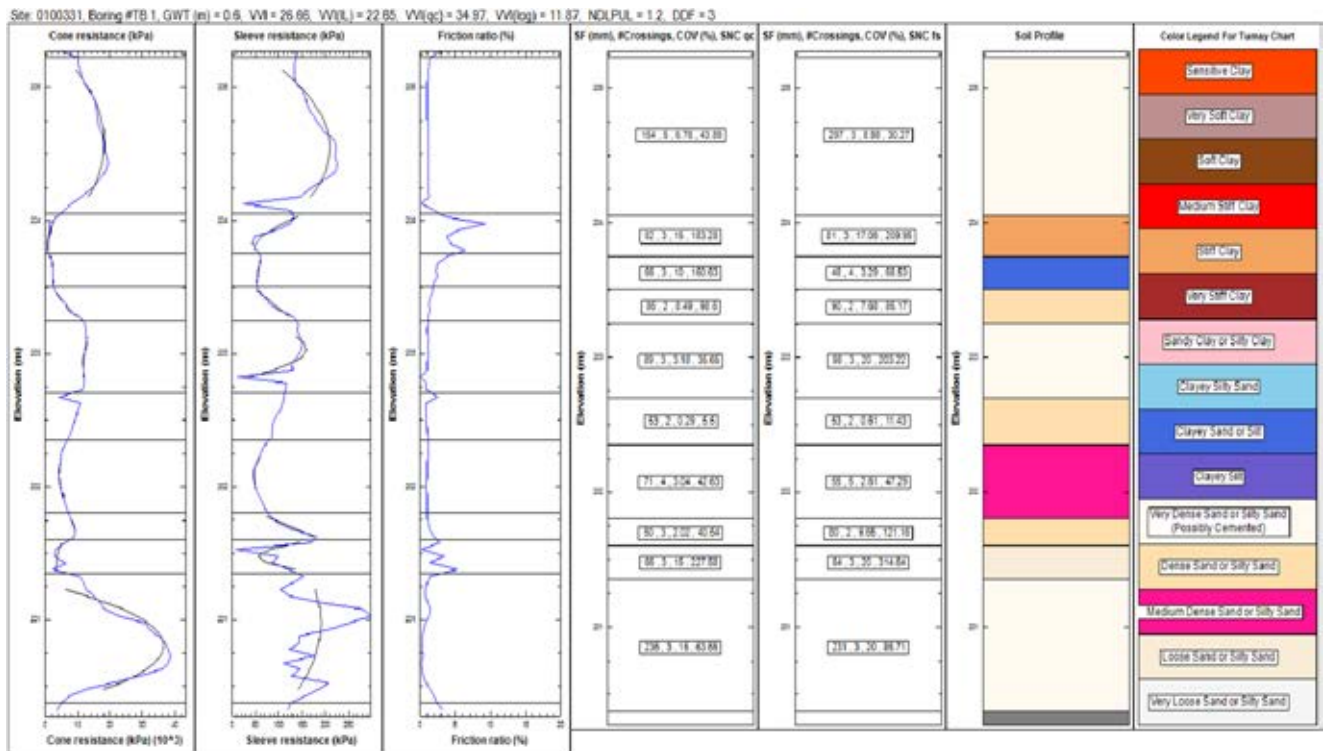


Figure 5.39 Vertical variability of sounding TB-1 of site 0100331 (LaPorte) for a 5 m soil profile length using the modified Tumay (1985) chart.

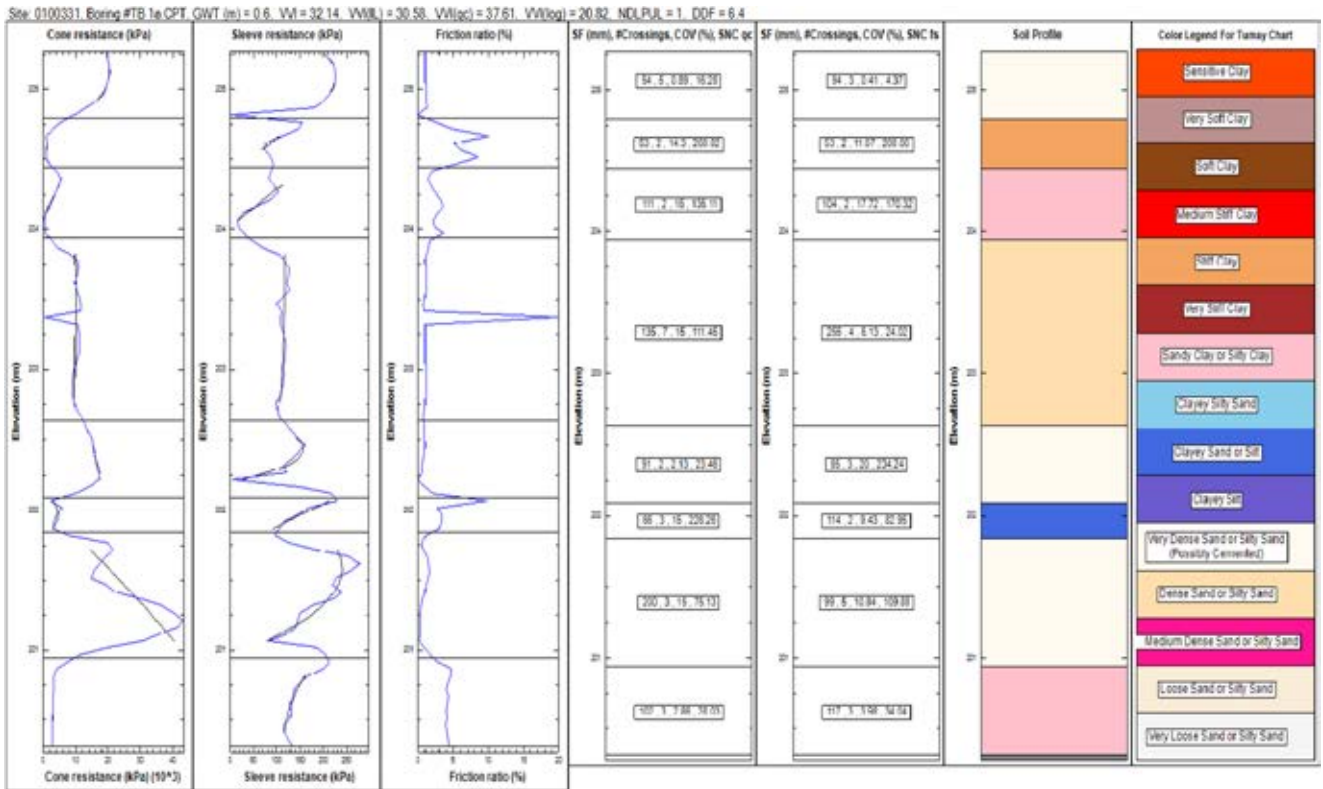


Figure 5.40 Vertical variability of sounding TB-1a of site 0100331 (LaPorte) for a 5m soil profile length using the modified Tumay (1985) chart.

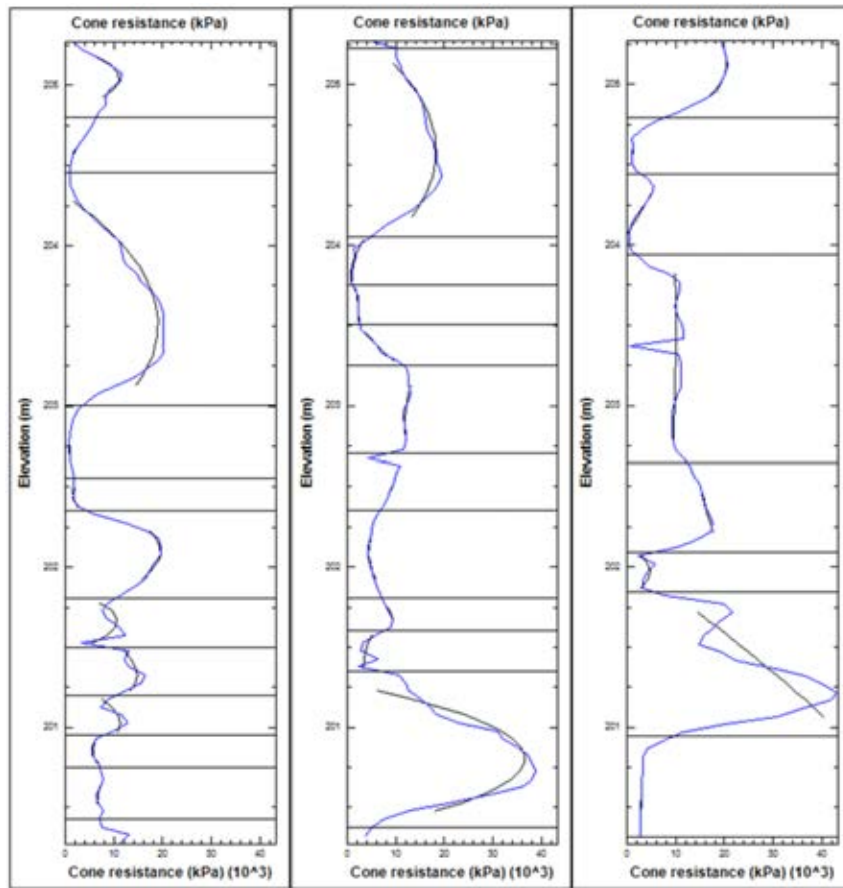


Figure 5.41 Side-by-side comparison of  $q_c$  profiles for soundings CPT 2, TB-1 and TB-1a of site 0100331 (LaPorte).

TABLE 5.5  
SVR results for 3 m soil profile length

DES#/Site Name	Location		Modified Tumay (1985) Chart			Modified Robertson (1990) Chart		
	County	District	Site VVI	Site HVI	SVR	Site VVI	Site HVI	SVR
100521	White	LaPorte	47	24	ML	55	24	ML
401113	Elkhart	Fort Wayne	50	31	ML	48	31	ML
600337	Howard	Greenfield	28	14	LL	29	14	LL
301142	Elkhart	Fort Wayne	39	17	ML	39	17	ML
901897	Daviess	Vincennes	37	25	ML	39	25	ML
8823155	Warrick	Vincennes	31	25	LL	35	25	ML
100331	LaPorte	LaPorte	30	73	LH	35	73	MH
1173689	Jasper	LaPorte	19	78	LH	22	78	LH
300970	Steuben	Fort Wayne	42	29	ML	49	29	ML
100385	Newton	LaPorte	23	30	LL	25	30	LL
301070	White	LaPorte	44	17	ML	46	17	ML
300310	Allen	Fort Wayne	31	42	LM	32	42	LM
301066	White	LaPorte	35	11	ML	38	11	ML
301143	Elkhart	Fort Wayne	25	17	LL	30	17	LL
301071	White	LaPorte	42	29	ML	48	29	ML
9904180 A	Adams	Fort Wayne	41	27	ML	45	27	ML
9031790	DeKalb	Fort Wayne	40	27	ML	46	27	ML
9700260	Allen	Fort Wayne	27	35	LM	31	35	LM
810115	Steuben	Fort Wayne	36	49	MM	39	49	MM
1006389	Decatur	Seymour	40	6	ML	40	6	ML
Purdue Campus	—	—	23	33	LL	26	33	LL
Frankfort	—	—	49	26	ML	48	26	ML
Fort Wayne	—	—	37	34	MM	35	34	MM
McCormick	—	—	35	16	ML	33	16	LL
Flora	—	—	65	29	ML	67	29	ML
Koleen	—	—	46	33	ML	48	33	ML
Romney	—	—	31	79	LH	33	79	LH

TABLE 5.6  
SVR results for 4 m soil profile length

DES#/Site Name	Location		Modified Tumay (1985) Chart			Modified Robertson (1990) Chart		
	County	District	Site VVI	Site HVI	SVR	Site VVI	Site HVI	SVR
100521	White	LaPorte	46	23	ML	50	23	ML
401113	Elkhart	Fort Wayne	50	27	ML	45	27	ML
600337	Howard	Greenfield	33	18	LL	33	18	LL
810115	Steuben	Fort Wayne	33	50	LM	38	50	MM
901897	Daviess	Vincennes	31	24	LL	34	24	ML
100331	LaPorte	LaPorte	28	69	LH	32	69	LH
1173689	Jasper	LaPorte	15	66	LH	20	66	LM
300970	Steuben	Fort Wayne	40	31	ML	46	31	ML
100385	Newton	LaPorte	21	27	LL	23	27	LL
301070	White	LaPorte	37	21	ML	39	21	ML
301143	Elkhart	Fort Wayne	35	29	ML	40	29	ML
8823155	Warrick	Vincennes	31	23	LL	32	23	LL
9031790	DeKalb	Fort Wayne	36	29	LL	41	29	ML
9700260	Allen	Fort Wayne	27	28	LL	31	28	LL
Koleen	—	—	46	33	ML	46	33	ML
Romney	—	—	31	79	LH	32	79	LH
McCormick	—	—	35	16	ML	36	16	ML
Flora	—	—	54	23	ML	52	23	ML

TABLE 5.7  
SVR results for 5 m soil profile length

DES#/Site Name	Location		Modified Tumay (1985) Chart			Modified Robertson (1990) Chart		
	County	District	Site VVI	Site HVI	SVR	Site VVI	Site HVI	SVR
100521	White	LaPorte	43	26	ML	45	26	ML
401113	Elkhart	Fort Wayne	48	25	ML	41	25	ML
600337	Howard	Greenfield	37	24	ML	36	24	ML
810115	Steuben	Fort Wayne	32	53	MM	36	53	MM
901897	Daviess	Vincennes	31	22	LL	34	22	ML
100331	LaPorte	LaPorte	28	76	LH	32	76	LH
1173689	Jasper	LaPorte	18	62	LM	20	62	LM
8823155	Warrick	Vincennes	29	22	LL	31	22	LL
9031790	DeKalb	Fort Wayne	32	29	LL	35	29	ML
9700260	Allen	Fort Wayne	26	24	LL	30	24	LL
Koleen	—	—	46	33	ML	46	33	ML
Romney	—	—	31	79	LH	32	79	LH
McCormick	—	—	35	16	ML	36	16	ML
Flora	—	—	54	23	ML	52	23	ML

TABLE 5.8  
Maximum and minimum variability values for 5 m soil profile length using the modified Tumay (1985) chart

	Tumay (1985) chart					
	VVI	DDF	NLDPUL	(VVI) <sub>IL</sub>	(VVI) <sub>log</sub>	COV <sub>(qc)</sub>
Min.	13.8	2.1	0.4	8.26	2.14	17.66
Max.	57.07	21.1	1.7	41.34	100	2.14

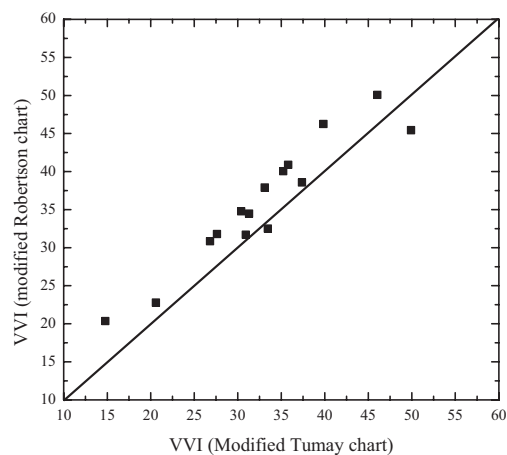


Figure 5.43 Comparison between VVIs obtained using the modified Tumay (1985) and modified Robertson (1990) charts for 4 m soil profile length.

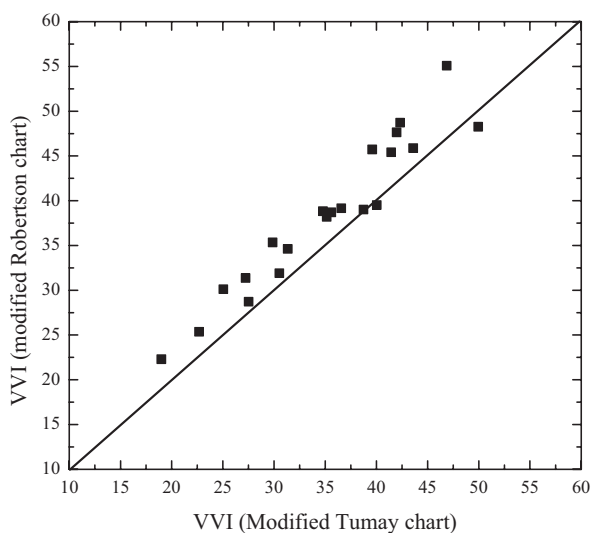


Figure 5.42 Comparison between VVIs obtained using the modified Tumay (1985) and modified Robertson (1990) charts for 3 m soil profile length.

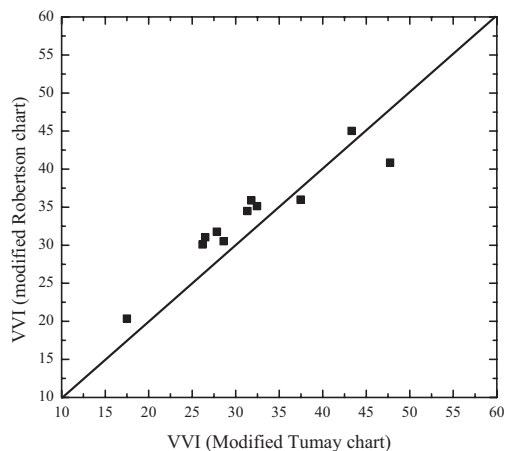


Figure 5.44 Comparison between VVIs obtained using the modified Tumay (1985) and modified Robertson (1990) charts for 5 m soil profile length.

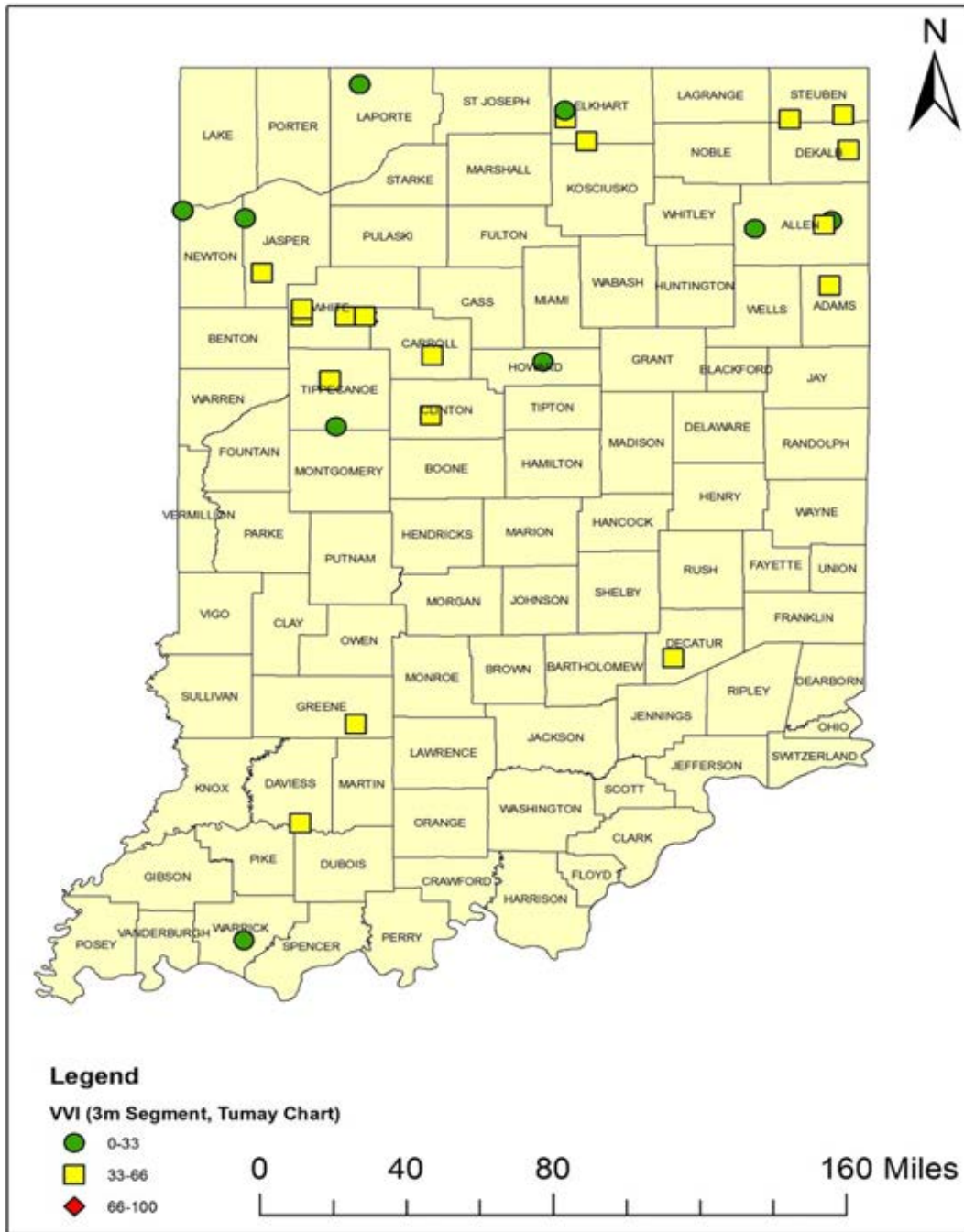


Figure 5.45 Site VVI for 3 m soil profile length using modified Tumay (1985) chart.

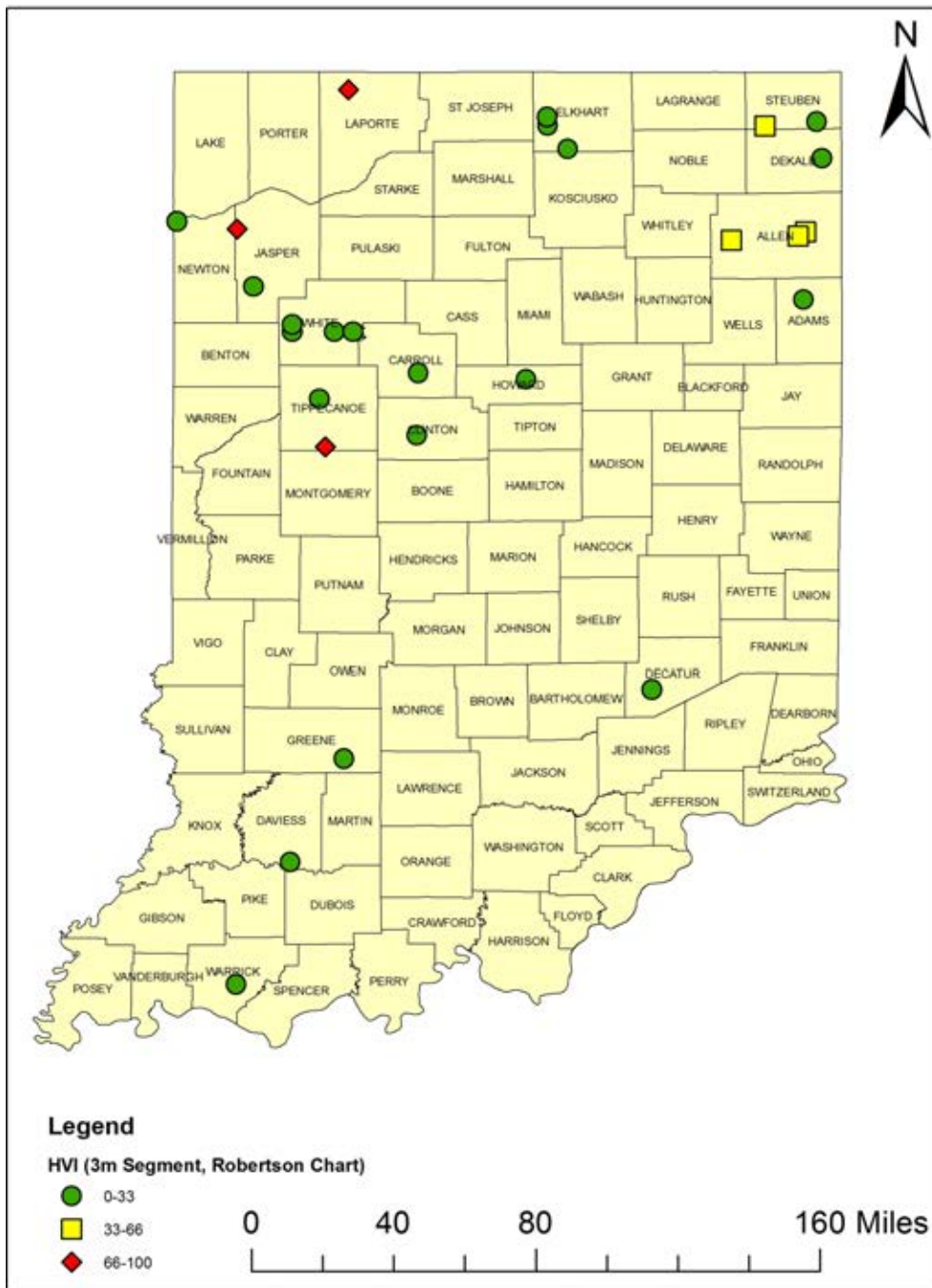


Figure 5.46 Site HVI for 3 m soil profile length using modified Tumay (1985) chart.

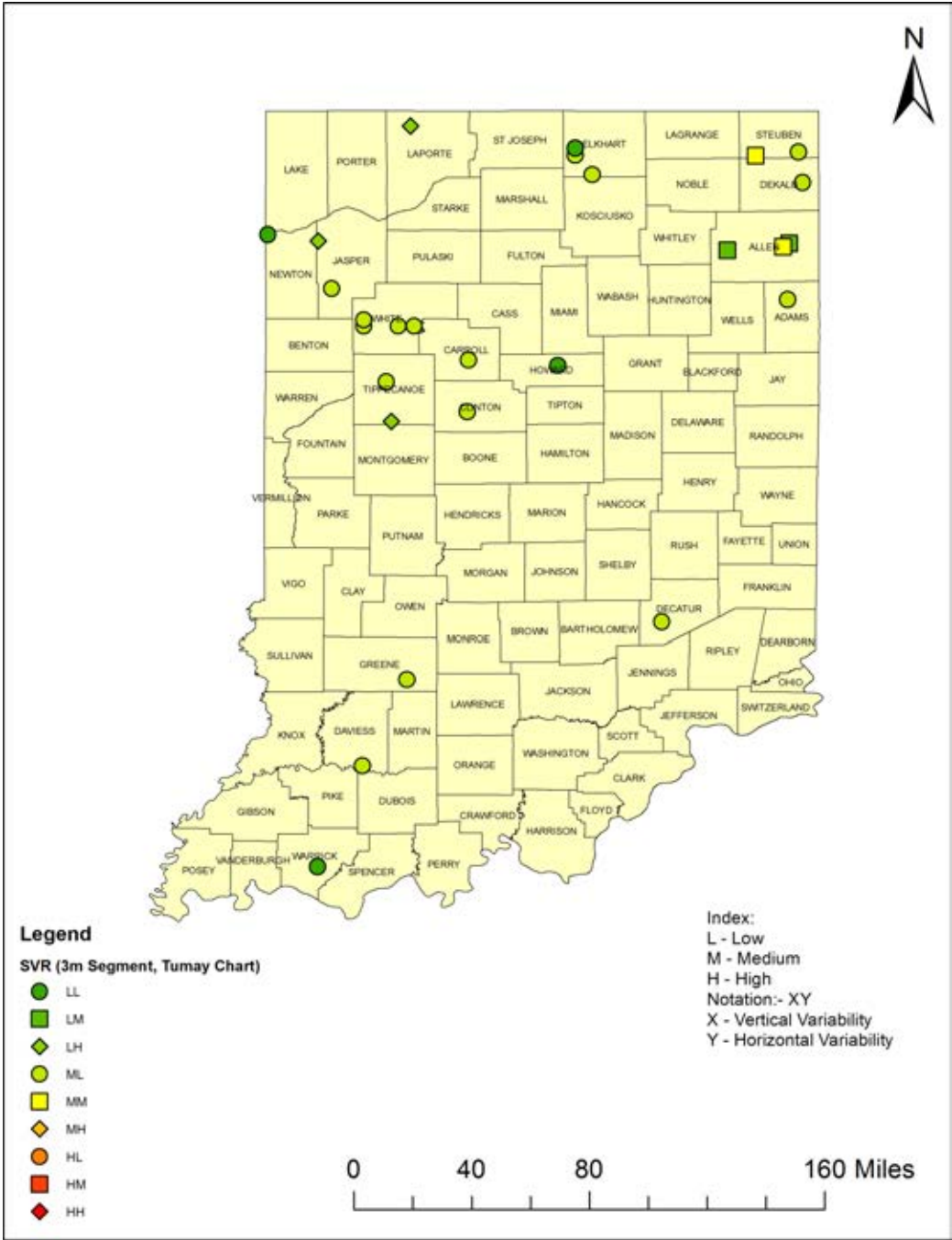


Figure 5.47 Site SVR for 3 m soil profile length using modified Tumay (1985) chart.

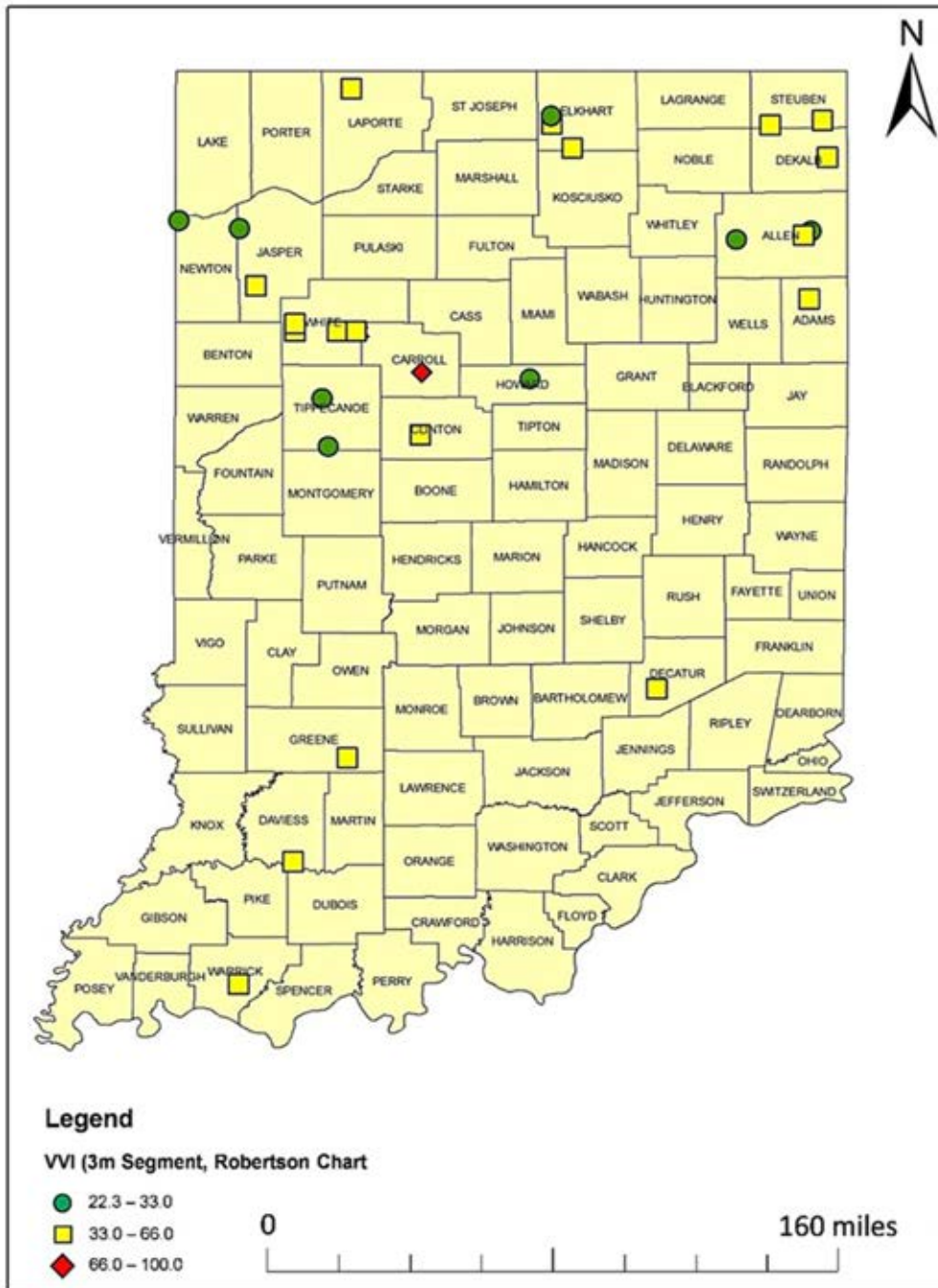


Figure 5.48 Site VVI for 3 m soil profile length using the modified Robertson (1990) chart.

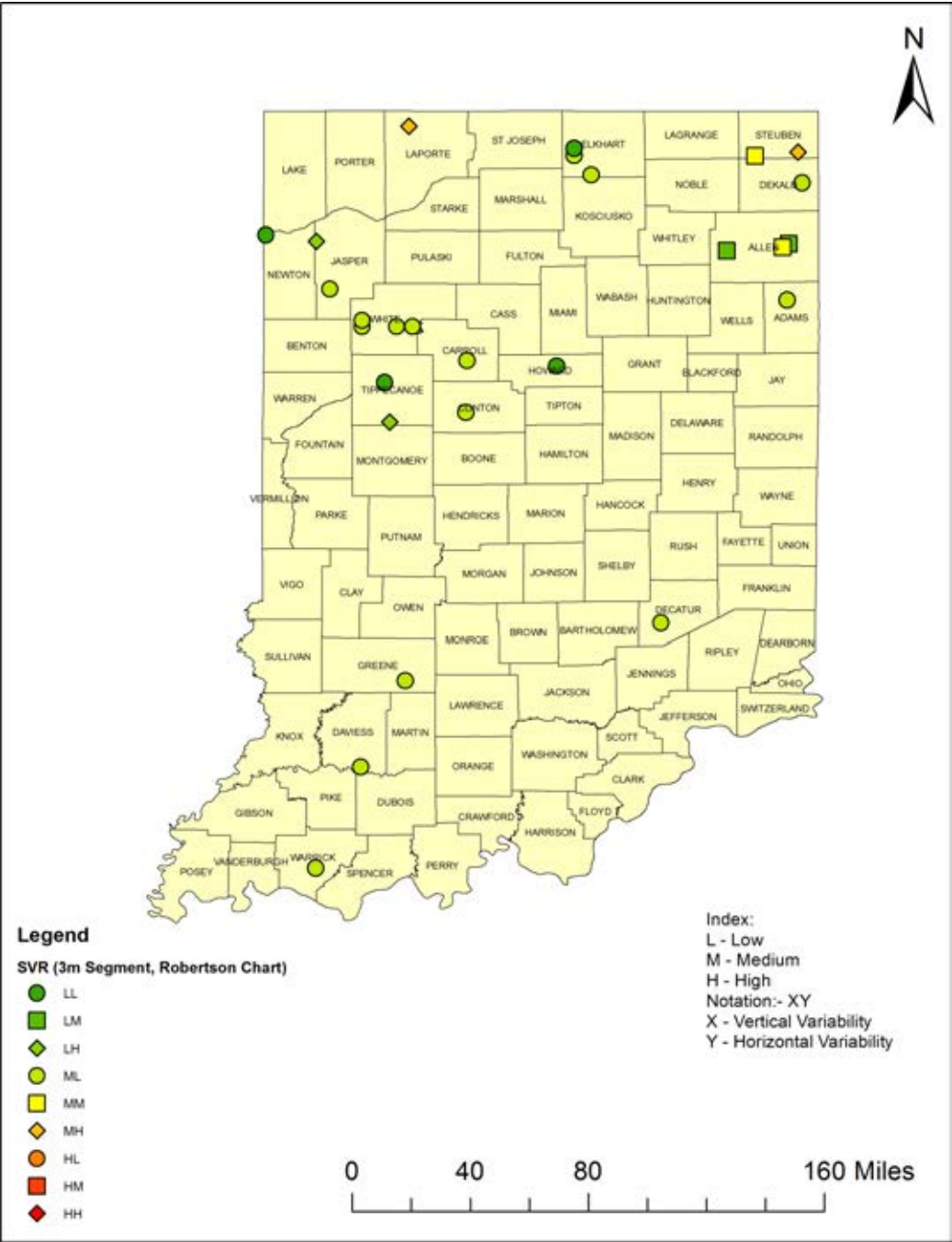


Figure 5.49 Site SVR for 3 m soil profile length using modified Robertson (1990) chart.

variability of the soil at the site. More CPTs must be performed if deemed necessary based on the engineering judgment of the site engineer.

## 6. DEVELOPMENT OF DATA ACQUISITION SYSTEMS

### 6.1 Introduction

A data acquisition system (DAQS) was developed for the CPT and another for the SPT. The CPT DAQS enables acquisition of data from a cone penetrometer and also enables processing of this data in a variety of ways. A soil profile can be generated and its variability quantified (as discussed in chapter 4). Additionally, CPT soundings can be stored to a site project, and the variability of the site quantified. Finally, the DAQ also assists the operator to decide on the spacing at which the next sounding should be performed. The SPT DAQS enables both measurement of energy ratio and automatic counting of blows. This chapter discusses both systems and their use.

### 6.2 CPT DAQ Hardware

The purpose of the DAQ hardware is to acquire data during the course of a cone penetration test. The data collected during a CPT come from a cone penetrometer and from an encoder, which measures the depth of penetration. The CPT data obtained from the cone consist of cone resistance, sleeve resistance, pore water pressure and inclination data. Figure 6.1 is a simple diagram to illustrate the different components of the DAQ hardware. A computer is used to operate the DAQ system. In the next sections, different components of the DAQ are discussed.

#### 6.2.1 Cone

Purdue University owns a 1995 Ford F-Super Duty truck with a CPT rig mounted on the frame of the truck, as shown in Figure 6.2. The CPT rig has a pushing capacity of ten tons. The truck has seven hydraulic levers, which are used to push the cone into the ground, raise the truck and level it, and drill two

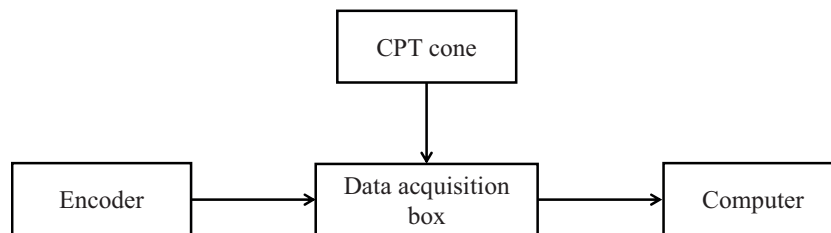


Figure 6.1 A simple diagram of CPT DAQ system.



Figure 6.2 Purdue CPT truck.



Figure 6.3 Analog cone.

augers into the ground to gain more pushing capacity. Purdue University owns two analog cones. Figure 6.3 shows one of these cones. Push rods are stored on the deck of the truck.

### 6.2.2 Encoder

A digital encoder is used for recording the penetration depth of the cone as it penetrates into the soil. The encoder is mounted on a steel bar. As the cone is pushed downward, a horizontal rod in the center of the encoder rotates. This rotation is recorded by the encoder, which is converted into distance by the DAQS. This distance is equal to the penetration length of the cone. Figure 6.4 is a photo of the encoder mounted on the backside of the hydraulic rams that push the cone.



Figure 6.4 Encoder (mounted).

### 6.2.3 DAQ Box

The data acquisition box is a closed steel box, as shown in Figure 6.5.

### 6.2.4 Power Source

An Omega power supply (model PSS D-12B) is used to provide power to the cone. It provides  $\pm 12$  VDC with a common ground at 0 VDC. Five terminals are located across the face of the power source. The two terminals on the left are for connecting an electrical cord that plugs into a 110 VAC outlet. The three rightmost terminals are the  $\pm 12$  VDC and common ground.

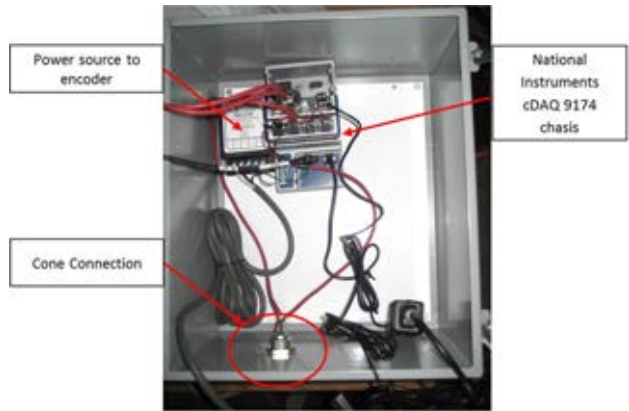


Figure . DAQ Box

Figure 6.5 DAQ box.

## 6.3 CPT DAQ and Variability Analysis Software

The CPT DAQS records the CPT data from the cone and depth data from the encoder and saves it in xml file format. It also enables sounding and site variability quantification (site variability quantification requires at least 3 soundings) and a more informed decision on sounding spacing based on observed inter-sounding/site variability. Figure 6.6 shows the interface of the CPT DAQS.

### 6.3.1 CPT DAQS Walkthrough

The CPT DAQS requires the user to choose the system of units and the cone penetrometer to be used and to provide the project name, site name, location, borehole number and operator name before the start of a test.

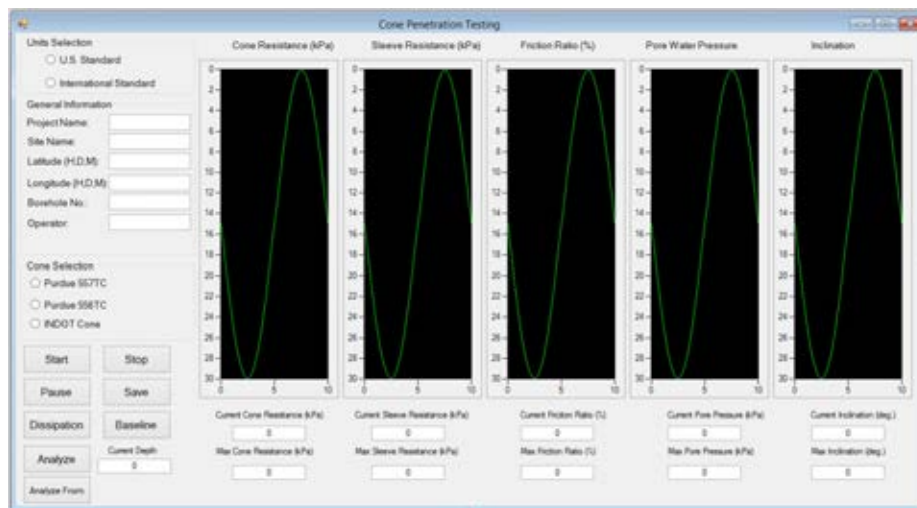


Figure 6.6 CPT DAQ software interface.

At first, a baseline reading of all the CPT cone outputs (i.e., cone resistance, sleeve resistance, pore pressure and inclination) are taken by clicking the **Baseline** button. Then the test is started by clicking the **Start** button and simultaneously starting to push the cone down. After every one meter of penetration, the test is paused by clicking the **Pause** button. The **Pause** button appears in the place of the **Resume** button when a test is running. After a test is paused, an extra push rod is added and, when the operator is ready to resume the test, the **Resume** button is pressed. At the end of the test, the **Stop** button is clicked. Then the cone is raised a few centimeters above the base of the hole. At this the moment, the baseline of all the CPT outputs are again taken by clicking the **Baseline** button. After taking the baseline, all the data are saved in an xml file format in a desired location in the computer by clicking the **Save** button. During the course of the test, all the data are also temporarily stored in the computer. Variability analysis can be performed on the recorded data to measure vertical variability of the current sounding by clicking the **Analyze** button.

The DAQS allows quantification of variability from previously collected CPT data. To do that, the **Analyze From** button (Figure 6.6) is clicked and the **Analyze Data** form, as shown in Figure 6.7, appears. We first need to input the CPT data. There are two ways to input the CPT data: either spreadsheets can be manually selected or an Excel spreadsheet containing links to the file locations can be selected (see Figure 6.7). Figure 6.8 shows the form to input data manually. First, the site name and the number of soundings available are input. The spreadsheet files, containing the CPT data, are selected by clicking on the **Get file #\_\_** buttons. The folder to save the analysis results are selected by clicking the **Browse Saving Folder** button (Figure 6.8). When the **Read Data** button is clicked, the program reads the CPT data from the computer memory and the form closes. At this moment, we are ready for variability assessment calculations. The different variability assessment options can be seen by clicking **Run** under the **Analyze** tab (see Figure 6.9).

The different analysis properties can be changed by going to **Properties** under the **Analyze** tab (Figure 6.9).

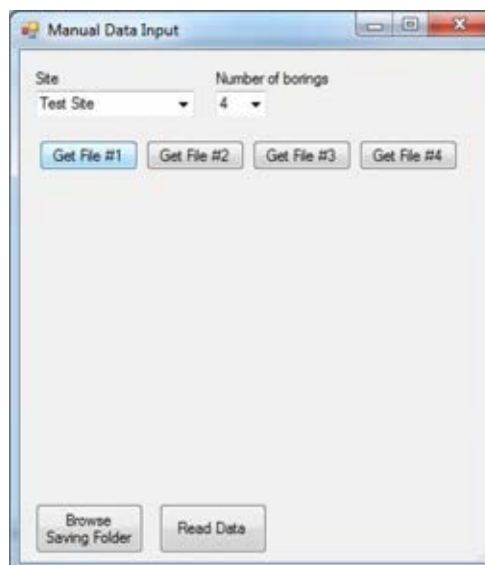


Figure 6.8 Input data to analyze.

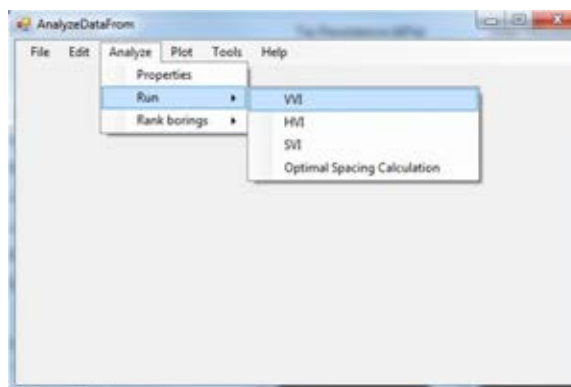


Figure 6.9 Variability assessment.



Figure 6.7 Analyze data form.

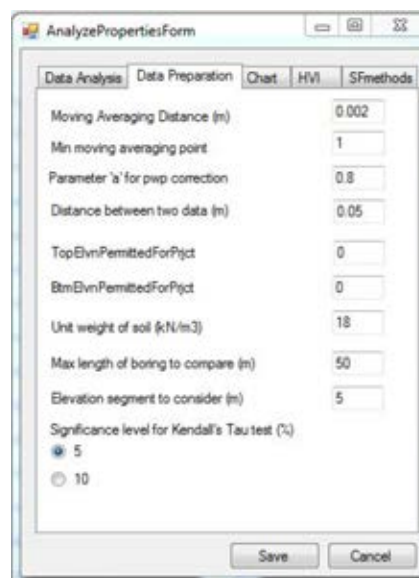


Figure 6.10 Analysis properties.



Figure 6.11 SPT instrumented rod.

Figure 6.10 shows the Analyze Properties form with the default values.

#### 6.4 SPT DAQ Hardware

The standard penetration test (SPT) is one of the most widely used *in situ* tests. The SPT DAQ system, developed in

this research, includes data acquisition hardware. The essential component of the instrumented SPT DAQS is an SPT rod instrumented with strain gauges and accelerometers, shown in Figure 6.11 and Figure 6.12. The instrumented rod is 2 feet in length. It is AWJ-threaded and therefore can be used with INDOT's SPT rig. National Instrument (NI) modules are used to collect and send strain and acceleration data from strain gauges and accelerometers wirelessly to a laptop.

##### 6.4.1 Using the Instrumented SPT Rod in the Field

The following steps are followed to use the instrumented rod in the field for the purpose of energy efficiency measurements:

1. The Instrumented Rod has AWJ threads, which are compatible with the type of rod INDOT currently uses for drilling operations. The instrumented rod is first connected to INDOT's drilling rod.
2. Clip the RJ-50 cables into the strain gage terminals of the instrumented rod.
3. Bolt the acceleration housing units onto the instrumented rod.
4. Place and tighten the anvil on top of the instrumented rod. The final assembly is shown in Figure 6.13
5. Begin the SPT testing and collect strain and acceleration data wirelessly to a laptop using SPT DAQ software.

#### 6.5 SPT DAQS

The SPT DAQS measures the energy transferred to the SPT rod by the hammer blow, allowing calculation of the energy ratio for that hammer and rig. Figure 6.14 shows the SPT DAQS interface.

The user inputs the boring number, boring location, and depth at which the SPT will be performed. At the time the operator is ready to start the test, the operator clicks on the **Start** button, and the drilling crew starts the test. The software records the strain data from 2 sets of strain gauges and acceleration data from the two accelerometers. After each blow, velocity (or acceleration) and force (or strain) measurements are plotted, as shown in Figure 6.14. At the end of an SPT, performed at a particular depth, the **Stop** button is clicked and the recorded data are saved in xml file format by clicking the **Save** button. When performing an



Figure 6.12 Accelerometer mounted on SPT rod.



Figure 6.13 Using instrumented SPT rod in field.

SPT at the next desired depth, the **New SPT** button is clicked. The user now inputs the new depth information, and runs the new test as before. To start an SPT at a new location (new boring), the **New Log** button is clicked. The user now inputs the new boring number and boring location information, and runs the test as before.

## 6.6 SPT Energy Measurement

The SPT is not a very reliable test because of the many sources of uncertainties. Several investigators have measured the hammer energy in various SPT systems and found considerable variability (Howie, Daniel, Jackson, & Walker, 2003). The amount of energy effectively transmitted to the rods varies with hammer type, the hardware in general and specific test procedures (Salgado, 2008).

The maximum theoretical energy applied by the hammer to the anvil can be calculated from the potential energy of the SPT hammer. The ratio of the actual energy transferred to the rods to this maximum theoretical energy is known as the energy ratio  $ER$ :

$$ER = \frac{\text{Transferred energy}}{\text{Maximum potential energy}} \quad (6.1)$$

For donut, safety and pin weight hammers, the energy ratios are reported as being roughly 45%, 60% and 70%. However, these are just approximate values, with dispersion around these values being potentially significant. In order to know with reliability the  $ER$  of an SPT system, the  $ER$  should be measured. There are two main methods of measuring the transferred energy to the rods during an SPT: through force integration (F-square method) and through integration over time of the product  $Fv$  of force by velocity. In order to obtain the transmitted energy, the force-velocity method requires the measurement of force from strain gauge readings and measurement of velocity from accelerometer readings.

In the  $Fv$  method, the energy  $EFV$  in the instrumented rod is obtained using:

$$EFV = \int_{t_1}^{t_2} F(t)v(t)dt \quad (6.2)$$



Figure 6.14 SPT DAQS interface.

where  $F$  is the force in the instrumented rod obtained from the strain gauge readings,  $v$  is the velocity obtained from the accelerometers,  $t_1$  is the time of impact by the SPT hammer and  $t_2$  is the time to the peak energy transferred to the rod.

The F-square method was developed at a time when there wasn't a satisfactory method to measure the acceleration in the rod. This method requires determination of only the force through the strain gauge readings. The following equation shows the relationship between particle velocity, force and rod impedance  $Z = EA/c$ :

$$v(t) = \frac{F(t)}{\frac{EA}{c}} \quad (6.3)$$

Combination of Equation 6.2 and Equation 6.3 leads to the energy EF2 transferred to the rod calculated by the F-square method:

$$EF2 = \frac{c}{EA} \int [F(t)]^2 dt \quad (6.4)$$

where  $v$  is particle velocity,  $EA/c$  is rod impedance,  $E$  is the elastic modulus of steel,  $A$  is the cross-sectional area of steel and  $c$  is the speed of wave propagation in steel.

The integration in Equation 6.4 is carried out from the time the downward compressive stress wave first passes the measurement point until the time  $t = 2L/c$ , where  $L$  is the length of the rod and  $c$  = speed of wave propagation in steel.

### 6.7 SPT Energy Measurement Results

The SPT DAQS and instrumented rod have been tested during SPTs performed at the Koleen site. The average energy ratios obtained from SPTs performed at several

TABLE 6.1  
ER (%) obtained from boring 1 at Koleen site

Number	Depth (ft)	Blow Count	ER (%)
1	3.5–5.5	5-6-6	66.44
2	8.5–10	3-3-5	65.17
3	13.5–15	2-3-4	67.43
4	18.5–20	3-3-7	66.54
5	23.5–25	0-0-3	68.26
6	28.5–30	3-2-4	64.74
Avg ER (%)			<b>66.43</b>

TABLE 6.2  
ER (%) obtained from SPT 3 at Koleen site

Number	Depth (ft)	Blow Count	ER (%)
1	3.5–5	4-6-8	60.48
2	8.5–10	2-3-4	71.77
3	13.5–15	2-2-3	58.6
4	18.5–20	0-1-3	68.57
5	23.5–25	4-5-7	64.54
6	28.5–30	3-3-4	67.95
Avg ER (%)			<b>65.32</b>

TABLE 6.3  
ER (%) obtained from SPT 4 at Koleen site

Number	Depth (ft)	Blow Count	ER (%)
1	3.5–5.5	5-5-5	66.00
2	8.5–10	3-4-5	70.81
3	13.5–15	1-1-2	62.43
4	18.5–20	0-1-2	72.8
5	23.5–25	1-2-2	—
6	28.5–30	0-1-2	71.44
7	33.5–35	0-1-2	68.10
8	38.5–40	0-2-2	70.54
9	43.5–45	3-3-4	62.53
10	48.5–50	2-8-4	69.66
Avg ER (%)			<b>68.26</b>

depths in 3 borings are shown in Table 6.1, Table 6.2 and Table 6.3.

## 7. CONCLUSIONS AND RECOMMENDATIONS

Geotechnical engineers are being called on to better quantify properties not only in an average sense but also in terms of their variability. In geotechnical engineering design, an assessment of the variability of soil properties, which are often obtained from a limited number of *in situ* or laboratory tests, should be performed for proper selection of representative soil properties for use in geotechnical design. In order to assess the variability of soil properties at a site, consideration of the correlation structure of soil properties is necessary. In LRFD, uncertainties related to loads are accounted for in the values of the load factors, while those associated with all the steps of the determination of soil resistances are accounted for in the values of the resistance factors. Design for low-variability sites is rewarded by use of higher resistance factors, while resistance factors are lower for highly variable sites. When this was first proposed by FHWA, site variability was introduced in a very qualitative manner. In this research, a site variability quantification methodology was developed that relies on cone penetration test data.

In order to develop a comprehensive methodology for site variability assessment, consideration should be given to inter- and intra-layer variability in a soil profile, and both vertical and horizontal variability. First, soil behavior type (SBT) charts (Tumay, 1985, and Robertson, 1990) are used to obtain the subsurface soil profiles from CPT parameters (e.g.,  $q_c$  and  $f_s$ ).

A soil profile generation algorithm was developed for this specific purpose. A vertical variability index (*VVI*), which reflects the intra-layer variability, the log variability and the COV of the cone resistance of the sounding, was defined to quantify the vertical variability in a CPT sounding. The average of the *VVIs* for all CPT soundings performed at a site is the site *VVI*. A site horizontal variability index (site *HVI*), based on the cross-correlation between the cone resistances of soundings and the spacing between them, was also developed to quantify the soil variability of a site in the horizontal direction. A site variability rating (SVR) system,

integrating the vertical and horizontal site variability, was developed to assess the overall site variability.

The soil profile generated using the soil profile generation algorithm depends on the SBT chart selected; however, the two charts tested in this research, which are by far the most common ones, produced comparable values of SVR. In order to illustrate the use of the algorithms for *VVI*, *HVI* and SVR calculations, CPTs from across the state of Indiana were analyzed. CPT data were obtained from Purdue's own database and INDOT's data repository. Site variability is calculated for specific soil profile lengths of interest. For example, the depth of interest will be shallower for shallow foundations than for deep foundations. It makes no sense to refer to site variability without specifying the depth of interest for the target design problem. For this research, 3 m, 4 m and 5 m depths were considered. Site variability rating maps (SVR maps) for these three soil profile lengths were constructed for the state of Indiana, illustrating the potential use of the site variability assessment methodology.

The SVR maps developed in this research can be used in the development of regional soil resistance factors to be used for LRFD design in the state of Indiana. The SVR maps are also helpful with the planning of site investigations for INDOT projects (a highly variable site would require a greater number of soundings or smaller spacing). In addition, an optimal CPT sounding spacing calculation methodology, which takes into account in real time the variability of previously performed soundings at a site, was also developed to make the site investigation process more efficient, cost-effective and reliable.

The variability assessment methodology proposed here is a powerful platform to plan and execute site investigation and design for geotechnical infrastructure. With the enlargement of databases and refinements to the methodology, it should develop into a tool that will enable geotechnical engineers to perform planning, design and construction activities with greater confidence.

## REFERENCES

- AASHTO. (2007). *AASHTO LRFD bridge design specifications* (4th ed.). Washington DC: American Association of State Highway and Transport Officials.
- ASTM D5778-12. (2012). *Standard Test Method for Electronic Friction Cone and Piezocone Penetration Testing of Soils*. West Conshohocken, PA: ASTM International.
- Begemann, H. K. S. (1965). The friction jacket cone as an aid in determining the soil profile. *Proceedings of the 6th International Conference on Soil Mechanics and Foundation Engineering, Vol. 1* (pp. 35–39). Toronto, Ontario: University of Toronto Press.
- Daniel, W. (1990). *Applied nonparametric statistics*. Boston, MA: PWS-Kent Publishing.
- Douglas, B. J., & Olsen, R. S. (1981). Soil classification using electric cone penetrometer. In G. M. Norris & R. D. Holtz (Eds.), *Proceedings of the Symposium on Cone Penetration Testing and Experience* (pp. 209–227). New York, NY: American Society of Civil Engineers.
- Eslami, A., & Fellenius, B. (1997). Pile capacity by direct CPT and CPTu methods applied to 102 case histories. *Canadian Geotechnical Journal*, 34(6), 886–904. <http://dx.doi.org/10.1139/t97-056>
- Fenton, G., & Griffiths, D. (2008). *Risk assessment in geotechnical engineering*. New York, NY: John Wiley & Sons.
- Foye, K. C. (2005). *A rational, probabilistic method for the development of geotechnical load and resistance factor design*. Doctoral dissertation. West Lafayette, IN: Purdue University.
- Foye, K. C., Abou-Jaoude, G., Prezzi, M., & Salgado, R. (2009). Resistance factors for use in load and resistance factor design of driven pipe piles in sands. *Journal of Geotechnical and Geoenvironmental Engineering*, 135(1), 1–13. [http://dx.doi.org/10.1061/\(ASCE\)1090-0241\(2009\)135:1\(1\)](http://dx.doi.org/10.1061/(ASCE)1090-0241(2009)135:1(1))
- Foye, K. C., Prezzi, M., & Salgado, R. (2011). Developing resistance factors for design of piles in sand. *Proceedings of Geo-Risk 2011: Risk Assessment and Management* (pp. 444–451). Reston, VA: American Society of Civil Engineers.
- Foye, K. C., Salgado, R., & Scott, B. (2006). Assessment of variable uncertainties for reliability-based design of foundations. *Journal of Geotechnical and Geoenvironmental Engineering*, 132(9), 1197–1207. [http://dx.doi.org/10.1061/\(ASCE\)1090-0241\(2006\)132:9\(1197\)](http://dx.doi.org/10.1061/(ASCE)1090-0241(2006)132:9(1197))
- Howie, J., Daniel, C., Jackson, R., & Walker, B. (2003). *Comparison of energy measurement methods in the standard penetration test, final report*. Vancouver, British Columbia: The University of British Columbia.
- Jaksa, M. B., Kaggwa, W. S., & Brooker, P. I. (1999). Experimental evaluation of the scale of fluctuation of a stiff clay. In R. E. Melchers & M. G. Stewart (Eds.), *Proceedings of the 8th International Conference on the Application of Statistics and Probability* (pp. 415–422). Rotterdam, Netherlands: Balkema.
- Jefferies, M. G., & Davis, M. P. (1991). Soil classification by the cone penetration test: Discussion. *Canadian Geotechnical Journal*, 28(1), 1–178. <http://dx.doi.org/10.1139/t91-023>
- Larsson, R., & Mulabdic, M. (1991). *Piezocone tests in clay* (Report No. 42). Linköping, Sweden: Swedish Geotechnical Institute.
- Olsen, R. (1994). *Normalization and prediction of geotechnical properties using the cone penetrometer test (CPT)* (Report No. GL-94-29). Washington, DC: U.S. Army Corps of Engineers.
- Olsen, R., & Mitchell, J. (1995). CPT stress normalization and prediction of soil classification. *Proceedings of International Symposium on Cone Penetration Testing, Vol. 2* (pp. 257–262). Linköping, Sweden: Swedish Geotechnical Society.
- Paikowsky, S. (2004). *Load and resistance factor design (LRFD) for deep foundations* (NCHRP Report 507). Washington, DC: Transportation Research Board.
- Phoon, K.-K., & Kulhawy, F. H. (1999). Characterization of geotechnical variability. *Canadian Geotechnical Journal*, 36(4), 612–624. <http://dx.doi.org/10.1139/t99-038>
- Ramsey, N. (2002). A calibrated model for the interpretation of cone penetration tests (CPTs) in North Sea quaternary soils. *Proceedings of Offshore Site Investigation and Geotechnics: Diversity and Stability* (pp. 341–356). London, UK: Society for Underwater Technology.
- Robertson, P. (1990). Soil classification using the cone penetration test. *Canadian Geotechnical Journal*, 27(1), 151–158. <http://dx.doi.org/10.1139/t90-014>
- Robertson, P. (2010). Soil behaviour type from the CPT: An update (Paper No. 2-56). 2nd International Symposium on Cone Penetration Testing, May 9–11, Huntington Beach, CA (pp. p.x).
- Robertson, P., & Campanella, R. (1983). Interpretation of cone penetration tests. Part I: Sand. *Canadian Geotechnical Journal*, 20(4), 718–733. <http://dx.doi.org/10.1139/t83-078>
- Robertson, P., Campanella, R. G., Gillespie, D., & Rice, A. (1986). Seismic CPT to measure in situ shear wave velocity. *Journal of Geotechnical Engineering*, 112(8), 791–803. [http://dx.doi.org/10.1061/\(ASCE\)0733-9410\(1986\)112:8\(791\)](http://dx.doi.org/10.1061/(ASCE)0733-9410(1986)112:8(791))

- Salgado, R. (2008). *The engineering of foundations*. New York, NY: McGraw-Hill.
- Sanglerat, G., Nhim, T., Sejourne, M., & Andina, R. (1974). Direct soil classification by static penetrometer with special friction sleeve. *Proceedings of the First European Symposium on Penetration Testing, ESPOT-1, Vol. 2.2* (pp. 337–344). Linköping, Sweden: Swedish Geotechnical Society.
- Schmertmann, J. (1978). *Guidelines for cone penetration test (performance and design)* (Publication No. FHWA-T5-78-209). Washington, DC: Department of Transportation.
- Schneider, J. A., Randolph, M. F., Mayne, P. W., & Ramsey, N. R. (2008). Analysis of factors influencing soil classification using normalized piezocone tip resistance and pore pressure parameters. *Journal of Geotechnical and Geoenvironmental Engineering*, 134(11), 1569–1586. [http://dx.doi.org/10.1061/\(ASCE\)1090-0241\(2008\)134:11\(1569\)](http://dx.doi.org/10.1061/(ASCE)1090-0241(2008)134:11(1569))
- Senneset, K., Sandven, R., & Janbu, N. (1989). Evaluation of soil parameters from piezocone tests. *Transportation Research Record*, 1235, 24–37.
- Tumay, M. (1985). *Field calibration of electric cone penetrometers in soft soils* (Publication No. FHWA/LA/LSU-GE-85/02). Washington, DC: Federal Highway Administration.
- Uzielli, M., Lacasse, S., & Nadim, F. (2007). Soil variability analysis for geotechnical practice. In K. K. Phoon, D. W. Hight, S. Leroueil, & T. S. Tan (Eds.), *Proceedings of the Second International Workshop on Characterisation and Engineering Properties of Natural Soils* (pp. 1653–1752). London, UK: Taylor and Francis.
- Uzielli, M., Vannucchi, G., & Phoon, K. (2005). Random field characterisation of stress-normalised cone penetration testing parameters. *Geotechnique*, 55(1), 3–20. <http://dx.doi.org/10.1680/geot.2005.55.1.3>
- Vanmarcke, E. (1977). Probabilistic modeling of soil profiles. *Journal of Geotechnical Engineering*, 103(11), 1227–1246.
- Vanmarcke, E. (1983). *Random fields: Analysis and synthesis*. Cambridge, MA: MIT Press.
- Wickremesinghe, D. (1989). *Statistical characterization of soil profiles using in situ tests*. Vancouver: The University of British Columbia.

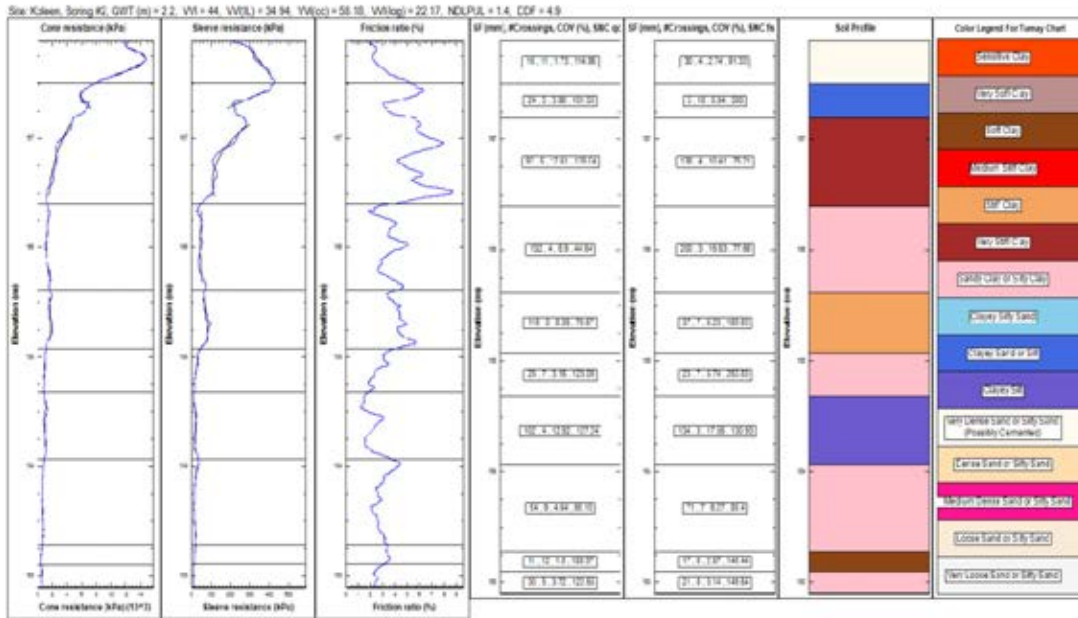
APPENDICES

APPENDIX A: GENERATED VS. ACTUAL SOIL PROFILE COMPARISON FOR INDIANA SITES

Site: Kolean Interstate 69 Expansion Site      Final Depth (m): 9.15  
 Date: 16-Jul-12      Groundwater Depth (m): 2.18  
 Boring: 2      Drill Rig: ATV  
 Surface Elevation (m): 158.84      Drilling Method: **R2.SLD/1650.D.** H.S.A.

Depth (m)	USCS	Description	N <sub>60</sub> (Blows)	Remarks
1.07-1.52	CL	Moist, stiff, lean CLAY	8.3	
2.59-3.05		grading wet	9.7	
4.12-4.57		grading firm	5.3	
5.64-6.10		grading soft	3.0	
7.16-7.62			2.2	
8.69-9.15			3.3	The boring was terminated at 9.15 meters.

(a)



(b)

**Figure A.1** *In situ* test profiles: (a) SPT profile (N<sub>60</sub> values and soil boring description) for SPT 02 and (b) CPT profile (cone resistance, sleeve resistance, friction ratio, variability indices and soil profiles generated using modified Tumay (1985) chart and modified Robertson (1990) chart) for CPT 02 at Kolean site.

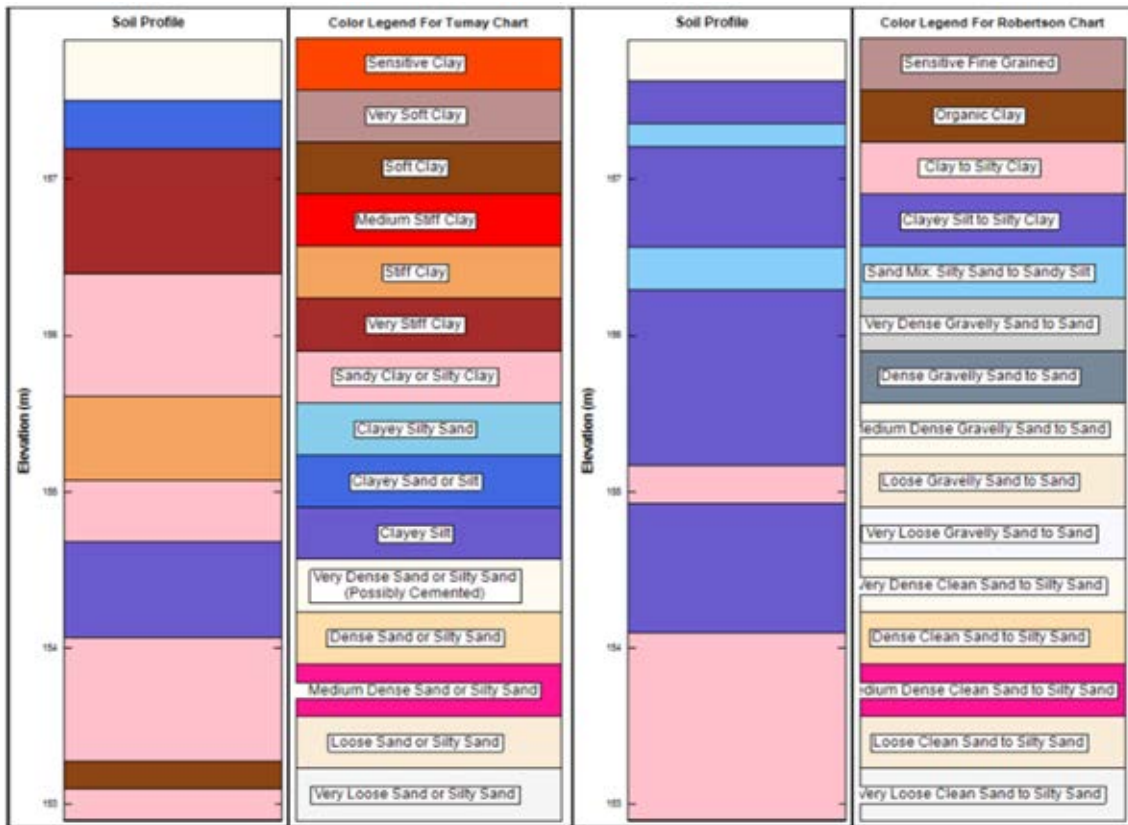
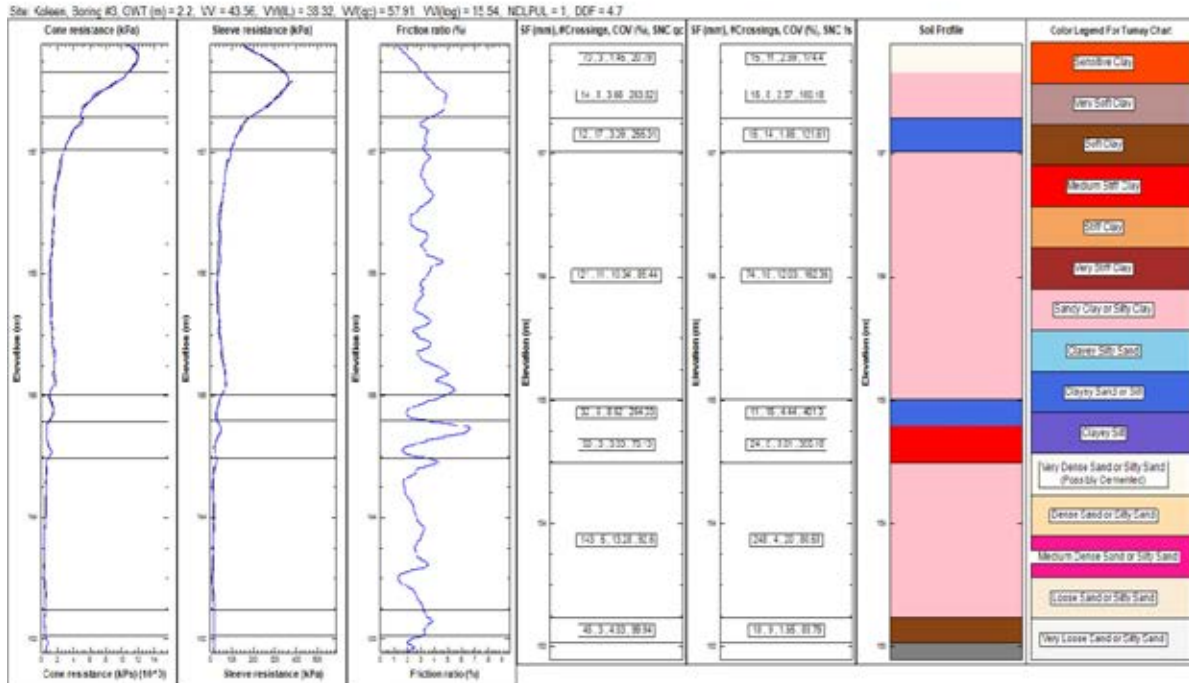


Figure A.2 Soil profiles generated using modified Tumay (1985) chart and modified Robertson (1990) chart for CPT 2 from Koleen site.

Site: Koleen Interstate 69 Expansion Site Final Depth (m): 15.24  
 Date: 19-Jul-12 Groudwater Depth (m): 2.18  
 Boring: 5 Drill Rig: ATV  
 Surface Elevation (m): 158.84 Drilling Method: **R2.SL.D./1650.D.** H.S.A.

Depth (m)	USCS	Description	N <sub>60</sub> (Blows)	Remarks
1.07-1.52	CL	Moist, stiff, lean CLAY	8.2	
2.59-3.05		grading wet and firm	7.9	
4.12-4.57		grading soft	3.2	
5.64-6.10			3.0	
7.16-7.62		grading firm	4.5	
8.69-9.15		grading soft	3.3	
10.21-10.67			3.5	
11.74-12.20		grading firm	4.7	
13.25-13.72	ML	Wet, firm, SILT	7.6	
14.79-15.24		grading stiff	14.7	The boring was terminated at 15.24 meters.

(a)



(b)

**Figure A.3** *In situ* test profiles: (a) SPT profile (N<sub>60</sub> values and soil boring description) for SPT 05 and (b) CPT profile (cone resistance, sleeve resistance, friction ratio, variability indices and soil profiles generated using modified Tumay (1985) chart and modified Robertson (1990) chart) for CPT 03 at Koleen site.

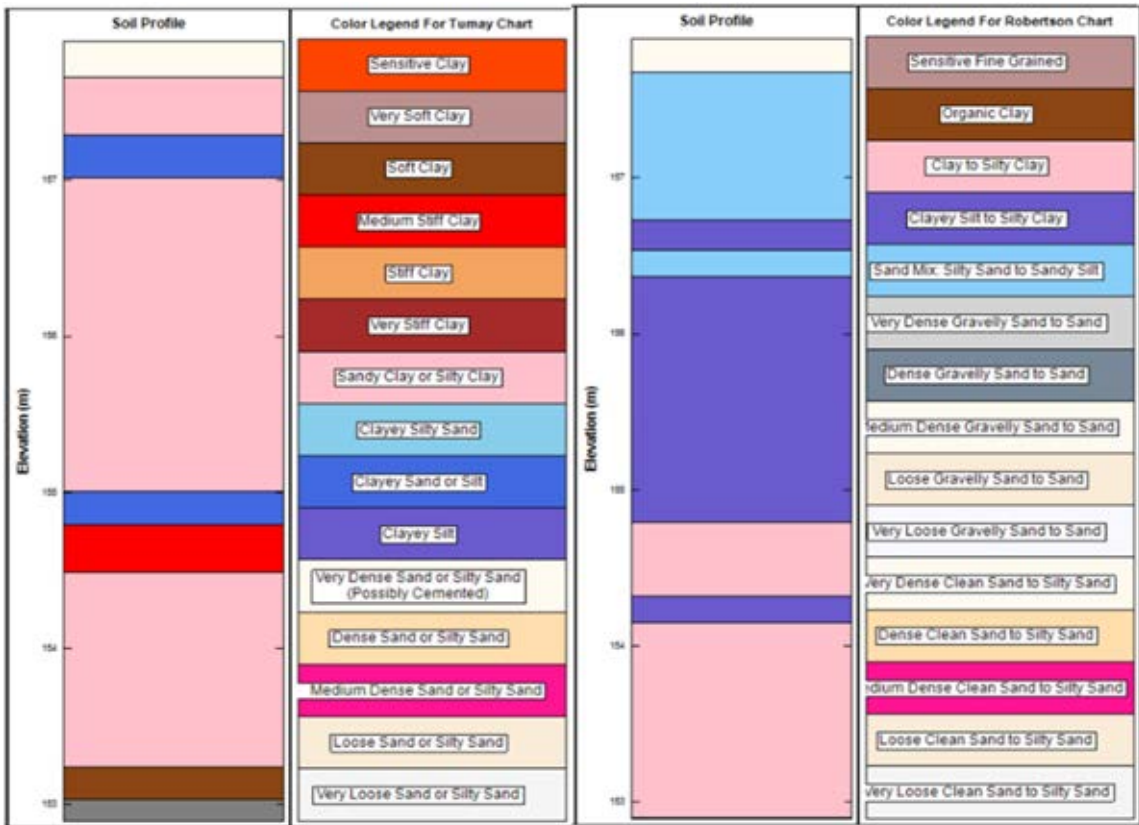


Figure A.4 Soil profiles generated using modified Tumay (1985) chart and modified Robertson (1990) chart for CPT 3 from Koleen site.



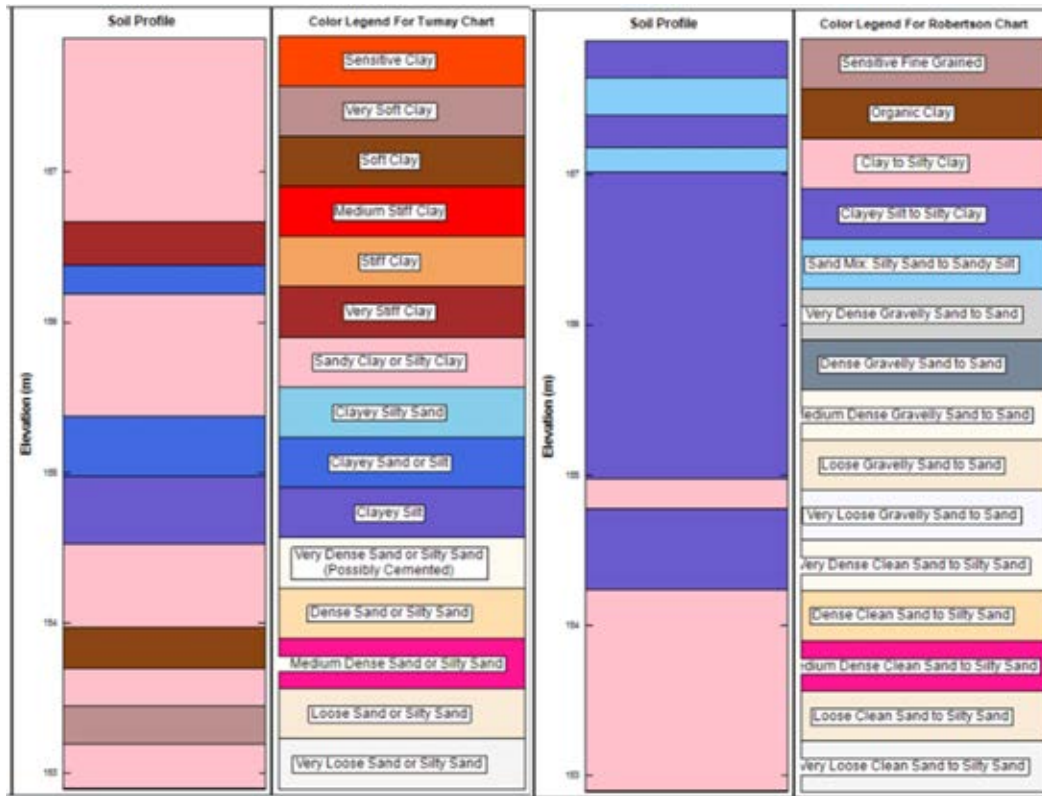
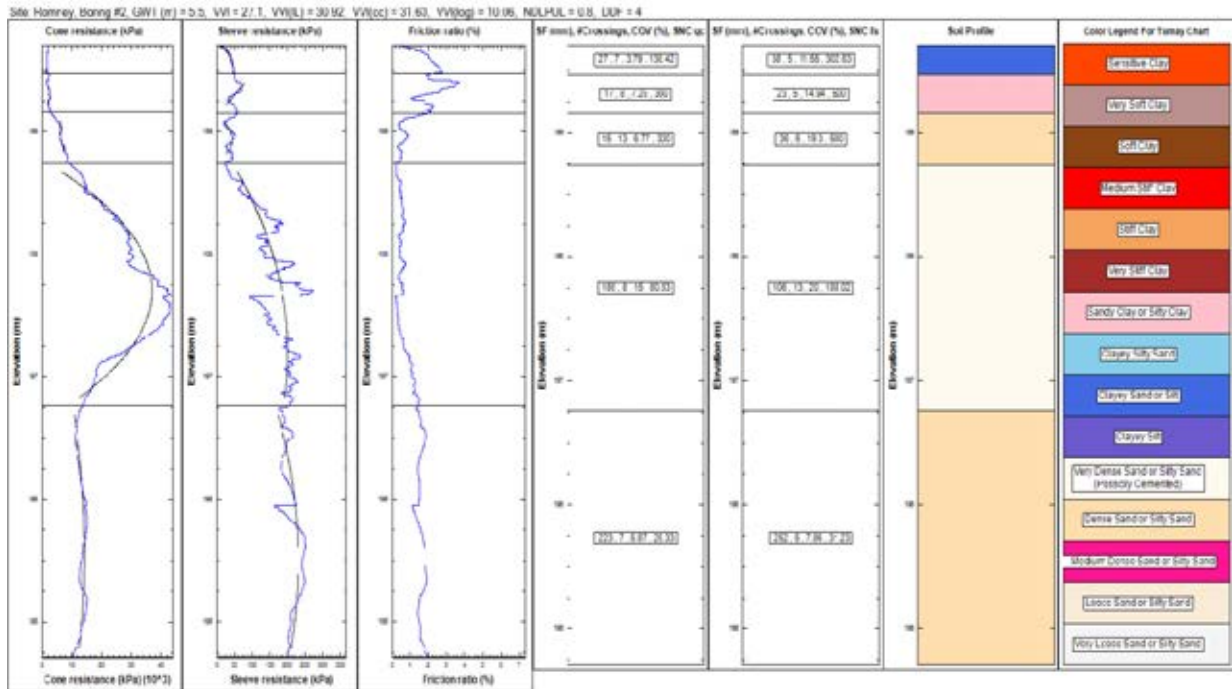


Figure A.6 Soil profiles generated using modified Tumay (1985) chart and modified Robertson (1990) chart for CPT 4 from Koleen site.

Site: Romney Maintenance Unit      Final Depth (m): 7.62  
 Date: 9-Jan-12      Groundwater Depth (m): 5.49  
 Boring: 2      Drill Rig: ATV  
 Surface Elevation (m): 233.23      Drilling Method: **R2.SLD**/1650.D, H.S.A.

Depth (m)	USCS	Description	N <sub>60</sub> (Blows)	Remarks
1.07-1.52	GW	Moist, dense, well-graded GRAVEL w/ sand	42.8	
2.59-3.05	ML	Moist, stiff, SILT	16.8	
4.12-4.57	SM	Moist, medium dense, silty SAND	20.9	Water table encountered at 5.49 meters.
5.64-6.10	ML	Wet, stiff, sandy SILT	16.0	
7.16-7.62		grading hard	38.1	The boring was terminated at 7.62 meters.

(a)



(b)

**Figure A.7** *In situ* test profiles: (a) SPT profile (N<sub>60</sub> values and soil boring description) for SPT 02 and (b) CPT profile (cone resistance, sleeve resistance, friction ratio, variability indices and soil profiles generated using modified Tumay (1985) chart and modified Robertson (1990) chart) for CPT 02 at Romney site.

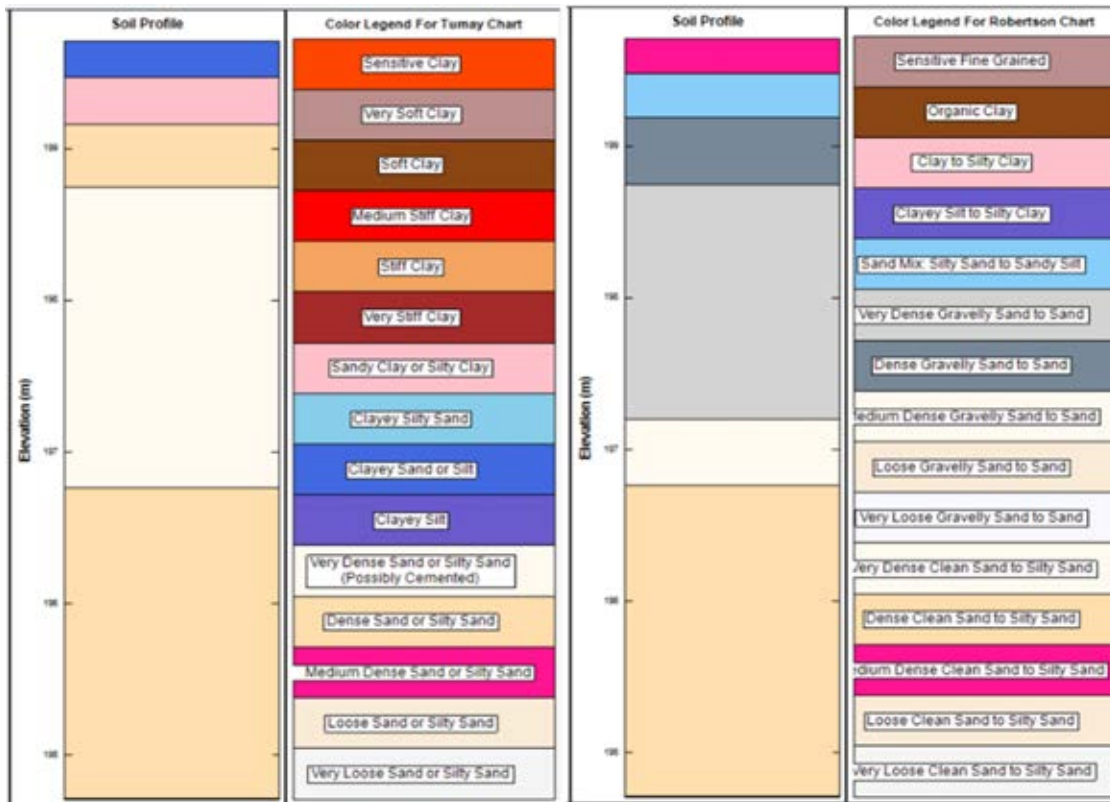
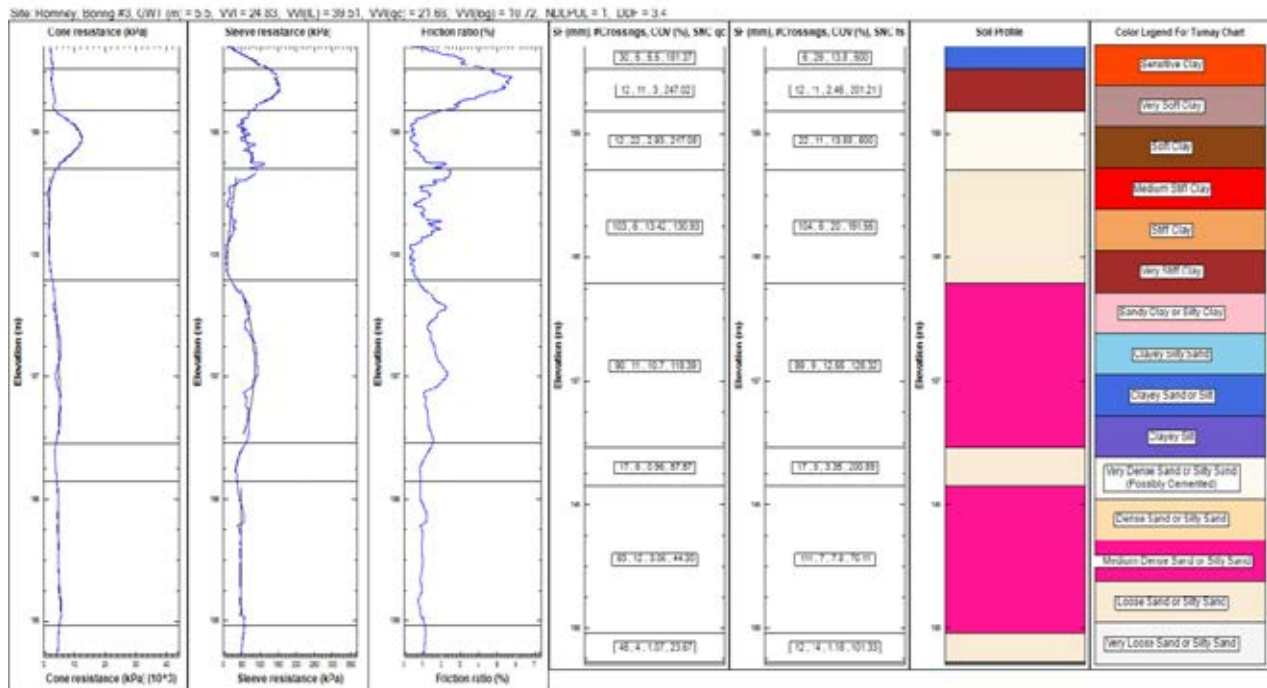


Figure A.8 Soil profiles generated using modified Tumay (1985) chart and modified Robertson (1990) chart for CPT 2 from Romney site.

Site: Romney Maintenance Unit      Final Depth (m): 6.10  
 Date: 9-Jan-12      Groundwater Depth (m): 5.49  
 Boring: 3      Drill Rig: ATV  
 Surface Elevation (m): 233.23      Drilling Method: **82.SLD/1650.D**, H.S.A.

Depth (m)	USCS	Description	N <sub>60</sub> (Blows)	Remarks
1.07-1.52	SP-SM	Moist, dense, poorly-graded SAND w/ silt and gravel	50.0	
2.59-3.05	SM	Moist, medium dense, silty SAND	25.0	
4.12-4.57			22.9	Water table encountered at 5.49 meters. The boring was terminated at 6.10 meters.
5.64-6.10	ML	Wet, very stiff, sandy SILT	19.9	

(a)



(b)

**Figure A.9** *In situ* test profiles: (a) SPT profile (N<sub>60</sub> values and soil boring description) for SPT 03 and (b) CPT profile (cone resistance, sleeve resistance, friction ratio, variability indices and soil profiles generated using modified Tumay (1985) chart and modified Robertson (1990) chart) for CPT 03 at Romney site.

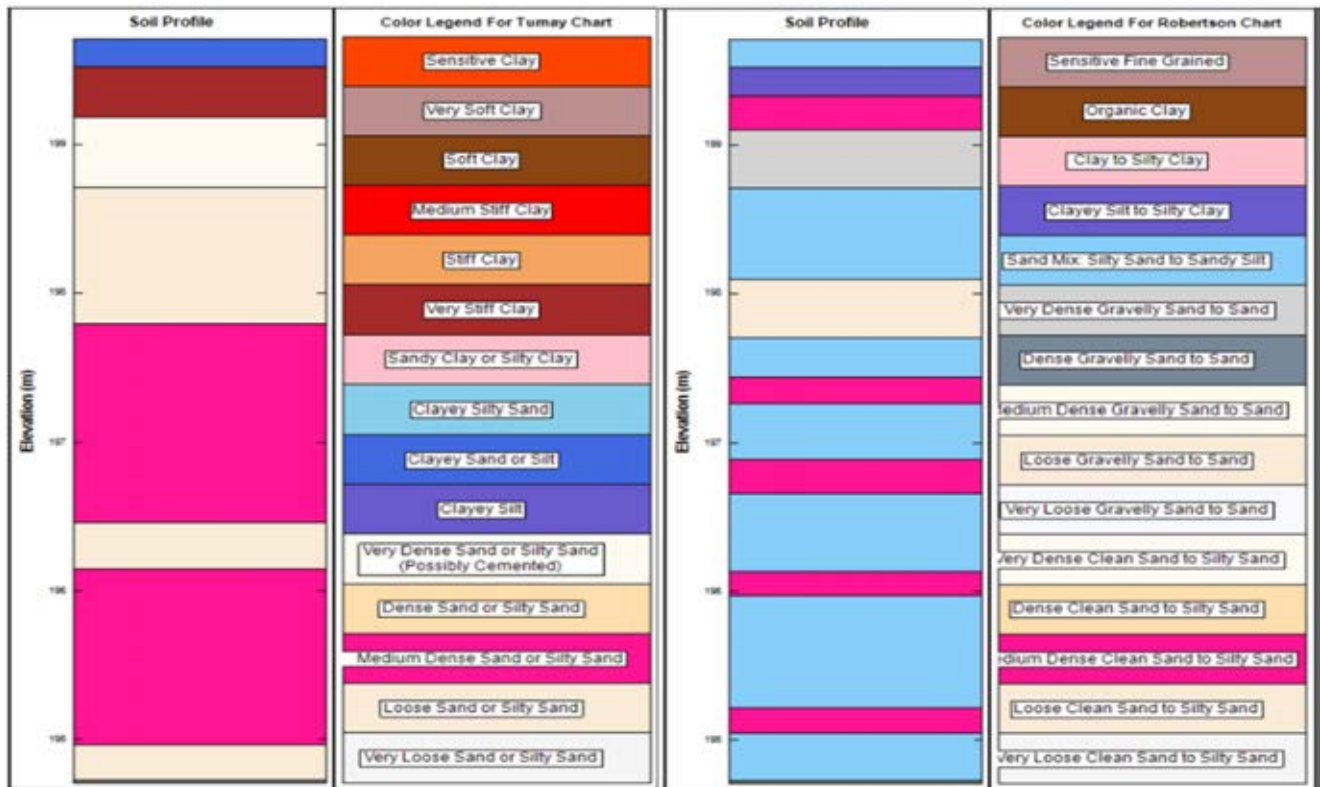


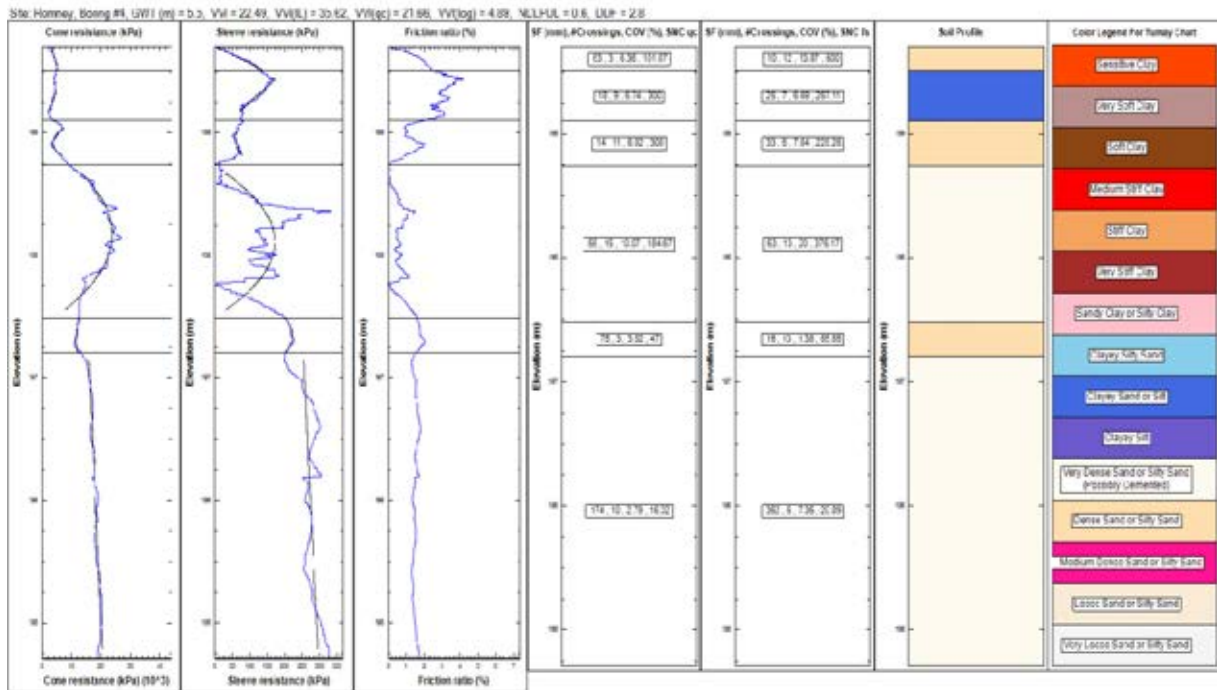
Figure A.10 Soil profiles generated using modified Tumay (1985) chart and modified Robertson (1990) chart for CPT 3 from Romney site.

Site: Romney Maintenance Unit  
 Date: 10-Jan-12  
 Boring: 4  
 Surface Elevation (m): 233.23

Final Depth (m): 6.10  
 Groundwater Depth (m): 5.49  
 Drill Rig: ATV  
 Drilling Method: **82.SLD/1650.D, H.S.A.**

Depth (m)	USCS	Description	N <sub>60</sub> (Blows)	Remarks
1.07-1.52	SP-SM	Moist, dense, poorly-graded SAND w/ silt and gravel	34.7	
2.59-3.05	SM	Moist, medium dense, silty SAND	20.6	
4.12-4.57			21.5	
5.64-6.10			19.9	Water table encountered at 5.49 meters. The boring was terminated at 6.10 meters.

(a)



(b)

**Figure A.11** *In situ* test profiles: (a) SPT profile (N<sub>60</sub> values and soil boring description) for SPT 04 and (b) CPT profile (cone resistance, sleeve resistance, friction ratio, variability indices and soil profiles generated using modified Tumay (1985) chart and modified Robertson (1990) chart) for CPT04 at Romney site.

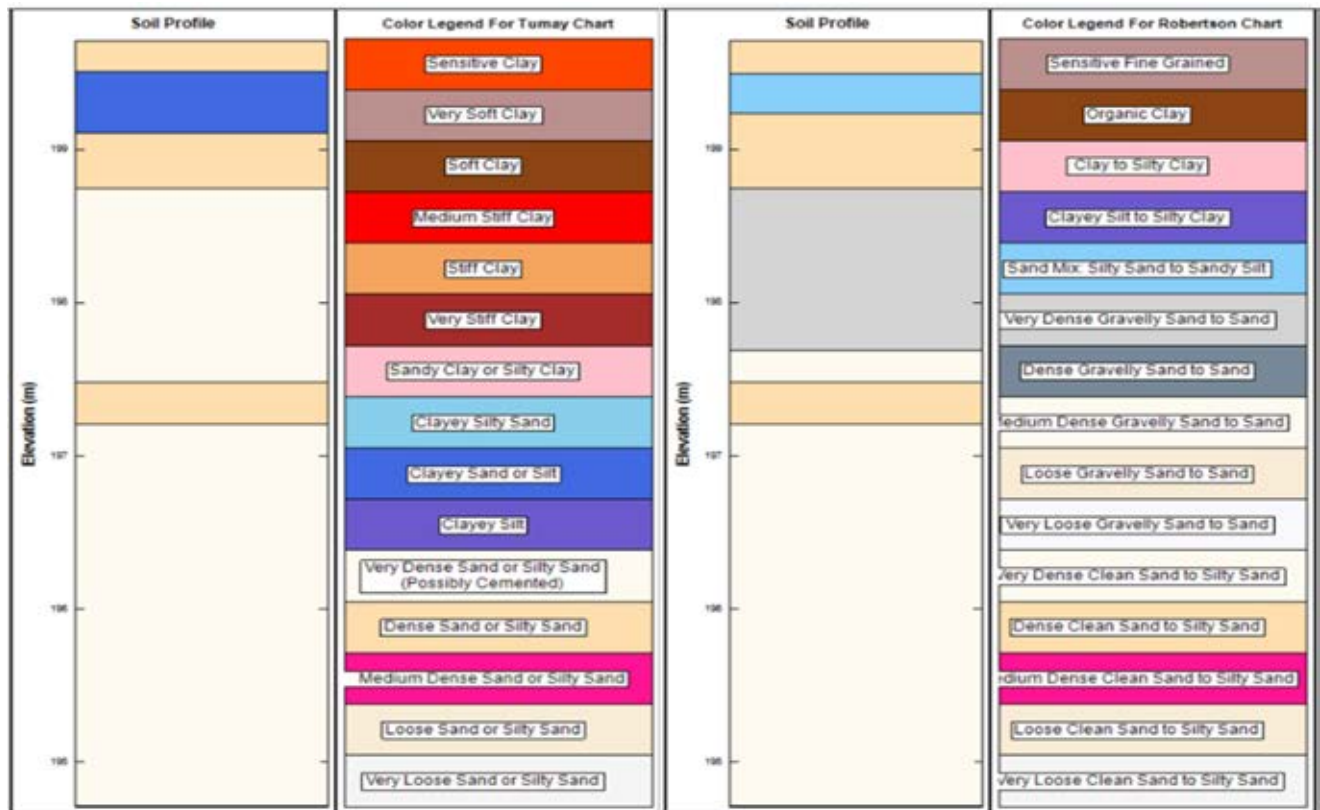
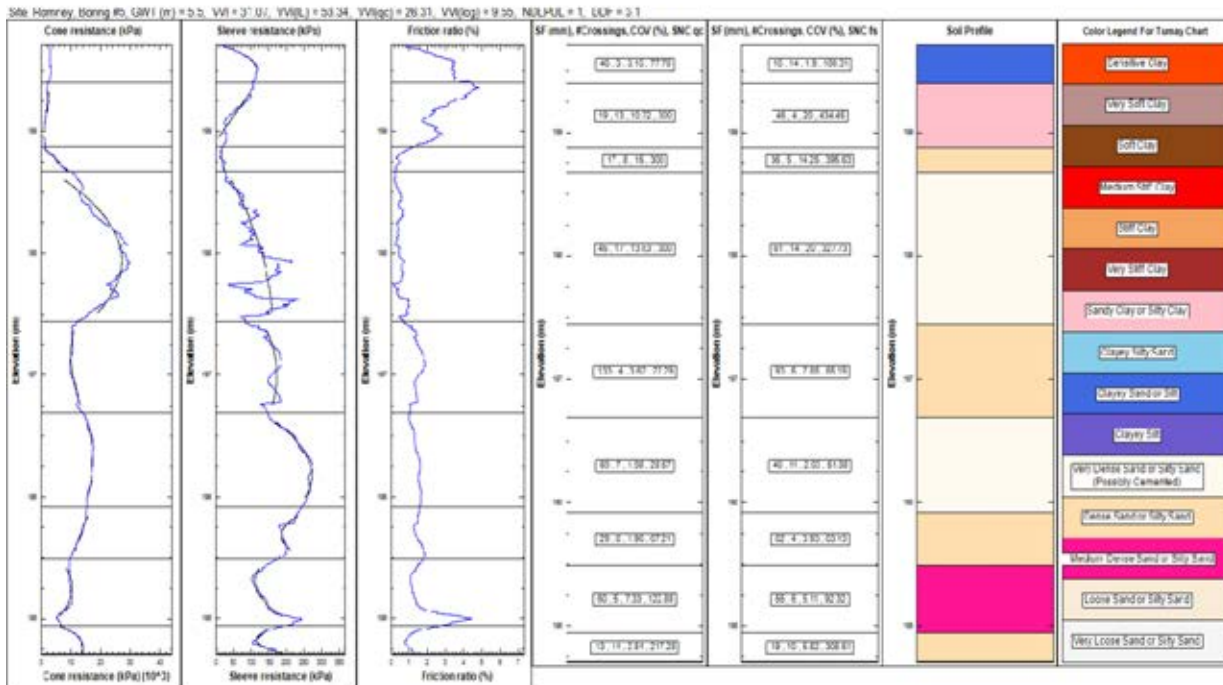


Figure A.12 Soil profiles generated using modified Tumay (1985) chart and modified Robertson (1990) chart for CPT 4 from Romney site.

Site: Romney Maintenance Unit      Final Depth (m): 6.10  
 Date: 10-Jan-12      Groundwater Depth (m): 5.49  
 Boring: 5      Drill Rig: ATV  
 Surface Elevation (m): 233.23      Drilling Method: **82.SLD./1650.D.** H.S.A.

Depth (m)	USCS	Description	N <sub>60</sub> (Blows)	Remarks
1.07-1.52	SP-SM	Moist, dense, poorly-graded SAND w/ silt and gravel	45.6	
2.59-3.05	ML	Moist, very stiff, SILT w/ sand	29.6	
4.12-4.57	SM	Moist, medium dense, silty SAND	25.7	
5.64-6.10	ML	Wet, very stiff, SILT	24.7	Water table encountered at 5.49 meters. The boring was terminated at 6.10 meters.

(a)



(b)

**Figure A.13** *In situ* test profiles: (a) SPT profile (N<sub>60</sub> values and soil boring description) for SPT 05 and (b) CPT profile (cone resistance, sleeve resistance, friction ratio, variability indices and soil profiles generated using modified Tumay (1985) chart and modified Robertson (1990) chart) for CPT 05 at Romney site.

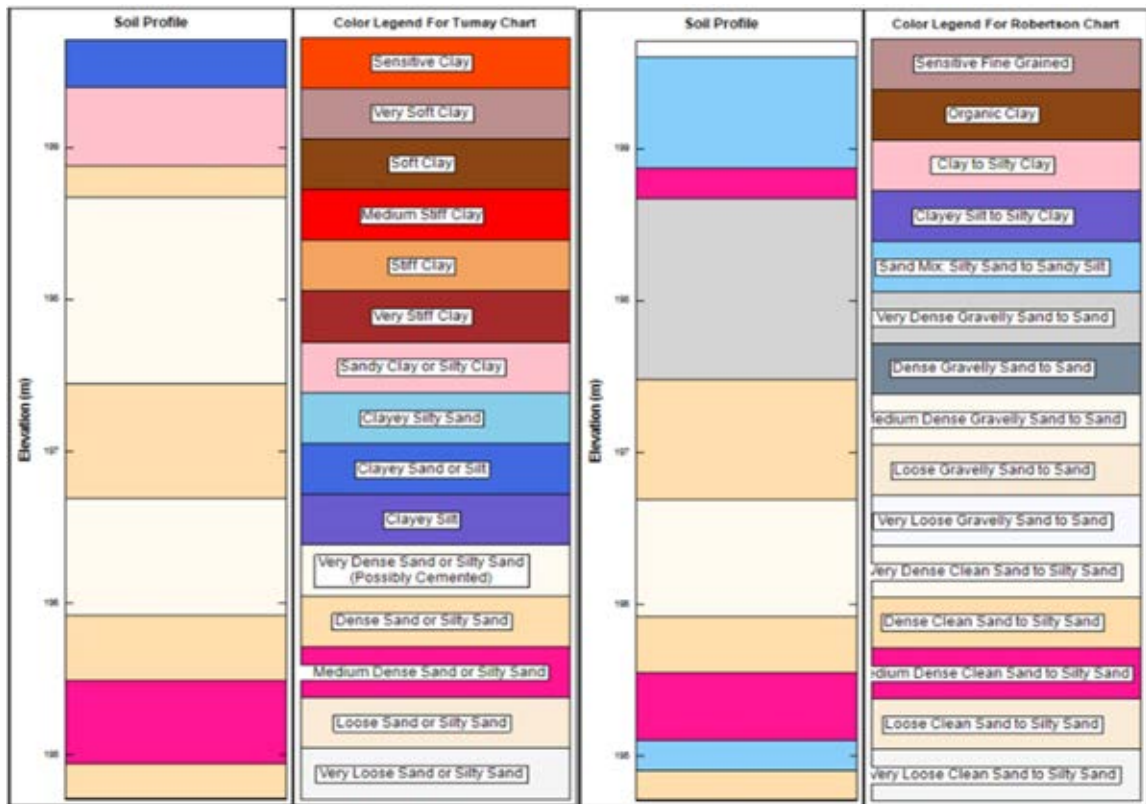
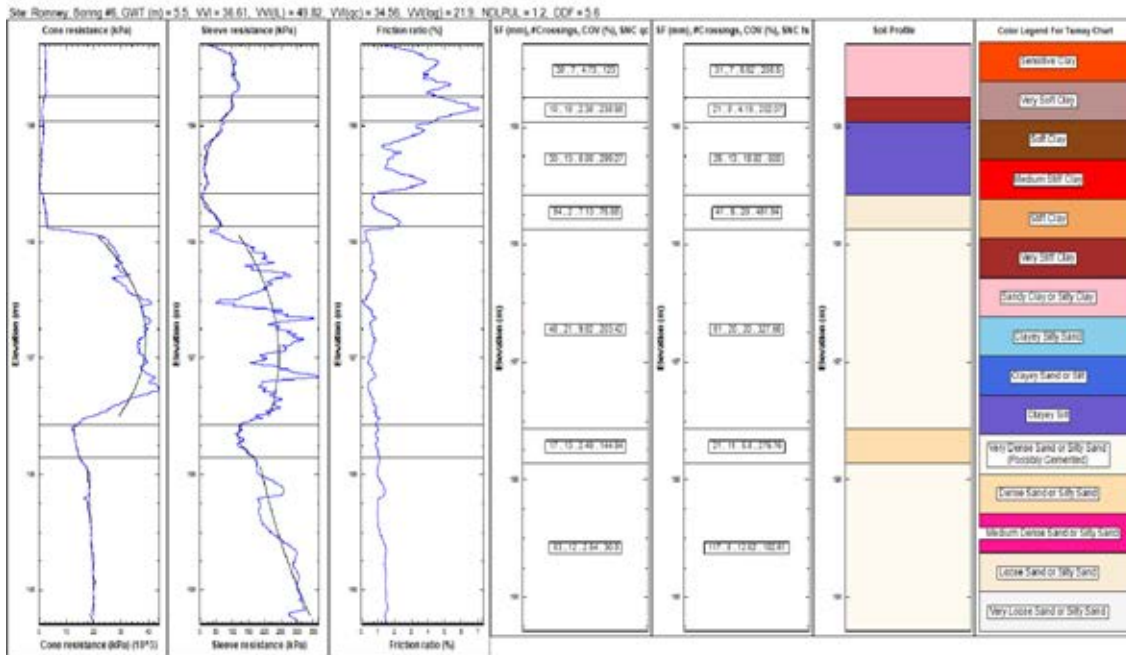


Figure A.14 Soil profiles generated using modified Tumay (1985) chart and modified Robertson (1990) for CPT 5 from Romney site.

Site: Romney Maintenance Unit      Final Depth (m): 6.10  
 Date: 10-Jan-12      Groundwater Depth (m): 5.49  
 Boring: 6      Drill Rig: ATV  
 Surface Elevation (m): 233.23      Drilling Method: **82.SLD./1650.D.** H.S.A.

Depth (m)	USCS	Description	N <sub>60</sub> (Blows)	Remarks
1.07-1.52	SP-SM	Moist, medium dense, poorly graded SAND w/ silt and gravel	21.7	
2.59-3.05	SM	Moist, medium dense, silty SAND w/ gravel	25.0	
4.12-4.57		grading out gravel	21.5	
5.64-6.10	ML	Wet, very stiff, sandy SILT	21.1	Water table encountered at 5.49 meters. The boring was terminated at 6.10 meters.

(a)



(b)

**Figure A.15** *In situ* test profiles(a) SPT profile (N<sub>60</sub> values and soil boring description) for SPT 06 and (b) CPT profile (cone resistance, sleeve resistance, friction ratio, variability indices and soil profiles generated using modified Tumay (1985) chart and modified Robertson (1990) chart) for CPT 06 at Romney site.

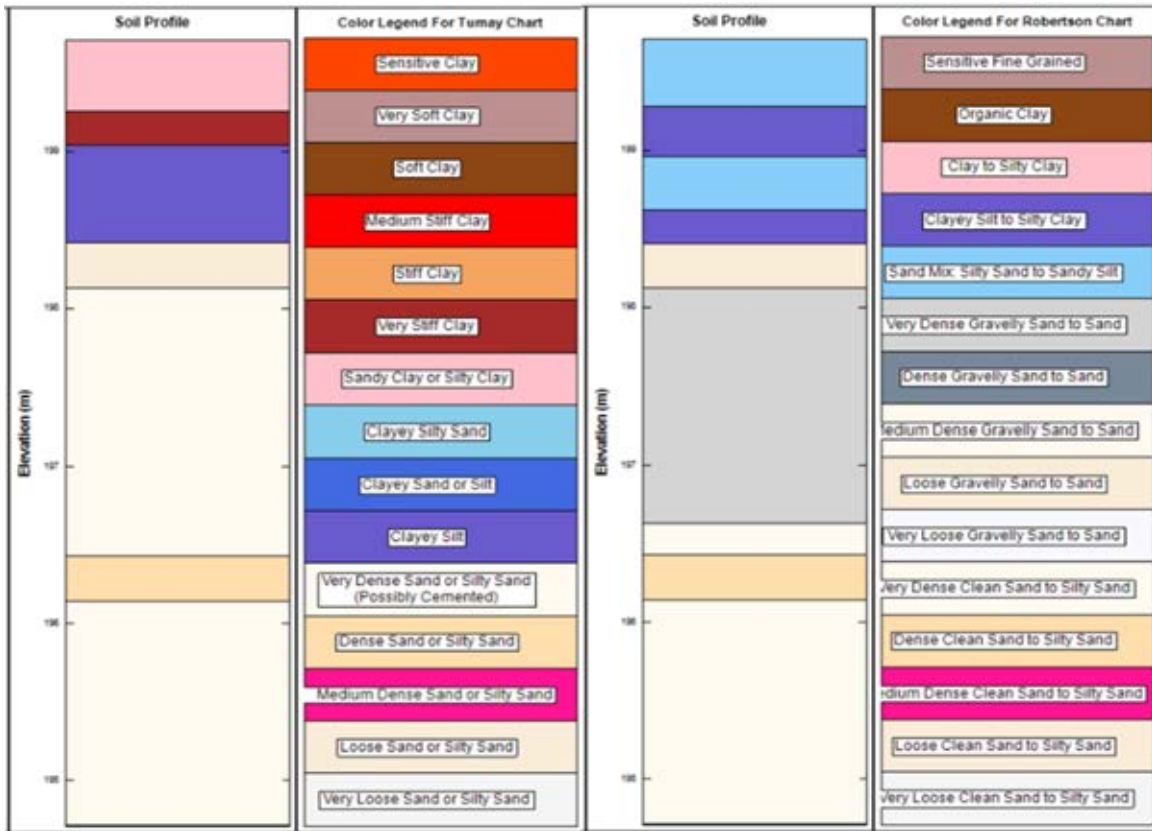
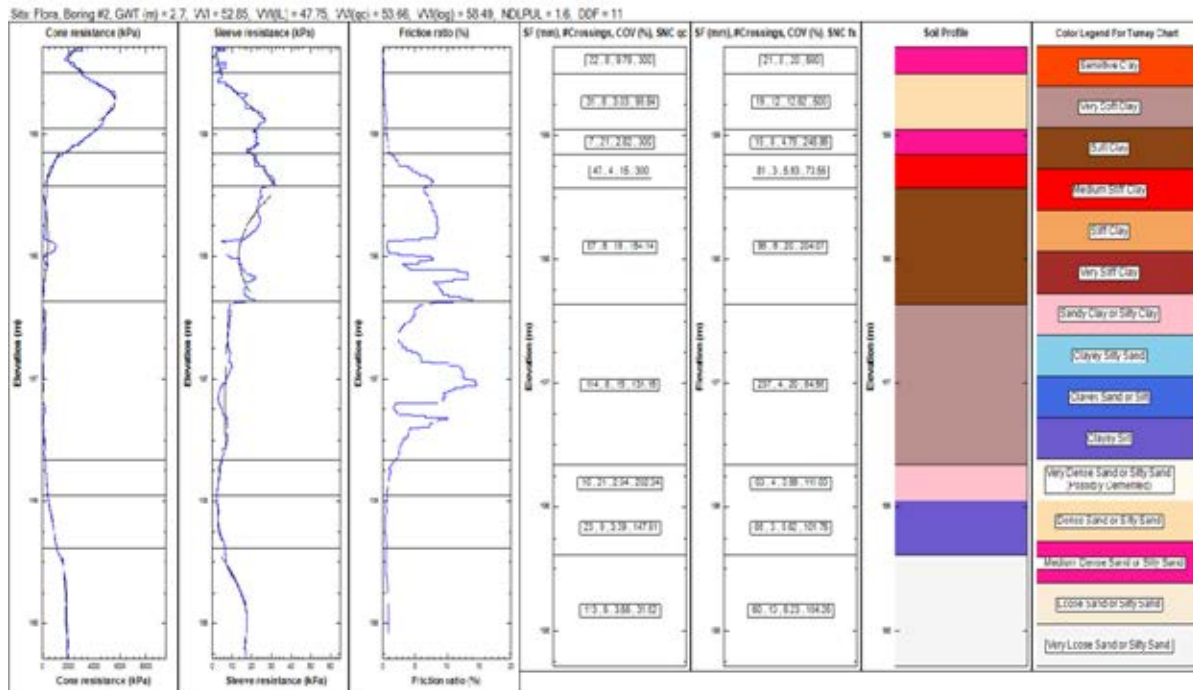


Figure A.16 Soil profiles generated using modified Tumay (1985) chart and modified Robertson (1990) chart for CPT 6 from Romney site.

Site: Flora Maintenance Unit      Final Depth (m): 4.57  
 Date: 9-Aug-11      Groundwater Depth (m): 2.74  
 Boring: 2      Drill Rig: Truck  
 Surface Elevation (m): 216.16      Drilling Method: **R2.SLD**/1650.D, H.S.A.

Depth (m)	USCS	Description	N <sub>60</sub> (Blows)	Remarks
1.07-1.52	CL	Moist, stiff, sandy lean CLAY	13.0	
2.59-3.05	SP	Wet, medium dense, poorly-graded SAND	13.7	Water table encountered at 2.74 meters.
4.12-4.57		grading wet	25.8	Sand was flowing into the hollow stem augers. The boring was terminated at 4.57 meters.

(a)



(b)

**Figure A.17** *In situ* test profiles: (a) SPT profile (N<sub>60</sub> values and soil boring description) for SPT 02 and (b) CPT profile (cone resistance, sleeve resistance, friction ratio, variability indices and soil profiles generated using modified Tumay (1985) chart and modified Robertson (1990) chart) for CPT 02 at Flora site.

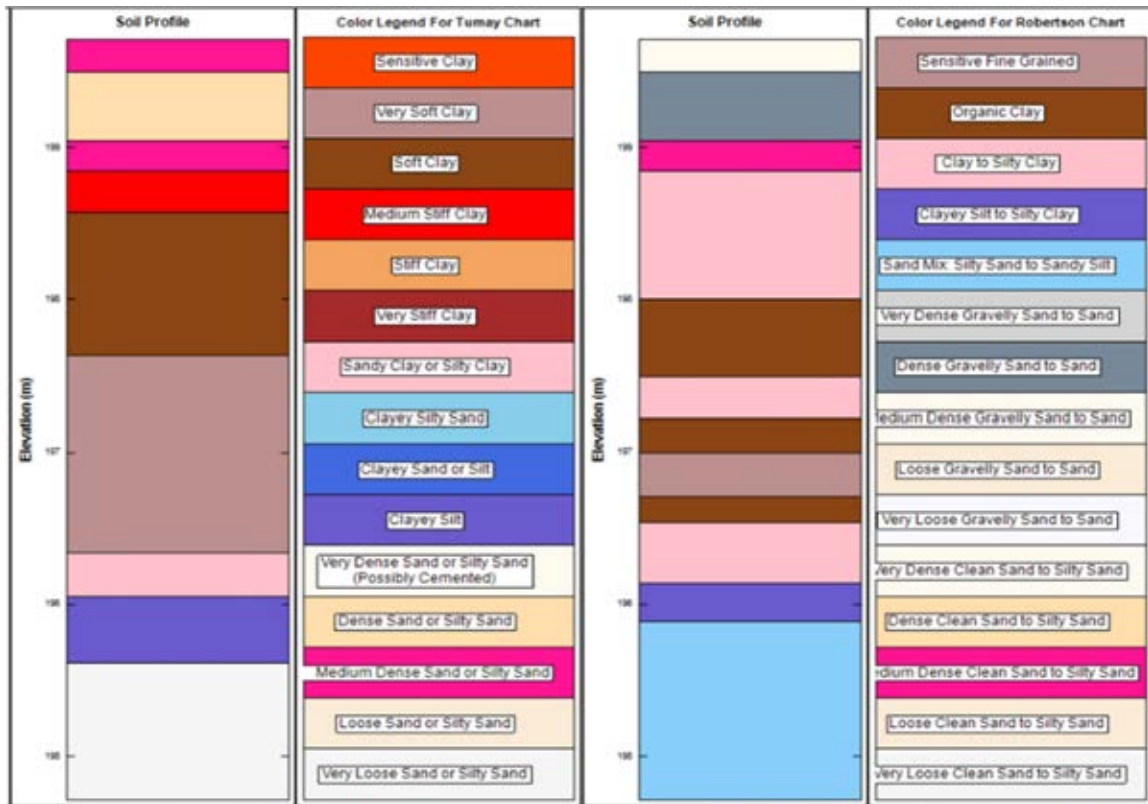
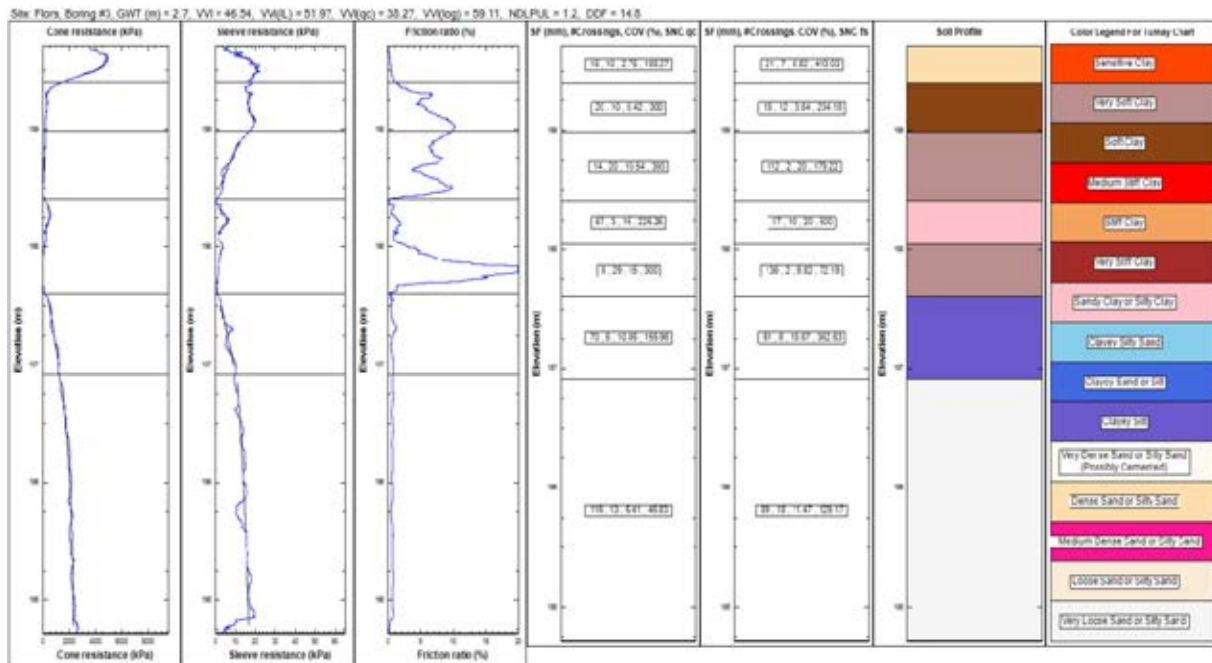


Figure A.18 Soil profiles generated using modified Tumay (1985) chart and modified Robertson (1990) chart for CPT 2 from Flora site.

Site: Flora Maintenance Unit      Final Depth (m): 4.57  
 Date: 9-Aug-11      Groundwater Depth (m): 2.74  
 Boring: 3      Drill Rig: Truck  
 Surface Elevation (m): 216.16      Drilling Method: **R2.SL.D./1650.D.** H.S.A.

Depth (m)	USCS	Description	N <sub>60</sub> (Blows)	Remarks
1.07-1.52	SC-SM	Moist, medium dense, silty clayey SAND	18.5	
2.59-3.05	SP-SC	Wet, medium dense, poorly-graded SAND w/ silty clay	13.7	Water table encountered at 2.74 meters.
4.12-4.57	SP	Wet, medium dense, poorly-graded SAND	14.7	Sand was flowing into the hollow stem augers. The boring was terminated at 4.57 meters.

(a)



(b)

**Figure A.19** *In situ* test profiles: (a) SPT profile (N<sub>60</sub> values and soil boring description) for SPT 03 and (b) CPT profile (cone resistance, sleeve resistance, friction ratio, variability indices and soil profiles generated using modified Tumay (1985) chart and modified Robertson (1990) chart) for CPT 03 at Flora site.

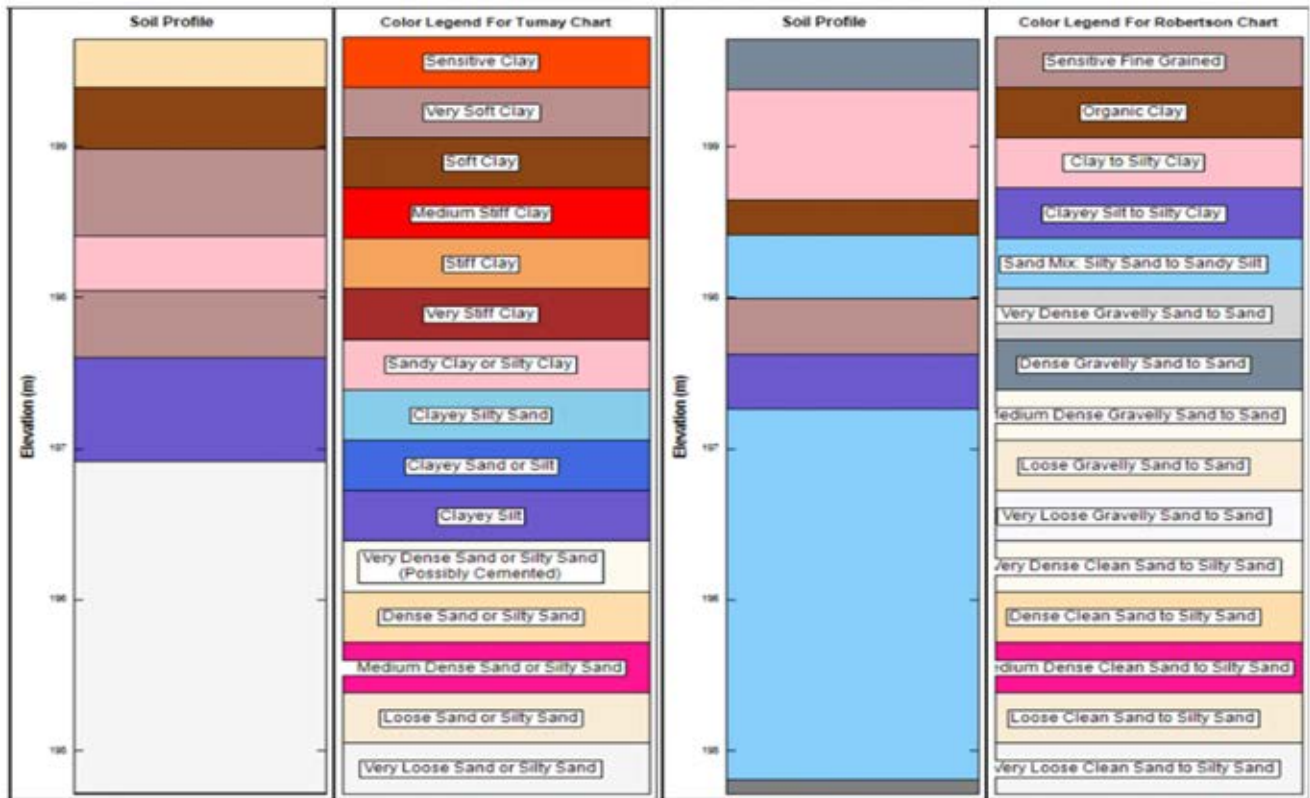


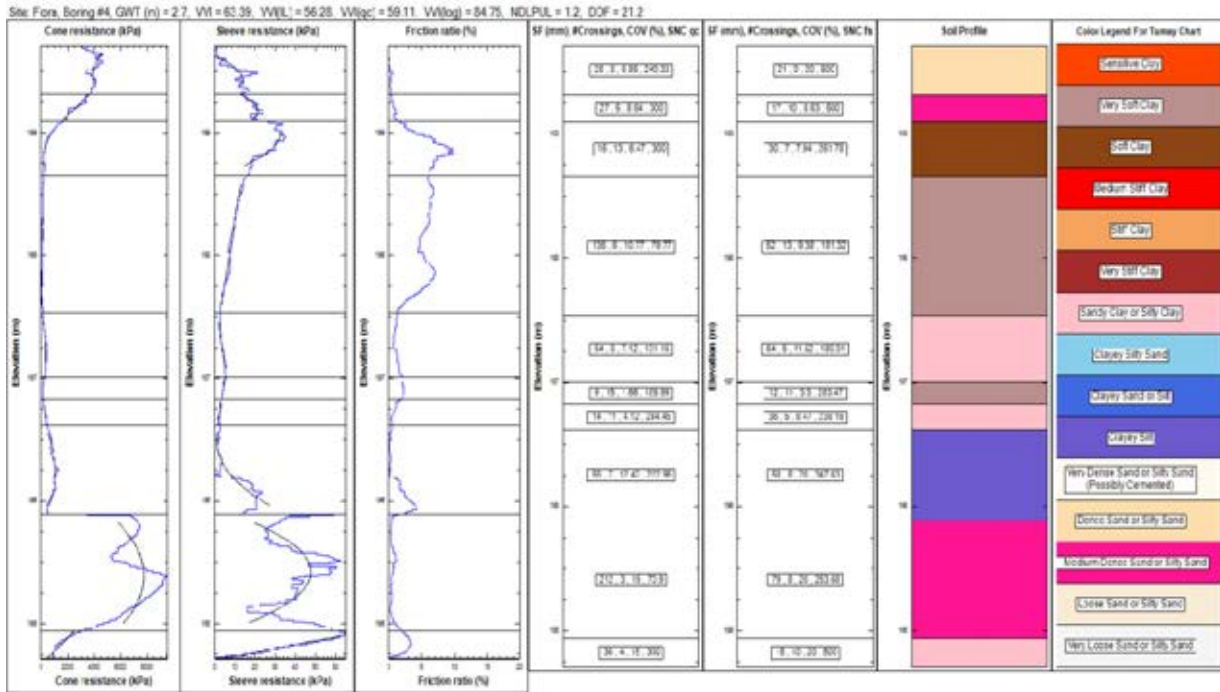
Figure A.20 Soil profiles generated using modified Tumay (1985) chart and modified Robertson (1990) chart for CPT 3 from Flora site.

Site: Flora Maintenance Unit  
 Date: 9-Aug-11  
 Boring: 4  
 Surface Elevation (m): 216.16

Final Depth (m): 4.57  
 Groundwater Depth (m): 2.74  
 Drill Rig: Truck  
 Drilling Method: **82.SI.D./1650.D.** H.S.A.

Depth (m)	USCS	Description	N <sub>60</sub> (Blows)	Remarks
1.07-1.52	SC-SM	Moist, medium dense, silty clayey SAND	14.8	
2.59-3.05	SP-SC	Wet, medium dense, poorly-graded SAND w/ silty clay	13.7	Water table encountered at 2.74 meters.
4.12-4.57	SC-SM	Wet, medium dense, poorly-graded SAND	13.5	Sand was flowing into the hollow stem augers. The boring was terminated at 4.57 meters.

(a)



(b)

**Figure A.21** *In situ* test profiles: (a) SPT profile ( $N_{60}$  values and soil boring description) for SPT 04 and (b) CPT profile (cone resistance, sleeve resistance, friction ratio, variability indices and soil profiles generated using modified Tumay (1985) chart and modified Robertson (1990) chart) for CPT 04 at Flora site.

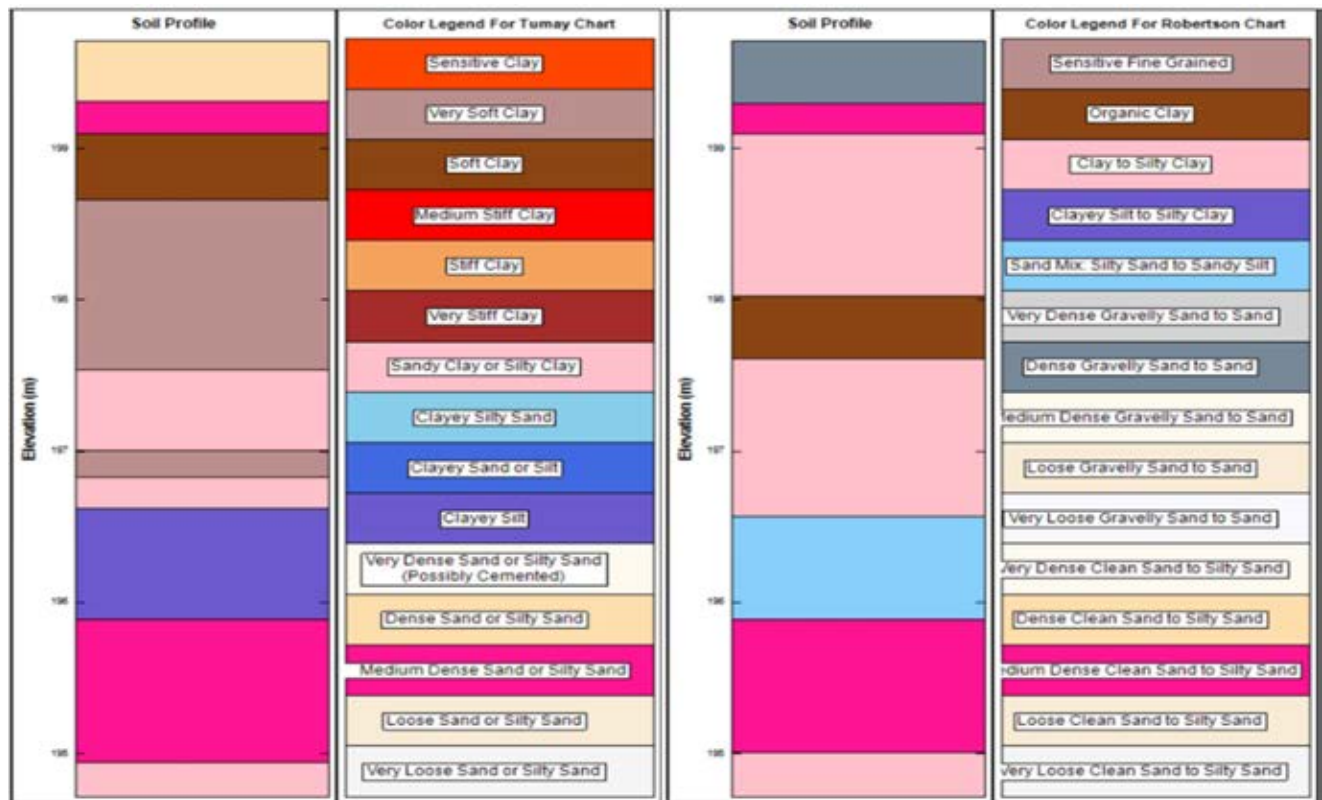
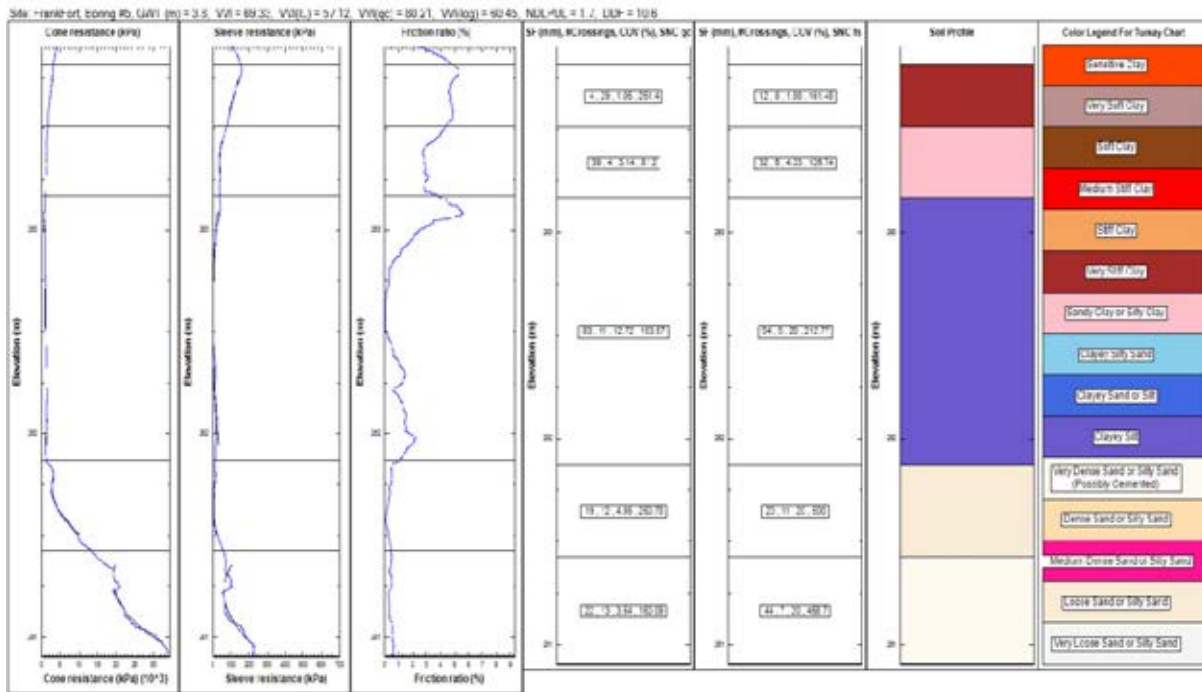


Figure A.22 Soil profiles generated using modified Tumay (1985) chart and modified Robertson (1990) chart for CPT 4 from Flora site.

Site: Frankfort Maintenance Unit      Final Depth (m): 4.57  
 Date: 5-Jan-12      Groundwater Depth (m): 3.81  
 Boring: 6      Drill Rig: ATV  
 Surface Elevation (m): 264.33      Drilling Method: **B2.5LD**/1650.D, H.S.A.

Depth (m)	USCS	Description	N <sub>60</sub> (Blows)	Remarks
1.07-1.52	SM	Moist, dense, silty SAND	36.9	
2.59-3.05		grading very dense	58.9	Water table encountered at 3.81 meters. The boring was terminated at 4.57 meters.
4.12-4.57	ML	Wet, hard, sandy SILT	43.8	

(a)



(b)

**Figure A.23** *In situ* test profiles: (a) SPT profile (N<sub>60</sub> values and soil boring description) for SPT 06 and (b) CPT profile (cone resistance, sleeve resistance, friction ratio, variability indices and soil profiles generated using modified Tumay (1985) chart and modified Robertson (1990) chart) for CPT 05 at Frank Fort site.

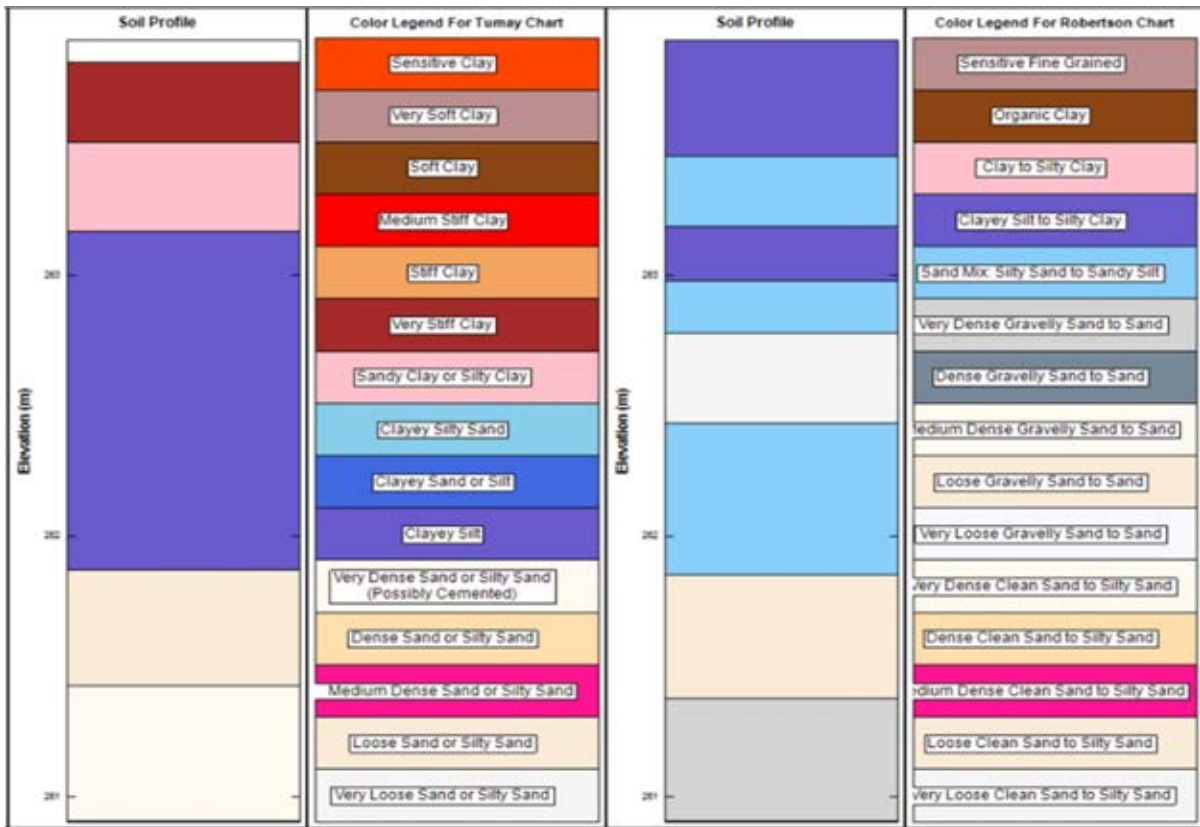
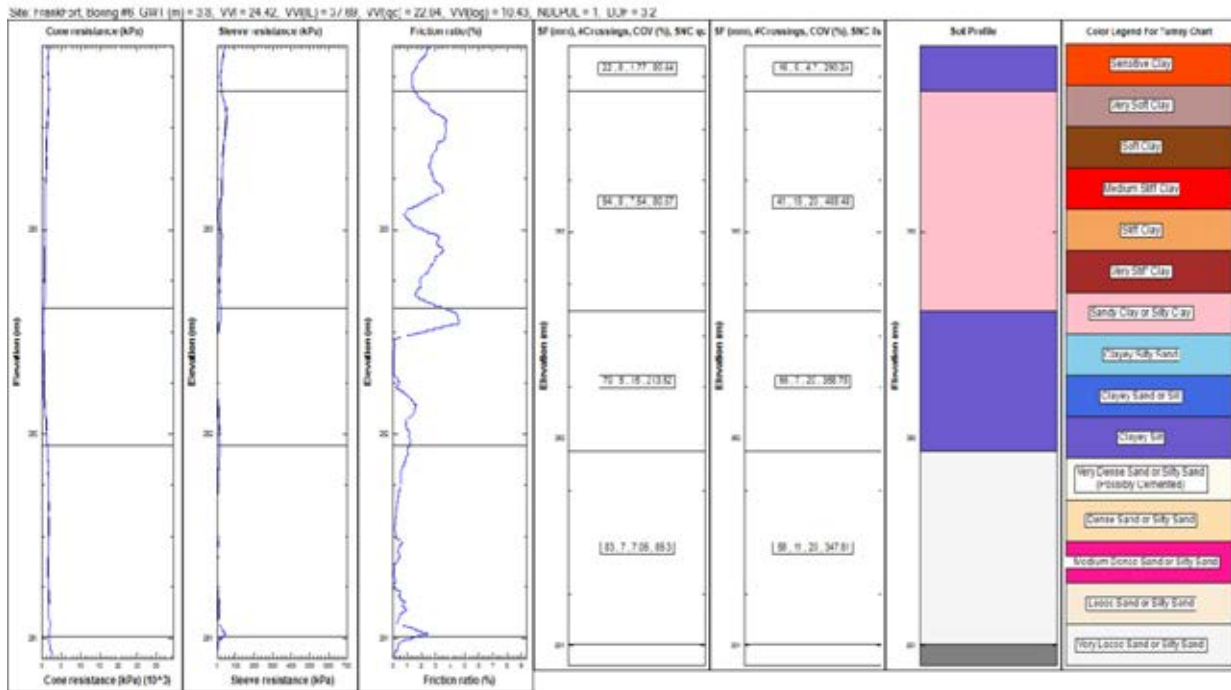


Figure A.24 Soil profiles generated using modified Tumay (1985) chart and modified Robertson (1990) chart for CPT 5 from Frank Fort site.

Site: Frankfort Maintenance Unit Final Depth (m): 4.57  
 Date: 6-Jan-12 Groundwater Depth (m): 3.81  
 Boring: 7 Drill Rig: ATV  
 Surface Elevation (m): 264.33 Drilling Method: **K2.SLD**/1650.D. H.S.A.

Depth (m)	USCS	Description	N <sub>60</sub> (Blows)	Remarks
1.07-1.52	CL	Moist, very stiff, sandy lean <u>CLAY</u>	18.2	
2.59-3.05	CL-ML	Moist, stiff, sandy silty <u>CLAY</u>	13.8	Water table encountered at 3.81 meters. The boring was terminated at 4.57 meters.
4.12-4.57		grading wet and hard	46.8	

(a)



(b)

**Figure A.25** *In situ* test profiles: (a) SPT profile ( $N_{60}$  values and soil boring description) for SPT 07 and (b) CPT profile (cone resistance, sleeve resistance, friction ratio, variability indices and soil profiles generated using modified Tumay (1985) chart and modified Robertson (1990) chart) for CPT06 at Frank Fort site.

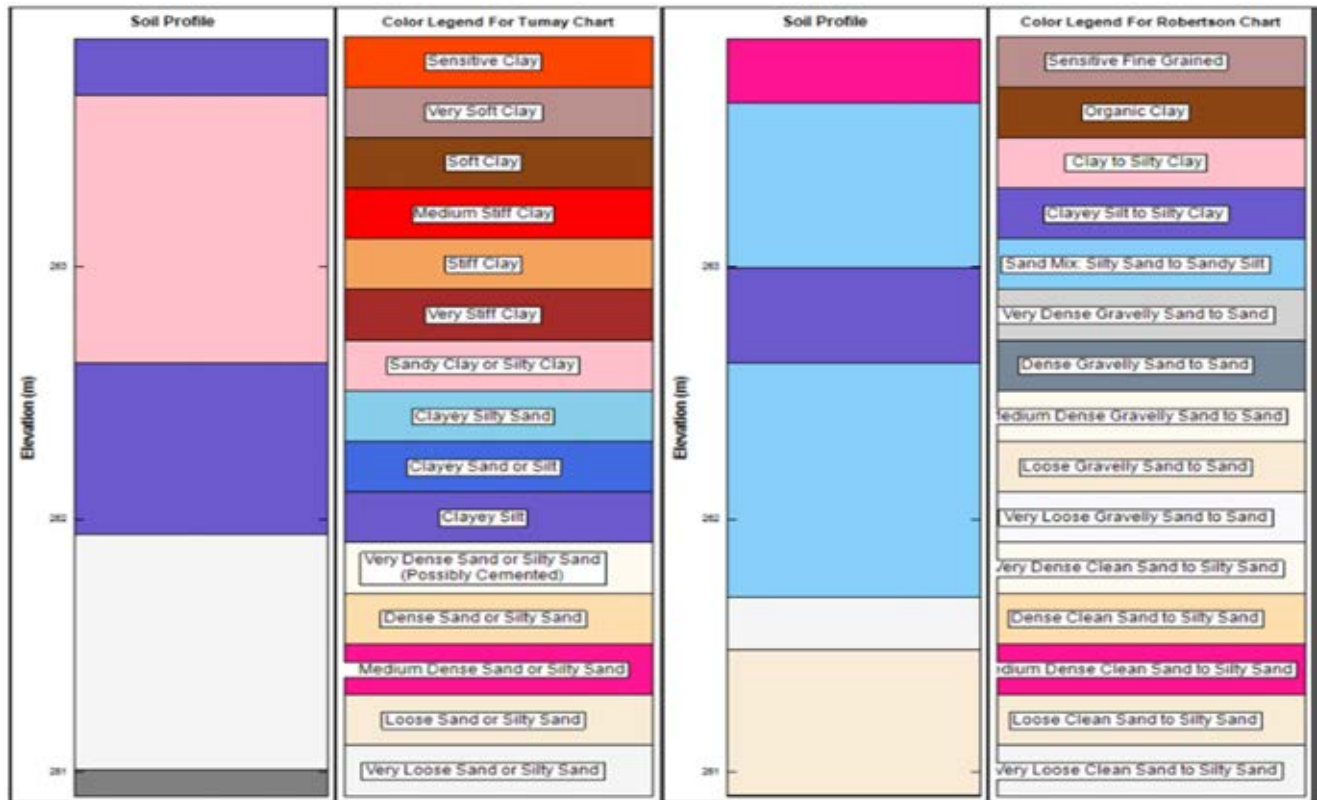
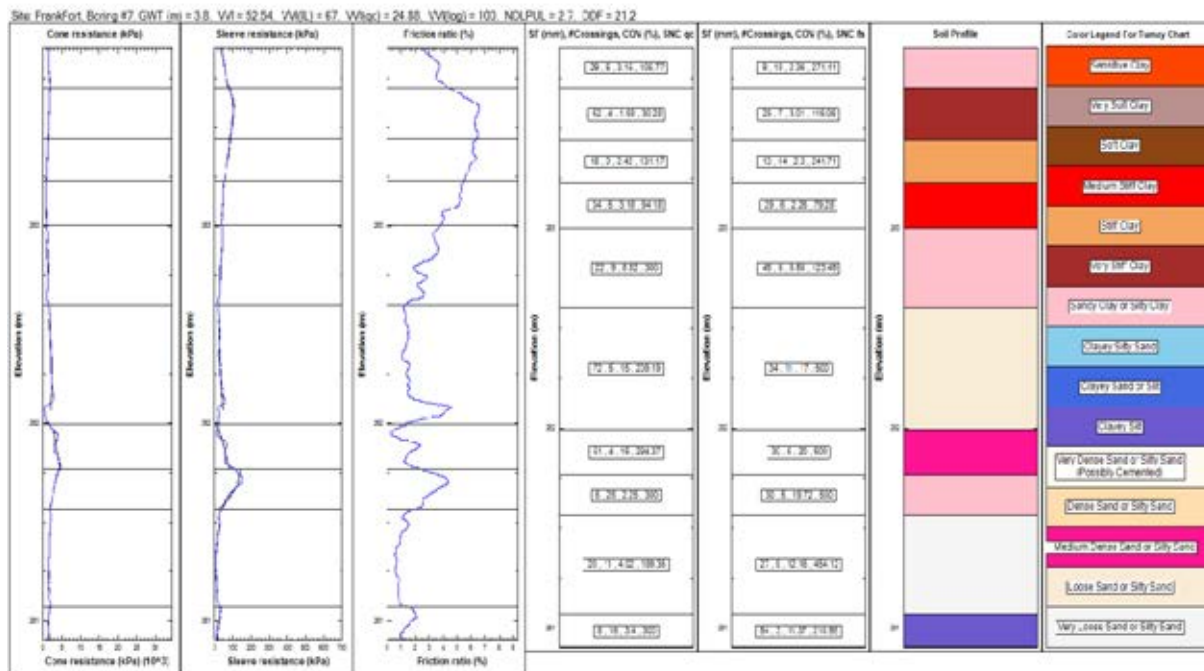


Figure A.26 Soil profiles generated using modified Tumay (1985) chart and modified Robertson (1990) chart for CPT 6 from Frank Fort site.

Site: Frankfort Maintenance Unit      Final Depth (m): 6.10  
 Date: 6-Jan-12      Groudwater Depth (m): 3.81  
 Boring: 8      Drill Rig: ATV  
 Surface Elevation (m): 264.33      Drilling Method: **82.SLD**/1650.D, H.S.A.

Depth (m)	USCS	Description	N <sub>60</sub> (Blows)	Remarks
1.07-1.52	CL	Moist, very stiff, lean <u>CLAY</u> w/ sand	18.2	
2.59-3.05		grading sandy	16.9	Water table encountered at 3.81 meters.
4.12-4.57	CL-ML	Wet, hard, sandy silty <u>CLAY</u>	59.5	
5.64-6.10	SM	Wet, medium dense, silty <u>SAND</u>	16.4	The boring was terminated at 6.10 meters.

(a)



(b)

**Figure A.27** *In situ* test profiles: (a) SPT profile (N<sub>60</sub> values and soil boring description) for SPT 08 and (b) CPT profile (cone resistance, sleeve resistance, friction ratio, variability indices and soil profiles generated using modified Tumay (1985) chart and modified Robertson (1990) chart) for CPT 07 at Frank Fort site.

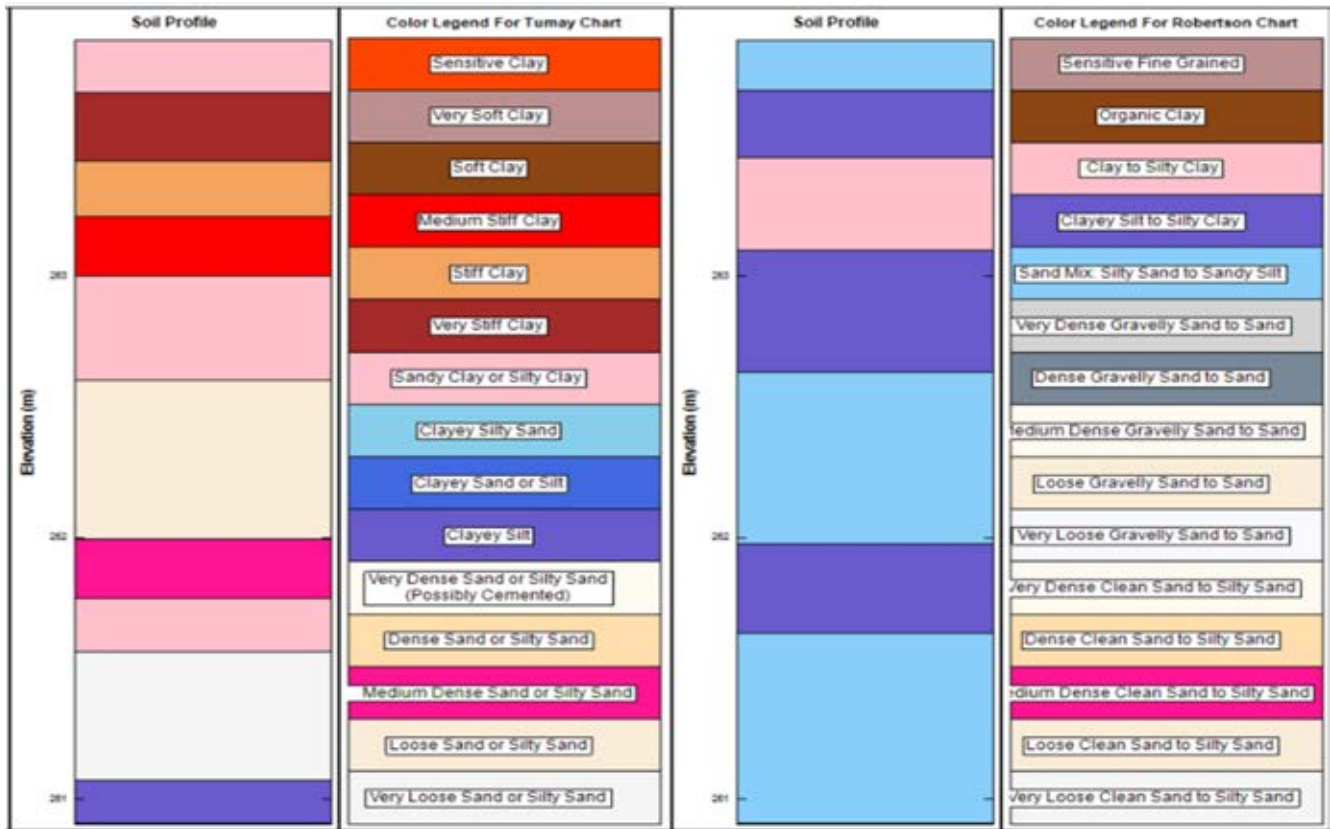


Figure A.28 Soil profiles generated using modified Tumay (1985) chart and modified Robertson (1990) chart for CPT 7 from Frank Fort site.

APPENDIX B: VARIABILITY MAPS FOR INDIANA

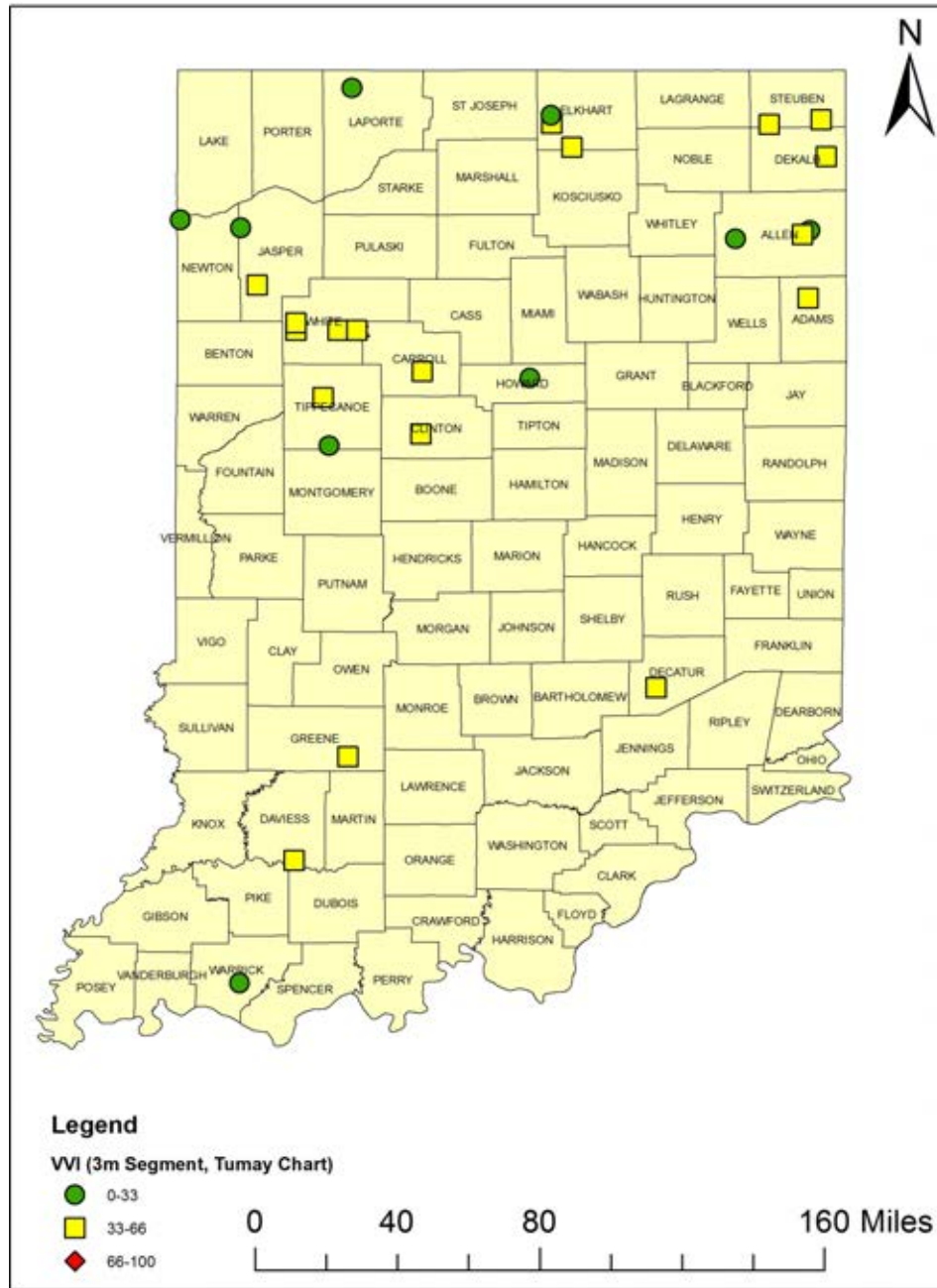


Figure B.1 Site VVI for 3 m soil profile length using modified Tumay (1985) chart.

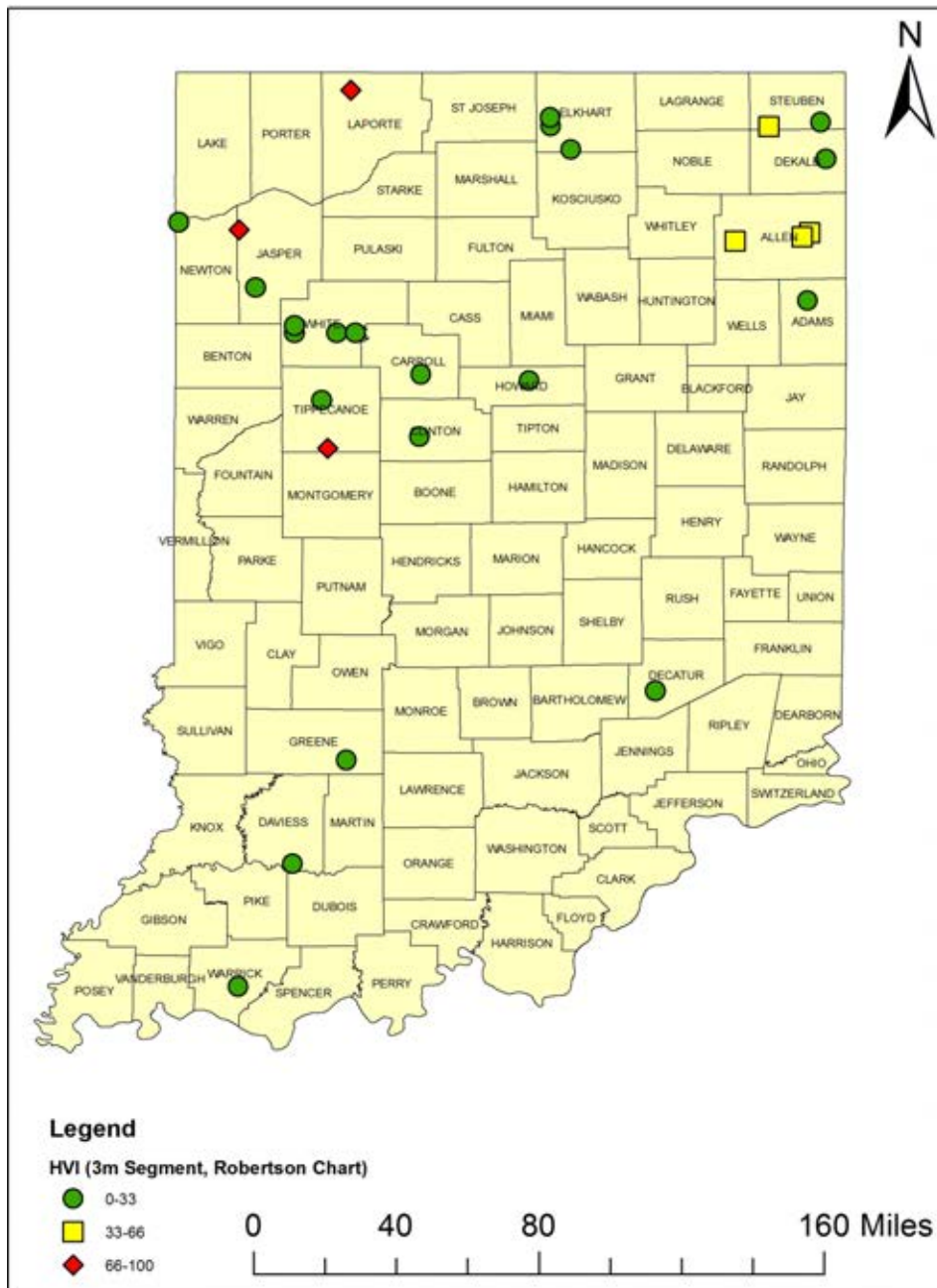


Figure B.2 Site HVI for 3 m soil profile length.

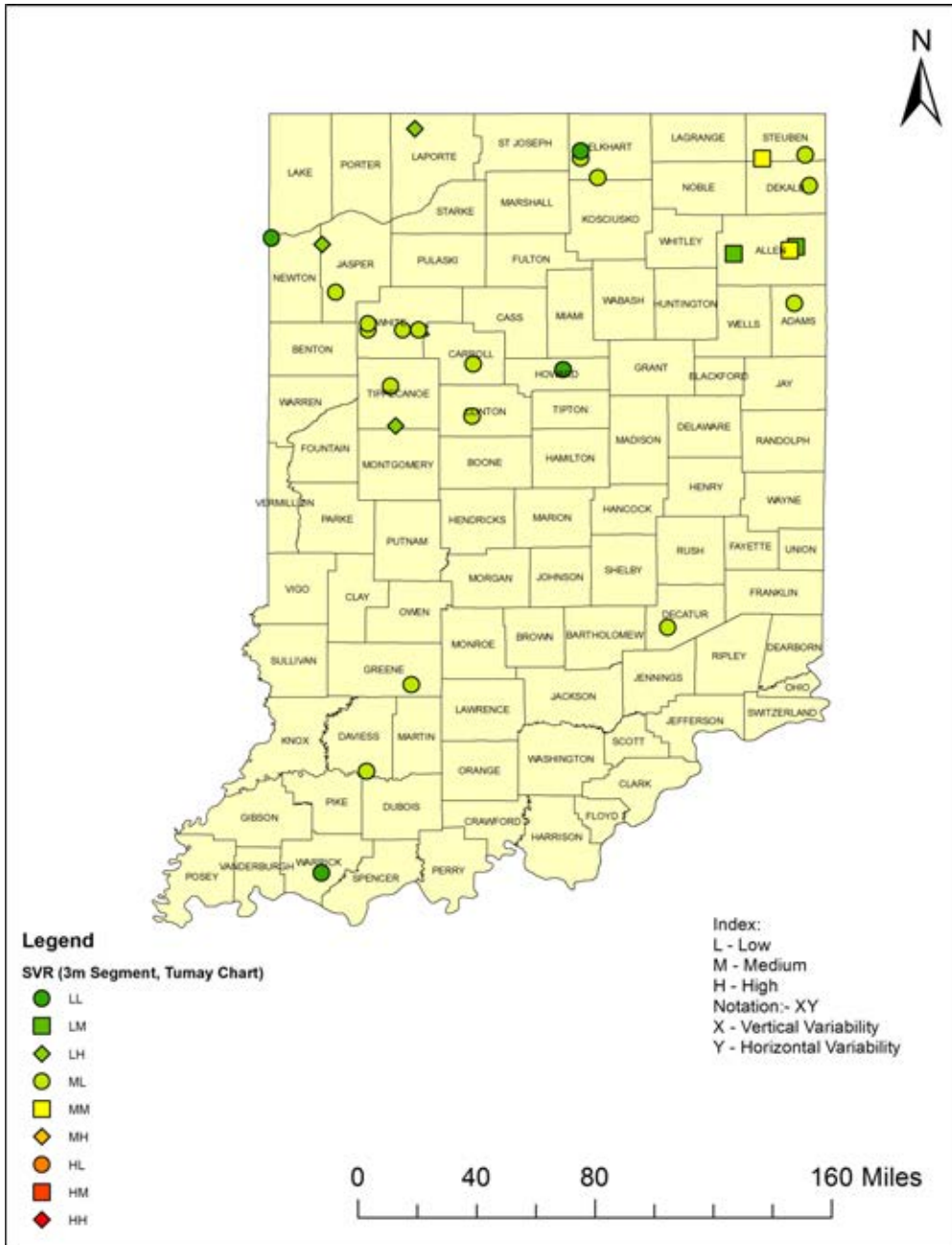


Figure B.3 SVR for 3 m soil profile length using modified Tumay (1985) chart.

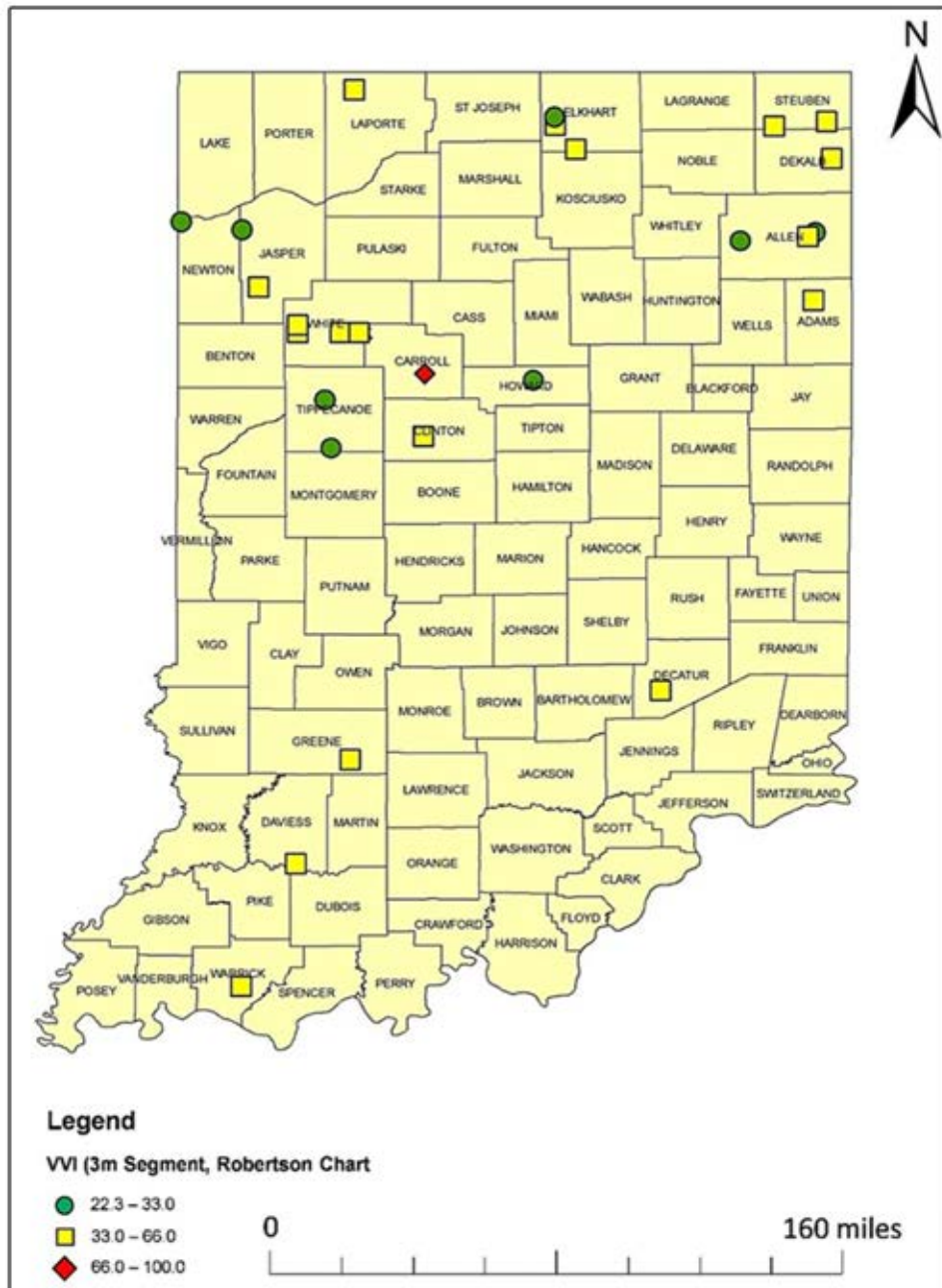


Figure B.4 Site VVI for 3 m soil profile length using modified Robertson (1990) chart.

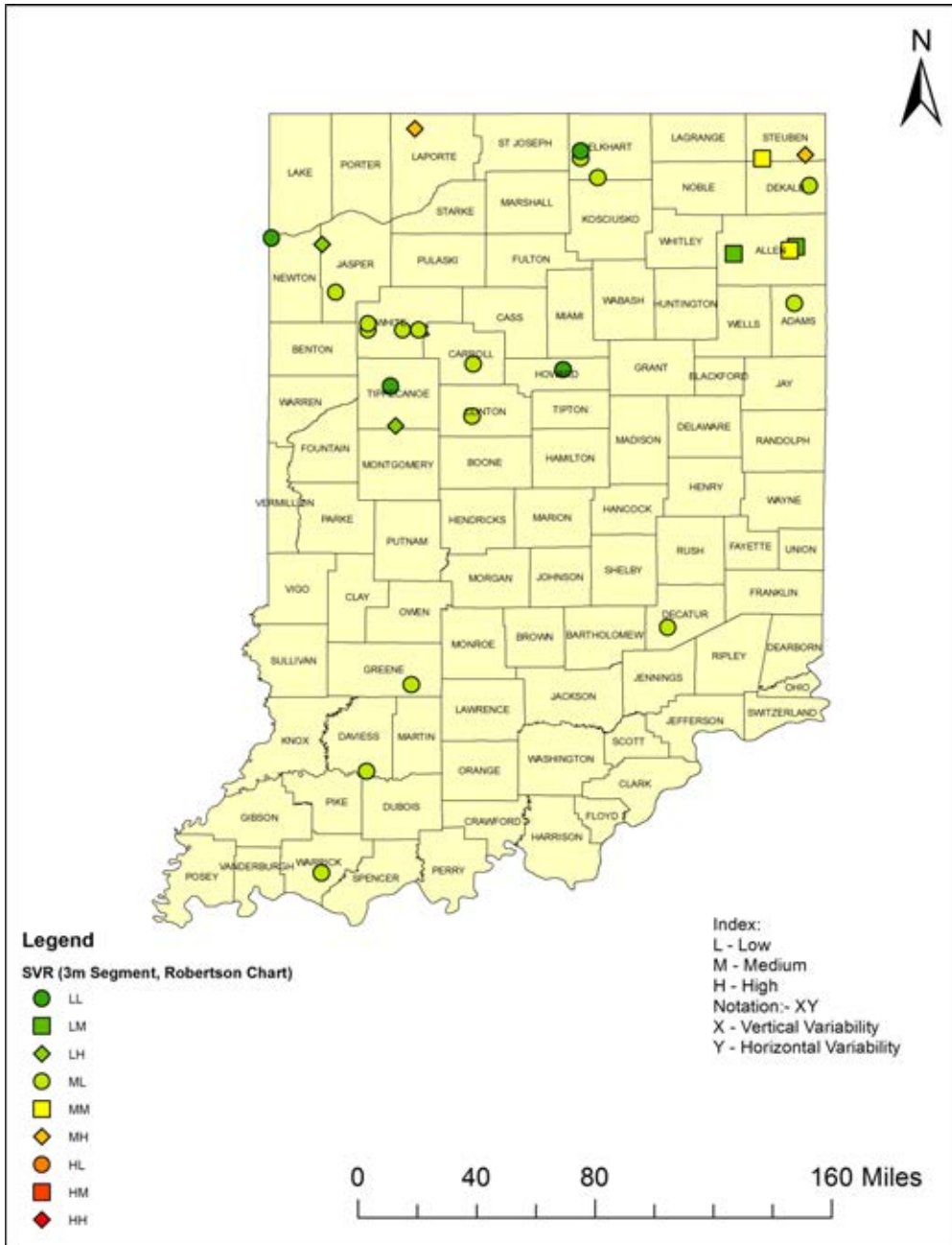


Figure B.5 SVR for 3 m soil profile length using modified Robertson (1990) chart.

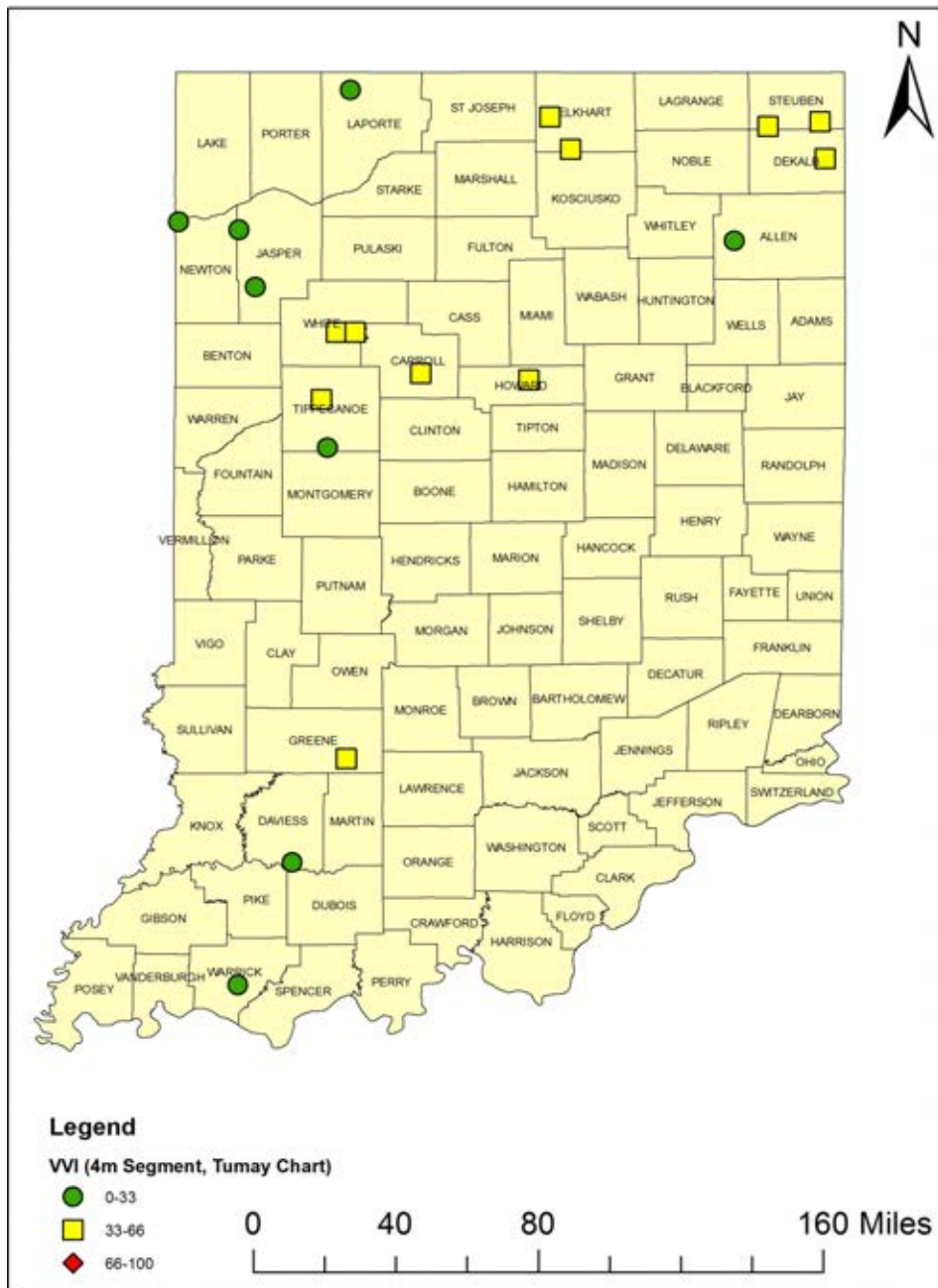


Figure B.6 Site VVI for 4 m soil profile length using modified Tumay (1985) chart.

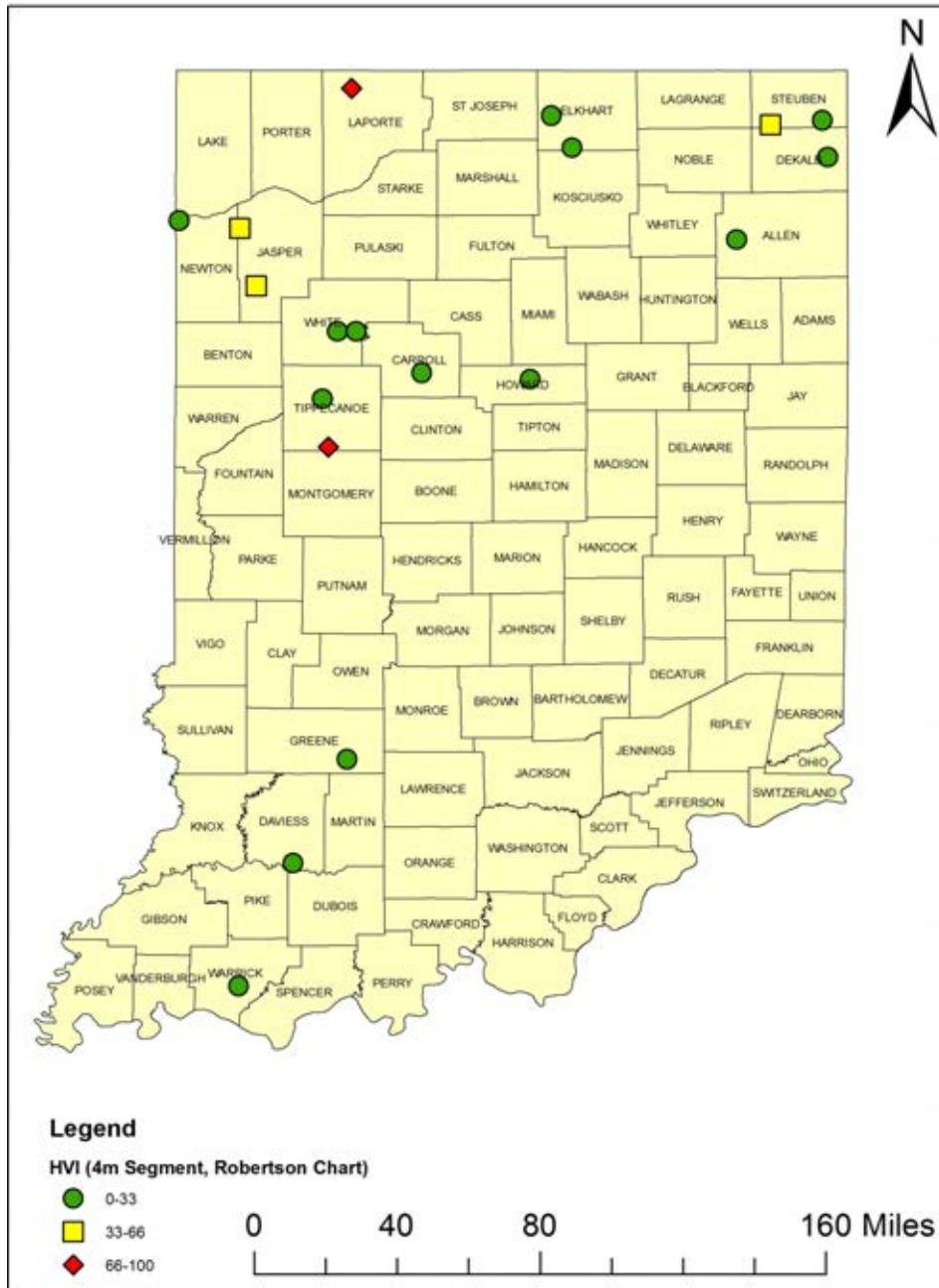


Figure B.7 Site HVI for 4 m soil profile length.

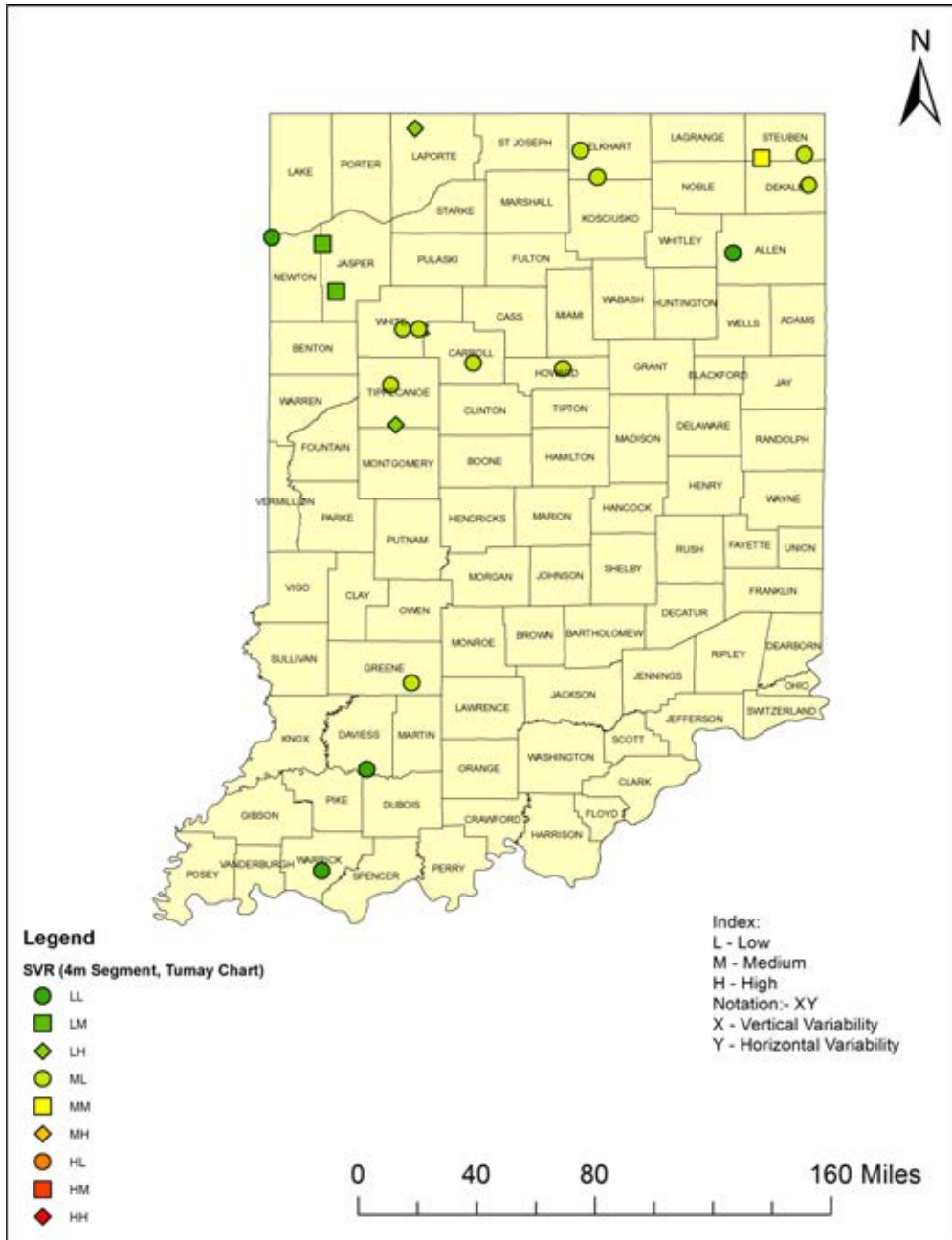


Figure B.8 SVR for 4 m soil profile length using modified Tumay (1985) chart.

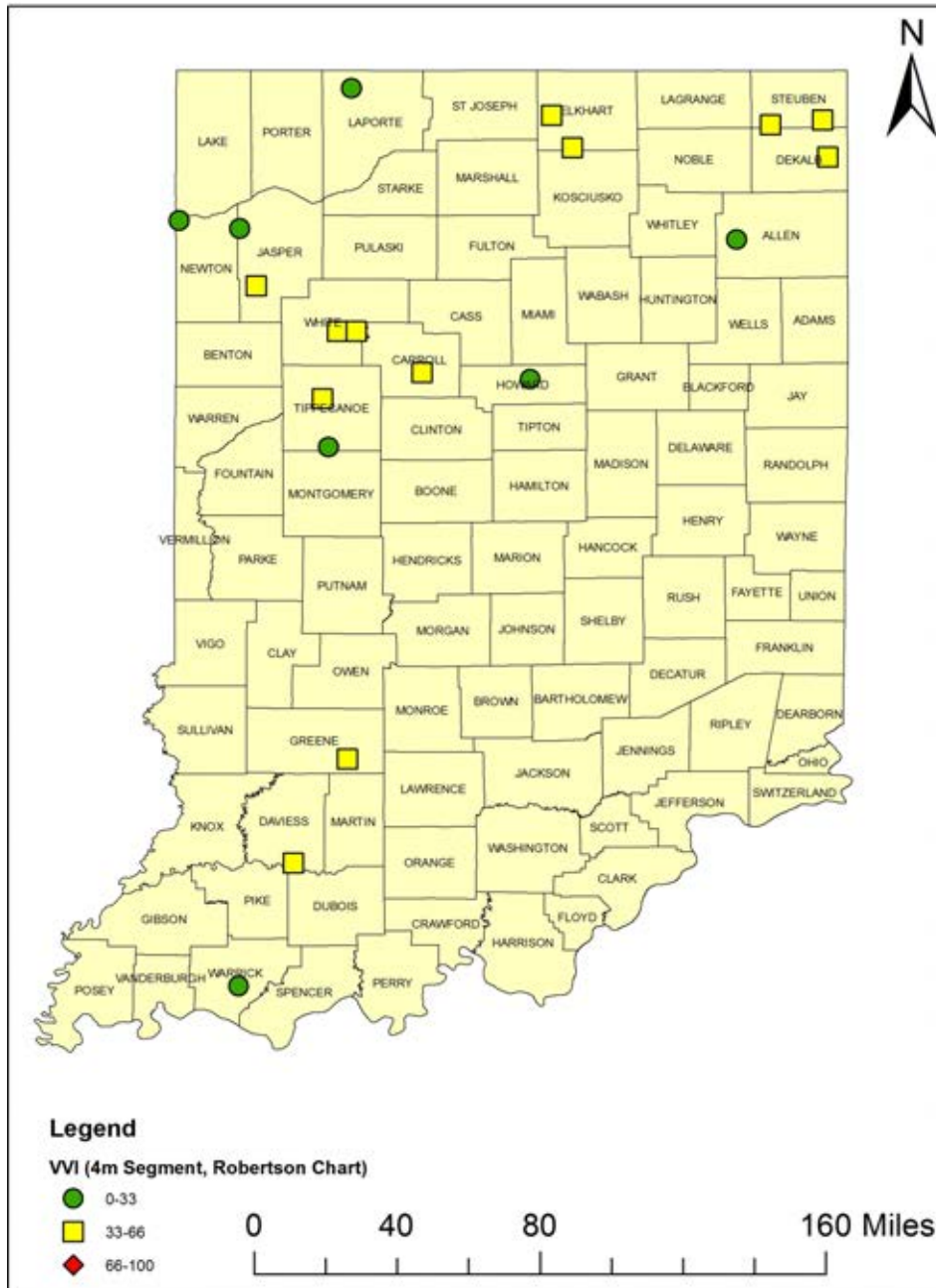


Figure B.9 Site VVI for 4 m soil profile length using modified Robertson (1990) chart.

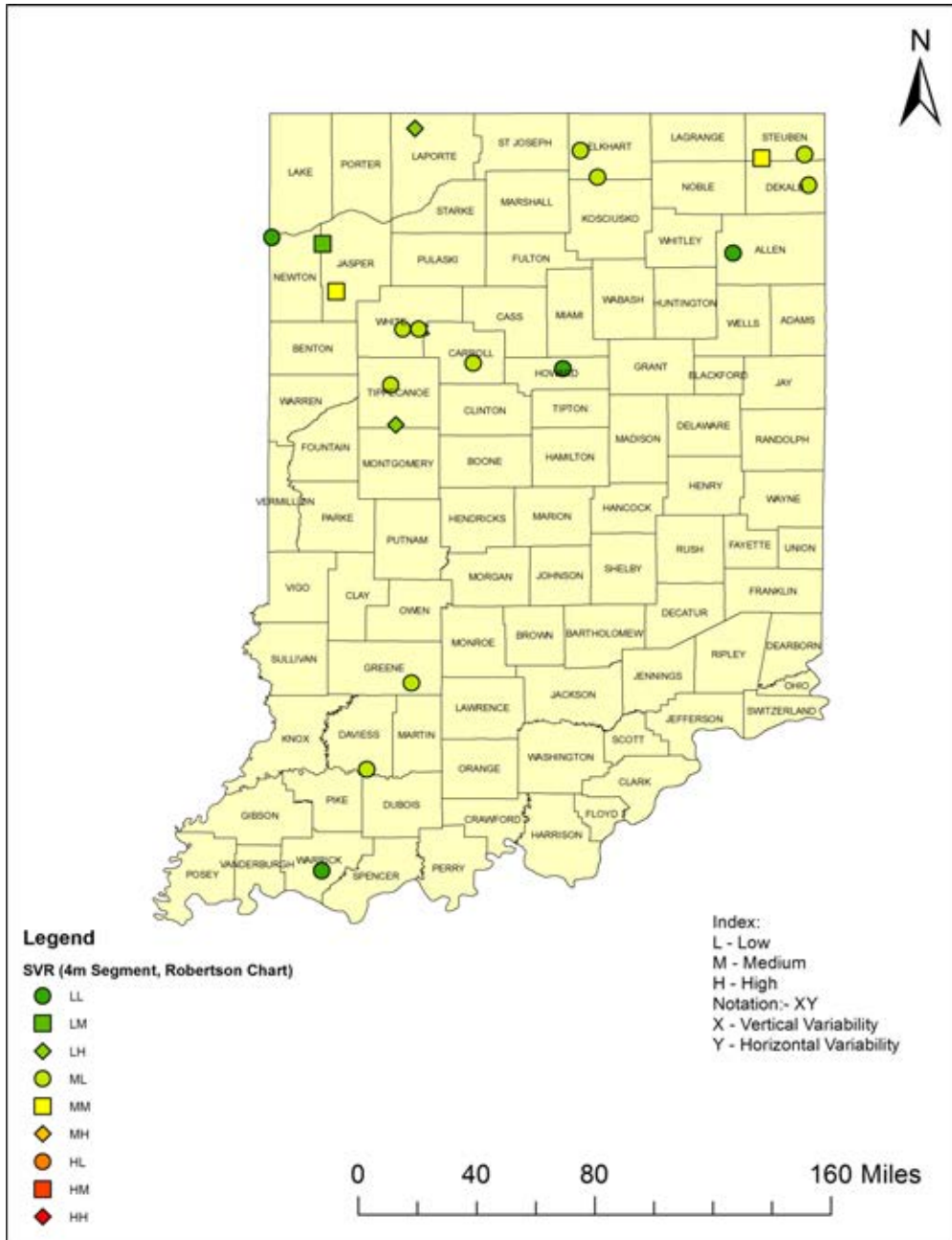


Figure B.10 SVR for 4 m soil profile length using modified Robertson (1990) chart.

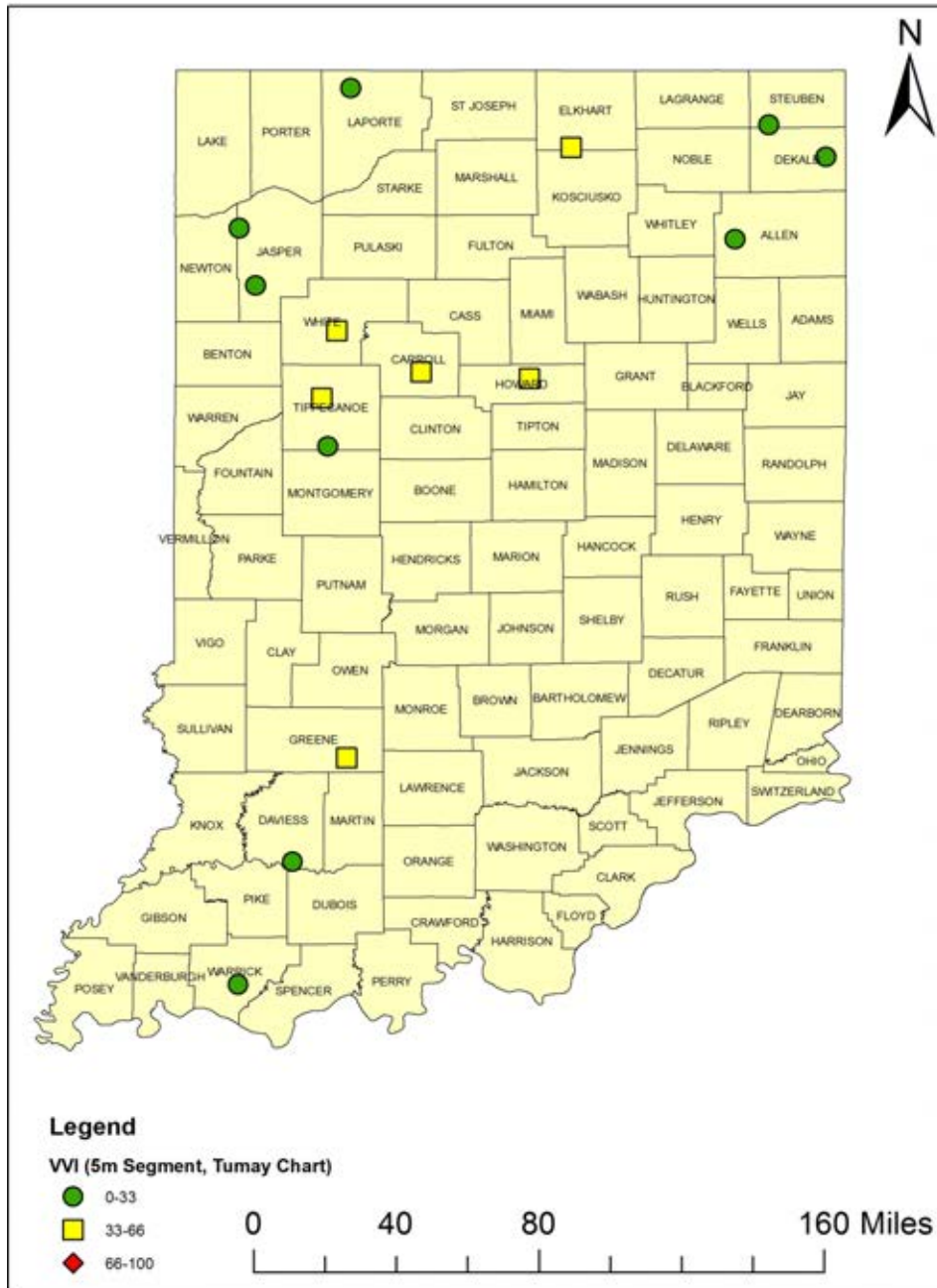


Figure B.11 Site VVI for 5 m soil profile length using modified Tumay (1985) chart.

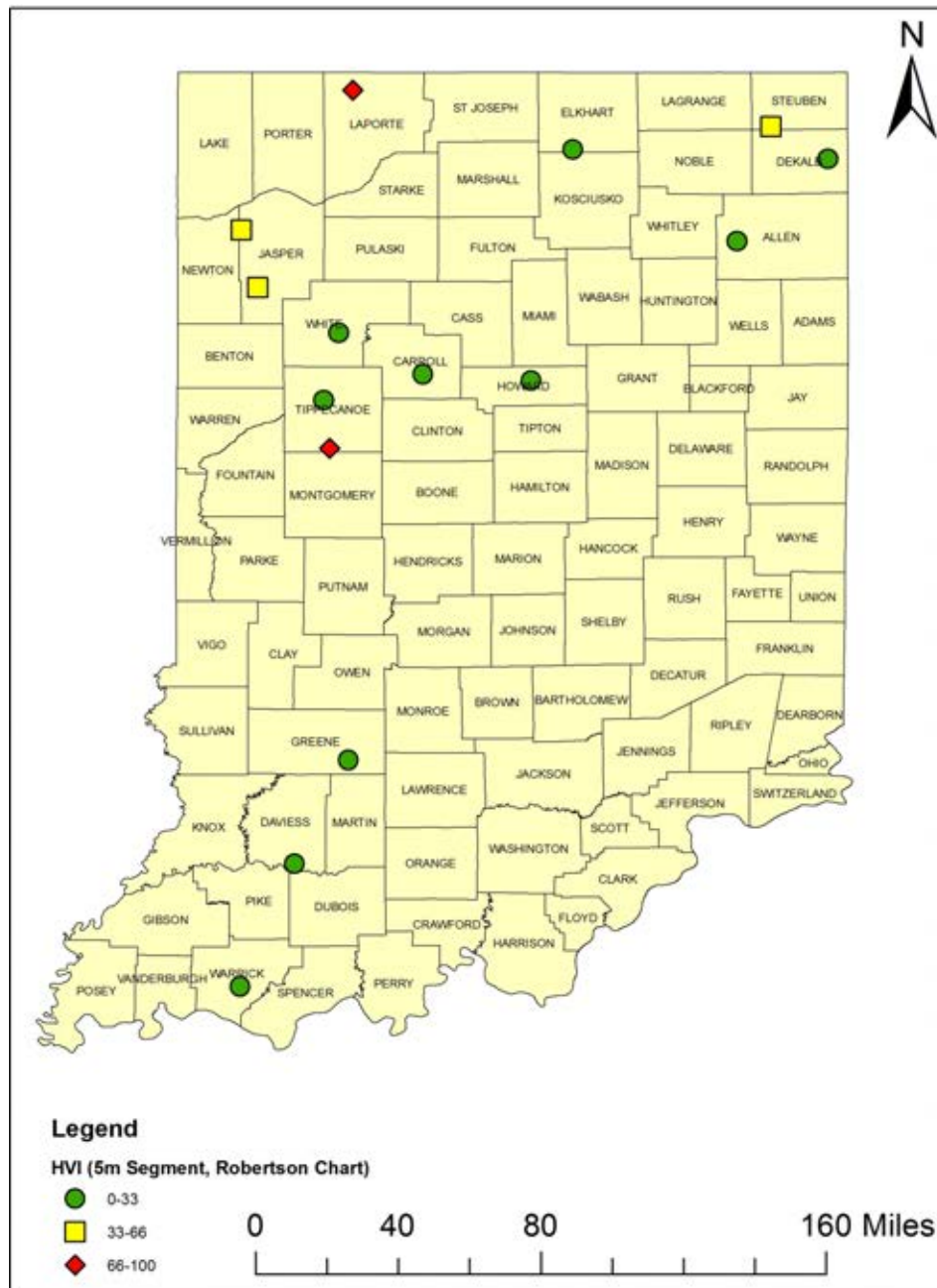


Figure B.12 Site *HVI* for 5 m soil profile length.

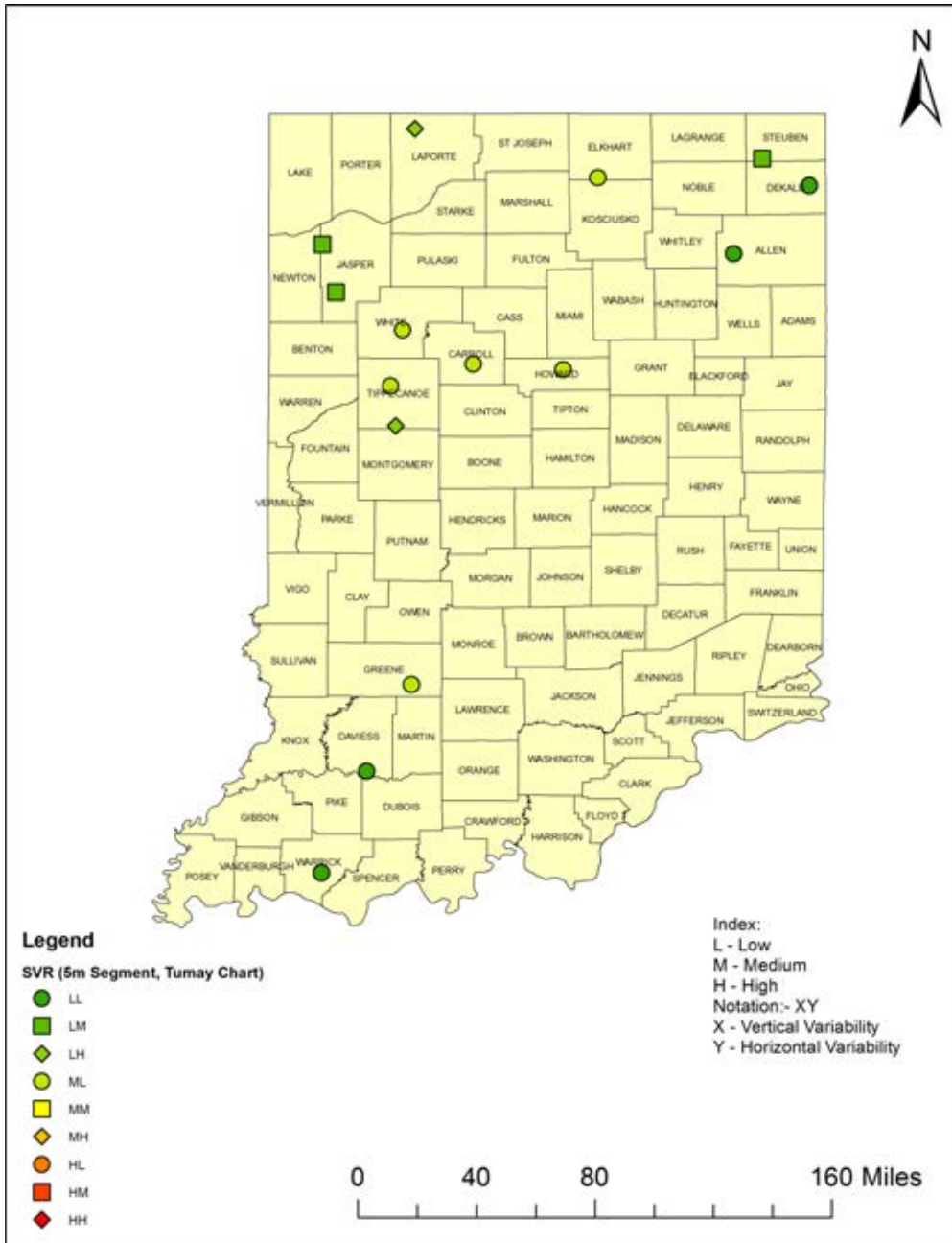


Figure B.13 SVR for 5m soil profile length using modified Tumay (1985) chart.

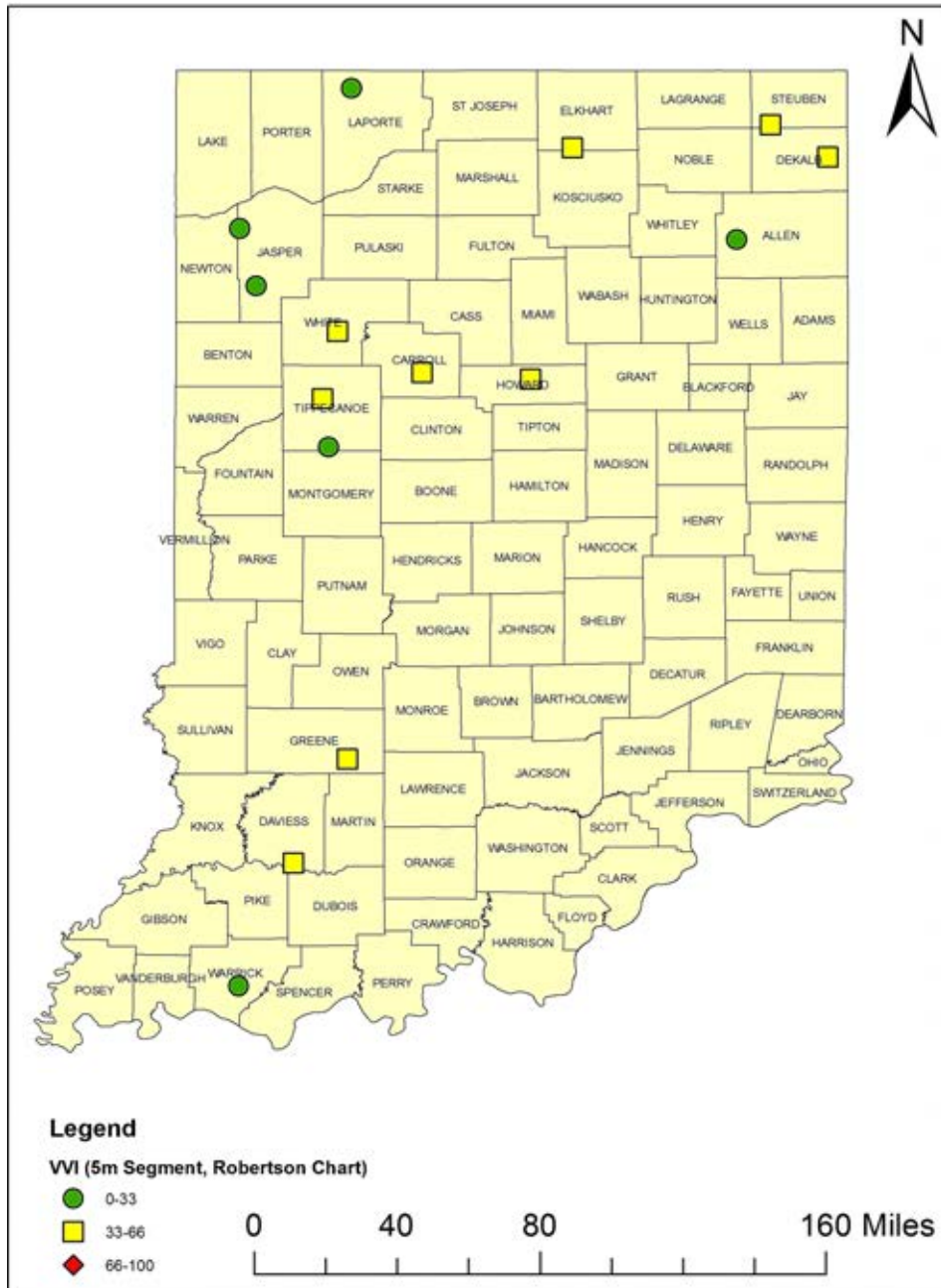


Figure B.14 Site VVI for 5 m soil profile length using modified Robertson (1990) chart.

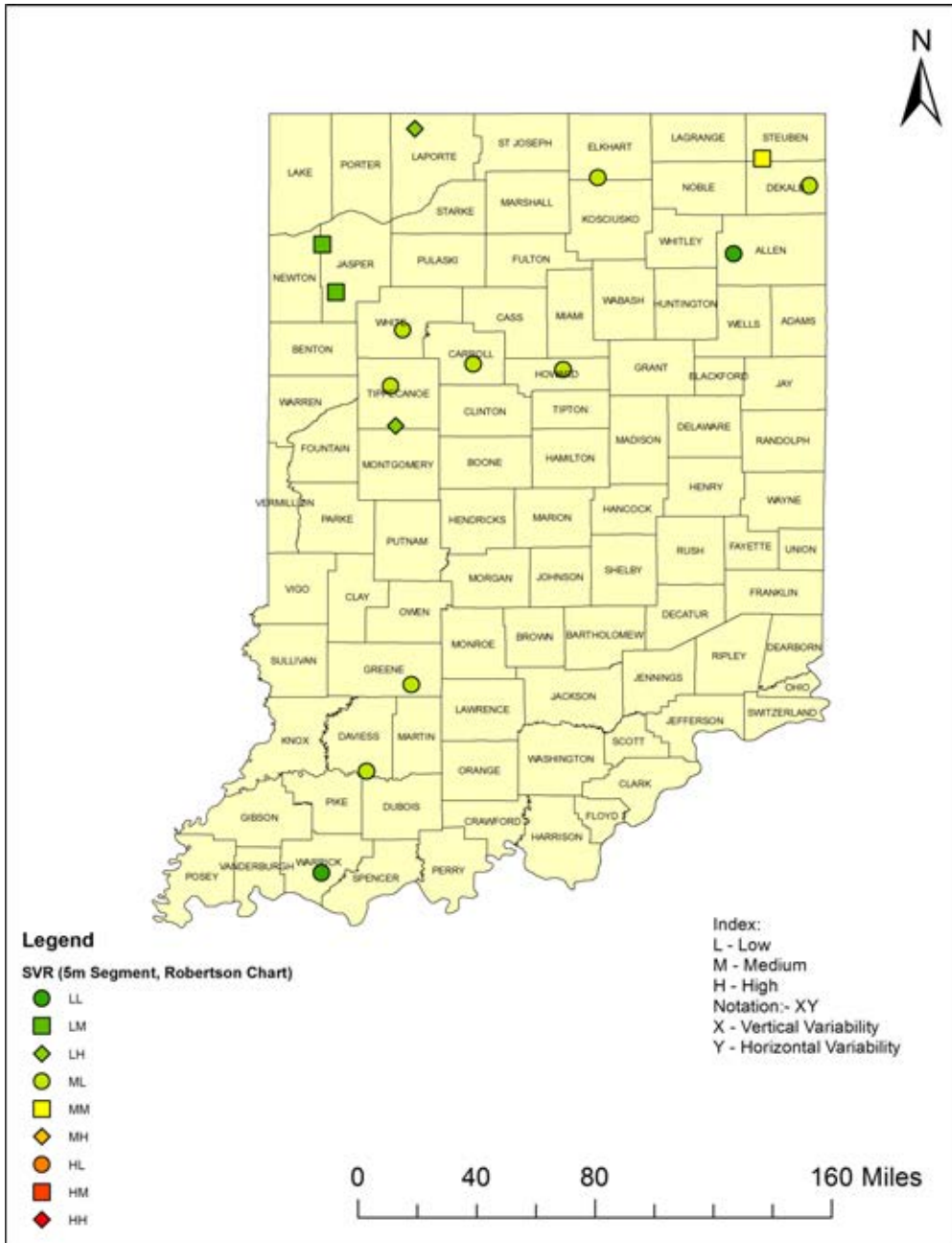


Figure B.15 SVR for 5m soil profile length using modified Robertson (1990) chart.

## About the Joint Transportation Research Program (JTRP)

On March 11, 1937, the Indiana Legislature passed an act which authorized the Indiana State Highway Commission to cooperate with and assist Purdue University in developing the best methods of improving and maintaining the highways of the state and the respective counties thereof. That collaborative effort was called the Joint Highway Research Project (JHRP). In 1997 the collaborative venture was renamed as the Joint Transportation Research Program (JTRP) to reflect the state and national efforts to integrate the management and operation of various transportation modes.

The first studies of JHRP were concerned with Test Road No. 1—evaluation of the weathering characteristics of stabilized materials. After World War II, the JHRP program grew substantially and was regularly producing technical reports. Over 1,500 technical reports are now available, published as part of the JHRP and subsequently JTRP collaborative venture between Purdue University and what is now the Indiana Department of Transportation.

Free online access to all reports is provided through a unique collaboration between JTRP and Purdue Libraries. These are available at: <http://docs.lib.purdue.edu/jtrp>

Further information about JTRP and its current research program is available at: <http://www.purdue.edu/jtrp>

## About This Report

An open access version of this publication is available online. This can be most easily located using the Digital Object Identifier (doi) listed below. Pre-2011 publications that include color illustrations are available online in color but are printed only in grayscale.

The recommended citation for this publication is:

Salgado, R., Prezzi, M., & Ganju, E. (2015). *Assessment of site variability from analysis of cone penetration test data* (Joint Transportation Research Program Publication No. FHWA/IN/JTRP-2015/04). West Lafayette, IN: Purdue University. <http://dx.doi.org/10.5703/1288284315523>